Kemijski optički senzori temeljeni na derivatima benzimidazola

Horak, Ema

Sveučilište u Zagrebu

FAKULTET KEMIJSKOG INŽENJERSTVA I TEHNOLOGIJE

Ema Horak

KEMIJSKI OPTIČKI SENZORI TEMELJENI NA DERIVATIMA BENZIMIDAZOLA

DOKTORSKI RAD

Zagreb, 2017.

University of Zagreb

FACULTY OF CHEMICAL ENGINEERING AND TECHNOLOGY

Ema Horak

CHEMICAL OPTICAL SENSORS BASED ON BENZIMIDAZOLE DERIVATIVES

DOCTORAL THESIS

Zagreb, 2017.

Sveučilište u Zagrebu
FAKULTET KEMIJSKOG INŽENJERSTVA I TEHNOLOGIJE

Ema Horak

KEMIJSKI OPTIČKI SENZORI TEMELJENI NA DERIVATIMA BENZIMIDAZOLA

DOKTORSKI RAD

Mentor: Izv. prof. dr. sc. Ivana Steinberg

Zagreb, 2017.

University of Zagreb
FACULTY OF CHEMICAL ENGINEERING AND TECHNOLOGY

Ema Horak

CHEMICAL OPTICAL SENSORS BASED ON BENZIMIDAZOLE DERIVATIVES

DOCTORAL THESIS

Supervisor: Ivana Steinberg, PhD, Associate professor

Zagreb, 2017.

Bibliografski podaci:

- UDK: 547.7:681.5(043.3)
- Znanstveno područje: prirodne znanosti
- Znanstveno polje: kemija
- Znanstvena grana: primijenjena kemija
- Institucija: Sveučilište u Zagrebu, Fakultet kemijskog inženjerstva i tehnologije, Zavod za opću i anorgansku kemiju
- Voditelj rada: izv. prof. dr. sc. Ivana Steinberg
- Broj stranica: 246
- Broj slika: 38
- Broj tablica: 8
- Broj priloga: 4
- Broj literaturnih referenci: 244
- Datum obrane: 02. lipnja 2017.
- Sastav povjerenstva za obranu:
  Izv. prof. dr. sc. Marijana Hranjec, Fakultet kemijskog inženjerstva i tehnologije
  Izv. prof. dr. sc. Stjepan Milardović, Fakultet kemijskog inženjerstva i tehnologije
  Dr. sc. Nikola Basarić, znanstveni suradnik, Institut Ruđer Bošković

- Rad je pohranjen u:
  Nacionalnoj i sveučilišnoj knjižnici u Zagrebu, Hrvatske bratske zajednice bb;
  Knjižnici Fakulteta kemijskog inženjerstva i tehnologije Sveučilišta u Zagrebu, Marulićev trg 20; Knjižnici Sveučilišta u Rijeci, Dolac 1;
  Knjižnici Sveučilišta u Splitu, Livanjska 5 i
  Knjižnici Sveučilišta u Osijeku, Europska avenija 24.

Tema rada prihvaćena je na 194. sjednici Fakultetskog vijeća Fakulteta kemijskog inženjerstva i tehnologije Sveučilišta u Zagrebu održanoj dana 24. veljače 2016. te odobrena na sjednici Senata Sveučilišta u Zagrebu održanoj dana 19. travnja 2016. godine.

“Isn’t it funny how day by day nothing changes, but when you look back everything is different?”

— C.S. Lewis

Rezultat svih mojih malih i velikih promjena posljednjih godina je utkan u ovaj doktorski rad. On se ne nalazi isključivo unutar ovog sveska papira, već se njegov odraz očituje u svim segmentima života. Stoga, dio ovog rada pripada svim ljudima koji su prolazno ili trajno bili dio mog života tijekom njegove izrade.

Najveće hvala mojoj mentorici, izv. prof. dr. sc. Ivani Steinberg, koja me od prvog dana smatrala ravnopravnom članicom istraživačkog tima i strpljivo vodila do konačnih rezultata. Hvala na predloženoj temi te svim savjetima i pomoći tijekom izrade ovog doktorskog rada.

Veliko hvala i dr. sc. Marijani Hranjec i dr. sc. Nataši Perin na vječitoj podršci, odličnoj suradnji i gostoprimstvu na Zavodu za organsku kemiju.

„Podrška“ nije dovoljno snažna riječ koja opisuje strpljivost i dobrotu mojih kolega sa Zavoda za opću i anorgansku kemiju, kojima bih od srca htjela zahvaliti na mnogočemu, a prvenstveno prijateljstvu. Svim starim i novim članovima Zavoda - hvala što ste dio mog svakog radnog dana.

Hvala ostalim kolegama s FKIT-a i IRB-a na ugodnoj suradnji, a osobito dr.sc. Robertu Vianellu, voditelju HRZZ projekta „Dizajn i sinteza novih dušikovih heterocikličkih fluorofora i fluorescentnih nanomaterijala kao kemijskih senzora za pH i metalne ione“ (IP-09-2014-3386) u sklopu kojeg je izrađen dio doktorskog rada.

Veliko hvala mojim curama, doživotnim iskrenim prijateljicama i čuvaricama. Mojoj obitelji na bezuvjetnoj podršci, a najviše roditeljima - kojima se zahvalnost za podršku i ljubav ne može opisati riječima.

Ema Horak

SAŽETAK

Temelj svakog kemijskog senzorskog sustava je receptor, odnosno kemosenzorska molekula sposobna prepoznati potencijalni analit. Optički kemijski senzori za ione kao receptore često primjenjuju konjugirane D-π-A heterocikličke molekulske sustave, koje osim funkcije prepoznavanja analita, osiguravaju i dobra optička svojstva poput snažne apsorpcije pri visokim valnim duljinama i izražene fluorescencije. Na taj način omogućuju jednostavnu i brzu metodu detekcije iona, često uočljivu i golim okom. Jedna od osnovnih gradivnih jedinica mnogih heterocikličkih senzorskih sustava je benzimidazol. Derivati benzimidazola, osim izražene biološke aktivnosti, pronalaze primjenu u tehnologiji lasera, optoelektronici, kao fluorescentne probe i kemosenzori. Benzimidazolna jezgra ugrađena u *push-pull* molekulski sustav (D-π-A sustav) može biti elektron-donorska jedinica ili dio konjugiranog mosta te znatno utjecati na fotofizička i senzorska svojstva molekule.

U ovom radu su istraženi novi heterociklički sustavi za primjenu u senzorima temeljeni na tri klase kromofora: akrilonitrilna benzimidazolna bojila, benzimidazo[1,2-*a*] kinolinski derivati i Schiffove baze funkcionalizirane benzimidazolnom jezgrom. Karakterizacijom njihovih fotofizičkih, kiselo-baznih i kompleksirajućih svojstava definirani su odnosi strukture i spektralnih svojstava te procijenjena njihova primjenjivost u senzorskim sustavima za pH i metale. Najbolji kandidati imobilizirani u polimerne senzorske matrice, optode, su pokazali vrlo izraženu fluorescenciju (u plavom, žutom i zelenom spektralnom području) i sposobnost reverziblnog praćenja pH vrijednosti u otopinama u fiziološki relevantnom području (pH 5-8). Istraživanjem su otkrivena jedinstvena fotofizička svojstva nekih od ispitivanih derivata benzimidazola, poput emisije uzrokovane nanoagregacijom molekula u vodenim otopinama. Promjenom pH vrijednosti otopine moguće je reverzibilno utjecati na proces stvaranja nanoagregata u otopini i na taj način uključivati i isključivati pojavu emisije pri 600 nm. Otkrivena svojstva mogu pronaći primjenu u senzorima, bio-oslikavanju i funkcionalnim materijalima. Definirane su smjernice za nastavak istraživanja kemosenzorskih mehanizama i materijala, posebno za praćenje interakcija s metalnim ionima i DNA molekulama. Na temelju dobivenih rezultata je zaključeno da benzimidazolna jezgra predstavlja multifunkcionalnu gradivnu jedinicu u optičkim kemijskim senzorima, s dokazanim potencijalom za razvoj novih funkcionalnih (nano)materijala.

Ključne riječi: senzor; pH; benzimidazol; emisija uzrokovana agregacijom, D-π-A sustav

SUMMARY

Chemosensing molecules capable of assaying cations or anions in solution ("receptors") are at the core of every optical chemical sensor. Conjugated D-π-A heterocyclic molecular systems play a dual role in optical chemical ion sensors: as receptors they recognise potential analytes and transform it into analytical signal due to their excellent optical properties, such as strong absorption and fluorescence at long wavelengths. This provides a fast and simple ion detection method, often visible by naked eye. A variety of heterocyclic molecules have been employed in the development of optical sensors in which the benzimidazole unit forms one of the key building blocks. In addition to their recognised biological activity, benzimidazole derivatives also find application in optical lasers and optoelectronics, as fluorescent probes and chemosensors. In recent years, emphasis has been placed on chemosensors that possess push-pull structures (D-π-A systems), where the benzimidazole unit may function as an electron-donating moiety or as a part of a conjugating system.

This thesis presents the investigation of three classes of novel benzimidazole functionalised heterocyclic chromophore systems as potential chemosensors: acrylonitriles, benzimidazo[1,2-*a*]quinolines and Schiff bases. The photophysical, acid-base and metal-ion complexing properties of all derivatives have been identified and their structure-property relationships discussed. Their potential for pH and metal-ion sensing has been evaluated, and the best candidates immobilised in polymer matrices (optodes). The optodes showed very strong fluorescence (in the blue, yellow and green spectral regions) and were able to reversibly monitor pH in solution in the physiologically relevant range (pH 5-8). The research has revealed the ability of some derivatives to form emissive nanoaggregates in aqueous solutions. Aggregation-induced emission (AIE) at 600 nm was found to be pH switchable and reversible, demonstrating great potential for applications in chemosensing, bioimaging and functional materials.

Further research in the field of benzimidazole based chromophores and materials, and their potential sensing mechanisms and interactions with metal ions and DNA molecules is proposed. The results of the thesis lead to the conclusion that the benzimidazole unit represents an important multifunctional building block in optical chemical sensors, with proven potential for development of novel functional (nano)materials.

Keywords: sensor, benzimidazole, aggregation induced emission, D-π-A system

SADRŽAJ

1. UVOD

Kemijski senzori odgovaraju na jedan od ključnih izazova moderne analitičke kemije: jednostavno, brzo i ekonomično određivanje ciljanog analita, na licu mjesta i bez referentnog uređaja. Optički kemijski senzori temelje se na mjerenju optičkog svojstva uzorka (apsorpcija, refleksija, emisija), a odlikuju ih visoka osjetljivost, dobra selektivnost, brzina odziva i jednostavnost priprave i uporabe. Također, potreba za minijaturizacijom i beskontaktnim mjerenjima je sve izraženija, zbog čega je područje istraživanja i razvoja optičkih senzora izrazito progresivno. Pritom se posebno ističu fluorescencijski senzori zbog niza prednosti u praćenju interakcija između senzorske molekule i analita, kao što je visoka osjetljivost i raznovrsnost raspoloživih mehanizama detekcije.

Heterociklički kromofori su jedna od najistraživanijih skupina kemosenzorskih molekula zbog mogućnosti detekcije različitih analita, odnosno promjene fotofizičkih svojstava u procesu selektivnog prepoznavanja anionskih ili kationskih vrsta. U literaturi je opisan velik broj heterocikličkih kromofora/fluorofora kao kemosenzorskih molekula i između ostalih uključuje Schiffove baze [1-4], kinoline [5-8], kumarine [9-12] te stirilna bojila [13-16]. Benzimidazolna jezgra može biti uključena kao gradivna jedinica u heterocikličkom molekulskom sustavu i pridonosi nizu novih svojstava posebno zanimljivih za senzorske i optoelektroničke primjene. Benzimidazol, u ulozi jezgre organskih kromofora (fluorofora), svojom rigidnom i planarnom strukturom može pridonositi rezonantnoj stabilnosti spoja i prijenosu naboja unutar konjugiranog sustava. Slobodni elektroni na atomima dušika u molekuli benzimidazola i različiti supstituenti na osnovnom molekulskom kosturu posredno ili neposredno utječu na kemosenzorska svojstva molekule, posebno u pogledu pH osjetljivosti i kompleksiranja metalnih kationa. Prisutnost metalnih kationa često je nužna za odvijanje velikog broja bioloških i kemijskih procesa, dok je poznavanje vrijednosti pH izrazito važno u medicini, biologiji i mnogim (bio)tehnološkim procesima. Stoga, iako je njihov potencijal za različitu primjenu često zasjenjen izvanrednom biološkom aktivnosti [17], ne čudi sve češća primjena benzimidazolnih derivata kao fluorescentnih proba ili kemosenzora [18].

Pregledom dostupnih znanstvenih radova uočena je potreba za sustavnim istraživanjem i razvojem novih klasa kromofora i fluorofora temeljenih na benzimidazolu kao gradivnoj jedinici. Metodologija razvoja novih senzorskih sustava započinje definiranjem osnovnih odnosa *struktura-svojstvo*, odnosno spektralnom karakterizacijom potencijalnih kemosenzorskih molekula u otopinama, definiranjem kiselo-bazne ravnoteže ionskih vrsta, određivanjem njihovih konstanti disocijacije (pK_a vrijednosti) te ispitivanjem utjecaja potencijalnih analita na fotofizička svojstva. Osim za senzorske primjene, ovakva

karakterizacija je nužna za primjene u optičkom obilježavanju bioaktivnih molekula ili u postupcima razvoja i primjene farmaceutika. Potom slijedi funkcionalizacija ili imobilizacija kemosenzorskih molekula, najčešće putem priprave funkcionalnih (nano)materijala prikladnih za integraciju u optički senzorski sustav. Funkcionalizirana kemosenzorska molekula ili senzorski materijal dobiven optimiranjem postupka imobilizacije molekula u prikladne matrice može imati znantno različita svojstva u odnosu na kemosenzorsku molekulu u otopini. Stoga je prikladnim odabirom matrice, to jest mikrookruženja u kojem se molekula nalazi, moguće utjecati na spektralna svojstva, vrijednosti pK_a, vrijeme života fluorescencije ili mogućnost kompleksiranja iona. U tom je pogledu posebno zanimljivo istraživanje novih heterogenih senzorskih shema i mehanizama koji u homogenom okruženju u otopinama nisu mogući.

Na Slici 1. shematski je prikazan optički kemosenzorski sustav temeljen na derivatu benzimidazola. Analitička funkcija sustava proizlazi iz dualne uloge kemosenzorske molekule koja uz selektivnu detekciju potencijalnog analita ima i sposobnost signaliziranja događaja prepoznavanja pomoću promjene nekog od spektroskopskih svojstava.

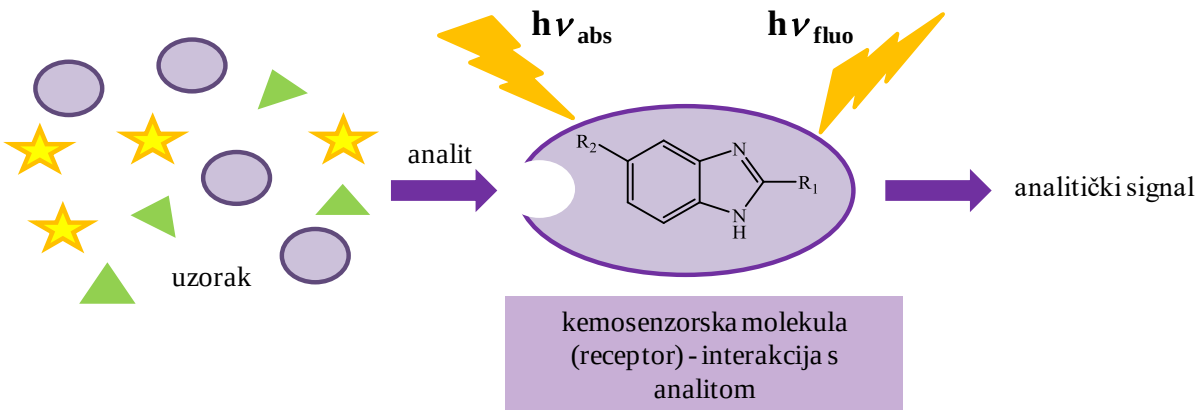

Slika 1. Shematski prikaz rada optičkog kemosenzorskog sustava u otopini temeljenog na derivatu benzimidazola.

U ovom su radu istraženi novi derivati benzimidazola s potencijalnim senzorskim djelovanjem podijeljeni prema strukturnim karakteristikama na nekoliko klasa spojeva: stiril-cijaninska bojila, benzimidazo[1,2-*a*]kinolinski derivati ili Schiffove baze temeljene na benzimidazolu (Slika 2). Spojevi su pripravljeni na Zavodu za organsku kemiju FKIT-a pod vodstvom izv. prof. dr. sc. Marijane Hranjec.

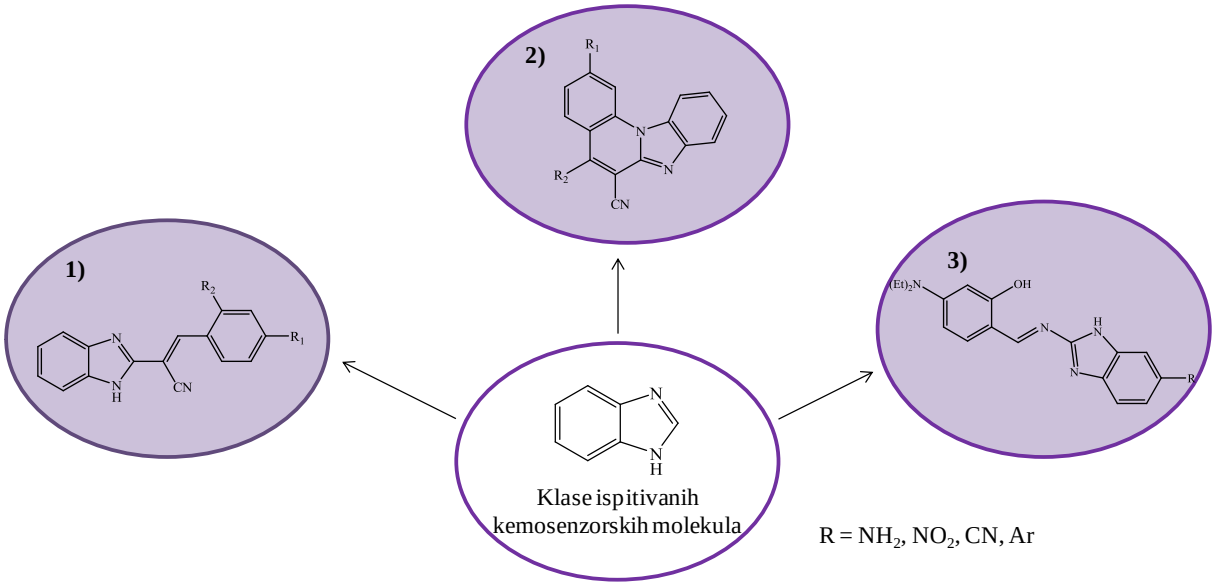

Slika 2. Klase ispitivanih kemosenzorskih molekula temeljenih na benzimidazolu.

Stiril-cijaninska bojila se široko primjenjuju u mnogim područjima znanosti [13]. Benzimidazolni derivati ove klase spojeva pružaju novu platformu za ispitivanje kiselo-baznih i kompleksirajućih svojstava novih kromofora (fluorofora) temeljenih na benzimidazolu. Benzimidazo[1,2-*a*]kinolini su tetraciklički derivati benzimidazola. Amino supstituirani derivati ove vrste spojeva pokazuju svojstva intenzivne fluorescencije što omogućuje razne mogućnosti primjene u optičkim senzorskim sustavima i funkcionalnim materijalima [14, 19, 20]. Schiffove baze su jedna od najistraživanijih skupina organskih kemijskih spojeva zahvaljujući izvanrednim mogućnostima kompleksiranja iona. Benzimidazolna jezgra u mnogočemu doprinosi fotofizičkim i senzorskim svojstvima ovih klasa spojeva.

U doktorskom radu su sustavno istražena navedena svojstva prikazanih kemosenzorskih molekula u otopinama i tankim polimernim filmovima, uočena je osnovna veza između njihove molekulske strukture i specifičnih fotofizičkih i senzorskih svojstava te na taj način definirana uloga benzimidazolne jedinice u tumačenju svojstava molekula.

2. OPĆI DIO

2.1. Kemijski senzori

Kemijski senzori su „*minijaturizirani analitički uređaji koji u stvarnom vremenu donose* on-line *informacije o prisustvu specifičnih spojeva ili iona u kompleksnom uzorku*“ [21]. Bitno je napomenuti da riječ „senzor“ nije jednoznačna u svim znanstveno - istraživačkim područjima. Supramolekulska kemija, primjerice, senzorom smatra bilo koju molekulu koja je u mogućnosti detektirati promjenu unutar sustava (stvaranje kompleksa metala i liganda i slično), za razliku od analitičke kemije koja kemijski senzor smatra analitičkim uređajem. **Senzorska molekula ili kemosenzor** se u analitičkim kemijskim senzorima naziva receptorom, te je upravo ona odgovorna za selektivnu detekciju analita i analitički odgovor senzora. Općeniti shematski prikaz kemijskog senzora i njegovih glavnih komponenti je prikazan na Slici 3.

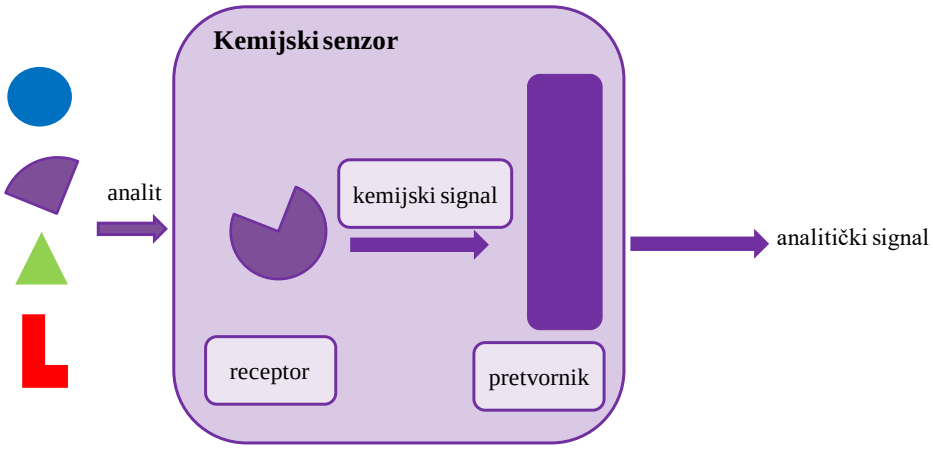

Slika 3. Shematski prikaz kemijskog senzora kao analitičkog uređaja.

Receptor se u analitičkom uređaju može bazirati na fizikalnim, kemijskim ili biokemijskim principima, ovisno potječe li analitički signal od fizikalnog svojstva molekule, kemijske ili biokemijske reakcije s analitom. Osim receptora, tipičan kemijski senzor se sastoji još od pretvornika i separatora (npr. membrane). Pretvornik pretvara kemijsku informaciju u analitički koristan signal te se najčešće upravo prema principu rada pretvornika vrši podjela kemijskih senzora na:

- Optičke senzore, koji pretvaraju kemijsku informaciju nastalu promjenom optičkih svojstava interakcijom analita i receptora u analitički signal.
- Elektrokemijske senzore, koji pretvaraju elektrokemijske informacije nastale interakcijom analita i elektrode u analitički signal.
- Električne uređaje, čiji signal proizlazi iz promjene električnih svojstava uzrokovanih reakcijom analita.
- Uređaje osjetljive na promjenu mase, koji analitički signal stvaraju promjenom mase uzrokovane akumulacijom analita na modificiranoj podlozi.
- Magnetske uređaje, čiji signal proizlazi od promjene paramagnetičkih svojstava analiziranog uzorka.
- Termometrijske uređaje bazirane na mjerenju topline specifičnih kemijskih reakcija [21].

2.2. Optički kemijski senzori

U današnje doba, jednostavno, brzo i ekonomično određivanje ciljanog analita na licu mjesta je izrazito važno. Navedeni zahtjevi omogućeni su uporabom optičkih kemijskih senzora, zbog čega je područje njihovog istraživanja i razvoja izrazito progresivno. Optički kemijski senzori se temelje na mjerenju optičkog svojstva uzorka, a odlikuju ih visoka osjetljivost, dobra selektivnost, brzina odziva i jednostavnost priprave i uporabe [22, 23].
Podjela optičkih senzora se najčešće temelji na optičkom svojstvu koje se detektira pa razlikujemo:

- apsorpcijske senzore,
- refleksijske senzore,
- fluorescencijske senzore,
- senzore temeljene na indeksu loma,
- senzore temeljene na optotermalnom efektu,
- senzore temeljene na raspršenju svjetla.

Razvoj kemijskog senzora je kompleksan proces koji uključuje logičan slijed istraživačkih radnji, počevši od ciljane sinteze kemosenzorske molekule do njezine 'ugradnje' u analitički sustav. Jedna od najjednostavnijih metoda priprave kemijskog senzora jest imobilizacija kemosenzorske molekule na određeni supstrat. Imobilizacijom heterocikličkih kromofora u

prikladne polimerne matrice nastaju funkcionalni senzorski materijali, koji su danas osim u senzorskim primjenama prikladni za razvoj nove generacije organskih optoelektroničkih komponenata, iskorištavanje sunčeve energije te raznih drugih inteligentnih i funkcionalnih bio-materijala. Procesom imobilizacije se mogu promijeniti brojne fizičke i kemijske karakteristike kemosenzorskih molekula, kao što su spektralna svojstva, vrijednosti pK_a, vrijeme života fluorescencije ili mogućnost kompleksiranja. Osim toga, odabir vrste polimernog materijala i način imobilizacije senzorske molekule znatno utječe na analitičke parametre senzorskog sustava kao što su vrijeme odziva, osjetljivost, radno područje i selektivnost. Fizičko zarobljavanje kemosenzorske molekule unutar polimerne matrice je najčešća metoda priprave jednostavnih optičkih senzorskih membrana ili *optoda*. Pojam *optoda* ili *optroda* je nastao prije 30-tak godina od „optička elektroda“ (engl. *optical electrode)* i redovito se koristi kao skraćenica za optički senzor. Oba pojma u suštini imaju isto značenje i naglasak daju na činjenicu da je signal optički, a ne elektrokemijski.

Ion-selektivne optode su vrsta optičkih membrana kod kojih je senzorski mehanizam temeljen na natjecateljskoj ionskoj izmjeni kroz cijeli profil polimerne matrice (*bulk membrane*). Izvedba senzora u obliku ion-selektivnih optoda je najpogodnija za brzu, jednostavnu i ekonomičnu uporabu, jer optoda sadrži sve sastojke potrebne za prepoznavanje analita. Sastav membrane izravno utječe na njezina ionsko-izmjenjivačka svojstva, a uglavnom se sastoji od polimerne matrice, omekšavala (plastifikatora), lipofilne soli, ionofora (prenosilac ciljanog iona, ligand), kromoionofora i otapala. Mehanizam rada ionsko-selektivne optode se temelji na stvaranju ionskih parova kromoionofora i lipofilnog dodatka pri čemu kromoionofor nije selektivan na ciljani ion (Slika 4.). Kompleksiranje ionofora s ciljanim analitom izaziva promjenu koncentracije protoniranog/deprotoniranog oblika kromoionofora u membrani, odnosno promjenu optičkog svojstva (apsorbancije, fluorescencije i slično). Ionofor u membrani mehanizmom difuzije prenosi na sebi ciljani ion (engl. *ion-carrier*) te je odgovoran za selektivno i reverzibilno vezanje određenog iona [22, 24, 25]. Kromoionofor može ujedno biti i prepoznavajuća jedinica (receptor), što dodatno olakšava izvedbu ionsko-selektivnih optoda.

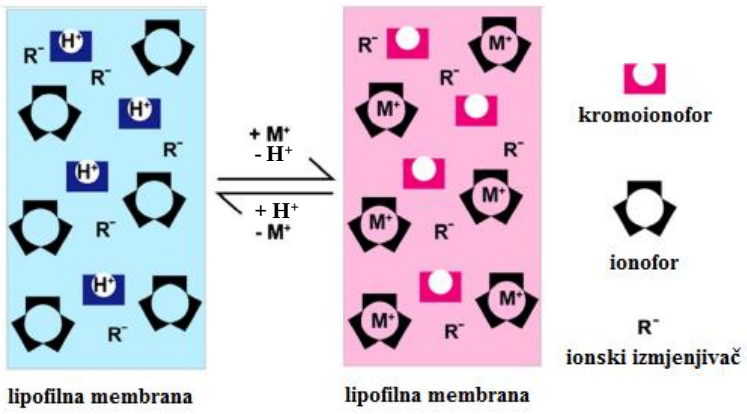

Slika 4. Mehanizam natjecateljske ionske izmjene kod ionsko-selektivnih optoda, adaptirano iz [25].

2.2.1. Fluorescencijski kemijski senzori

Fluorescencijski senzori se posebno ističu u skupini optičkih senzora zbog niza prednosti u praćenju interakcija između senzorske molekule i analita, prvenstveno visoke osjetljivosti i raznovrsnosti raspoloživih mehanizama detekcije. Ključni napredak u razvoju fluorescentnih senzora su predstavili Lakowicz i Valeur [26-28] definiranjem temeljnih znanja o fluorescenciji i fluorescentnoj spektroskopiji, Demchenko [29], predstavljanjem ključnih primjera fluorescentnih molekulskih sustava za senzorsku primjenu, de Silva detaljnom karakterizacijom i razvojem novih senzorskih molekulskih sustava [30] te Wolfbeis razvojem optičkih senzora u obliku optoda, optičkih vlakana, nanomaterijala i slično [23, 31, 32]. Dizajn fluorescencijskih kemijskih senzora se temelji na prikladnom odabiru fluorofora i jedinice za prepoznavanje analita (receptora). Većina fluorescencijskih senzora se bazira na jednostavnim strukturama, gdje su fluorofor i receptor povezani kemijskom vezom, strukturnom razmaknicom (engl. *spacer*) ili su integrirani (Slika 5.).

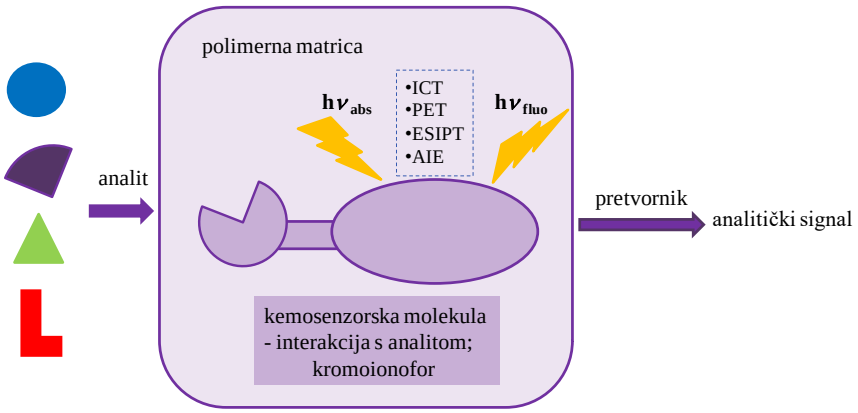

Slika 5. Shematski prikaz fluorescencijskog kemijskog senzora. Ukoliko se radi o senzorskoj membrani, primjerice ionsko-selektivnoj optodi, komponente su imobilizirane u polimernu matricu.

Kemosenzorska molekula (receptor) selektivno i specifično prepoznaje analit te proizvodi optički odogovor (fluorescenciju). Pretvornikom se smatra uređaj, najčešće minijaturiziran, pomoću kojeg se optički signal prevodi u analitički korisnu informaciju. Sofisticirani uređaj poput spektrofluorimetra može biti prikladan pretvornik za određene analitičke primjene, no analitička funkcija optičkih senzora može se postići i uz manje zahtjevnu instrumentaciju, čak i bez pretvornika, koristeći ljudsko oko za detekciju. Upravo ova karakteristika optičkih senzora donosi im znatnu prednost u određenim primjenama u odnosu na druge vrste kemijskih senzora. To se posebno očituje u širokoj primjeni kolorimetrijskih i fluorimetrijskih senzorskih shema razvijenim na pasivnim mikrofluidičkim platformama, poput testova za trudnoću i drugih dijagnostičkih imunotestova izvedenim na celuloznim podlogama.

Kreiranje novih fluorescencijskih senzorskih shema temelji se na promjenama fotofizičkih svojstava kemosenzorskih molekula u interakciji s molekulama analita. U fotofizičkom smislu, fluorescencija, kao i fosforescencija, je vrsta luminiscencije kod koje se pobuda zbiva apsorpcijom energije fotona. Molekule koje su apsorbirale energiju fotona prelaze u elektronski pobuđeno stanje te se emisijom zračenja vraćaju u osnovno stanje. Povratak molekule iz pobuđenog u osnovno stanje može se odvijati određenim radijativnim mehanizmom (na primjer fluorescencijom) ili neradijativnim mehanizmima, kao što su unutarnja pretvorba (eng. *Internal conversion*, IC), međusustavno križanje (engl. *Intersystem Crossing*, *ISC*) i konformacijske promjene.

Dijagram Jablonskog pruža jednostavnu vizualizaciju mogućih procesa pri pobudi molekule svjetlosnim zračenjem (Slika 6.). Osnovno singletno elektronsko stanje je označeno S_0 (potom slijede S_1, S_2), a tripletna elektronska stanja su označena T_1, T_2.

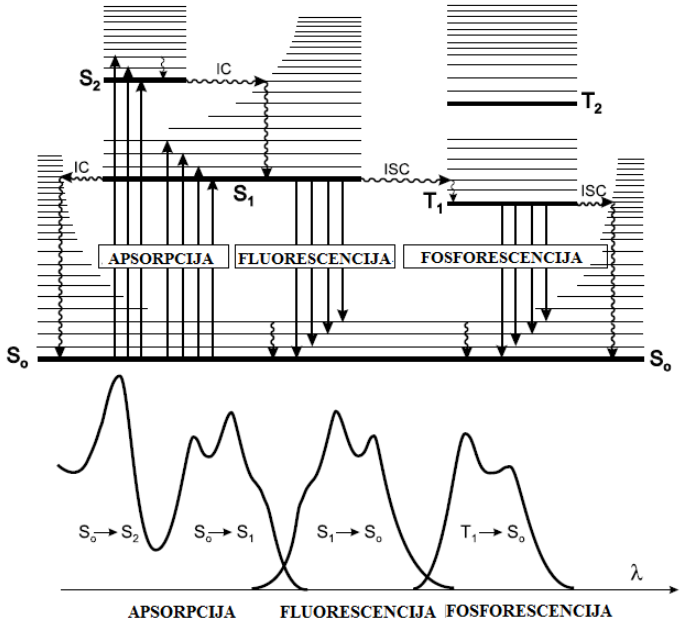

Slika 6. Dijagram Jablonskog i ilustracija relativnih položaja apsorpcijskog, fluorescencijskog i fosforescencijskog spektra, adaptirano iz [9].

Apsorpcija fotona može dovesti molekulu do jednog od vibracijskih nivoa singletnih stanja S_1, S_2 itd. Emisija fotona koju prati $S_1 \rightarrow S_0$ relaksacija se naziva fluorescencija. Emisija fotona je spontan proces te je jednako brza kao i apsorpcija fotona. Međutim, pobuđene molekule obično ostaju u S_1 stanju nekoliko desetaka pikosekundi do nekoliko stotina nanosekundi (ovisno o vrsti molekule i medija u kojem se nalazi), stoga se nakon pobude molekula veoma kratkim pulsom svjetlosti intenzitet fluorescencije eksponencijalno smanjuje s vremenom, na čemu se mogu temeljiti mjerenja vremena života fluorescencije. Valna duljina emisije će uvijek biti veća od valne duljine apsorpcije zbog gubitka energije u procesima vibracijskih relaksacija (Slika 6.). Fizikalni i kemijski parametri mikrookoliša koji utječu na fluorescentne karakteristike molekula su temperatura, viskoznost, pH, vodikove veze i polarnost [33], no najveći utjecaj ima molekulska struktura. Većina fluorescentnih spojeva su aromatske strukture kod kojih povećanjem stupnja konjugacije dolazi do pomaka apsorpcijskog i fluorescencijskog spektra prema većim valnim duljinama. Efekt supstituenata na fluorescentna svojstva aromatskih spojeva je veoma kompleksan. Primjerice, prisutnost teškog atoma kao supstituenta unutar aromatske molekule (npr. Br, I) uzrokuje gašenje fluorescencije zbog povećane vjerojatnosti međusustavnog križanja (efekt teškog atoma). Supstitucija elektron-donorskim grupama (OH, -OR, $-NH_2$, -NHR, $-NR_2$) često uzrokuje povećanje molarnog apsorpcijskog koeficijenta i pomak apsorpcijskog i fluorescencijskog

spektra prema većim valnim duljinama, jer su slobodni elektronski parovi na supstituentima direktno uključeni u konjugaciju aromatskog sustava [29].

Utjecaj molekulske strukture i mehanizama stvaranja i prijenosa signala kod fluorescentnih senzorskih molekula je široko i atraktivno područje istraživanja. Najčešći mehanizmi stvaranja i prijenosa signala su fotoinducirani prijenos elektrona (engl. *Photoinduced Electron Transfer*, PET), intramolekulski prijenos naboja (engl. *Intramolecular Charge Transfer*, ICT) i prijenos protona u pobuđenom stanju stanju (engl. *Excited-State Intramolecular Proton Transfer*, ESIPT), a bitno je još spomenuti i rezonantni prijenos energije (engl. *Flourescence Resonance Energy Transfer*, FRET) te stvaranje ekscimera i ekscipleksa [29].

2.2.1.1. Mehanizmi stvaranja i prijenosa signala kod fluorescentnih senzorskih molekula

Molekula u pobuđenom stanju može reagirati na način koji u osnovnom stanju nije moguć. Primjerice, prijenos elektrona, protona ili parcijalnog naboja u pobuđenom stanju može znatno promijeniti fotofizička svojstva molekule pri interakciji s analitom. Takvi mehanizmi stvaranja signala su temelj rada fluorescentnih senzora.

Fotoinducirani prijenos elektrona (PET)

U procesu fotoinduciranog prijenosa elektrona (engl. *Photoinduced Electron Transfer*, PET) elektron prelazi s pobuđenog donorskog mjesta na akceptorsko mjesto ili obrnuto, pri čemu su ključni faktor njihovi oksido-redukcijski potencijali. Sustavi u kojima je moguć fotoinducirani prijenos elektrona su molekule čija se struktura temelji na donorskoj i akceptorskoj jedinici povezanoj π-konjugiranim mostom (Slika 7.). Jedan od mogućih procesa kod ove vrste senzorskih molekula jest prijenos elektrona od receptorskog do fluoroforskog dijela molekule prilikom pobude fluorofora, takozvano „*off*“ stanje. Energija pobuđenog stanja fluorofora pritom mora biti dovoljna za redukciju fluorofora i oksidaciju receptora. Ukoliko pobuda fluorofora rezultira fluorescencijom, PET proces je onemogućen i senzorska molekula se nalazi u takozvanom „*on*“ stanju. PET proces se lako onemogućava vezivanjem analita, primjerice H^+, koji elektrostatski privlače elektrone i pritom povisuju oksidacijski potencijal receptora. U svom najjednostavnijem obliku, PET senzori se mogu promatrati kao sustavi u kojem dolazi do prijenosa elektrona ukoliko je oksidacijski potencijal receptora niži od oksidacijskog potencijala fluorofora. Pažljivim odabirom fluorofora, receptora i

konjugirane poveznice moguće je fino podešavanje fluorescentnog odgovora ovakvih molekula. Stoga, ne čudi što je dugi niz godina dizajn i priprava PET senzora široko i opsežno područje istraživanja.

Primjer senzora čija se struktura temelji na fluorofor – π konjugirana poveznica – receptor sustavu, te kod kojeg dolazi do fotoinduciranog prijenosa elektrona ("on-*off*" stanje) je prikazan na Slici 7. Ako se kation veže na elektron-donorsku skupinu (receptor), energija HOMO donora se snižava zbog pozitivnog naboja. Energija HOMO donora tada postaje niža od energije HOMO akceptora i onemogućuje fotoinducirani prijenos elektrona, odnosno omogućuje fluorescenciju ("*on*" stanje). Fluorofor pritom postaje jaki emiter svjetlosti, omogućavajući tako senzorsku uporabu u takozvanim „*on-off* senzorima" [30, 34].

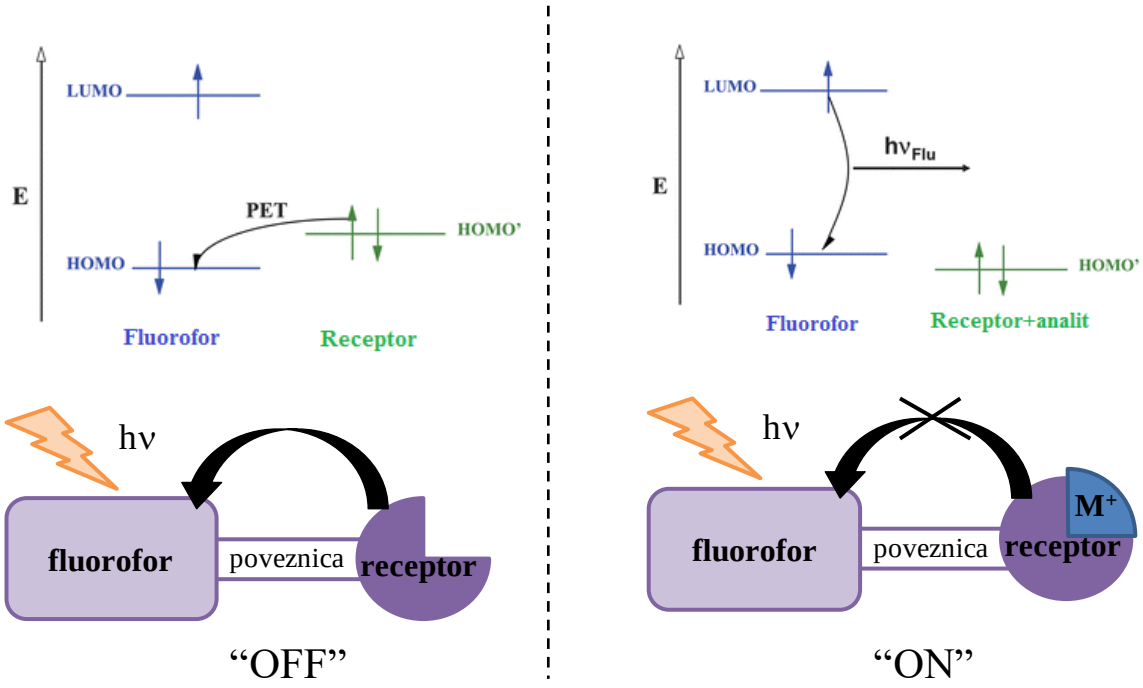

Slika 7. Shematski prikaz energetskog dijagrama u procesu fotoinduciranog prijenosa elektrona fluorescentne kemosenzorske molekule (lijevo) i molekule u interakciji s kationom (desno), adaptirano iz [34].

Intramolekulski prijenos naboja (ICT)

Jedan od mehanizama stvaranja signala kod fluorescencijskih kemosenzorskih molekula je intramolekulski prijenos naboja (engl. *Intramolecular charge transfer*, ICT) [30]. Intramolekulski prijenos naboja je prvenstveno omogućen geometrijom molekule, odnosno strukturnim rasporedom supstituenata na suprotnim krajevima π-konjugiranog sustava (engl. *push – pull*). Najčešće se u ICT sustavima na jednom kraju molekule nalazi elektron-donorska, '*push*' grupa, a elektron-odvlačeća, '*pull*' grupa se nalazi na drugom kraju molekule π-konjugiranog fluorofora [35]. Unutar *push-pull* sustava dolazi do polarizacije unutar same molekule ICT procesom te je elektronski prijelaz prilikom pobude fluorofora praćen gotovo trenutnom promjenom u dipolnom momentu fluorofora (Slika 8.). U pobuđenom stanju se pojačava donorski efekt elektron-donorske grupe, kao i akceptorski elektron-akcpetorske grupe, što dovodi do značajne polarizacije molekule u pobuđenom stanju. Nastali dipol međudjeluje s dipolima iz okolnog medija i može uzrokovati promjenu molekulske strukture (npr. nastajanje takozvanih TICT stanja) ili reorganizaciju molekula otapala oko fluorofora. ICT se očituje u velikim Stokesovim pomacima i osjetljivosti tako polarizirane molekule na mikrookolinu (npr. otapalo ili vezivanje analita), što čini temelj rada ICT senzora.

Mehanizam stvaranja i prijenosa signala kod ICT senzora se najčešće temelji na promjeni emisijskih svojstava molekule prilikom vezivanja analita, ovisno proizlazi li emisija iz lokalnog pobuđenog stanja ili ICT stanja. Tako se, na primjer, smanjuje donorski utjecaj elektron-donorske grupe ukoliko ona stupa u interakciju s analitom ili je izravno vezana na ionofor. Stupanj konjugacije se pritom smanjuje te se uočava plavi spektralni pomak. Nasuprot tome, ako se interakcija s analitom (kationom) događa na akceptorskom dijelu molekule, pojačava se elektron-odvlačeći efekt i uočava se crveni spektralni pomak i porast molarnog apsorpcijskog koeficijenta (Slika 8.)

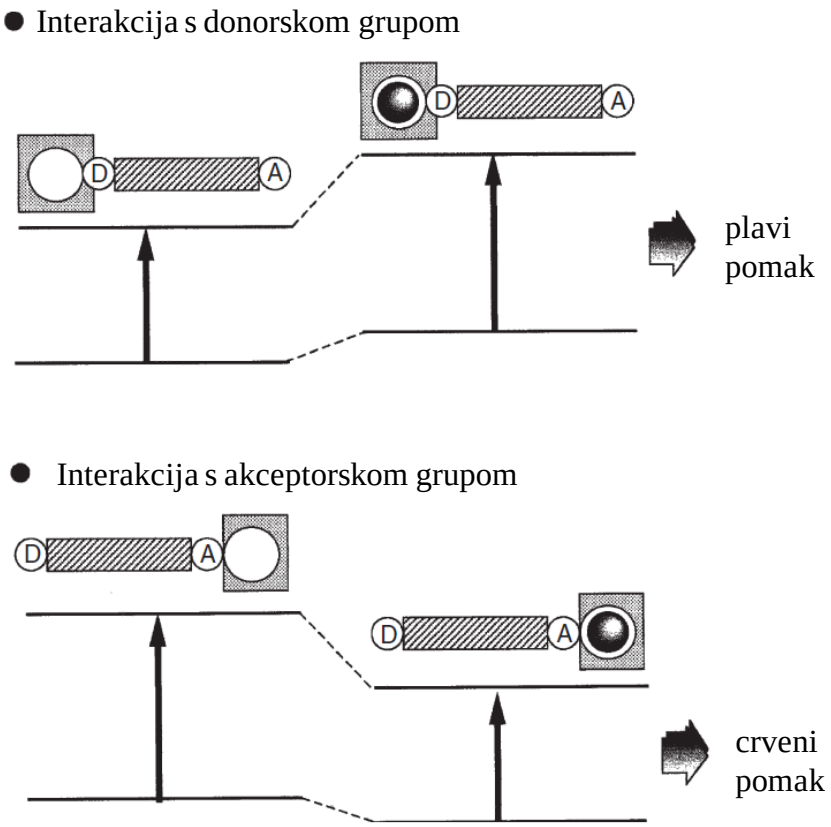

Slika 8. Spektralni pomaci kod ICT senzorskih molekula uzrokovani vezivanjem kationa na elektron-donorsku ili elektron-akceptorsku grupu, adaptirano iz [29].

Bitno je spomenuti i TICT mehanizam stvaranja signala (izvijeni intramolekulski prijenos naboja, engl. *Twisted intramolecular charge transfer*) gdje se stvaranje signala temelji na zakretanju ravnina receptorskog i fluorofornog dijela molekule (donorskog i akceptorskog dijela) povezanog preko jednostruke veze (Slika 9.). Tijekom prijenosa naboja unutar TICT molekulskog sustava dolazi do gubitaka u energiji zbog rotiranja dijela molekule oko jednostruke veze, što uzrokuje emisiju pri višim valnim duljinama. Često se kod TICT fluorofora zapažaju dvije emisijske vrpce koje odgovaraju emisiji iz lokalnog pobuđenog stanja i TICT emisiji [36, 37].

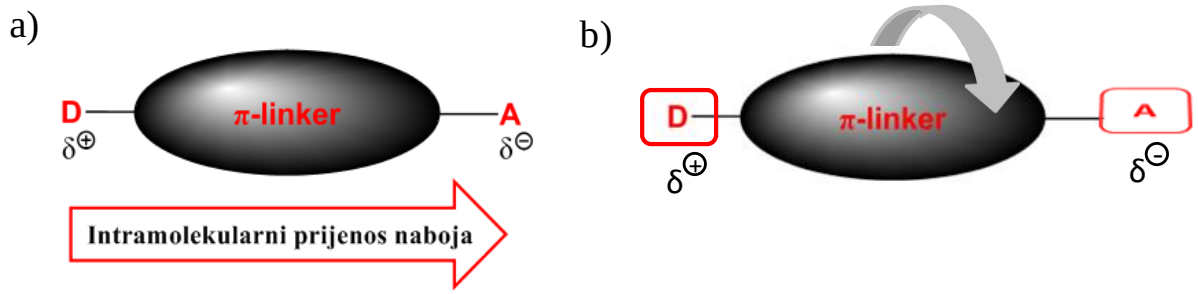

Slika 9. a) Shema sustava s intramolekulskim prijenosom naboja (ICT), adaptirano iz [38]; b) Shematski prikaz TICT sustav – rotiranje akceptorskog dijela konjugiranog molekulskog sustava oko jednostruke veze.

Intramolekulski prijenos protona u pobuđenom stanju (ESIPT)

Prijenos protona u pobuđenom stanju (engl. *Excited-State Intramolecular Proton Transfer*, ESIPT) jedan je od fundamentalnih procesa stvaranja signala kod fluorofora s intramolekulskom vodikovom vezom. Kod ovog fotokemijskog procesa dolazi do stvaranja tautomera u pobuđenom stanju, čija se svojstva razlikuju od osnovne pobuđene vrste (normalna emisija). Glavni preduvjet za ESIPT je prisutnost kisele i bazične skupine unutar molekule i prikladna geometrija sustava koja ne sprječava prijenos protona. Najčešće korištene proton donorske skupine su –OH i $–NH_2$, dok su bazični centri najčešće =N– i karbonilni kisik –C=O. Kisela (proton donorska) i bazična (proton akceptorska) skupina prilikom elektronske pobude doživljavaju povećanje kiselosti, odnosno bazičnosti. Proton se prilikom pobude svjetlosnim zračenjem prenosi s donorskog mjesta na akceptorsko, te se u pobuđenom stanju stvara tautomer. Tautomer emitira pri većim valnim duljinama zbog gubitka energije u procesu tautomerizacije, stoga je Stokesov pomak kod ove vrste fluorofora velik [39]. Često se kod ESIPT fluorofora uočavaju dvije emisijske vrpce - emisija enolne forme na nižoj valnoj duljini (normalna emisija) i emisija keto forme na višoj valnoj duljini (ESIPT emisija). Shematski prikaz ESIPT procesa na primjeru 2-(2-hidroksifenil)-benzotiazola je prikazan na Slici 10.

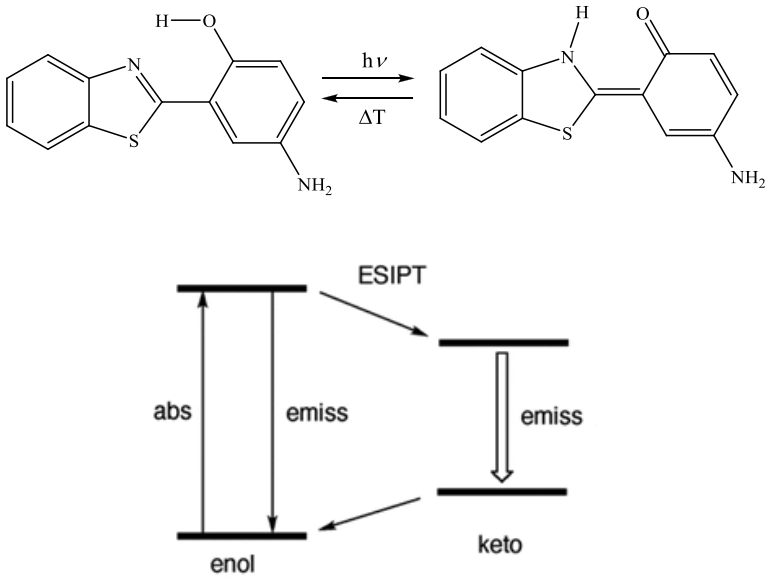

Slika 10. Shematski prikaz ESIPT procesa na primjeru 2-(2-hidroksifenil)-benzotiazola, preuzeto iz [29].

Svojstva ESIPT fluorofora, poput velikih Stokesovih pomaka, dvostruke emisijske vrpce i spektralne osjetljivosti na okolni medij, često se koriste u dizajnu novih senzorskih sustava. Sve se više istražuju ESIPT fluorfori u čvrstom stanju koji mogu emitirati u cijelom vidljivom spektralnom spodručje i proizvesti emisiju bijelog svjetla.
Zanimljivo je spomenuti da su do sada najraširenija skupina ESIPT fluorofora derivati benzazolnih molekula: 2-(2'-hidroksifenil)benzimidazola, 2-(2'-hidroksifenil)benzoksazola i 2-(2'-hidroksifenil)benztiazola.

2.2.1.2. Donorsko – akceptorski π-konjugirani sustavi

Poželjno je da organska fluorescentna bojila, odnosno kemosenzorske molekule, posjeduju svojstva kao što su :

- Visoki molarni apsorpcijski koeficijent, ε. Molarni apsorpcijski koeficijent je parametar koji definira sposobnost molekule da apsorbira svjetlost pri određenoj valnoj duljini.
- Visok kvantni prinos fluorescencije, Φ, tj. visoku vrijednost omjera broja emitiranih i apsorbiranih fotona. Kvantni prinos fluorescencije je važan je parametar pri karakterizaciji fluorescentnih molekula.

- Velik Stokesov pomak. Stokesov pomak je razlika između valnog broja apsorpcije i emisije. Detekcija fluorescentnih vrsta je puno lakša što je Stokesov pomak veći jer ne dolazi do preklapanja signala i neželjenih nuspojava poput samogašenja fluorescencije (engl. *Inner Filter Effect*).
- Optimalna valna duljina apsorpcije i emisije u vidljivom području između 400 i 800 nm.
- Fotostabilnost. Kvalitetni fluorofori mogu proći kroz do 10^5 ciklusa pobude i emisije prije njihovog raspada.
- Optimalna topljivost ili reaktivnost u danim sustavima.

Navedene poželjne karakteristike fluorescentnih kemosenzora posebno dolaze do izražaja kod prethodno spomenutih donorsko-akceptorskih π-konjugiranih sustava zbog mogućnosti prijenosa naboja s donora na akceptor. Organske molekule koje sadrže elektron-donorsku (D) i elektron-akceptorsku (A) grupu na suprotnim krajevima π elektronskog konjugiranog mosta nazivamo *push-pull* strukturama, odnosno strukturama s elektron-donorskom i elektron-akceptorskom jedinicom povezanom π-konjugiranim mostom (D-π-A). U D-π-A sustavima donorske i akceptorske grupe pružaju asimetriju naboja, dok π konjugirani most osigurava put za delokalizaciju elektrona. Optimizacija fotofizičkih svojstava takvih fluorofora je moguća ciljanim uvođenjem supstituenata na osnovni molekulski kostur, zbog čega su široko korišteni za mnoge napredne tehnologije poput nelinearnih optičkih uređaja (NLO), organskih svjetlećih dioda (OLED) i slično [40].

Različiti π-konjugirani mostovi između donora i akceptora u malim kromoforima izravno utječu na optoelektronička svojstva sustava [41]. Imidazol se pokazao pogodnom središnjom π-konjugiranom poveznicom u mnogim donorsko-akceptorskim sustavima [41, 42] (Slika 11.). U svojoj strukturi sadrži dva atoma dušika različite elektronske prirode, kemijski je stabilan te se lako sintetizira i dalje funkcionalizira.

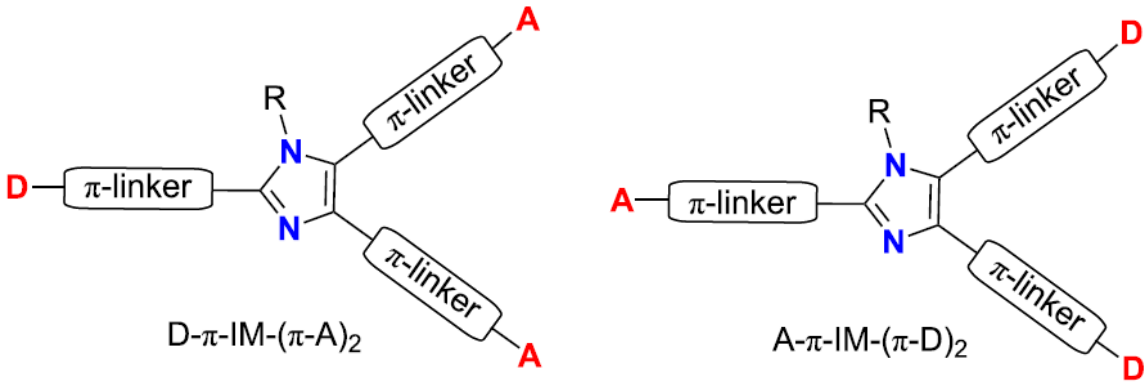

Slika 11. Derivati imidazola u D-*π*-A kromoforima, preuzeto iz [41].

Druga vrlo česta poveznica unutar D-*π*-A kromoforskih i/ili senzorskih sustava su triazoli, čija se uporaba osobito raširila razvojem „*click*“ kemije [43]. "C*lick*-reakcija" je jedna od često korištenih reakcija u suvremenoj sintetskoj kemiji jer je jednostavna, učinkovita i selektivno i lako dovodi do željenog produkta, uz vrlo malo nusprodukata. U „*click*“ reakciji dolazi do bakom katalizirane cikloadicije azida na alkin (CuAAC), uz nastajanje triazolnog prstena (Slika 12.). Triazoli formirani *„click“* reakcijom mogu imati funkciju liganada u optičkim senzorima ili služiti kao mostovi za povezivanje receptorskog i fluorofornog dijela molekule. Osim toga, triazolni prsten može doprinositi konjugaciji i proširivanju *π*-sustava [44-46].

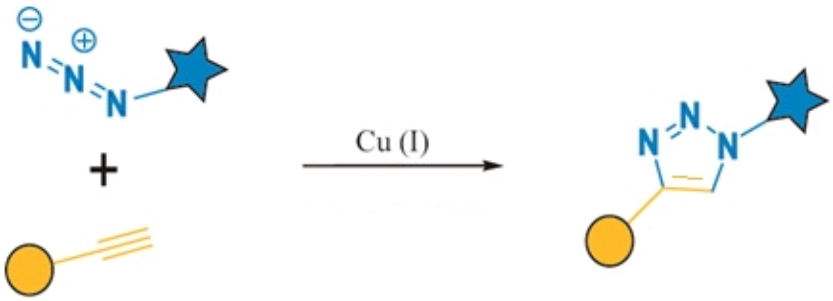

Slika 12. Shematski prikaz primjene „*click*“ kemije u stvaranju 1,2,3-triazola kao poveznice unutar D-*π*-A kromoforskih i/ili senzorskih sustava.

2.3. Karakterizacija optičkih kemijskih senzora

2.3.1. Metode karakterizacije optičkih kemijskih senzora

Za karakterizaciju optičkih kemijskih senzora poželjno je koristiti brze, jednostavne i nedestruktivne metode. Sve metode karakterizacije se baziraju na interakciji svjetlosti i materije, kao što su apsorpcija, difrakcija, raspršenje, interferencija ili refleksije svjetlosti. Najčešći odabir u istraživanju i razvoju optički osjetljivih molekula i materijala su spektroskopske i mikroskopske metode karakterizacije. Apsorpcijska i fluorescencijska spektroskopija predstavljaju ključan alat u karakterizaciji novih optičkih kemosenzorskih molekula, dok je fluorescencijska mikroskopija izraženija u kemosenzorskim primjenama u području biologije i biokemije. U sljedećim poglavljima je predstavljen kratki teorijski pregled odabranih spektroskopskih i mikroskopskih metoda koje su najzastupljenije u karakterizaciji ove vrste senzora.

Spektroskopske metode karakterizacije

Spektralnom karakterizacijom kemosenzorskih molekula ili materijala dobivaju se bitne informacije o kompleksiranju ili interakciji analita i receptora unutar sustava. Iako nije nužno, vrlo je atraktivno i korisno ako se kemijska promjena unutar sustava može uočiti golim okom, odnosno da se promjene događaju u vidljivom dijelu spektra.

UV-vidljiva **apsorpcijska spektroskopija** je najrašijenija spektroskopska metoda u karakterizaciji optički osjetljivih molekula. Organski spojevi, a osobito spojevi s visokim stupnjem konjugacije, apsorbiraju fotone UV i vidljivog dijela elektromagnetskog spektra. UV-vidljiva spektroskopija se koristi u širokom rangu istraživačkih područja za određivanje kvalitativnih i kvantitativnih karakteristika molekula, molekulskih kompleksa ili kemijskih reakcija. Za kvantitativno određivanje koncentracije analita u nekom uzorku se koristi metoda koja slijedi Beer-Lambertov zakon:

$$A = \log (I_0/I) = \varepsilon \times c \times L \qquad (2)$$

gdje je A apsorbancija, I_0 je intenzitet upadnog snopa zraka svjetlosti određene valne duljine, I je intenzitet izlaznog snopa zraka, L je duljina puta kojeg je svjetlost prešla, ε je molarni apsorpcijski koeficijent, a c je koncentracija uzorka.

UV-vidljivi spektrofotometar mjeri intenzitet zrake svjetlosti koja prolazi kroz uzorak i uspoređuje ga s intenzitetom ulazne zrake. Osnovni dijelovi spektrofotometra su izvor svjetla, mjesto za uzorak, monokromator ili prizma koja odvaja zrake svjetlosti određene valne duljine i detektor (Slika 13.).

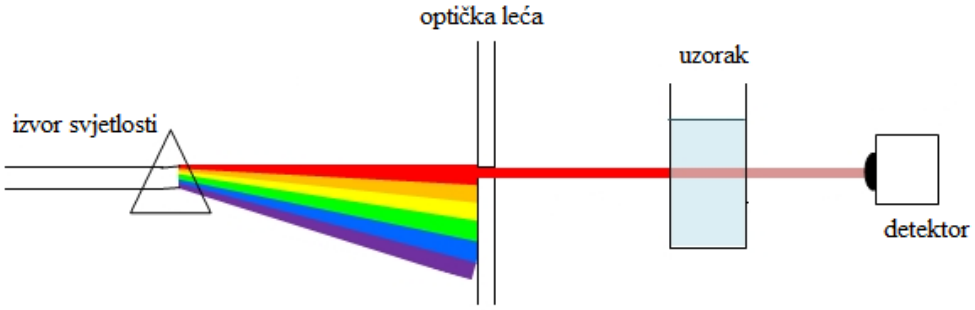

Slika 13. Shema spektrofotometra.

Uzorci za UV-vidljivu spektrometriju su najčešće otopine, iako se u nekim slučajevima može mjeriti i apsorbancija plinova i krutina, pa tako i polimernih filmova nanesenih na prozirnu podlogu (poput ionsko-selektivnih optoda).

Pri analizi tehnikama **fluorescencijske spektroskopije** molekula analita se pobuđuje zračenjem određene valne duljine, pri čemu emitira zračenje druge valne duljine. Dobiveni emisijski spektar nam pruža informacije za kvalitativnu i kvantitativnu analizu uzorka. Fluorescencija odgovara relaksaciji molekule iz pobuđenog singletnog stanja u singletno osnovno stanje uz emisiju svjetlosti, stoga se bilanca energije za fluorescenciju može napisati kao

$$E_{\text{fluor}} = E_{\text{aps}} - E_{\text{vib}} - E_{\text{otap.relax}} \qquad (3)$$

pri čemu je E_{fluor} energija emitiranog svjetla, E_{abs} energija apsorbiranog svjetla prilikom pobude molekule, E_{vib} energija izgubljena prilikom vibracijske relaksacije, a izraz $E_{\text{otap.relax}}$ opisuje reorganizaciju molekula otapala. Učinkovitost fluorescencije se može definirati veličinom koju nazivamo kvantni prinos fluorescencije Φ:

$$\Phi = N_{\text{e}} / N_{\text{a}} \qquad (4)$$

gdje je N_e broj emitiranih fotona, a N_a broj apsorbiranih fotona.

Instrument koji se koristi za analizu fluorescencijskom spektroskopijom se naziva spektrofluorimetar. Tipičan spektrofluorimetar sadrži izvor svjetlosti, mjesto za uzorak i detektor fluorescencije. Molekule u otopini se pobuđuju svjetlom određene valne duljine, a izvor pobude je najčešće deuterijska ili ksenonska lampa. Monokromator propušta samo zrake određene valne duljine, a detektor detektira fluorescenciju.

Fluorimetrijske metode su široko upotrebljavane metode detekcije. Osim mjerenja intenziteta fluorescencije, moguće je karakterizirati fluorescentnu molekulu i mjerenjem života fluorescencije (engl. *fluorescence lifetime*). Vrijeme života fluorescencije (τ) je vrijeme potrebno da se intenzitet fluorescencije nakon pobude snizi na 1/e svoje početne vrijednosti, a kreće se od nekoliko pikosekundi do mikrosekunda, najčešće 2 do 20 ns. Vrijeme života je recipročna vrijednost zbroja konstanti brzina reakcija prvog reda svih procesa koji uzrokuju nestajanje pobuđenog stanja molekule:

$$\tau = 1/k = 1/\Sigma_i k_i \qquad (5)$$

Postoji nekoliko metoda za mjerenje vremena života fluorescencije, poput pulsne metode gdje se uzorak pobuđuje kratkim pulsom svjetlosti, ili metoda fazne modulacije gdje se uzorak pobuđuje sinusoidalno moduliranim zračenjem. Senzori temeljeni na mjerenju vremena života fluorescencije su uglavnom indikatorske molekule kod kojih brzina povratka iz pobuđenog stanja izravno ovisi o koncentraciji druge kemijske vrste, odnosno gasitelja (engl. *quenchers*). Odnos vremena života u prisutnosti (τ) i odsutnosti gasitelja (τ_0) je prikazana Stern-Volmerovom jednadžbom:

$$\frac{\tau_0}{\tau} = 1 + k_0 \times \tau_0[Q] \qquad (6)$$

gdje je k_0 konstanta gašenja, a [Q] množinska koncentracija gasitelja.

Osim UV-vidljivih spektroskopskih metoda, karakterizacija kemosenzorskih molekula i senzorskih materijala se može odvijati i u drugim područjima valnih duljina koristeći metode poput infracrvene spektroskopije, Ramanove spektroskopije ili Rendgenske spektroskopije. **Infracrvena spektroskopija** (IR) je jedna od važnijih spektroskopskih tehnika u istraživačkoj kemiji, a temelji se na uspoređivanju spektara nepoznatog uzorka sa spektrom poznate molekule, to jest usporedbom dijela spektra koji se naziva "otisak prsta" (engl. *finger print region*). IR područje se dalje dijeli na blisko (*near* IR, NIR), srednje (*mid* IR, MIR) i daleko

(*far* IR, FIR) infracrveno područje. Mnogi se senzori u zadnjih nekoliko godina baziraju na radu u blizu – infracrvenom (NIR) području, zbog prikladnosti takvih senzora za biološke analize. Stoga je vrlo poželjno dizajnirati nove molekulske probe i senzore čija se apsorpcija ili fotoluminiscencija nalazi u spektralnom području iznad 700 nm.

Spektroskopske metode koje ne uključuju apsorpciju energije, odnosno pobuđivanje, temelje se na interakcijama poput difrakcije, raspršenja ili disperzije, mogu pružiti velik broj korisnih informacija o istraživanom mediju (otopini ili polimernoj membrani) ili molekuli od interesa (agregacija, raspodjela veličina čestica i slično). Metode mjerenja **raspršenja svjetlosti** temelje se na pojavi raspršenja fotona u koliziji s pokretnim česticama, na primjer česticama koje se nalaze u uzorku. Metode se široko primjenjuju u biologiji, biokemiji i znanosti o materijalima (engl. *Light-Scattering Methods, Photon Correlation Spectroscopy*) [47]. Ovisno o mehanizmu nastanka, postoji više vrsta raspršenja svjetlosti poput Rayleighovog, Mie, Tyndallovog, Brillouinovog ili Ramanovog raspršenja. Razlikujemo statičko i dinamičko raspršenje svjetlosti (SLS i DLS), ovisno o eksperimentalnom parametru koji se mijenja. U prvoj mjernoj tehnici određuje se intenzitet raspršene svjetlosti u vremenskom prosjeku, dok druga mjerna tehnika proučava promjene intenziteta ovisno o vremenu. Princip mjerenja prosječnog intenziteta raspršene svjetlosti metodom dinamičkog raspršenja (DLS) je prikazan na Slici 14.

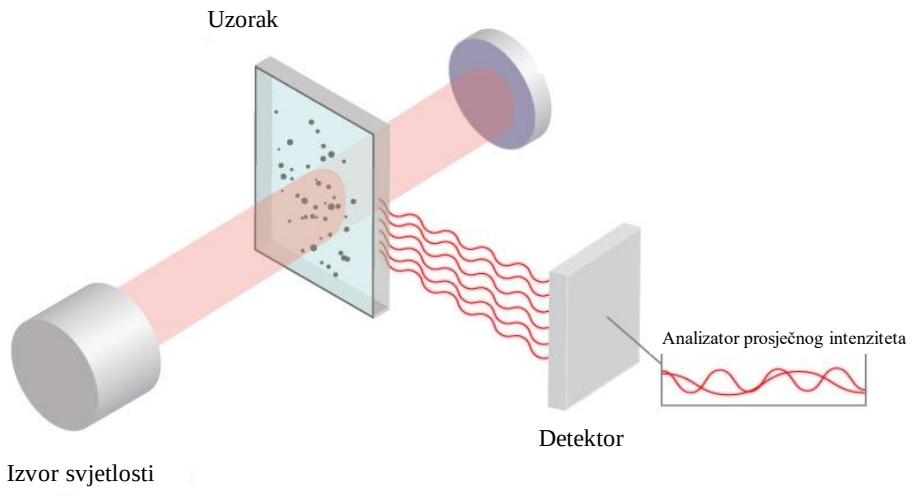

Slika 14. Princip mjerenja prosječnog intenziteta raspršene svjetlosti metodom dinamičkog raspršenja (DLS).

Uz fluorescencijsku spektroskopiju, DLS metoda predstavlja najvažniju metodu karakterizacije fluorescentnih nanočestica. Metoda omogućava dokazivanje nastanka fluorescentnih molekulskih nanoagregata u otopinama, definiranje njihove veličine i praćenje utjecaja interakcija s potencijalnim analitom u prilikom razvoja novih kemosenzorskih sustava [48, 49].

Fluorescencijske mikroskopske metode karakterizacije

Tanki polimerni filmovi s potencijalnom uporabom u kemijskim senzorima se često karakteriziraju različitim mikroskopskim tehnikama, čime se dobivaju vrlo korisni podaci o morfološkoj strukturi, homogenosti, debljini filma te se omogućava dinamička analiza funkcije senzorskog odziva na mikroskopskoj razini.

Posebno važanu metodu u senzorskim primjenama predstavlja **fluorescencijska mikroskopija** koja koristi pojavu fluorescencije ili fosforescencije za proučavanje svojstava uzorka. Ako uzorak ne posjeduje autofluorescenciju, postoji nekoliko metoda za stvaranje fluorescentnih uzoraka: označavanje s fluorescentnim bojilima ili fluorescentnim proteinima. Fluorescencijski mikroskop je moćan alat u biologiji jer omogućuje specifična i osjetljiva bojenja uzoraka te *fluorescencijsko oslikavanje* (engl. *fluorescent imaging*). Pri tome se primjenjuju različite vrste uređaja, od jednostavnog epifluorescencijskog mikroskopa do složenog konfokalnog fluorescencijskog mikroskopa koji koristi optičko seciranje za postizanje bolje rezolucije. Današnje metode fluorescencijske analize omogućuju ne samo kvalitativni prikaz obojenih stanica i tkiva, već kvantitavnu analizu funkcije promatranog biološkog sustava uz pomoć prikladnih fluorescentnih molekulskih proba i kemosenzora. Stoga je razvoj novih fluorofora za potrebe fluorescentnog obilježavanja stanica u usponu, a sve je više naglašen i razvoj „pametnih“ molekula i nanostruktura čija se funkcija u organizmu također može pratiti fluorescencijom [32, 50].

2.3.2. Analitički parametri optičkih kemijskih senzora

Spektroskopska karakterizacija kemosenzorskih molekula je neophodna za procjenu njihove potencijalne primjenjivosti. Zbog izrazitog utjecaja mikrookoline na senzorska svojstva molekule, kemosenzorska molekula u otopini i kemosenzorska molekula imobilizirana na određeni substrat mogu posjedovati sasvim različita svojstva. Stoga, razvoj optičkog senzorskog sustava uključuje optimiranje najbitnijh značajki senzora čije vrijednosti određuju zahtjevi specifične namjene. Analitičke značajke senzorskog sustava o kojima treba voditi brigu u postupku dizajna specifičnih senzora su:

- osjetljivost
- selektivnost
- stabilnost senzora
- mjerno područje
- vrijeme odziva
- granica detekcije.

Osjetljivost i selektivnost su najvažnije značajke senzorskog sustava. Osjetljivost se definira kao mjera promjene vrijednosti izmjerenog signala senzora po jedinici koncentracije analita. Za selektivno i reverzibilno vezivanje analita u senzorskim sustavima je odgovoran ionofor (receptor). Selektivnost se definira kao mogućnost dobivanja signala koji potječu isključivo od određivanog analita. Na stabilnost odziva senzora kod optičkih sustava najviše utječe fotokemijska razgradnja komponenata u membrani i njihovo ispiranje. Mjerno područje senzora je područje u kojem promjena signala linearno ovisi o promatranom svojstvu analita, a određeno je najmanjom i najvećom vrijednošću aktiviteta (koncentracija) analita u području linearnosti. Vrijeme odziva senzora je vrijeme koje je potrebno da se postigne 95 % stabilnog mjernog signala, dok se granica detekcije definira kao najmanja količina analita koja se može pouzdano mjeriti [22].

2.4. Benzimidazoli i njegovi derivati

Benzimidazolna jezgra je jedna od važnih heterocikličkih gradivnih jedinica, a sastoji se od imidazolnog prstena vezanog na benzensku jezgru (Slika 15.). Potvrdom da je benzimidazolna jezgra sadržana u strukturi vitamina B_{12}, započet je trend istraživanja derivata benzimidazola za biološke i farmaceutske primjene, koji od 1950. godine do danas ne prestaje.

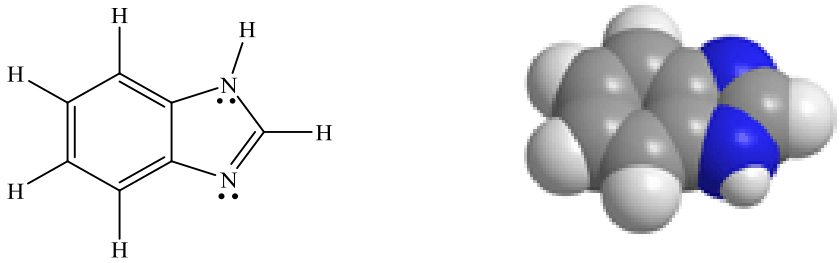

Slika 15. Struktura benzimidazola

Benzimidazol je strukturni izomer purina koji ima ključnu ulogu u strukturi mnogih biološki važnih spojeva te njegovi derivati lako stupaju u interakciju s biomolekulama poput DNA, RNA ili različitih proteina [51]. Mnogi derivati benzimidazola pokazuju širok i raznolik spektar bioloških aktivnosti, kao što su antitumorska, antivirusna, antibakterijska, antifungalna, antihipertenzivna i antihistaminska aktivnost (Slika 16.) [17, 52]. Međutim, derivati benzimidazola imaju potencijal za puno širi spektar primjene, primjerice u optičkoj senzorskoj tehnologiji zahvaljujući velikom broju konjugiranih veza i protonabilnih dušikovih atoma u benzimidazolnoj jezgri. Većina derivata ove klase spojeva posjeduje dobra kromoforska i ionoforska svojstva [53]. Različiti supstituenti na osnovnom molekulskom kosturu mogu bitno utjecati na fotofizička i kiselo-bazna svojstva. Ciljanim uvođenjem supstituenta na benzimidazolnu jezgru moguće je optimirati spektralna i senzorska svojstva novih kromofora. Stoga, uz izraženu biološku aktivnost, derivati benzimidazola sve češće pronalaze primjenu u optoelektronici [54], tehnologiji lasera [55], kao fluorescentne probe ili kemosenzori [56].

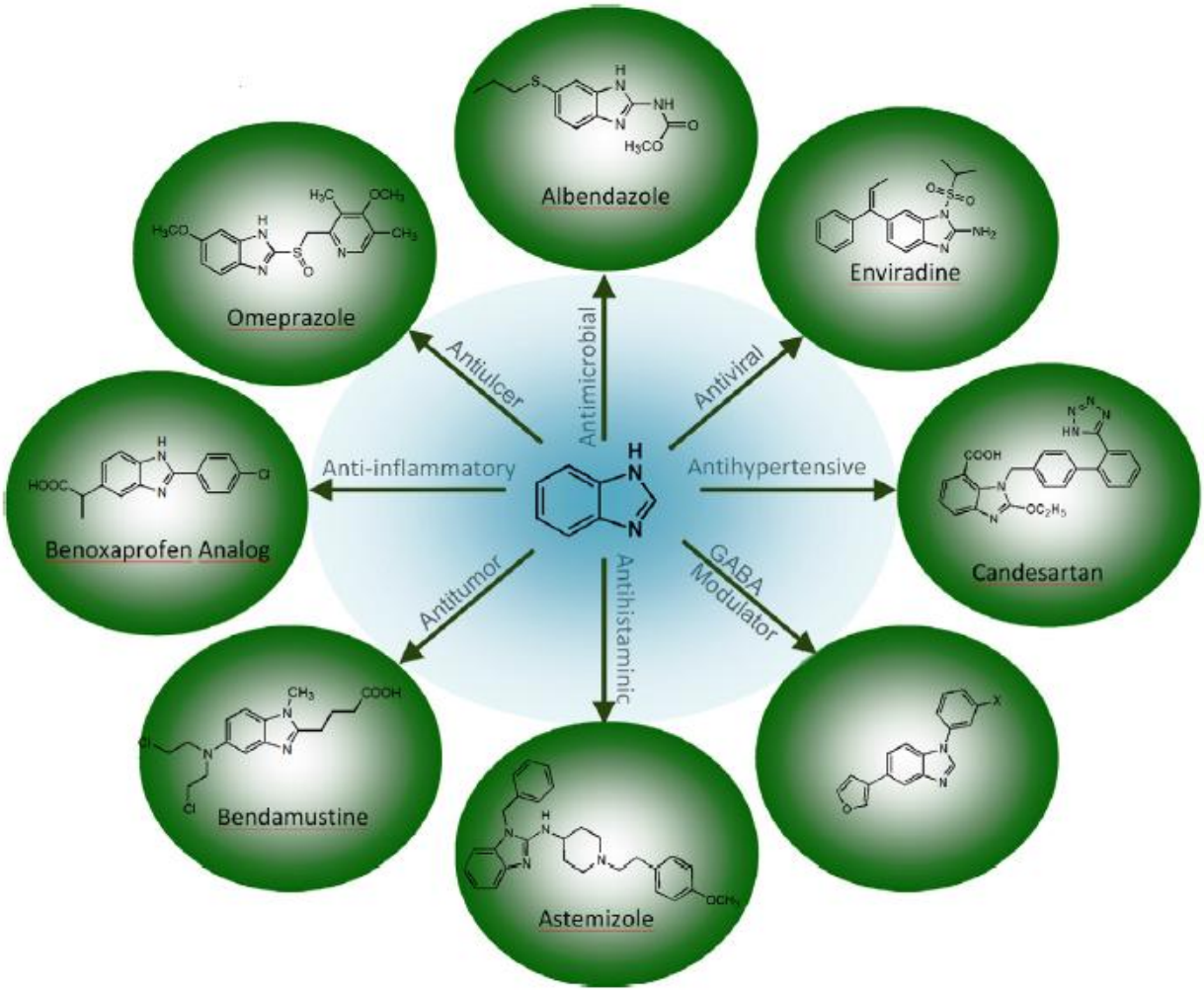

Slika 16. Derivati benzimidazola korišteni u farmaceutskoj industriji, slika preuzeta iz [17].

Istraživanje spektralnih svojstava derivata benzimidazola u otopinama je važan prvi korak u razvoju i primjeni novih senzorskih molekula. Objavljen je velik broj eksperimentalnih i teorijskih istraživanja sličnih klasa spojeva s fokusom u različitim aspektima fotofizičkih i fotokemijskih svojstva kao što su kiselo-bazna ravnoteža [57], intermolekularni prijenos naboja (engl. *Intermolucular charge transfer*, ICT) [58] i prijenos protona u pobuđenom stanju (engl. *Excited state intermolecular proton transfer*, ESIPT) [59]. Jedno od najznačajnijih otkrića u sintezi novih π-konjugiranih heterocikličkih sustava je upotreba struktura s elektron-donorskom i elektron-akceptorskom jedinicom na suprotnim krajevima konjugirane molekule (D-π-A sustava), u kojima benzimidazol može biti dio konjugiranog mosta ili receptorska jedinica [41].

Pregled kemosenzorskih molekula i senzorskih materijala za primjenu u optičkim kemijskim senzorima temeljenih na derivatima benzimidazola predstavljen je kroz sljedećih nekoliko poglavlja.

3. LITERATURNI PREGLED

Heterociklički kromofori su jedna od najistraživanijih skupina optičkih senzorskih molekula zahvaljujući odličnim spektralnim svojstvima i mogućnosti detekcije različitih iona. Benzimidazol sve više zaokuplja pažnju znanstvenika kao jedna od gradivnih jedinica kemosenzorskog heterocikličkog sustava. Pregledom najnovijih znanstvenih istraživanja omogućen je uvid u područje razvoja i primjene optičkih kemosenzora temeljenih na benzimidazolu. Kritičkim pregledom literature utvrđene su prednosti i nedostaci postojećih kromofora (fluorofora) temeljenih na benzimidazolu te su određeni ključni izazovi u dizajniranju, pripravi, karakterizaciji i primjeni navedene klase organskih spojeva u optičkim kemijskim senzorima.

Pretragom literature s ključnim riječima '*benzimidazo**' i '*sensor*' u sustavu WoS, dobiva se uvid u 308 znanstvenih publikacija u posljednjem desetljeću. Sužavanjem pretrage na isključivo optičke sustave od interesa, te proširivanjem pretrage uvrštavanjem ključne riječi '*probe*' dobiven je rezultat od **96 znanstvena rada**. Interes u ovom znanstvenom području iz godine u godinu raste, što možemo zaključiti i po raspodjeli broja publikacija po godinama, gdje se vidi konstantan rast uz najveći broj publiciranih radova u 2015. godini. U sljedećih nekoliko poglavlja prikazan je pregled znanstvenih publikacija objavljenih u prošlom desetljeću vezanih uz benzimidazolne derivate kao optičke senzorske sustave. U poglavlju 3.1. prikazani su uglavnom radovi čiji rezultati daju uvid u važne spoznaje o povezanosti strukture derivata benzimidazola s fotofizičkim i fotokemijskim svojstvima koja čine temelj njihove potencijalne kemosenzorske aktivnosti. U poglavljima od 3.2. do 3.5. su predstavljeni radovi fokusirani na kemosenzorski aspekt derivata benzimidazola i klasificirani su prema analitima koje detektiraju (pH, kationi, anioni i neutralne molekule). U poglavlju 3.6. prikazan je kritički osvrt na kemosenzorske (nano)materijale s benzimidazolnom jezgrom, a u poglavlju 3.7. sumarno su navedeni zaključci literaturnog pregleda i definirani pravci razvoja ove skupine kemosenzora.

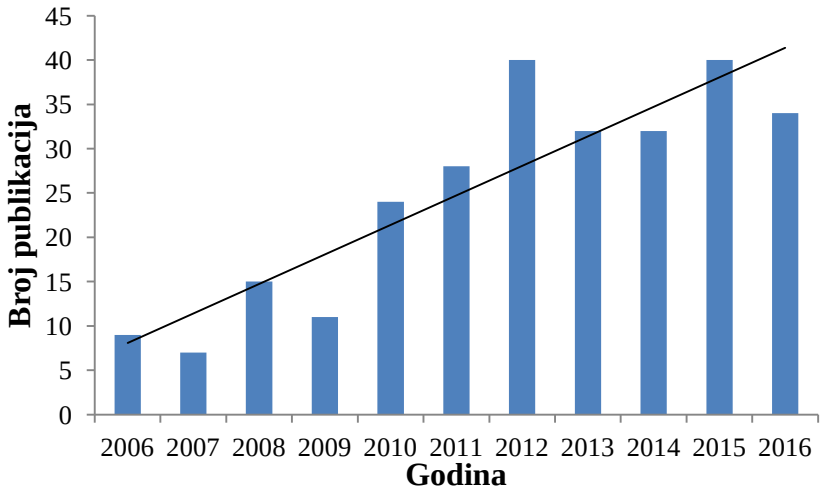

Slika 17. Rezultati pretrage literature s ključnim riječima '*benzimidazo**' i '*sensor*' u sustavu Scopus.

3.1. Razvoj benzimidazolnih fluoro(iono)fora

3.1.1. Istraživanje odnosa strukture i svojstva derivata benzimidazola

Dizajn novih fluorescencijskih kemosenzorskih sustava te optimiranje i fino podešavanje njihovih svojstava temelji se na poznavanju i tumačenju mehanizama prijenosa signala pod utjecajem vezanja analita. Najvažniji mehanizmi su fotoinducirani prijenos elektrona (engl. *Photo induced electron transfer* – PET) [34], intramolekulski prijenos protona u pobuđenom stanju (engl. *Excited state intermolecular proton transfer* – ESIPT) [39] ili intramolekulski prijenos naboja (engl. *Internal charge transfer mechanism* – ICT, *Metal induced charge transfer*- MICT) [29]. Upravo kontrola nad raznovrsnim fluorescentnim odgovorima molekule otvara nove funkcionalne mogućnosti. Optimiranje svojstava fluorofora se najčešće istražuje kod donorsko-akceptorskih struktura (D-π-A sustava) gdje su fotofizička svojstva molekule određena procesima unutarmolekulskog prijenosa naboja [41, 42, 60]. Umetanjem različitih premosnica između donora i akceptora u malim donorsko-akceptorskim kromoforima moguće je podesiti međusobna sprezanja, odnosno optoelektronička svojstva kromofora. Znanstvenici su prepoznali navedeno svojstvo D-π-A sustava kao izrazitu prednost u stvaranju i prijenosu signala unutar novih senzorskih sustava [61]. Benzimidazol sve više pronalazi primjenu kao dio D-π-A molekulskih sustava. Objavljen je velik broj eksperimentalnih i teorijskih istraživanja spektralnih svojstava derivata benzimidazola, s

naglaskom na različita fotofizička i fotokemijska svojstva vezana uz kiselo-bazne ravnoteže [57, 62, 63], intermolekulski prijenos naboja [58] i prijenos protona u pobuđenom stanju [59, 64].

Pioniri u istraživanju fotofizičkih svojstava derivata benzimidazola su indijski znanstvenici S. K. Dogra i suradnici. Mehanizmi stvaranja i prijenosa signala, kiselo-bazna ravnoteža i utjecaj otapala su sustavno tumačeni kroz niz derivata benzimidazola, ciljano uvodeći nove supstituente i mijenjajući eksperimentalne parametre. Po prvi puta se detaljno tumačila veza strukture i kiselo-baznih svojstava ove klase spojeva te je vrlo jasno predstavljena kroz niz radova navedenih autora prikazanih u Tablici 1.

Tablica 1. Sustavna karakterizacija fotofizičkih i kiselo-baznih svojstava derivata benzimidazola koje je objavila više grupa znanstvenika (N-neutralni, MC-monokationski, DC-dikationski, MA-monoanionski oblik molekule).

Spoj	**pK_a**	**λ_{abs} / nm**	**Referenca**
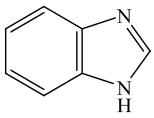 **1**	pK_{a1} =5,6 pK_{a2} =12,8	**N**: 270 **MC**: 244	Donkor i sur. (1993.) [65]
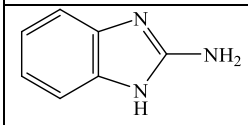 **2**	pK_{a1} =7,18	-	Schenkeveld i sur. (2002.)
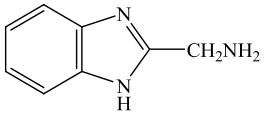 **3**	pK_{a3} =3,1 pK_{a1} =8,1 pK_{a2} =12,8	**N**: 243, 271, 277 **MC**: 244, 272, 278 **DC**: 269, 277 **MA**: 280, 286	Sinha i sur. (1985.) Mishra i sur. (1985.) [66-68]
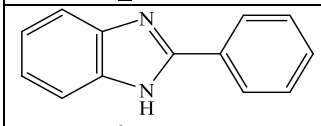 **4**	pK_{a1} =5,23 pK_{a2} =11,91	**N**: 302 **MC**: 290, 240 **DC**: / **MA**: 308	Walba i sur. (1961.) Mishra i sur. (1983.) [69, 70]
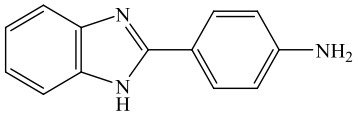 **5**	pK_{a1} =1,40 pK_{a2} =5,05 pK_{a3} =13,0	**N**: 313 **MC**: 330 **DC**: 295, 230 **MA**: 320, 260	Mishra i sur. (1985.) [63, 68]
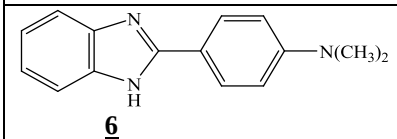 **6**	pK_{a3} =1,4 pK_{a1} =5,6 pK_{a3} =12,1	**N**: 329 **MC**: 360 **DC**: 298,241 **MA**: 322,263	Dey i sur. (1994.) Krishnamoorthy i sur. (1999.) [71, 72]
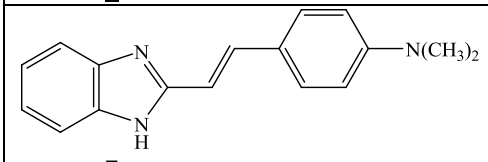 **7**	pK_{a1} =3,41 pK_{a3} =6,04	**N**: 360 **MC**: 420 **DC**: 320 **MA**: /	Mishra i sur. (2013.) [58]

Utjecaj strukture na reaktivnost i ostala molekulska svojstva može se podijeliti u tri kategorije: induktivni (ili elektrostatski) efekti, sterički efekti i rezonancijski (konjugacijski) efekti. Induktivni utjecaj podrazumijeva polarizaciju jedne veze djelovanjem susjedne polarne veze ili skupine. Induktivni efekti su najjače izraženi na susjednim vezama i naglo slabe s povećavanjem udaljenosti između međudjelujućih skupina. Sterički efekti su strukturni utjecaji do kojih dolazi zbog prostornog međudjelovanja između kemijskih skupina. Uzrok rezonancijskog efekta su delokalizirani elekroni, odnosno činjenica da je rezonancijski hibrid energetski povoljniji od bilo koje doprinoseće rezonancijske strukture. U π-konjugiranim sustavima, kao što su derivati benzimidazola, rezonancijski efekt je najizraženiji. Stoga, utjecaj strukture na spektralna i kiselo-bazna svojstva spojeva najčešće se tumači upravo delokalizacijom elektrona.

Uočeni trend u spektralnim karakteristikama i kiselo-baznim svojstvima derivata benzimidazola, opisan u radovima navedene skupine autora, i danas je temelj za dizajn novih kromofora i fluorofora baziranih na benzimidazolu. Tako je primjerice, pomak apsorpcijske vrpce prema višim valnim duljinama (crveni pomak) uočen pri protonaciji imino dušika na benzimidazolnoj jezgri ili deprotonaciji amino dušika zbog bolje delokalizacije elektrona. Ukoliko postoji dodatni amino supstituent čija deprotonacija destabilizira molekulu, uočava se apsorpcijski pomak prema nižim valnim duljinama (plavi pomak u odnosu na neutralnu molekulu) (Slika 18., Tablica 1, spoj **7**).

Također, autori su prvi odredili trendove u ovisnosti strukture i kiselo-baznih svojstava derivata benzimidazola. Zanimljiva je činjenica da se u gotovo svim ispitivanim derivatima prikazanim u Tablici 1. prvo protonira dušik na benzimidazolu, unatoč mogućnosti protonacije drugih amino supstituenata, bliskih po vrijednosti pK_a. Supstituenti na osnovnom molekulskom kosturu utječu na prijenos naboja i raspodjelu elektronske gustoće unutar sustava, što posredno određuje mogućnost protoniranja određenih atoma u molekuli, odnosno bazičnost protonabilnih dušika u molekuli. Sustavna karakterizacija spektralnih i kiselo-baznih svojstava neutralnih (N) i monokationskih (MC) oblika derivata benzimidazola ispitanih u navedenoj grupi autora prikazana je u Tablici 1. Osim navedenih svojstava, u istoj grupi autora detaljno su ispitane i reakcije prijenosa protona u osnovnom i pobuđenom stanju [57] i mehanizmi intramolekulnog prijenosa naboja prilikom protoniranja [73], o čemu će biti riječ kasnije u tekstu.

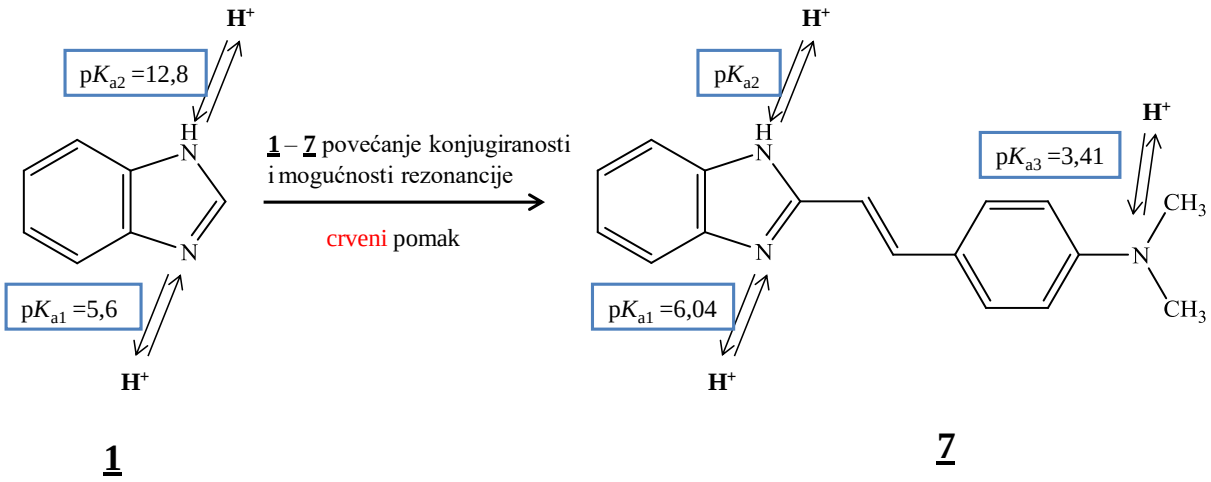

Slika 18. Sustavna karakterizacija spektralnih i kiselo-baznih derivata benzimidazola **1** – **7** (prikazani u Tablici 1.) prikazana kroz publikacije Dogre i suradnika.

Uslijedila je karakterizacija složenijih benzimidazolnih struktura, kao što je molekula *Hoechst*. *Hoechst 33258* je bis-benzimidazolni derivat često korišten kao fluorescentna proba u živim organizmima [74]. Njegovo protuparazitsko djelovanje i svojstvo vezivanja u mali utor DNA su detaljno ispitani prethodnim istraživanjima, no nije bio poznat podatak kako kiselo-bazna svojstva navedene molekule utječu na vezivanje DNA. Određivanje konstanti disocijacije i protonacijskih mjesta molekule *Hoechst*-a je vrlo izazovno, jer molekula sadrži 7 ionizibilnih mjesta (4 bazična i 3 kisela), odnosno 2^7 = 128 protonacijskih stanja.

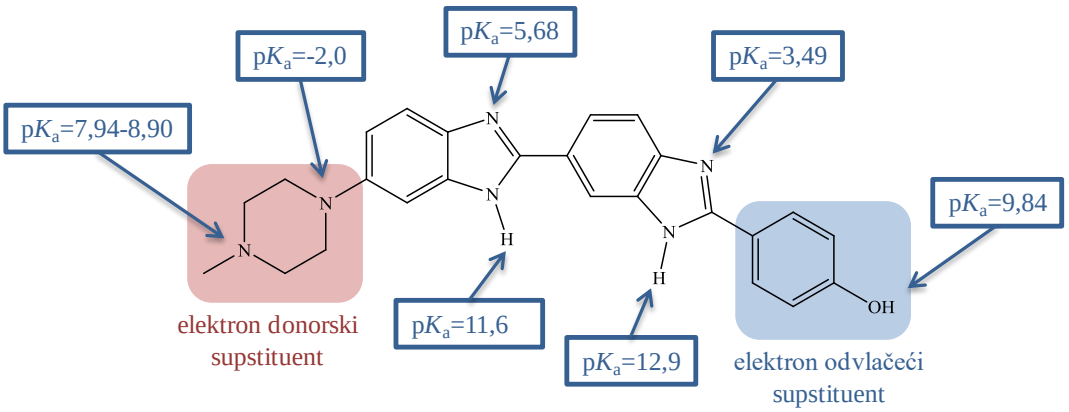

Slika 19. Ionazibilna mjesta molekule **8** (*Hoechst 33258*) [74].

Kombiniranim teorijskim i eksperimentalnim pristupom, spektralno su određene konstante disocijacije i odgovarajuća protonacijska mjesta te raspodjela vrsta pri određenim vrijednostima pH. Pažljivim spektrofotometrijskim titracijama molekule *Hoeschst*, kao i njezinih zasebnih podjedinica, utvrđene su vrijednosti pK_a prikazane na Slici 19. [74]

Ponovno možemo utvrditi da utjecaj strukture molekule izrazito utječe na njena spektralna i kiselo bazna svojstva. Piperazinski prsten i fenolni prsten svojim elektron-donorskim svojstvima znatno utječu na konstantu disocijacije benzimidazolnog dušika povećavajući gustoću naboja na susjednim atomima. Molekula *Hoechst* je većinom u monokationskom obliku pri vrijednosti pH ≈ 7 pri čemu je protoniran vanjski sp^3 hibridiziran dušik na piperazinskom supstituentu, što su autori potvrdili računanjem raspodjele ionskih vrsta u otopini [74]. Protoniranje benzimidazolnog dušika i ostalih ionazibilnih mjesta slijedi prema vrijednostima pK_a na Slici 19.

ESIPT benzimidazolni fluorofori

Veliku skupinu istraživanih benzimidazolnih derivata čine fluorofori temeljeni na prijenosu protona u pobuđenom stanju (engl. *Excited-state intramolecular proton transfer*, ESIPT). Dobra svojstva ESIPT fluorofora, kao što je veliki Stokesov pomak, omogućila su njihovu primjenu u laserima, fotostabilizatorima, solvatokromnim probama i slično. Stoga je istraživanje utjecaja elektron-donorskih i elektron-odvlačećih skupina na takvu vrstu benzimidazolnih spojeva vrlo bitno područje za napredak i razvoj navedene klase fluorofora.

Utjecaj cijano, metoksi, dimetilamino ili tiazolilnih supstituenata na različitim položajima π-konjugiranog sustava na fotofizička svojstva fluorofora ispitivan je na primjeru benzimidazolnih derivata **9a-k** (Slika 20.). Henary i suradnici su pokazali koliko je izazovno predviđanje fotofizičkih procesa, jer jednostavne strukturne pretpostavke ovise o velikom broju faktora. Male promjene koje se dovode u sustav mogu znatno utjecati na fotofizička svojstva molekula [64]. Prijenos protona u pobuđenom stanju je uočen kod svih ispitivanih derivata prikazanih na Slici 20, što se manifestira jednom emisijskom vrpcom ESIPT tautomera (T*). Derivati **9b** i **9d** posjeduju dodatnu drugu emisijsku vrpcu više energije, koja se pripisuje emisiji normalnog tautomera (Nc*).

U smislu razvoja novih ESIPT fluorofora za biološke primjene, derivati **9c** i **9d** posjeduju najmanju energiju i ujedno najveći potencijal za primjenu (emisija na visokim valnim duljinama). Izraženi kvantni prinos fluorescencije se uočava kod spoja **9c**. Senzorska primjena promatrane skupine fluorofora se za većinu derivata zasniva na stvaranju monoprotonirane vrste (pK_a = 4,43 – 8,02) ili deprotonaciji sulfonamidne grupe (pK_a = 6,75 – 9,33). Pri protonaciji, odnosno deprotonaciji spojeva, ometa se prijenos protona što uzrokuje izražene spektralne pomake zbog nestanka ESIPT vrpce.

Mjerene vrijednosti pK_a za deprotonaciju sulfonamidne grupe monosupstituiranih derivata su izrazito ovisne u supstituentu, odnosno rezonancijskom ili induktivnom efektu koji supstituent dovodi u sustav. Primjerice, metoksi grupa u para položaju naspram sulfonamidne grupe povisuje vrijednost pK_a za 0,3 (**9f**) zbog toga što rezonancijski efekt prevladava naspram induktivnog efekta uzrokovanog elektronegativnim kisikom. U meta položaju se uočava pad 0,4 pK_a (**9e**) zbog toga što prevladava induktivni efekt. Autori su također utvrdili da položaj i vrsta supstituenta na π konjugiranoj molekuli te njegova donorska ili akceptorska snaga izravno utječu na Stokesove pomake. Veći Stokesov pomak se uočava kod derivata s najjačim elektron-donorskim supstituentima. Dobivene spoznaje o odnosu strukture i fotofizičkih svojstava pružaju smjernice za daljnji dizajn raciometrijskih senzora optimiranih svojstava ili metalnih senzora za biološku primjenu.

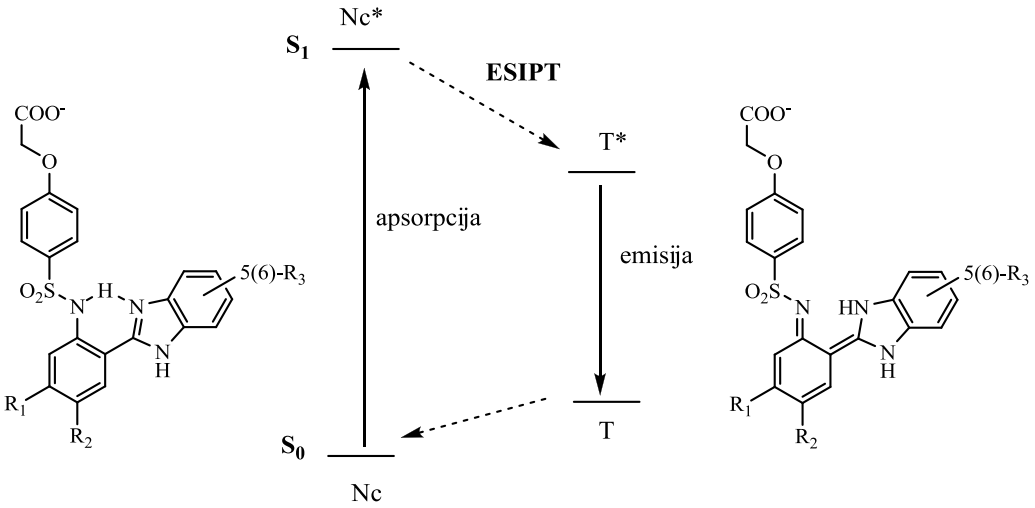

	R_1	R_2	R_3
9a	H	H	H
9b	CN	H	H
9c	CN	H	OCH_3
9d	2-tiazolil	H	H
9e	OCH_3	H	H
9f	H	OCH_3	H
9g	H	$N(CH_3)_2$	H
9h	H	OCH_3	CN
9i	H	H	CN
9j	H	H	OCH_3
9k	$-OCH_2O-$	$-OCH_2O-$	H

Slika 20. Primjer derivata benzimidazola s ESIPT mehanizmom stvaranja fluorescentnog odgovora [64].

Potreba za novim fluoroforima s većim Stokesovim pomacima i činjenica da ESIPT kod benzazolnih derivata omogućuje veću razliku u energiji apsorpcije i emisije (veći Stokesov pomak), potaknula je mnoge istraživačke grupe na sintezu i karakterizaciju novih ESIPT benzimidazolnih derivata. ESIPT je istraživan u strukturama poput 2-supstituiranih benzazolnih derivata [59, 75] ili naftalenskih derivata [76].

ICT benzimidazolni fluorofori

Intramolekulski prijenos naboja (engl. *Intramolecular charge transfer*, ICT) je jedan od fenomena na kojem se temelji rad fluorescentnih senzorskih sustava. Imidazolna jedinica poprima sve veći značaj u dizajnu ICT flurofora zbog jednostavnog i efikasnog uklapanja u D-π-A strukture [41]. Benzimidazolna jezgra je najčešće elektron-odvlačeća jedinica te se svojom planarnom i konjugiranom strukturom idealno uklapa u D-π-A sustave. Eelektron-akceptorski afinitet također svrstava benzimidazolnu jezgru u privlačnu gradivnu jedinicu novih optoelektroničkih materijala i uređaja. I kod ove vrste fluorofora ciljevi su povećati Stokesov pomak i omogućiti optički signal fluorofora u području viših valnih duljina kako bi se olakšala primjena u biološkim sustavima.

Intramolekulski prijenos naboja kod benzimidazolnih derivata je olakšan ukoliko je benzimidazol vezan na drugu konjugiranu jedinicu. Stvaranje takvih benzimidazolnih derivata rezultira povećanjem stupnja konjugacije i većim Stokesovim pomacina. Primjer konjugata benzimidazola i druge heterocikličke jedinice su fenotiazinski derivati prikazani na Slici 21. Fenotiazini su važna klasa spojeva u farmaceutskoj znanosti, no ujedno i potencijalno primjenjive molekule u optoelektroničkim sustavima. Utjecaj supstituenata na spektralna svojstva prikazanih spojeva, odnosno mogućnost optimiranja HOMO i LUMO energetskih nivoa kod asimetričnih 3-(benzimidazol-2-il)-10-heksilfenotiazinskih i simetričnih 3,7-bis(benzimidazol-2-il)-10-heksilfenotiazinskih derivata **10** – **15** su istraživali Zhang i suradnici [77].

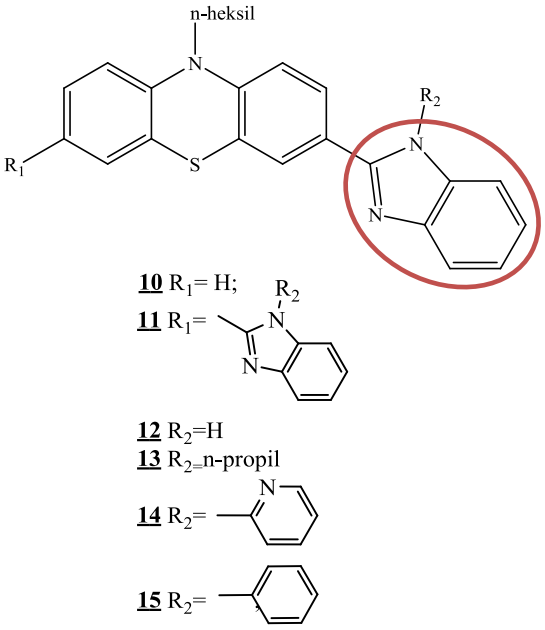

Slika 21. Primjer benzimidazolnih derivata s ICT karakteristikama – konjugat benzimidazola i fenotiazinske jezgre [77].

Najbolji primjer ovisnosti spektralnih svojstava o supstituentima na π-konjugiranom kosturu je predstavljen za stiril-benzimidazolna bojila, zbog tipične D-π-A strukture čija je glavna karakteritstika izražen intramolekulski prijenos naboja. Osim pomaka apsorpcijskih vrpci prema području viših valnih duljina povećanjem konjugiranosti molekule (Slika 22), supstituenti izravno utječu i na sam ICT proces. Porast dipolnog momenta u pobuđenom stanju neposredno je povezan s porastom Stokesovog pomaka u polarnim otapalima, odnosno prijenos naboja unutar molekulskog sustava i polarizacija molekule izravno utječu na spektralna svojstva. Osnovne fotofizičke karakteristike te utjecaj različitih supstituenata na stirilnim benzimidazolnim fluoroforima istraživan je kroz nekoliko znanstvenih publikacija [61, 78].

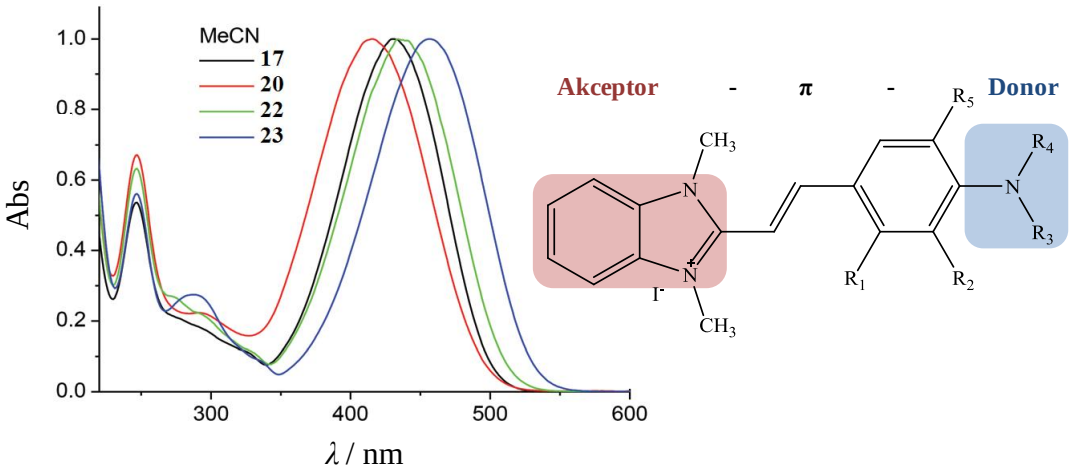

	R_1	R_2	R_3	R_4	R_5
16	-	-	Me	Me	-
17	-	-	Et	Et	-
18	Me	-	Me	Me	-
19	-	-	$-CH_2-CH_2-CH_2-CH_2-$		-
20	-	-	$-CH_2-CH_2-CH_2-CH_2-CH_2-$		-
21	-	$\_-CH_2-CH_2-$	$-CH_2-CH_2-$		-
22	-	$-CH_2-CH_2-CH_2-$		Me	-
23	-	$-CH_2-CH_2-CH_2-$		$-CH_2-CH_2-CH_2-$	
24	-	-	Ph	Ph	-

Slika 22. Pomak apsorpcijskih vrpci prema području viših valnih duljina promjenom supstituenata na molekulskom kosturu, primjer stiril-benzimidazolnih bojila temeljenih na ICT [78].

Fotofizička svojstva i intramolekulski prijenos naboja pri protoniranju *trans*-2-[4-(dimetilamino)stiril]benzimidazola **25** eksperimentalno i teorijski su opisani u radu Mishre i suradnika [58]. Apsorpcijski spektar molekule **25** se nalazi na nižim valnim duljinama nego apsorpcijski spektar benzoksazolnog **26** i benztiazolnog analoga **27**, no niže je energije naspram spektra spoja bez stirilne poveznice, 2-[4-(dimetilamino)fenil]benzimidazola. Polarnost otapala znatno utječe na apsorpcijski i emisijski spektar ICT bojila te se uočava batokromni pomak s porastom polarnosti otapala. Reorganizacija molekula otapala u pobuđenom stanju snižava energiju polarizirane molekule, što se očitava crvenim pomakom u emisijskom spektru. Međutim, spektralna svojstva spoja u vodi odudaraju od očekivanog ponašanja ICT molekula u polarnim otapalima. Kako je prethodnim istraživanjima utvrđeno, spektralne vrpce se pomiču prema višim valnim duljinama pri stvaranju vodikovih veza ili protonaciji imino dušika na benzimidazolu, dok protonacija dimetilamino grupe u sličnim

benzimidazolnim strukturama uzrokuje pomak prema nižim valnim duljinama. Plavi pomak spektralnih vrpci u vodi, naspram spektralnih svojstava u ostalim otapalima, autori tumače kao redukciju konjugacije zbog stvaranja vodikovih veza u vodi. Naime, stvaranjem vodikovih veza slobodni elektronski par na imidazolnom dušiku prestaje sudjelovati u konjugaciji. Pomak emisijskog maksimuma u ovisnosti o polarnosti otapala za tipične ICT fluorofore je prikazan na primjeru spoja **25**, Slika 23.

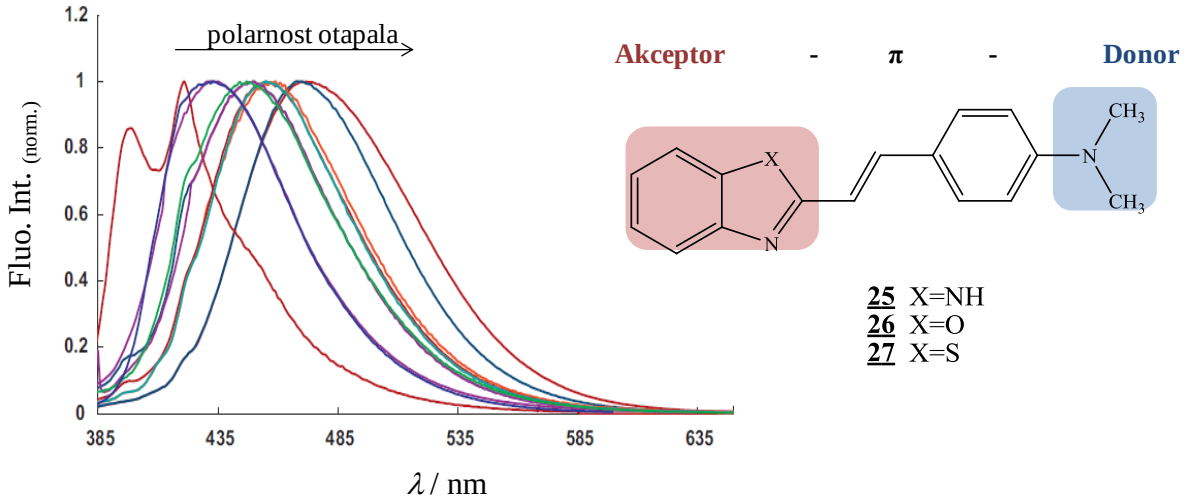

Slika 23. Pomak emisijskog maksimuma u ovisnosti o polarnosti otapala za tipične ICT fluorofore [58].

Tablica 2. Spektralna svojstva ICT fluorofora **25** u različitim otapalima [58].

Otapalo	λ^{ab}_{max}, **nm**	λ^{fl}_{max}, **nm**	Φ_f
Cikloheksan	367	399,421	0,12
Dioksan	371	432	0,18
Etilacetat	369	436	0,16
Dimetil formamid	376	457	0,28
1-propanol	372	449	0,13
Etanol	374	452	0,15
Acetonitril	372	459	0,13
Metanol	375	462	0,08
Glikol	384	471	0,35
Glicerol	385	473	0,88
Voda	363	490	

Heteroatom unutar sustava znatno utječe i na kiselo-baznu ravnotežu spoja. Primjerice, protonacija benztiazolnog derivata **27** u vodi se odvija na dušiku dimetiamino skupine, što se može lako pretpostaviti po bazičnosti prisutnih ionizabilnih mjesta. Međutim, kod benzimidazolnog derivata **25** se protoniranjem uočava crveni spektralni pomak, što dovodi do zaključka da se protonira imino dušik unutar benzimidazolne jezgre. Razlike u svojstvima molekula benztiazolnog i benzimidazolnog derivata uzrokovane kiselo-baznom ravnotežom, pripisuju se upravo prijenosu naboja unutar molekule. U svim promatranim sustavima (X= NH, O i S), prijenos naboja s *N*,*N*-dimetilamino skupine na benzazolni dio molekule u pobuđenom stanju uzrokuje smanjenje elektronskog naboja na *N*,*N*-dimetilaminskom dušiku i povećanje elektronske gustoće na azolnom dušiku, što omogućuje protonaciju azolnog dušika. Međutim, azolni dušik se protonira samo u slučaju benzimidazolnog derivata, dok u slučaju benztiazolnog i benzoksazolnog derivata sumpor i kisik smanjuju gustoću naboja na dušiku unutar prstena zbog svoje elektron-odvlačeće prirode te se protonacija odvija na *N*,*N*-dimetilaminskom supstituentu.

Navedenu teoriju potvrđuju i vrijednosti pK_a monokationskih vrsta koju kod navedenih sustava eksperimentalno i teorijski tumače Mishra i suradnici [58]. Konstante disocijacije imino dušika su niže za benztiazolni **27** i benzoksazolni derivat **26**. Veća bazičnost dušika u promatranim sustavima omogućuje protonaciju dimetilamino skupine (Tablica 3).

Spektralni pomaci za neutralni i protonirane oblike ispitivanog benzimidazolnog derivata slijede trendove uočene u literaturi, gdje se protoniranjem imino dušika uočava crveni spektralni pomak, a dimetilamino skupine plavi spektralni pomak. Primjer opisanih trendova u spektralnim pomacima prilikom protoniranja / deprotoniranja benzimidazolnog derivata **25** je prikazan na Slici 24.

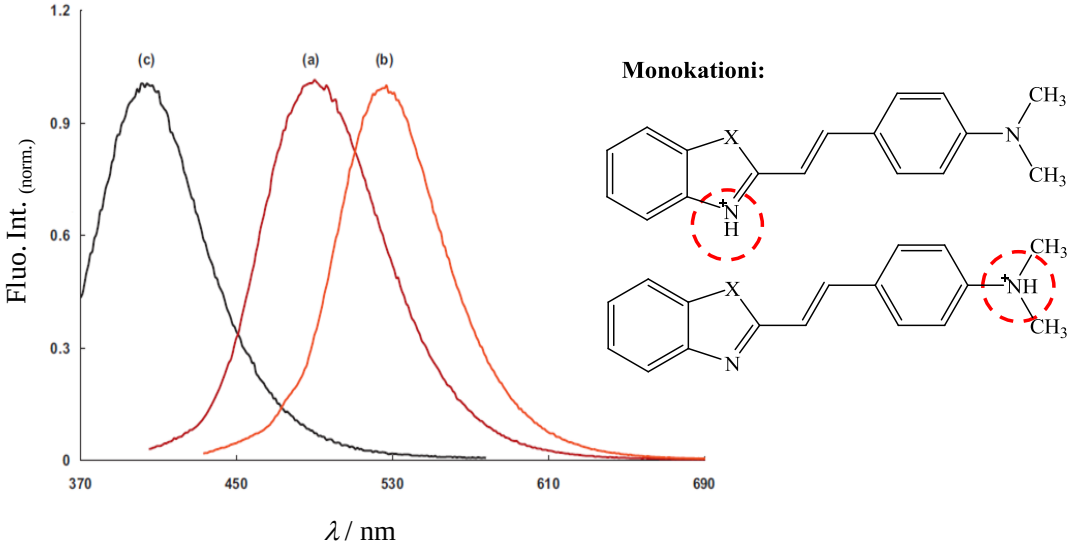

Slika 24. Emisijski spektar (a) neutralne, (b) monokationske i (c) dikationske vrste **25** u vodi, adaptirano iz [58].

Tablica 3. pK_a i pK_a* vrijednosti za imino dušik u promatranim sustavima.

Spoj	pK_a	pK_a*
25	6,04	10,87
26	2,6	7,15
27	4,8	8,47

Osim što su intenzivno istraživani kao novi fluorofori poboljšanih optičkih svojstava, *push-pull* derivati benzimidazola su okupirali pažnju istraživača i zbog svojih nelinearnih optičkih svojstava [79]. Visoka kemijska, termalna i fotokemijska stabilnost, ekonomična sinteza i mogućnost jednostavne funkcionalizacije omogućili su primjenu ove vrste kromofora u razvoju i unapređivanju optičkih vlakana [80], organskih emitirajućih dioda OLED [81, 82], solarnih ćelija DSSC [54, 83] i tehnologiji lasera [84]. Poznato je da su fluorofori s izraženim ICT mehanizmom vrlo osjetljivi na polarnost okoline, pa su tako predstavljeni *push-pull* derivati benzimidazola s potencijalnom primjenom kao solvatokromne probe [85].

TICT benzimidazolni fluorofori

Benzimidazolna jezgra je jedinstvena zbog mogućnosti vezivanja više okomitih π-konjugiranih jedinica, čime je omogućeno stvaranje novih optički osjetljivih sustava s mogućnosti višestruke primjene. Novo područje istraživanje u kemiji benzimidazola jest optimizacija svojstava molekula, ne samo supstituentima već kompletnom geometrijom sustava. Podrijetlo fotofizičkih pojava kod različitih prostorno strukturiranih derivata benzimidazola istraživali su Inouchi i suradnici [86, 87]. Vezivanje protona, metalnih iona ili aniona u takvim sustavima mijenja i povećava konjugaciju molekule ili elektron akceptorsku prirodu benzimidazolne jedinice, čime se mijenja intenzitet i boja optičkog signala (apsorpcije ili emisije). U posljednjih nekoliko godina intenzivno se istražuje geometrija π-konjugiranih sustava temeljenih na benzimidazolu s ciljem razvoja novih fluorofora u obliku slova T [86, 88], slova L [89] ili tzv. križastih fluorofora [90].

Istraživanje novih L- ili T- oblikovanih fluorofora znatno doprinosi razumijevanju fotofizičkih pojava unutar sustava. Mehanizam odgovoran za stvaranje signala kod T-oblikovanih fluorofora s benzimidazolnom jezgrom je intramolekulski prijenos naboja zakretanjem (engl. *Twisted intramolecular charge transfer*, TICT). Zakretanje (engl. t*wisting*) feniltiofenske jedinice naspram ravnine u kojoj leži benzimidazolna jezgra uzrokuje snažan pomak emisijskog spektra prema višim valnim duljinama i veliki Stokesov pomak. U radu Inouchija i suradnika je opisan TICT mehanizam za ovu vrstu fluorofora, usporedbom T-oblikovanih fluorofora s njihovim linearnim analozima koji emitiraju iz lokalnog pobuđenog stanja [87].

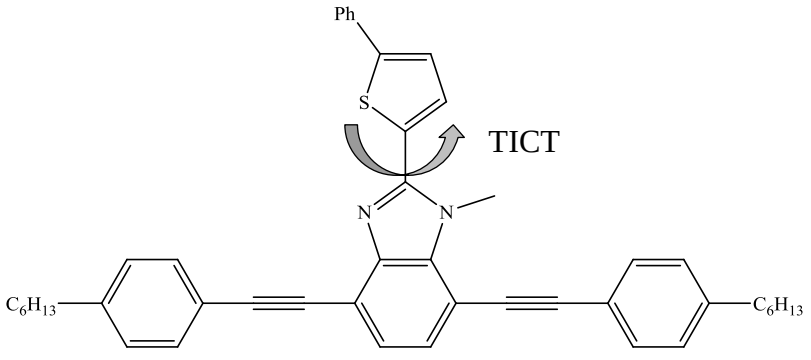

28

Slika 25. T-fluorofor temeljen na benzimidazolu [87].

Lirag i suradnici su pripravili i karakterizirali skupinu L-fluorofora temeljenih na benzimidazolu (Slika 26.) [89]. L-fluorofori su jednostavniji geometrijski oblik tzv. križastih fluorofora pripravljenih u istoj skupini autora [90]. Naime, uvođenjem prikladnih supstituenata, križaste strukture lokaliziraju svoje HOMO i LUMO orbitale na suprotne 'ruke' molekule, što izravno utječe na razliku energije HOMO-LUMO, odnosno optički signal proizveden prije i nakon vezivanja analita. Svih devet L-derivata je pokazivalo spektroskopski odgovor na prisutnost kiseline, baze, ili aniona. Detaljnije su uspoređivani derivati **29** i **34**, gdje je izravno uključen i prijenos naboja unutar molekule zbog donorskih i akceptorskih supstituentata (dimetilanilin i piridin).

HOMO i LUMO orbitale su delokalizirane unutar molekule **29**, za razliku od molekule **34** gdje je većina elektronske gustoće LUMO smještena oko piridinskog dijela molekule, dok je gustoća HOMO smještena duž elektronima bogate dimetilanilinske grupe.

Istraživana su kiselo-bazna svojstva takvih derivata, no utvrđena je samo pK_a vrijednost 12,8 koja odgovara deprotonaciji dušika na benzimidazolu. Vrijednost konstante za prvu protonaciju je grubo određena iznosi oko 2,30, no nije definirano na kojem atomu se molekula protonira.

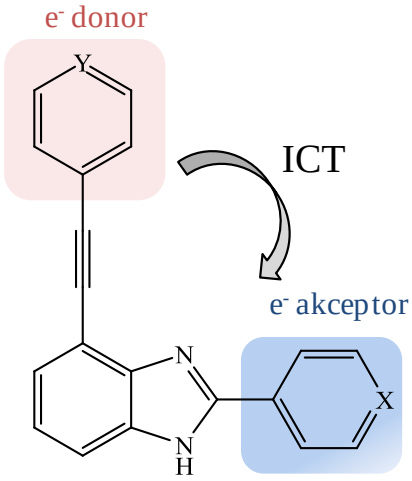

29 X = Y = CH
30 X = CH, Y = C-NMe_2
31 X = CH, Y = N
32 X = C-NMe_2, Y = CH
33 X = Y = C-NMe_2
34 X = C-NMe_2, Y = N
35 X = N, Y = CH
36 X = N, Y = C-NMe_2

Slika 26. L-fluorofori temeljeni na benzimidazolu [89].

PET fluorofori

Kako je prethodno opisano, proces fotoinduciranog prijenosa elektrona (engl. *Photoinduced Electron Transfer*, PET) je izravno ovisan o oksido-redukcijskim potencijalima donorskog i akceptorskog mjesta unutar molekulskog sustava. Sustavi u kojima je moguć fotoinducirani prijenos elektrona su sustavi s elektron-donorskom i elektron-akceptorskom grupom smještenim na suprotnim krajevima konjugirane molekule, stoga se u razvoju novih PET fluorofora najviše pažnje usmjerava na optimizaciju fotofizičkih svojstava pametnim dizajnom molekulskog kostura, odnosno položaja i kompatibilnosti supstituenata. Benzimidazolni PET fluorofori su često opisivani u literaturi, no naglasak se pritom stavlja na senzorsku primjenu takvih spojeva. Naime, PET senzori pružaju mogućnost tzv. *on – off* fluorescentnog odgovora baziranog na fotoinduciranom prijenosu elektrona, što pruža jedinstvenu platformu za razvoj novih senzora. Detaljniji opis benzimidazolnih PET fluorofora je prikazan u poglavlju „3.2. pH senzori temeljeni na benzimidazolu“.

AIE fluorofori

Emisija izazvana agregacijom molekula (engl. *Aggregation induced emission*, AIE) je fenomen opisan u posljednjem desetljeću [91]. Park i suradnici su paralelno s Tangom i suradnicima uočili neobičnu pojavu da agregacija molekula kod određenih fluorofora uzrokuje značajno intenzivniju fluorescenciju, nasuprot očekivanom gašenju fluorescenije [92, 93].

Agregacija je nepoželjna nuspojava pri uporabi klasičnih fluorofora, stoga flurofori koji u agregiranom obliku emitiraju svjetlost većeg inteziteta pokazuju potencijal za primjenu u sustavima poput OLED-a, solarnih ćelija ili optičkih senzora [48]. Mehanizam ovog neobičnog fenomena je istraživan kroz nekoliko znanstvenih publikacija [94-96]. U suštini se podrijetlo fluorescencije molekula u agregiranom obliku pripisuje onemogućavanju molekulskih gibanja (engl. *Restriction of rotation*, RIR i *Restriction of vibration*, RIV), pa tako i onemogućenju intramolekulskog prijenosa naboja zakretanjem (TICT) [97]. Veliki potencijal za primjenu fluorescentnih agregata privukao je pozornost znanstvenika te je publiciran velik broj radova o novim klasama spojeva kod kojih je uočen ovaj fenomen [98]. Primjena AIE mehanizma u kemijskim senzorima je izazovno područje, jer su molekule koje posjeduju AIE uglavnom temeljene na rigidnim tetrafeniletilenskim i sličnim strukutrama

koje najčešće ne posjeduju prikladna receptorska mjesta. Benzimidazolni derivati kao AIE emiteri su predstavljeni u nekoliko radova kao strukturne jedinice novih AIE fluorofora za detekciju pirofosfata [99], fluoridnog iona [100], te općenito kao nova klasa AIE emitera u otopinama [101, 102] ili materijalima [103].

Gogoi i suradnici su opisali AIE senzor temeljen na benzimidazolu za detekciju pirofosfata [99], pri čemu benzimidazolna jezgra ima funkcionalnu ulogu u stvaranju agregata i prepoznavanju pirofosfatnog aniona. Kao što je prikazano na Slici 27., dodavanjem „lošeg“ otapala (H_2O) u otopinu spoja **37** u „dobrom“ otapalu (THF) dolazi do π-π pakiranja molekula i stvaranja nanostruktura s izraženom emisijom na λ = 530 nm. Spoj **37** ne emitira u THF-u, no emisija je vrlo izražena u vodi te je uočen Stokesov pomak od 125 nm. Prisutnost nanostruktura je potvrđena mikroskopskim tehnikama i eksperimentima dinamičkog raspršenja svjetlosti. Emitirajući agregati su potom demonstrirani kao senzor za pirofosfatni anion. Prisutnost pirofosfatnog aniona je pojačala AIE karakter sustava zbog utjecaja na veličinu formiranih agregata. Autori su predstavili osjetljivost kemosenzora **37** na pirofosfatni anion i u imobiliziranom obliku, na trakicama filter papira. Shematski prikaz stvaranja agregata **37** i AIE mehanizam detekcije pirofosfata je prikazan na Slici 28.

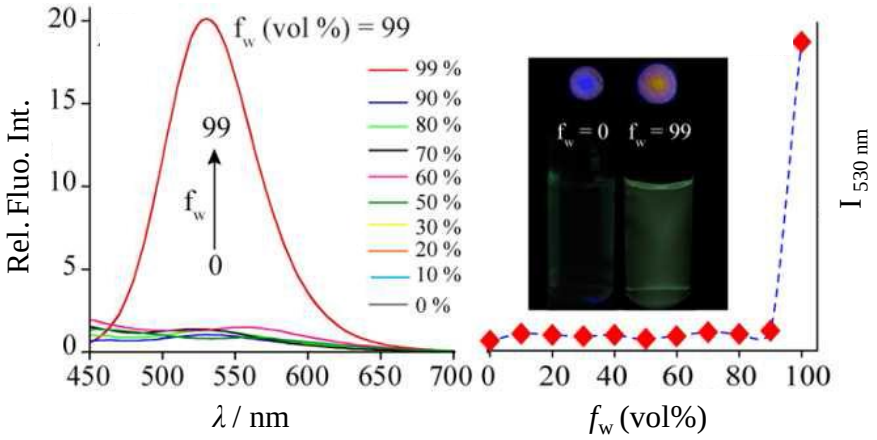

Slika 27. Emisija uzrokovana agregacijom derivata benzimidazola; stvaranje agregata je uzrokovano promjenom sastava otapala, preuzeto iz [99].

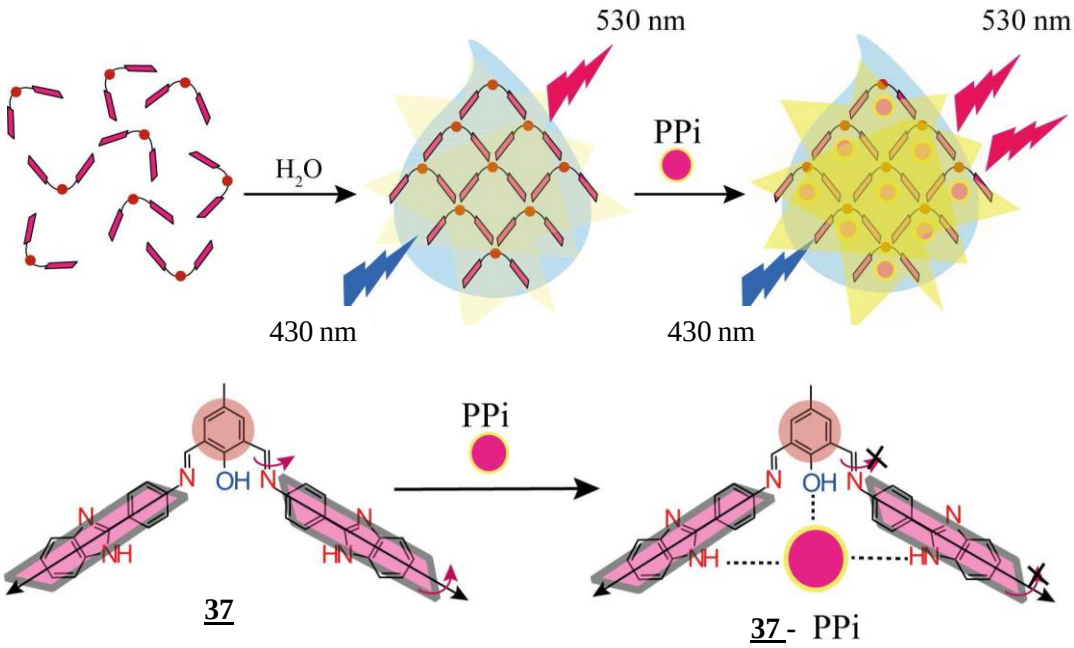

Slika 28. Shematski prikaz stvaranja agregata **L** i AIE mehanizam detekcije pirofosfata, preuzeto iz [99].

Noviji pristupi u razvoju benzimidazolnih fluorofora

Pregledom novije literature uočeni su određeni smjerovi razvoja novih benzimidazolnih fluorofora te su u ovom poglavlju opisani njihovi predstavnici.

Bor-dipirometenska bojila (BODIPY) i njihovi kompleksi su vrlo istraživana skupina spojeva zbog visokog molarnog apsorpcijskog koeficijenta, dobre termalne i fotokemijske stabilnosti te mogućnosti raznovrsne funkcionalizacije [104]. Fuzija BODIPY jezgre s aromatskim jedinicama, kao što su karbazol – BODIPY – benzimidazol konjugati, logičan je slijed istraživanja spektralnih mogućnosti benzimidazola [105, 106]. Integriranje BODIPY jezgre s aromatskim jedinicama poput benzimidazola rezultira proširenjem π konjugacije sustava, dok dušik na mezo spojnici BODIPY uzrokuje spektralni pomak prema višim valnim duljinama u odnosu na nekonjugirani BODIPY.

Maeda i suradnici su integrirali tiazolnu, benztiazolnu, imidazolnu, benzimidazolnu, 1,2,3-triazolnu ili indolonsku jedinicu s karbazolnom jezgrom [105]. Pripravljeni spojevi fluoresciraju u krutom stanju, što je ponukalo navedenu grupu autora na detaljniju analizu utjecaja supstituenta na intenzitet i boju emitirane svjetlosti. Iako su u radu predstavljeni rezultati dobiveni za benztiazolni derivat supstituiran različitim elektron donorskim ili

elektron odvlačećim supstituentima na karbazolnoj jedinici, osnovne smjernice za daljnja istraživanja i trend u fotofizičkim svojstvima bi se mogao odnositi i na benzimidazolni derivat **41**. Promjene u spektralnim svojstvima prate uočene literaturne trendove; derivati s elektron-odvlačećim supstituentima pokazivali su pomak maksimuma apsorpcije i emisije prema manjim valnim duljinama (plavi pomak), dok je crveni pomak uočen kod derivata s elektron-donorskim supstituentima. Metoksi supstituent je uzrokovao najveći pomak apsorpcijske vrpce zahvaljući ICT mehanizmu, no ujedno i najmanji intenzitet fluorescencije.

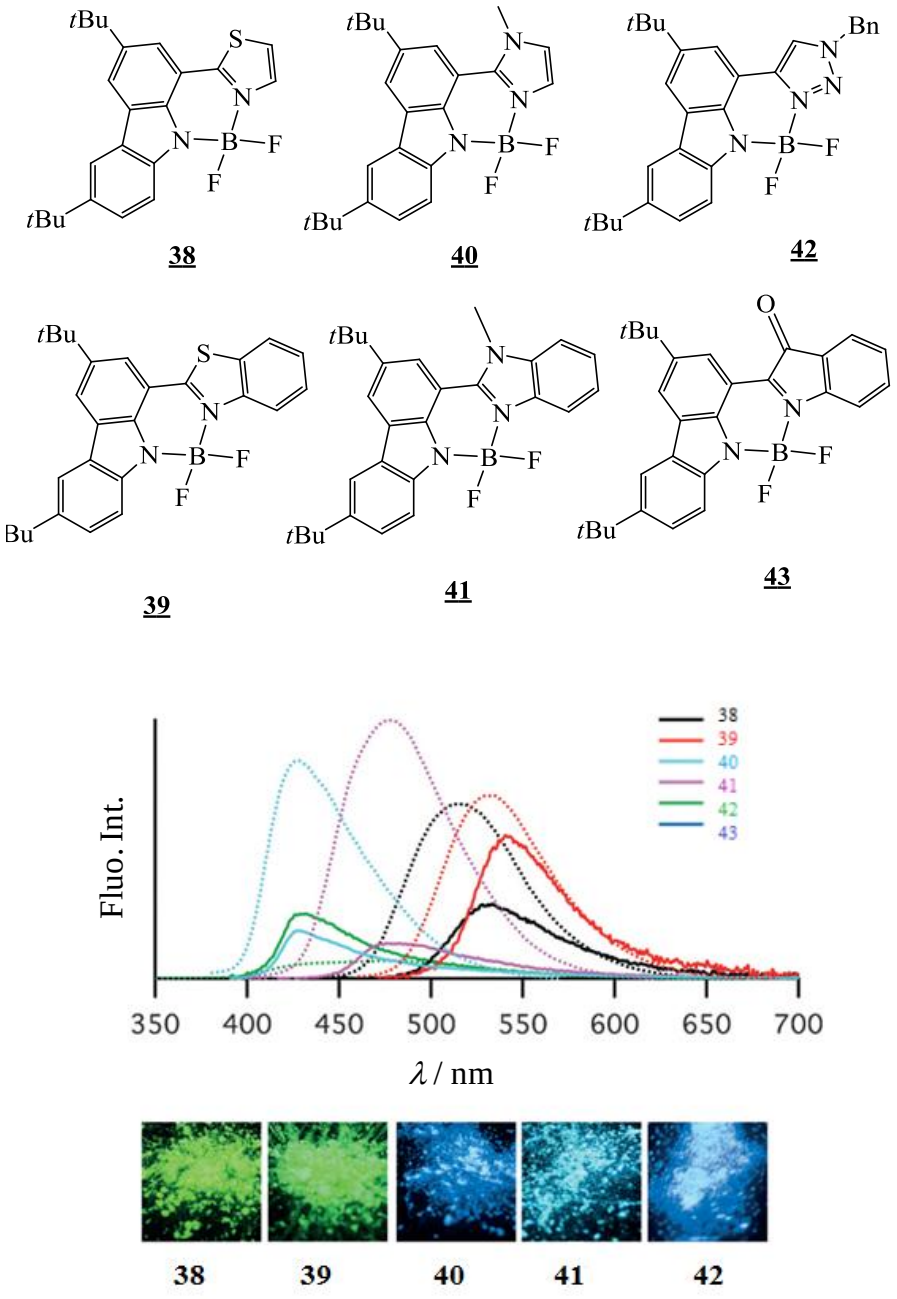

Slika 29. BODIPY fluorofori (**41** sadrži benzimidazolnu jezgru), preuzeto iz [105].

Fluorescencijski maksimum spojeva **38** i **39** u krutom stanju je pomaknut prema većim valnim duljinama obzirom na otopinu, što ukazuje na stvaranje agregata *J* – tipa. Pakiranje molekula u *J*-agregate pridonosi fluorescenciji spojeva u krutom stanju jer dokazano slaganje molekula u takozvane *cik – cak* strukture znatno minimiziraju mogućnost autoapsorpcije i samo-gašenja fluorescencije. Autori su također zaključili da je fluorescencija spojeva u krutom stanju intenzivnija kod derivata s prostorno većim supstituetima, zbog onemogućavanja intermolekulskih interakcija.

Tablica 4. Fotofizička svojstva karbazolnih BODIPY derivata u otopini (CH_2Cl_2) i čvrstom stanju [105].

Spoj	λ_{abs} (nm)	λ_{em} (nm)	$\Delta\nu_{St}$ (cm^{-1})	Φ_F (CH_2Cl_2)	λ_{prah} (nm)	Φ_F (prah)
38	436	513	3440	0,334	530	0,165
39	458	534	3110	0,320	542	0,214
40	394	427	1960	0,424	428	0,130
41	419	477	2900	0,547	478	0,141
42	382	477	5210	0,074	431	0,150
43	663	793	2470	< 0,001	-	-

Pomak spektralnih svojstava novih derivata benzimidazola za primjenu u optoelektroničkim sustavima istraživali su Sakai i suradnici [107]. Karboheliceni su policiklički aromatski spojevi zanimljivih optičkih svojstava, no karboheliceni sa svojstvom emisije u crvenom spektralnom području do tada nisu bili pripravljeni. Planarni i prošireni π konjugirani sustav u ovakvim strukturama najčešće znači i manju razliku u energiji HOMO i LUMO, odnosno crveni pomak u spektroskopim svojstvima, što je ostvareno pripravom konjugata [5]karbohelicena i benzimidazola. Protonacijom benzimidazolne jezgre dolazi do smanjenja razlike energije HOMO i LUMO energetske razine i emisije crvene svjetlosti (Slika 30).

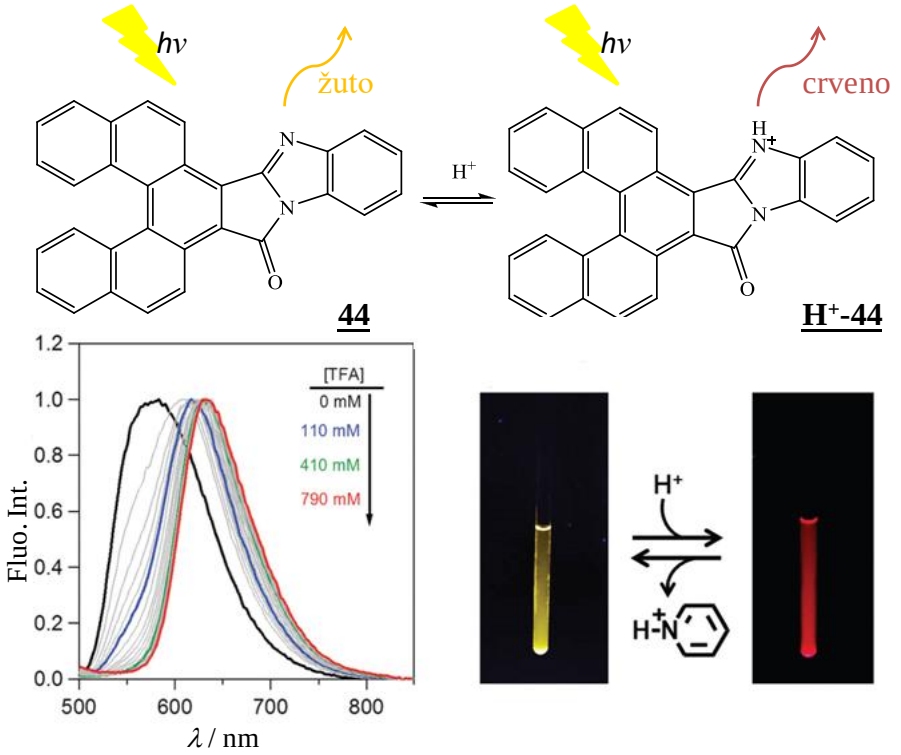

Slika 30. Karbohelicenski sustavi za primjenu u optoelektroničkim sustavima.

3.2. pH senzori temeljeni na benzimidazolu

Razvoj novih kemosenzorskih molekula je vrlo izražen i u području određivanja pH zbog niza prednosti jednostavnih optičkih senzora nad drugim metodama detekcije H^+ iona [108]. Optički pH kemijski senzori posjeduju brojne prednosti naspram standardnih pH elektroda, kao što su lakša mogućnost minijaturizacije i beskontaktnog mjerenja [109-111]. Molekula koja pokazuje razliku u boji ili intenzitetu fluorescencije između svog protoniranog i deprotoniranog oblika sposobna je dati kvantitativnu informaciju o kiselosti otopine. Vrijednost pH je bitan parametar u raznim biološkim i kemijskim procesima, a brzo i jednostavno određivanje pH je često nužno potrebno u medicini, biologiji i tehnološkim procesima. Poznavanje kiselo-bazne ravnoteže indikatora i poznavanje konstanti disocijacije (pK_a vrijednosti) je vrlo koristan fizikalno-kemijski podatak, prvenstveno u proizvodnji i razvoju farmaceutika. Ukoliko govorimo o senzorskim materijalima, pH ima ključnu ulogu u radu velikog broja optičkih senzora. Primjerice, bazičnost kromoionofora u ion-selektivnim optodama je bitna stavka koja određuje selektivnost i dinamički odziv optode [22].

Dugo vremena su apsorpcijski pH senzori istraživani više nego fluorescencijski, što u današnje doba nije slučaj zbog niza prednosti fluorescencijskih senzora. Poželjna svojstva fluorescentnih pH indikatora su pK_a vrijednost između 6 i 8 (idealno fiziološka vrijednost pH = 7,4), visoki kvantni prinos fluorescencije (Φ_F), visoki molarni apsorpcijski koeficijent (ε), ekscitacijski maksimumi u vidljivom dijelu spektra, dobra topljivost u vodi, kemijska stabilnost, fotostabilnost, veliki Stokesov pomak te dostupnost i niska cijena.

Protonabilni dušik unutar benzimidazolne jezgre omogućuje primjenu derivata benzimidazola kao senzora za pH. Dostupan je velik broj znanstvenih radova temeljenih na istraživanju protonacijskih mjesta, konstanti disocijacije i fotofizičkih svojstava različitih ionskih vrsta derivata benzimidazola (opisano u poglavlju 3.1.1) [58, 74]. Manji broj radova proučava potencijalnu primjenu derivata benzimidazola kao pH senzora i oni su predstavljeni u Tablici 5. Tablica se temelji na pretrazi literature po ključnim riječima „*benzimidazo**“ i „*sensor*“ .

Tablica 5. pH senzori temeljeni na derivatima benzimidazola.

Konjugirana jedinica	**pK_a**	**Primjena**	**Mehanizam stvaranja signala**	**Referenca**
antracen	-	pH senzor	PET	Tolpygin i sur. (2012) [112]
naftalen	4,9 – 6,1	Probe za kiseli pH u stanicama tkivima	-	Kim i sur. (2013) [113]
spiropiran	5,9	pH proba	ESIPT	You i sur. (2013) [114]
rodamin	-	pH proba	ESIPT	Xue i sur. (2014) [115]
BODIPY	3,46	pH proba	PET	Sevinç i sur. (2014) [116]
kinolin	6,67	pH senzor	PET	Liu i sur. (2015) [117]
nitrofenilfuran	11-12	kemosenzor	-	Zhu i sur. (2015) [118]
BODIPY	5,2	Unutarstanični pH	ICT	Li i sur. (2016) [119]
karbazol	-	Određivanje kiselosti	ICT	Aich i sur. (2016) [120]

Najizraženiji razvoj se uočava u području priprave i karakterizacije novih fluorescentnih proba za obilježavanje stanica koje funkcioniraju po principu promjene spektralnih svojstava u određenom području pH (6/9 znanstvene publikacije) [113]. Bitno je spomenuti i razvoj novih funkcionalnih materijala temeljenih na derivatima benzimidazola, poput pH osjetljivih polimernih nanočestica [121]. Zanimljivo je uočiti da se svi navedeni primjeri pH senzora temelje na protoniranju dušika unutar benzimidazolne jezgre. Benzimidazol je u pH senzorima konjugiran s različitim aromatskim jezgrama, primjerice antracenskom [112], naftalenskom [113] ili bordipirometenskom (BODIPY) jezgrom [116]. Najveći trud znanstvenika uložen je u razvoj novih pH senzora za biološke primjene, stoga je poželjno da senzorska molekula apsorbira pri većim valnim duljinama (crveno spektralno područje) i posjeduje velik Stokesov pomak. BODIPY derivati su, kako je već spomenuto, često korištena grupa fluorofora zbog svoje izražene fluorescencije te mogućnosti finog podešavanja spektralnih svojstava kroz cijelo vidljivo područje elektromagnetskog spektra.

Benzimidazolni senzori za pH se temelje na različitom mehanizmu stvaranja fluorescentnog odgovora, a najčešće se radi o tzv. *on-off* senzorima baziranim na fotoinduciranom prijenosu elektrona. Primjer PET senzora temeljen na konjugatu benzimidazola i BODIPY jezgre predstavili su Sevinç i suradnici (Slika 31.) [116]. Autori su opisali novi pH osjetljiv fluorescentni sustav kod kojeg dolazi do gašenja fluorescencije zbog fotoinduciranog prijenosa elektrona između BODIPY jezgre i benzimidazolne jedinice. Teorijskim računima HOMO i LUMO u neutralnom i protoniram obliku dokazan je PET proces. Naime, energijski nivoi orbitala BODIPY jezgre smješteni su između nivoa benzimidazolne jedinice, stoga u neutralnom stanju fluorescencija proizlazi iz LUMO BODIPY. Protonacijom se energijski nivou benzimidazola smanjuju te se LUMO benzimidazolne jedinice nalazi na nižem nivou nego LUMO BODIPY, što uzrokuje prijenos elektrona od BODIPY do benzimidazolne jedinice u pobuđenom stanju, odnosno gašenje fluorescencije.

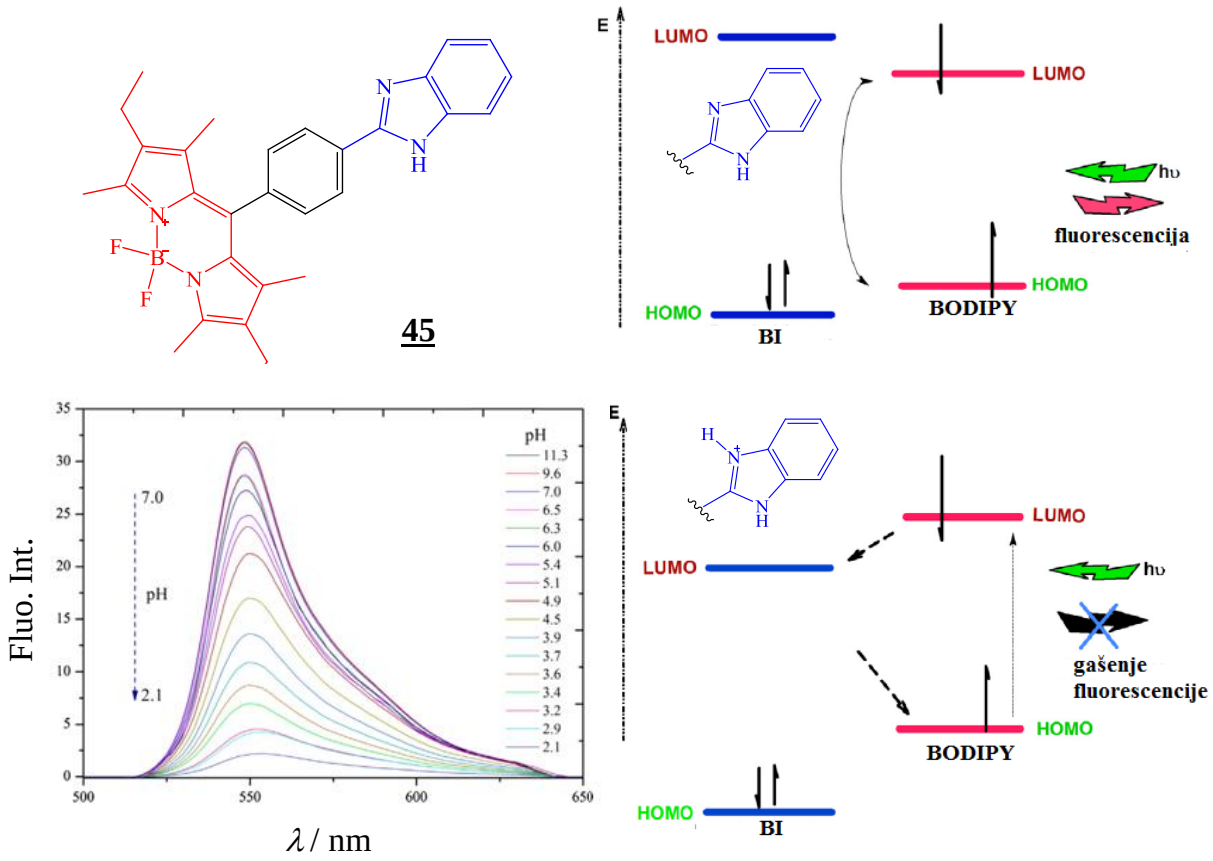

Slika 31. Primjer pH senzora temljenog na benzimidazolu, adaptirano iz [116].

3.3. Kationski senzori temeljeni na benzimidazolu

Prisutnost metalnih kationa je često ključan parametar za odvijanje raznih bioloških i kemijskih procesa. Tako su, primjerice, alkalijski i zemnoalkalijski metali izravno uključeni u biološke procese poput prijenosa živčanih impulsa, rad mišića i regulacije rada stanica. Metalni kationi u ulozi katalizatora su ključan faktor u radu mnogih enzima. Također, liječenje mnogih bolesti je povezano s prisutnošću metala u organizmu. Primjerice, znanstveno je dokazana povezanost Alzheimerove bolesti i koncentracije aluminija u organizmu [122]. Teški metali su općenito opisani kao metali visoke gustoće, velike atomske mase i atomskog broja. Među njih ubrajamo kadmij (Cd), krom (Cr), živu (Hg), arsen (As), bakar (Cu), olovo (Pb), cink (Zn), željezo (Fe), kositar (Sn) i druge metale. Neki teški metali su esencijalni za normalno funkcioniranje organizma (primjerice bakar, željezo ili cink), no u većim količinama mogu izazvati razne bolesti. Također, mnogi metali su izrazito toksični za organizme, primjerice živa, arsen, kadmij ili aluminij. Teški ioni također predstavljaju problem u okolišu, gdje su se s razvojem industrije i prometa počeli nakupljati u većim količinama. Poznavanje koncentracije teških metala u organizmu i okolišu je vrlo bitno, stoga su fluorescentni senzori za metalne katione koristan alat za brzu i jednostavnu detekciju.

Molekulski sustavi za prepoznavanje analita se često oslanjaju na načela supramolekulske kemije, gdje su komponente međusobno povezane reverzibilnim međumolekulskim silama (elektrostatske i vodikova veza, π-π interakcije i van der Waalsove sile) [123]. Najčešći mehanizmi prepoznavanja metala kod optičkih kemijskih senzora temeljeni su na stvaranju koordinativne veze između metala i prikladnih organskih liganada ili na selektivnim elektrostatskim privlačenjima, poput ion – dipolnih interakcija (primjer je stvarajne kompleksa kalija i valinomicina). Koordiniranjem metalnog iona, fluorescencija molekulskog sustava može postati intenzivnija (engl. *Chelation Enhanced Fluorescence effect*, CHEF) ili se gasiti (engl. *Chelation Enhancement Quenching effect*, CHEQ). Mehanizmi prijenosa i stvaranja signala pri detekciji metalnih iona su već spomenuti fotoinducirani prijenos elektrona (PET), intramolekulski prijenos naboja (ICT), intramolekulski prijenos naboja s metala na ligand (MLCT), fluorescencijski prijenos energije rezonancijom (FRET) te stvaranje ekscimera i ekscipleksa. Osim toga, metal može promovirati ireverzibilnu kemijsku reakciju pri čemu se praćenjem spektralnih odziva reaktanata i produkata mogu odrediti analitički parametri. Takvi ireverzibilni senzori se nazivaju kemodozimetri [124].

Danas u literaturi postoji velik broj kemijskih senzora za određivanje metala, stoga je istraživanje i razvoj novih kemosenzorskih sustava usmjereno prema poboljšanju analitičkih parametara postojećih senzora ili razvoju novih sustava za točno određenu i ciljanu primjenu. Dizajn novih senzora se temelji na postojećim i dobro istraženim mehanizmima, no bitno je pomicati granice osjetljivosti i selektivnosti te omogućiti reverzibilnost i višestruku primjenu [28]. Određivanje metala u organizmima je konstantni izazov, stoga su senzori temeljeni na biološki prihvatljivim spojevima od ključne važnosti [125]. Također, u mnogim klasičnim kationskim senzorima za prijelazne metale, gašenje fluorescencije se pripisuje paramagnetičnom atomu u blizini fluorofora koji omogućuje međusustavno križanje te se kompleksirana molekula vraća iz pobuđenog u osnovno stanje procesima bez zračenja [126]. Stoga je poželjan dizajn takozvanih *on – off* senzora, temeljenih najčešće na fotoinduciranom prijenosu elektrona, jer je njihova uporaba u mnogim slučajevima najjednostavnija. Razvijeni su mnogi optički kemijski senzori visoke osjetljivosti i selektivnosti za određivanje alkalijskih i zemnoalkalijskih metala, kao i za metale prijelaznih skupina elemenata Cu^{2+}, Hg^{2+}, Ag^{+}, Fe^{2+}/Fe^{3+}, Pb^{2+}, Mn^{2+} i Zn^{2+} i lantanide [28, 125, 127-132]. Benzimidazolna jedinica je često uključena u senzorski sustav za određivanje metalnih kationa, prvenstveno zbog slobodnog elektronskog para na dušiku koji omogućuje interakciju s kationom.

Brz i izražen napredak u optičkoj senzorskoj tehnologiji te velik značaj kemosenzorskih molekula koje omogućuju određivanje kationa ili aniona u otopini glavni je razlog za sintezu i karakterizaciju novih π-konjugiranih spojeva. Ugradnjom benzimidazolne jezgre u takve sustave moguć je razvoj senzora točno određenih i poželjnih fotofizičkih svojstava. Pregled optičkih kemijskih senzora temeljenih na benzimidazolu za metalne katione u posljednjem desetljeću prikazani su u Tablici 6. Vremenski okvir je odabran prema broju radova dostupnih u literaturi, prema čemu je velika većina publicirana nakon 2005. godine. Kako je prethodno rečeno, porast broja radova do 2015. godine usko prati i broj citata vezanih za benzimidazolne senzore. Iz rezultata prikazanih u Tablici 6. može se zaključiti da su benzimidazolni sustavi za detekciju kationskih vrsta najbrojnija skupina kemosenzora (59/96 literaturnih referenci, 61 % ukupnog broja prikazanih publikacija).

Tablica 6. Optički kemijski senzori za metalne katione temeljeni na benzimidazolu.

Analit	**Mehanizam nastajanja signala**	**Spektralno područje**	**Granica detekcije**	**Referenca**
Ag^{+}	-	500-700 nm	$2{,}8 \times 10^{-12}$ M	Firooz i sur. (2012) [133]
	-	300-500 nm	-	Zhaoi sur. (2015) [134]
	-	200-400 nm	$4{,}4 \times 10^{-7}$ M	Chen i sur. (2016) [135]
Al^{3+}	ICT	200-500 nm	$5{,}3 \times 10^{-7}$ M	Jeyanthi i sur. (2013) [136]
	PET	500-600 nm	$0{,}99 \times 10^{-6}$ M	Velmurugan i sur. (2015) [137]
Al^{3+} / F^{-}	-	300-600 nm	$3{,}41 \times 10^{-7}$M $9{,}189 \times 10^{-8}$M	Iniya i sur. (2015) [138]
Al^{3+} / Zn^{2+}	ESIPT	400-600 nm	$5{,}98 \times 10^{-6}$ M $3{,}3 \times 10^{-6}$ M	Cao i sur. (2014) [139]
Al^{3+} / Cd^{2+}	ESIPT	250-500 nm	65×10^{-6} M 75×10^{-6} M	Dhaka i sur. (2016) [140]
Al^{3+} / Cu^{2+}	-	400-600 nm	$0{,}31 \times 10^{-6}$ M $0{,}54 \times 10^{-6}$ M	Liu i sur. (2016) [141]
Cd^{2+} i Zn^{2+}	-	300-600 nm	$6{,}5 \times 10^{-5}$ M	Li i sur. (2016) [142]
Co^{2+} / Cu^{2+}	MLCT	400-600 nm	$4{,}1 \times 10^{-7}$ M $5{,}5 \times 10^{-7}$ M	Cimen i sur. (2015) [143]
Cr^{3+}, Fe^{3+} i Ba^{2+}	PET	300-500 nm	$3{,}0 - 6{,}0 \times 10^{-6}$ M	Lal i sur. (2014) [144]
Cu^{2+} / S^{2-}	ESIPT	350-600 nm	$3{,}5 \times 10^{-7}$ M $1{,}35 \times 10^{-6}$ M	Tang i sur. (2013) [145]
Cu^{2+}	-	350-600 nm	$0{,}98 \times 10^{-6}$ M	Saluja i sur. (2012) [146]
	PET	250-450 nm	-	Jayabharathi i sur. (2012) [147]
	PET	200-400 nm	$12{,}5 \times 10^{-6}$ M	Mahiya i sur. (2013) [148]
	FRET	500-600 nm	$3{,}1 \times 10^{-6}$ M	Goswami i sur. (2014) [149]
	PET	300-600 nm	$3{,}4 \times 10^{-7}$ M	Liu i sur. (2014) [150]
Cu^{2+} i Al^{3+}	PET	250-550 nm	$4{,}2 \times 10^{-8}$ M $8{,}1 \times 10^{-7}$ M	Kumar i sur. (2015) [151]
Cu^{2+} / CN^{-}	PET	400-600 nm	$3{,}8 \times 10^{-7}$ M $1{,}86 \times 10^{-5}$ M	Tang i sur. (2013) [152]
Cu^{2+} i Fe^{3+}	-	350-550 nm	$2{,}3 \times 10^{-5}$ M $2{,}1 \times 10^{-5}$ M	Lee i sur. (2010) [153]
Cu^{2+} i Fe^{3+}	ESIPT	250-550 nm	-	Chipem i sur. (2014) [154]
Cu^{2+} /S^{2-}	ESIPT	350-600 nm	$4{,}47 \times 10^{-7}$ M	Tang i sur. (2014) [155]

			$9{,}12 \times 10^{-7}$ M	
	PET / displacement approach	250-400 nm		Kar i sur. (2013) [156]
	displacement approach	350-550 nm	$2{,}77 \times 10^{-6}$ M $2{,}51 \times 10^{-6}$ M	Fu i sur. (2014) [157]
	PET / displacement approach	300-550 nm	$1{,}6 \times 10^{-9}$ M $5{,}2 \times 10^{-6}$ M	Paul i sur. (2015) [158]
Cu^{2+} /$H_2PO_4^-$	displacement approach	400 – 550 nm	$9{,}76 \times 10^{-6}$ M $1{,}41 \times 10^{-6}$ M	Goh i sur. (2016) [159]
Cu^{2+} / dopamin	-	200-450 nm	-	Khattar i sur. (2013) [160]
Cu^{2+} / hlapivi organski spojevi	-	500-750 nm	-	Yu i sur. (2015) [161]
Fe^{3+}	-	350-550 nm	-	Jung i sur. (2008) [162]
	PET	300-500 nm	$9{,}45 \times 10^{-6}$ M	Lal i sur. (2014) [163]
	Otvaranje spiro-prstena	400-600 nm	$2{,}74 \times 10^{-6}$ M	Li i sur. (2016) [164]
	ESIPT	300-400 nm	5×10^{-5} M	Prakash i sur. (2016) [165]
	PET	500-600nm	$1{,}5 \times 10^{-8}$ M	Li i sur. (2011) [166]
	-	350-550nm	250×10^{-6} M	Lee i sur. (2011) [167]
	PET	300-650 nm	9×10^{-8} M	Wang i sur. (2017) [168]
Fe^{3+} / $H_2PO_4^-$	-	350-50 nm	1.0×10^{-9} M	Liu i sur. (2014) [169]
Fe^{3+} i Hg^{2+}	PET	250-550 nm	-	Yang i sur. (2014) [170]
Fe^{3+} i Cu^{2+}	-	350-550nm	$1{,}19 \times 10^{-5}$ M $1{,}86 \times 10^{-5}$ M	Lee i sur. (2011) [171]
Fe^{3+} /PO_4^{3-}	-	300-500 nm	-	Saikia i sur. (2011) [172]
Hg^{2+}	-	500-700 nm	$0{,}77 \times 10^{-6}$ M	Madhu i sur. (2013) [173]
	-	300-500 nm	$9{,}56 \times 10^{-9}$ M	Hu i sur. (2015) [174]
	MLCT	400-600 nm	$2{,}54 \times 10^{-7}$ M	Zhong i sur. (2014) [175]
Hg^{2+} i Cu^{2+}	TICT	300-600 nm	$3{,}4 \times 10^{-7}$ M $2{,}9 \times 10^{-6}$ M	Tan i sur. (2008) [176]
		350-600 nm	70×10^{-9} M $1{,}202 \times 10^{-7}$ M	Gao i sur. (2017) [18]
Hg^{2+} / I⁻	PET	300-550 nm	1×10^{-9} M	Liu i sur. (2014) [177]
Mg^{2+} i Cr^{3+}	-	250-550 nm	$3{,}2\text{-}100 \times 10^{-6}$	Saluja i sur. (2012) [178]

			M 79,4-340 × 10^{-6} M	
Ni^{2+}		300-700 nm	0,14 × 10^{-6} M	Sarkar i sur. (2016) [179]
Zn^{2+}	-	250-650 nm	1,62 × 10^{-3} M	Mashraqui i sur. (2006) [180]
		350-550 nm		Lohar i sur. (2013) [181]
	PET	250-550 nm	1,5 × 10^{-5} M	Velmurgan (2015) [182]
	-	250-400 nm	8,28 × 10^{-7} M	Mashraqui i sur. (2016) [183]
	ESIPT	250-550 nm	-	Akutsu i sur. (2016) [184]
	ESIPT	250-500 nm	1,4 × 10^{-6} M	Sharma i sur. (2016) [185]
Zn^{2+} i Fe^{3+}	-	350-550 nm	2,1 × 10^{-6} M 3,5 × 10^{-6} M	Razavi i sur. (2016) [186]
Zn^{2+} i Cu^{2+}	-	280-350 nm	3 ×10^{-9} M	Majzoub (2009) [187]
Zn^{2+} / S^{2-}	ESIPT	350-600 nm	6.21 ×10^{-7} M 3,46 × 10^{-6} M	Tang i sur. (2013) [188]
	ESIPT	350-600 nm	7,34 ×10^{-8} M 1,53 × 10^{-7} M	Tang i sur. (2014) [189]
multikationski	-	300-550 nm	-	Esteves i sur. (2016) [190]

Prema HSAB teoriji (teorija tvrdih i mekih kiselina i baza) baziranoj na polarizibilnosti i sličnim fizikalno-kemijskim parametrima, donorski imini su meki ligandi pogodni za vezanje prijelaznih metala. Rezultat toga jest razvoj većeg broja senzora temeljenih na benzimidazolu za prijelazne metale, no vrlo mali broj senzora za alkalijske i zemnoalkalijske metale. Jedan od rijetkih senzora temeljen na benzimidazolu za element 2. skupine razvili su Saluja i suradnici [178]. Kolorimetrijsko određivanje **magnezija** omogućeno je veličinom pseudošupljine senzorske molekule koja se sastoji od benzimidazola i dva fenilna prstena povezana imino vezom, supstituirana hidroksi i nitro supstituentom. Vezivanje magnezijeva iona u šupljinu pogodne veličine uzrokuje promjenu apsorpcijskih svojstava, odnosno povećanje intenziteta apsorpcijskih vrpci u UV području. Molekula je također selektivna na kromov ion, no za razliku od apsorpcijskog određivanja magnezija, određivanje kroma se zasniva na promjeni fluorescencijskih svojstava. Navedeni primjer je ujedno i jedan od rijetkih benzimidazolnih senzora temeljenih na apsorbanciji.

Bakar je jedan od esencijalnih elemenata u ljudskom organizmu. Aktivator je i sastavni dio mnogih enzima te sudjeluje u mnogim biološkim procesima. Poznavanje koncentracije bakra je često nužno u biologiji i medicini, stoga je brzo, jednostavno i

selektivno određivanje bakra od izuzetne važnosti. Mnogo napora se ulaže u razvoj senzora koji mogu djelovati u vodenom mediju, prikladnih za detekciju metala *in vivo*. Kako je već navedeno, senzori temljeni na PET mehanizmu su poželjni zbog jednostavnosti izvedbe mjerenja („*ON-OFF"* princip). Stoga je većina senzora za bakar razvijena na temelju PET mehanizma koji omogućuje pojavu fluorescencije pri kompleksiranju s bakrom („*turn – ON*"). Primjer senzora navedenih karakteristika jest konjugat benzimidazola i naftalimida (plavo) s aminopiperazinskim (crveno) supstituentom kao receptorom prikazan na Slici 32. [150]. Dizajn kemosenzorske molekule se temelji na strukturi u kojoj su fluoroforna i receptorska jedinica odvojene konjugiranom razmaknicom, pri čemu je aminopiperazinski dio molekule (crveno) receptor, a benzimidazolna jezgra je dio aromatskog fluorofornog sutava. Bakar je također poznat kao jedan od gasioca fluorescencije, što je dodatni izazov za razvoj "*turn-ON*" senzora.

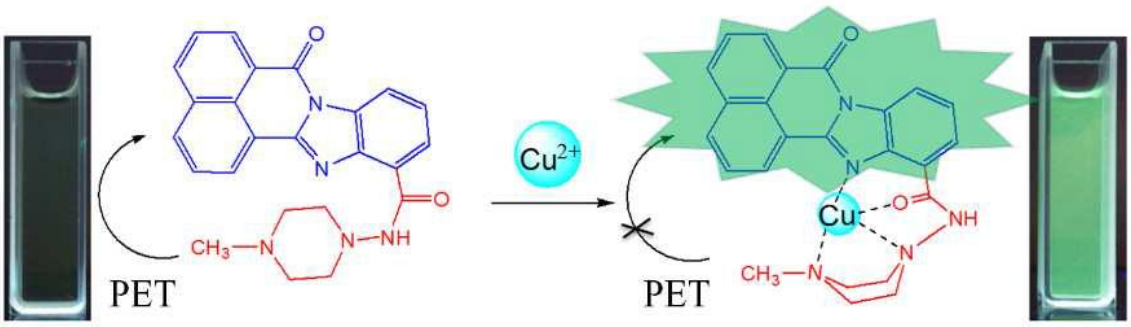

46 **47**

Slika 32. „*Turn-ON*" senzor za bakar temljen na benzimidazolu, preuzeto iz [150].

Proces kompleksiranja derivata benzimidazola i bakra je istraživan u brojnim znanstvenim publikacijama. Postoji čitav niz znanstvenih radova koji opisuju organometalne komplekse s bakrom i tumače prirodu nastalih kompleksa. Iako takvi radovi često niti ne spominju potencijal molekula za uporabu u kemijskim senzorima, istraživanje kompleksiranja derivata benzimidazola i bakra te svojstva novonastalog kompleksa mogu pružiti puno informacija o potencijalnoj senzorskoj primjeni benzimidazolnog liganda. Primjer takvog istraživanja su radovi usmjereni prema razvoju novih materijala ili senzora temeljenih na kompleksima s bakrom, čineći pritom sekundarni senzorski materijal. Naime, velik broj benzimidazolnih derivata koji tvore komplekse s bakrom predstavljeni su kao posredni senzori za anione, temeljem interakcije aniona i organometalnog kompleksa (engl. *displacement approach*). Ovakvim pristupom razvoja senzora se najčešće detektiraju sulfidi [157], no razvijeni su

senzori i za cijanidni ion [155], dopamin [160] ili novi materijali poput organometalnih mreža (engl. *metal organic framework*, MOF) za detekciju hlapivih organska otapala (Slika 33.) [161].

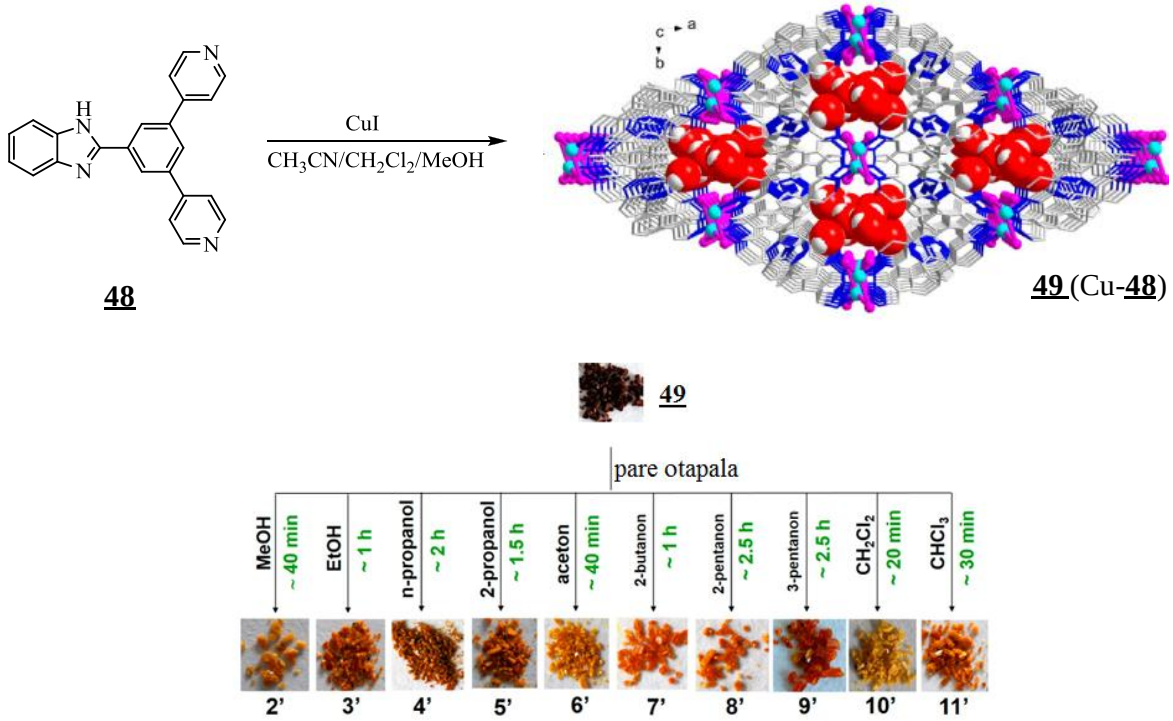

Slika 33. Organometalna mreža **49** (derivat benzimidazola **48** i Cu^{2+}) za detekciju hlapivih organskih otapala, adaptirano iz [161].

Cink je iznimno važan metal za normalno funkcioniranje viših organizama [191]. Sudjeluje u sintezi DNA i RNA, regulira rast stanica i zarastanje rana te je povezan s raznim neurološkim poremećajima, poput Alzheimerove bolesti i epilepsije [192]. Razvoj kemosenzora za cink temeljenih na benzimidazolu je dugo godina aktivno područje istraživanja zbog prikladne veličine iona cinka i većine benzimidazolnih senzorskih sustava. Mnogi istraživači su svoju pažnju usmjerili na dizajn novih malih kemosenzorskih sustava, najčešće vođeni ESIPT mehanizmom [184], no najniža granica detekcije svih razvijenih sustava tek je na mikromolarnoj razini [188]. ESIPT mehanizam se pokazao najboljim mehanizmom za detekciju cinkovih iona upravo zbog veličine atoma koji kompleksira u malu šupljinu takvih spojeva. Onemogućavanje interferencija u sustavu, kao i snižavanje granice detekcije te pomak optičkih svojstava na više valne duljine su i dalje ciljevi u razvoju novih kemosenzorskih sustava za detekciju cinka.

Živa se smatra jednim od najtoksičnijih metala za okoliš i živi organizam. Živin (II) ion je kancerogena supstanca s visokom staničnom toksičnosti. Snažan je neurotoksin te

izaziva niz ozbiljnih zdravstvenih problema kod ljudi, zbog čega je poznavanje koncentracije žive u okolišu vrlo bitno [193]. Razvoj novih osjetljivih i selektivnih senzora za živu je široko područje istraživanja, pri čemu optički senzori omogućuju niz prednosti kao što su visoka osjetljivost, selektivnost, jednostavnost izvedbe, ekonomičnost, brzina izvedbe mjerenja i primjenjivost na licu mjesta. Fluorescentni senzor temeljen na derivatu benzimidazola za određivanje žive s najnižom granicom detekcije razvili su Hu i suradnici [174]. Autori su predstavili konjugat kinolina i benzimidazola koji pokazuje izrazito osjetljivu promjenu boje emisije iz plave u bezbojnu u prisutnosti živinog (II) iona u vodenom mediju. Kinolinski dio molekule se ponaša kao fluorofor, dok je benzimidazol receptorska jedinica predstavljenog senzora. Koordinacija molekule omogućuje reverzibilno vezivanje živinog iona. ^{1}H NMR spektroskopijom utvrđeno je da živa tvori kompleks kelirajući između N atoma benzimidazola i N atoma kinolina, narušavajući pritom konjugiranu i planarnu strukturu što vodi do gašenja fluorescencije. Granica detekcije živinog (II) iona je na nanomolarnoj razini, što čini predstavljeni senzor prikladnim za primjenu u pitkim vodama. Autori su razvili i test trakice za određivanje Hg^{2+} koristeći filter papir kao mikrofluidičku platformu. Trakice filter papira uronjene u koncentriranu otopinu senzorske molekule pružaju informaciju o koncentraciji žive u uzorku golim okom (Slika 34.).

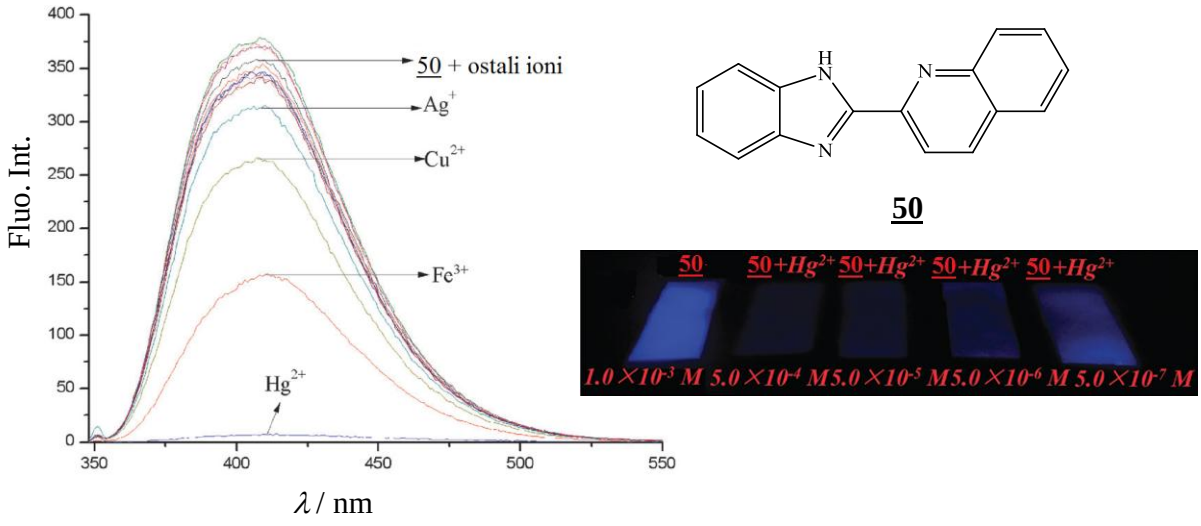

Slika 34. Optički kemijski sezor za živu temljen na derivatu benzimidazola **50**; gašenje fluorescencije uzrokovano koordiniranjem živinog iona (lijevo); test trakice za određivanje žive u uzorku (desno) adaptirano iz [174].

Najveći izazov u razvoju senzora za živu, kao i ostale metale, jest topljivost spojeva u vodi. Većina derivata benzmidazola su netopivi u vodi, što znatno ograničava njihovu primjenu.

Drugi nedostatak je niska valna duljina na kojoj se uočava optički signal, vjerojatno zbog toga što veličina iona žive sprječava korištenje većih π-konjugiranih sustava. Međutim, razvijeni benzimidazolni sustavi ipak su primjenjivi za detekciju metala i u živim organizmima. Uporaba matičnih otopina pripravljenih u organskom otapalu (nevodeni medij) ima i praktičnu primjenu, a dizajnom benzimidazolnog senzora s konjugiranom BODIPY jedinicom znatno su se poboljšala optička svojstva senzora (apsorpcija na većim valnim duljinama) [173].

Željezo je jedan od najvažnijih iona u organizmu. Prijenosnik je kisika u hemoglobinu i sudjeluje u brojnim biokemijskim reakcijama u organizmu. Nedostatak željeza je povezan s brojnim bolestima, kao što su anemija, dijabetes, oštećenje jetre i bubrega, Parkinsonova i Alzheimerova bolest [194]. Senzori za željezo su jedna od najistraživanijih skupina senzora, no i u ovom slučaju je najveći izazov razvoj senzora topljivih u vodi. Konjugat rodamina i benzimidazola predstavljen kao fluorescentni senzor za željezo jedan je od rijetkih primjera benzimidazolnog senzora topljivog u vodi [164]. Kompleksiranjem željeza uočava se izraziti pomak apsorpcijske vrpce (promjena boje iz bezbojnog u crveno, uz izraziti porast molarnog ekstinkcijskog koeficijenta) te povećanje intenziteta fluorescencije. Autori tumače drastičnu promjenu apsorpcijskih svojstava navedenog senzorske molekule kroz otvaranje rodamidnog prstena, što je moguće u području pH 5,8 – 7,4, području bliskom fiziološkim uvjetima. Senzor je također uspješno ispitan kao fluorescentna proba za Fe^{3+} u živim stanicama.
Kompleksi željeza i derivata benzimidazola također mogu biti sekudnarni senzori za anione metodom izmjene kationa / aniona [169] ili novi materijali za biološke primjene [172].

Možda najveći izazov u razvoju benzimidazolnog senzora za metalne katione je priprava senzora koji mogu djelovati u 100% vodenim otopinama. Rješavanju navedenog problema su pristupili Lal i suradnici [163] dizajniranjem benzimidazolnih soli s mogućnosti prepoznavanja metalnih iona (Slika 35.). Autori su također ciljanim dizajnom senzorskih molekula pokušali razviti „*turn-ON*“ senzor za željezo i krom, poseban izazov zbog njihove tendencije gašenja fluorescencije. PET mehanizam kod dva razvijena benzimidazolna sustava je izravno ovisan o dostupnosti i položaju slobodnih elektronskih parova receptora, što su autori iskoristili za moduliranje fluorescentnog odgovora. Sustavi se temelje na benzimidazolu kao fluoroforu, metilenskom i etilenskom mostu kao razmaknicama (engl. *spacer*) te morfolinskoj ili piperidinskoj jedinici kao receptorima.

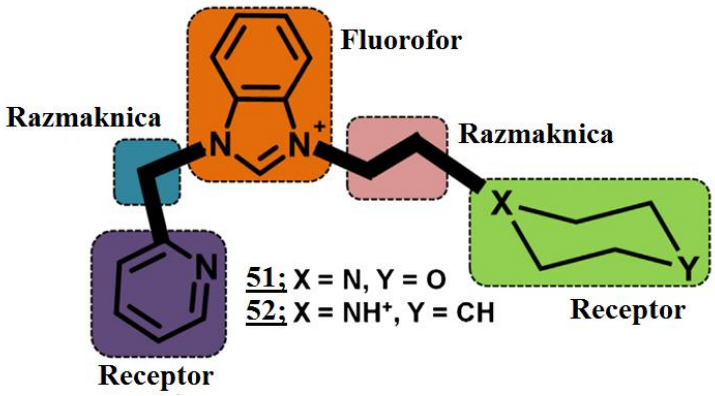

Slika 35. „*Turn-ON*“ optički kemijski sezor za željezo i krom temeljen na derivatu benzimidazola **51** i **52**, adaptirano iz [163].

PET proces je, zbog prisutnosti dva receptora piridina i morfolina, vrlo izražen kod **51**, stoga je intenzitet fluorescencije puno manji nego kod **52**, gdje je PET onemogućen u piperidinskom receptoru. Ispitivanjem utjecaja metalnih iona ne emisijski spektar, utvrđeno je kako je doista spoj **51** „*turn-on*“ senzor za krom, željezo i barij, no neočekivano svojstvo „*turn-OFF“* svojstvo je pokazao **52** za željezo. Željezo je uzročnik gašenja fluorescencije zbog paramagnetičnih svojstava.

Ovakav sustav za određivanje kroma, željeza i barija temeljen na benzimidazolu koji može djelovati u 100% vodenoj otopini ima veliki potencijal za uporabu u biologiji i biokemiji, obzirom da krom i željezo igraju veliku ulogu u mnogim metabolitičkim procesima unutar stanica.

3.4. Anionski senzori temljeni na benzimidazolu

Anioni imaju važnu ulogu u biološkim i industrijskim procesima te procesima koji se odvijaju u okolišu, stoga je razvoj novih malih molekula kao anionskih senzora atraktivno područje istraživanja. Principi određivanja aniona se temelje uglavnom na tri vrste interakcija koje izazivaju promjenu svojstava molekulskog sustava i stvaranje signala: 1) sustavi s proton-donorskom grupom; 2) sustavi temeljeni na izmjeni aniona i indikatora vezanog nekovalentnim vezama; 3) kemijskom reakcijom u prisutnosti aniona (kemodozimetri) [195, 196].

Pregled optičkih kemijskih senzora za anione, temeljenih na derivatima benzimidazola, prikazan je u Tablici 7. Vremenski okvir je odabran prema broju radova dostupnih u literaturi, prema čemu je većina publicirana nakon 2005. godine. Kako je prethodno rečeno, porast broja radova do 2015. godine usko prati i broj citata vezanih za benzimidazolne anionske senzore. Iz rezultata prikazanih u tablici 7. može se zaključiti da su benzimidazolni sustavi za detekciju anionskih vrsta manje zastupljeni od kationskih (24/96 literaturnih referenci, 25 % ukupnog broja prikazanih publikacija). Bitno je napomenuti da je u prethodnom poglavlju prikazan određen broj znanstvenih radova koji opisuju kompleksiranje derivata benzimidazola i metalnog kationa, nakon čega je organometalni kompleks sposoban prepoznati određeni anion. Očito je takav način prepoznavanja aniona (engl. *displacement method*) prikladniji za benzimidazolne senzore. Međutim, određeni broj radova prikazanih u Tablici 7. su uspješno predstavljeni kao direktni anionski senzori.

Tablica 7. Optički kemijski senzori za anione temeljeni na benzimidazolu.

Analit	**Struktura i mehanizam stvaranja signala**	**Granica detekcije**	**Referenca**
COO^-	Bis-benzimidazol, raciometrijski senzor	$2{,}0 \times 10^{-6}$ M	Joo i sur. (2007) [197]
	Bis-benzimidazol	-	Chetia i sur. (2011) [198]
	antracen	-	Kumar i sur. (2012) [199]
multi-anioni	Ciklo[2]benzimidazol, ESIPT	-	Abraham i sur. (2011) [200]
Cl^-	Fenantrolin, PET	-	Shao i sur. (2009) [201]
CN^-	Bis-benzimidazol	270×10^{-6} M	Kumar i sur. (2009) [202]
	Naftalen, ICT	$8{,}8 \times 10^{-8}$ M	Li i sur. (2014) [203]
	Kinazolin, MLTC	$4{,}0 \times 10^{-6}$ M	Wang i sur. (2015) [204]
CN^-/ Cu^{2+}	ESIPT	2×10^{-6} M 1×10^{-6} M	Sen Gupta i sur. (2016) [205]
CN^- / Pb^{2+}	kinazolin	$0{,}05 \times 10^{-6}$ M	Luxami i sur. (2015) [206]
F^-			Yu i sur. (2007) [207]
	Bis-benzimidazol	10^{-7} M	Chetia i sur. (2014) [208]
	BODIPY, PET	93×10^{-9} M	Madhu i sur. (2014) [209]
	Zvjezdolika BI molekula, PET	$0{,}28\text{-}0.56 \times 10^{-6}$ M	Wu i sur. (2016) [210]
F^- i AcO^-	Bis-benzimidazol		Moon i sur. (2007) [211]
F^- / CN^-	ESIPT	$2\text{-}200 \times 10^{-6}$ M $4\text{-}400 \times 10^{-6}$ M	Sen Gupta i sur. (2016) [212]
HSO_3^-	ICT	$0{,}4 \times 10^{-3}$ M	Wang i sur. (2013) [213]
	-	$5{,}3 \times 10^{-8}$ M	Dai i sur. (2015) [214]
SO_3^{2-}	ICT	76×10^{-9} M	Zhang i sur. (2016) [215]
SO_3^{2-} i S^{2-}	Kumarin, FRET	-	Roubinet i sur. (2015) [216]
I^-	Simetrični kompleksni spoj s polidentantnim ligandima	$2{,}1 \times 10^{-6}$ M	Singh i sur. (2007) [217]
	antracen	-	Ghosh i sur. (2010) [218]
ClO_4^-	Bis-benzimidazolni kompleks sa simetričnim ligandima	100×10^{-9} M	Kumar i sur. (2012) [219]
$C_4O_4^{4-}$	Antracen, bis-benzimidazol	-	Ghosh i sur. (2011) [220]

Ciljevi koje istraživači pokušavaju doseći pri razvoju novih anionskih senzora su reverzibilnost, mogućnost višekratne uporabe i optička svojstva u području viših valnih duljina. Navedene karaktersistike su ostvarili Madhu i suradnici [209] uporabom bor-dipirometenskih derivata (BODIPY). Kako je prethodno spomenuto, BODIPY derivati posjeduju atraktivna svojstva, kao što su oštra apsorpcijska vrpca, intenzivna fluorescencija, visoki kvantni prinos fluorescencije i dobru kemijsku i fotokemijsku stabilnost. Uvođenjem različitih supstituenata na BODIPY jezgru, omogućava se fino podešavanje optičkih i kiselo-baznih svojstava sustava. Poznato je također da benzimidazolni i imidazolni derivati posjeduju proton donorsku skupinu (=NH) u svojoj prstenastoj strukturi, što je potencijalno bitna karakteristika za anionske senzore [221]. Reverzibilni kemosenzor za detekciju fluoridnih iona razvijen je konjugacijom benzimidazolne jezgre kao anionskog receptora (crveno) i BODIPY jedinice kao fluorofora (crno) te prikazan na Slici 36 [209]. Detekcija fluoridnog iona se uočava i golim okom, promjenom boje od fluorescentne roze do nefluorescentne plave pri vezivanju aniona. Mehanizam stvaranja signala autori pripisuju fotoinduciranom prijenosu elektrona (PET) od benzimidazolne do BODIPY jedinice, koji je omogućen prekidom intramolekulskih vodikovih veza između dvije jedinice vezivanjem fluoridnog iona te povećanjem elektronske gustoće imidazolnog dijela molekule. Stoga se dodatkom fluoridnih iona uočava spektralni pomak u apsorpcijskom spektru i značajni pad intenziteta fluoresencije. Dodatak drugih aniona nije uzrokovao spektralne promjene. Svojstva senzora su ispitana titracijom fluoridnim ionima spektrofotometrijskim i elektrokemijskim tehnikama, te je ispitivan utjecaj pH. Protoniranjem molekule (protoniranjem benzimidazolnog imino dušika) ponovno se onemogućuje fotoinducirani prijelaz elektrona te se optička svojstva molekule vraćaju u prvobitno stanje.

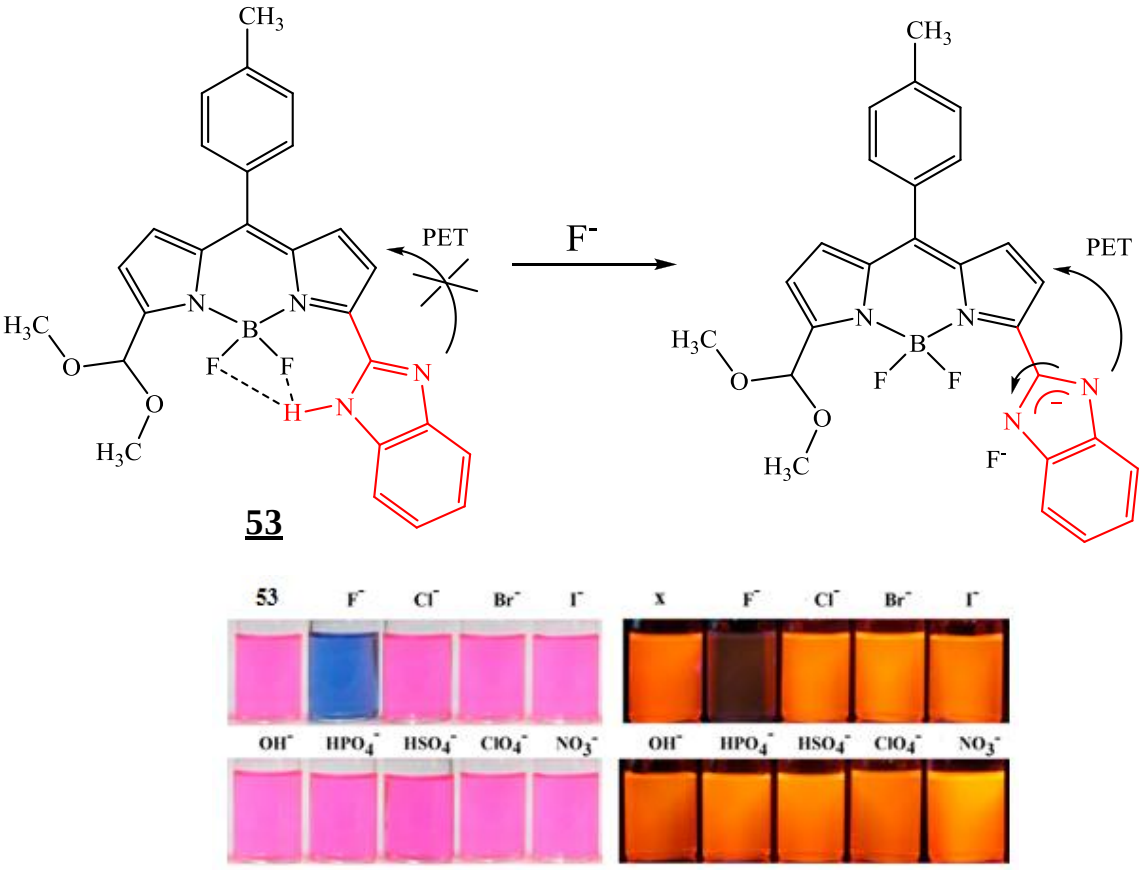

Slika 36. Senzor za F^- temeljen na fotoinduciranom prijenosu elektrona između benzimidazolne i BODIPY jedinice, adaptirano iz [209].

3.5. Senzori za neutralne molekule temeljeni na benzimidazolu

Određivanje i praćenje velikog broja neutralnih molekula i biomolekula u organizmu i okolišu je izuzetno važno za zdravlje ljudi ili odvijanje niza bioloških ili ekoloških procesa, pri čemu optički senzori pružaju mogućnost jednostavne uporabe i visoke osjetljivosti. Razvoj optičkih senzora za molekule kao što su dopamin i drugi neurotransmiteri, aminokiseline, CO_2 i glukoza, od izuzetne je važnosti za napredak ljudskog zdravlja i očuvanje okoliša. Senzori za neutralne molekule temeljeni na benzimidazolu su rijetki te se njihov mehanizam prepoznavanja uglavnom odvija u više stupnjeva (stvaranje primarnog kompleksa s metalom, deprotonacija i slično).

Benzimidazolni derivati mogu biti sastavni dio organometalnih mreža za prepoznavanje lako hlapivih spojeva [161], a predstavljeni su i senzorski sustavi za heparin, vodu, ATP i slično (Tablica 8.). Iz rezultata prikazanih u Tablici 8, uočava se da je broj benzimidazolnih spojeva kao senzora za neutralne molekule znatno manji naspram broja senzora za katione i anione (13/96 literaturnih referenci, 14 % ukupnog broja publikacija). I u ovom slučaju, kao i kod kationskih senzora, bitno je napomenuti da u literaturi postoje radovi u kojima se opisuje reaktivnost benzimidazola s neutralnim molekulama u smislu razvoja novih lijekova i slično. Benzimidazolna jezgra je često primjenjivana u farmaceutici i biologiji, a biološka aktivnost benzimidazolnih spojeva je dominantna u istraživanju ove klase spojeva. Stoga, takve publikacije vrlo slabo spominju derivate benzimidazola kao potencijalne senzore za neutralne molekule, no svakako mogu pružiti korisne informacije o karakteristikama benzimidazolnih senzorskih molekula.

Tablica 8. Optički kemijski senzori za neutralne molekule temeljeni na benzimidazolu.

Analit	Konjugirana jedinica	Mehanizam stvaranja signala	Granica detekcije	Referenca
anilin	Bis-BI i piridin	Stabilni supramolekulski adukt	-	Zhang i sur. (2009) [222]
CO_2	Aza-indacen	-	$4{,}1 \times 10^{-7}$ M	Ishida i sur. (2013) [223]
cistein	Benzimidazolil trikation	PET	48×10^{-9} M	Singh i sur. (2015) [224]
glukoza	kompleks derivata BI i vanadija	MLCT	-	Fernandez i sur. (2016) [225]
heparin	Benzimidazolil sustav	-	$0{,}1\text{-}10 \times 10^{-6}$ M	Wang i sur. (2008) [226]
voda	rodamin	FRET	0,0026 v/v%	Pal i sur. (2014) [227]
		ICT	0,565 v/v%	Nandi i sur. (2016) [228]
ATP	Piperazin kao most	-	-	Ghosh i sur. [229]
NO	naftalen	-	-	Oujang i sur. (2008) [230]
Asparaminska i glutaminska kiselina	piridin	-	-	Das i sur. (2010) [231]
H_2S	-	-	-	Ding i sur. (2013) [232]
DNA	-	-	-	Dumat i sur. (2016) [233]
homocistein	-	ESIPT	$9{,}02 \times 10^{-6}$ M	Tang i sur. (2016) [234]

Primjer senzora temeljenog na benzimidazolu za detekciju neutralnih molekula je senzor za CO_2 prikazan na Slici 37. Molekulski senzor je temeljen na šesteročlanoj prstenastoj strukturi povezanoj trifluormetil metinskim mostom [223]. Sustav može djelovati kao kolorimetrijski i fluorimetrijski senzor za CO_2 uz prethodnu deprotonaciju -NH skupine na pirolu uz pomoć fluoridnog aniona. Stvaranje kompleksa s fluoridnim anionom, odnosno deprotonacija -NH na pirolnom prstenu, uzrokuje batokromni pomak u apsorpcijskom spektru i gašenje fluorescencije. Ukoliko je uzorak spoja izložen struji plina CO_2, u apsorpcijskom i fluorescencijskom spektru se uočavaju izrazite promjene koje se pripisuju strukturi početnog spoja **54**, odnosno senzor je reverzibilan.

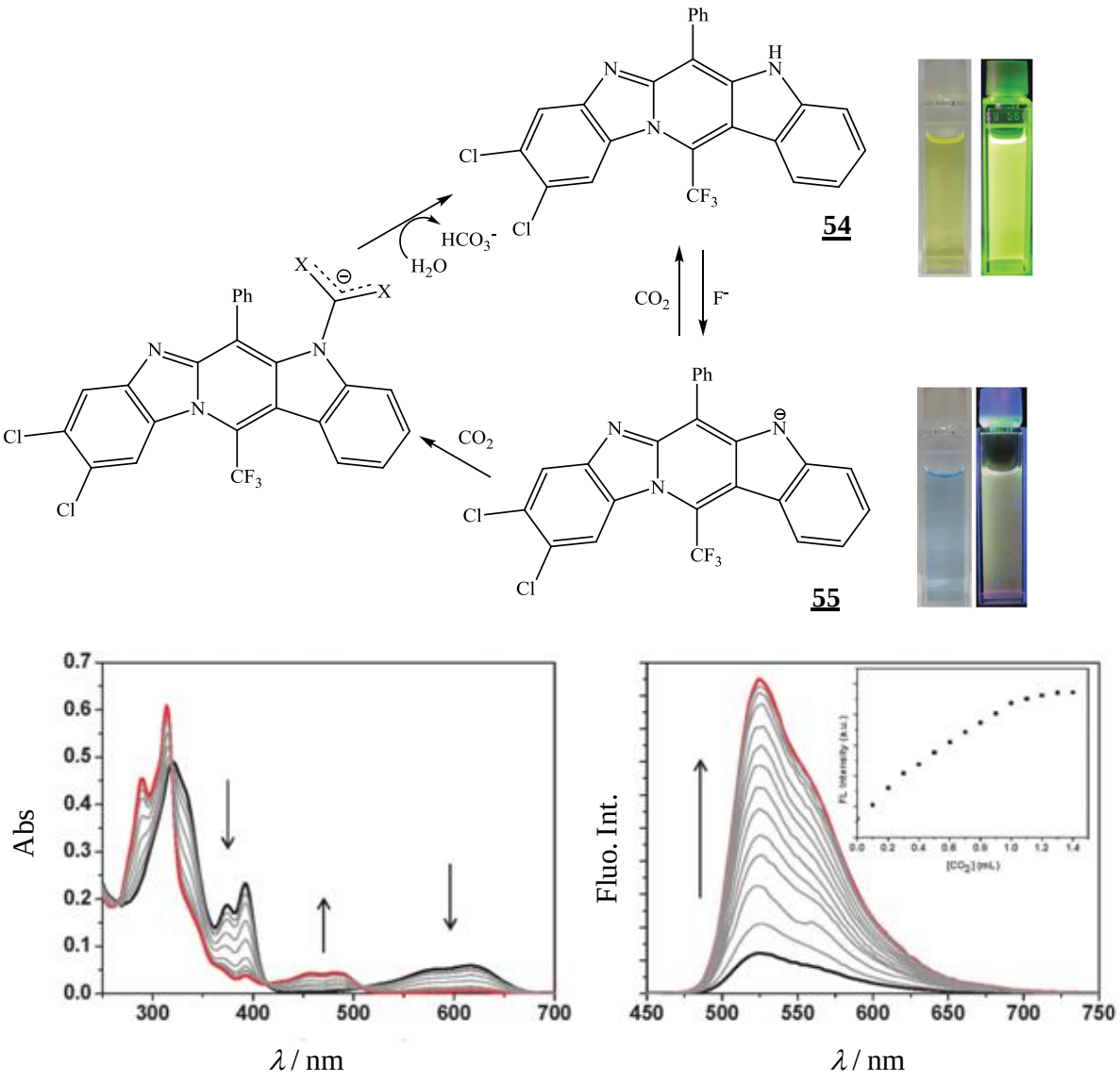

Slika 37. Optički kemijski senzor za CO_2 temeljen na derivatu benzimdiazola, adaptirano iz [223].

3.6. Senzorski materijali temeljeni na derivatima benzimidazola

Kontrola nad raznovrsnim fluorescentnim odgovorima molekule otvara nove funkcionalne mogućnosti i primjenu kemosenzorskih sustava u razvoju optički osjetljivih materijala. Stvaranje pametnih molekulskih senzora je omogućeno imobilizacijom na površinu heterogenih sustava [28, 31, 235] ili integracijom u nanočestice [32, 236-238]. Najjednostavnija izvedba senzorskog materijala je priprava polimera unutar kojeg je fizički zarobljena kemosenzorska molekula. Izbor polimera ovisi o propusnosti polimera za određeni analit, njegovoj stabilnosti, dostupnosti i sposobnosti imobilizacije. Mikrookruženje polimera ima jak utjecaj na spektralna svojstva imobilizirane molekule, vrijednosti pK_a i vrijeme života fluorescencije. Najčešće korišteni polimeri u pripravi kemijskih optičkih senzora su derivati celuloze i hidrogelovi zbog odličnih mehaničkih svojstava, stabilnosti pri različitim temperaturama i vrijednostima pH te visoke propusnosti za vodu, ione ili neotopljene plinove. Polimeri kao što su poliuretan i pHEMA su kompatibilni s biološkim materijalima, što otvara nove mogućnosti primjene takvih senzora. Zanimljivo je uočiti činjenicu da u pretrazi literature u sklopu ovog rada nije pronađen velik broj radova o senzorskim materijalima temeljenim na derivatima benzimidazola. Predstavljene su PVC ion-selektivne optode za mjerenje iona srebra [133], no većina ostalih literaturno dostupnih PVC membrana temeljenih na derivatima benzimidazola se zasniva na elektrokemijskim postupcima detekcije analita [239, 240].

Primjer novog polimernog materijala osjetljivog na prisutnost željeza i fosfata u uzorku sline su predstavili Saikia i sur. [172]. Neutralni poli(9,9-bis(60-benzimidazol)heksil)fluoren-alt-1,4-fenilen (PBP) **56** je fluorescentni polimer čiji se fluorescentni odgovor izrazito pojačava ili smanjuje u prisutnosti analita, toliko da ga autori nazivaju „supergasiocem“.

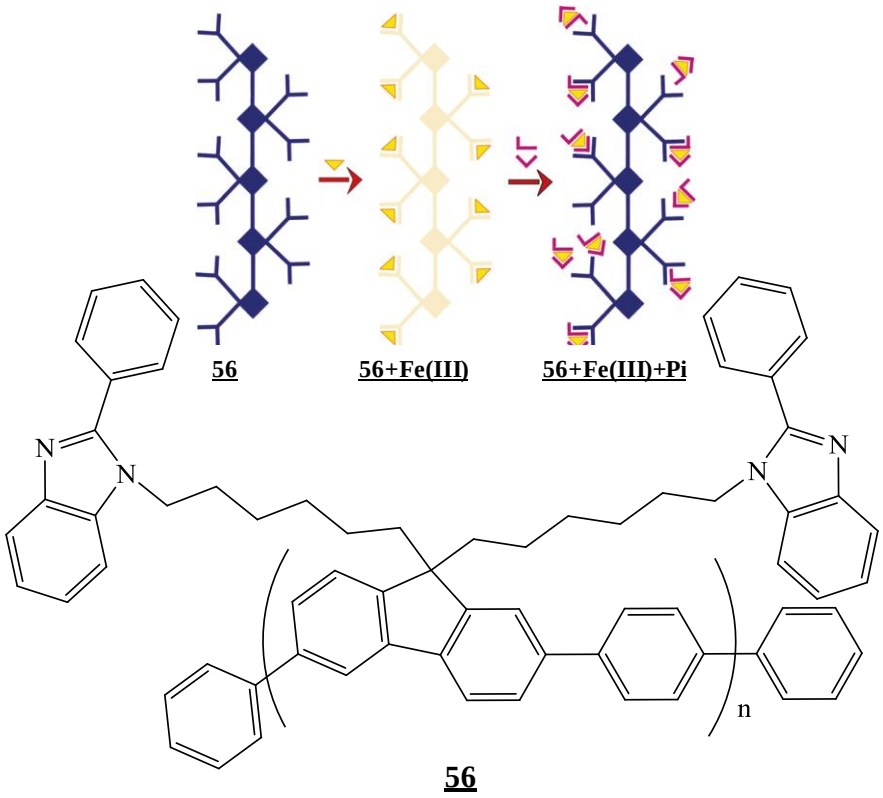

56

Slika 38. Primjer fluorescentnog polimera temeljenog na derivatu benzimidazola, adaptirano iz [172].

Sol-gel postupak je česta metoda priprave optičkih kemijskih senzora [241]. Sol je stabilna disperzija koloidnih čestica ili polimera u otapalu, dok se gel sastoji od trodimenzionalne kontinuirane mreže (na primjer mreže SiO_2) koja zatvara tekuću fazu. Sol-gel materijali su vrlo popularni za izradu nanosenzora. Porozni su kako bi analit slobodno mogao difundirati, robusni i biokompatibilni, što ih čini pogodnim za unutarstanična mjerenja. Indikatorske molekule su obično zarobljene unutar pora takvih sustava. Hoffman i sur. su predstavili nove fluorescentne materijale temeljene na benzimidazolu pripravljene sol-gel postukom [242].

Prethodno spomenuti flurofori s mogućnosti intenzivne fluroescencije u agregiranom stanju (AIE emiteri) se također mogu opisati kao novi materijali [99, 101-103]. Naime, fluorofori koji emitiraju u krutom stanju su izrazito rijetki zbog koncentracijskog efekta koji najčešće uzrokuje gašenje fluorescencije. Crveni flurofori su pritom najmanje raširena skupina spojeva, no promatranjem i tumačenjem spojeva kroz fenomen emisije izazvane agregacijom omogućuje se dizajn i priprava novih pametnih fluorofornih sustava. Njihova primjena je izrazito potrebna u području razvoja optoelektroničkih uređaja, no i kemijski senzorski sustavi se mogu temeljiti na selektivnim promjenama spektralnih svojstava agregiranih fluorofora u otopinama ili čvrstom stanju.

3.7. Zaključci pregleda i pravci razvoja

Pregledom literature o optičkim kemijskim senzorima temeljenim na derivatima benzimidazola omogućen je uvid u područje razvoja i primjene ove klase spojeva. Izvedeni su zaključci o prednostima i manama postojećih fluorofora i kemosenzorskih molekula te su određene smjernice za daljnji dizajn i razvoj novih kemosenzorskih sustava.

Benzimidazolna jezgra u većini opisanih kemosenzorskih sustava ima ključnu ulogu u stvaranju analitičkog signala. Planarna benzimidazolna jezgra znatno doprinosi konjugiranosti sustava, zbog čega je sastavni dio velikog broja fluorofora. Svi prikazani derivati benzimidazola posjeduju svojstvo fluorescencije, stoga većina senzora temeljenih na benzimidazolu koristi fluorescenciju kao analitički signal. Utjecaj elektron-donorskih i elektron-odvlačećih supstituenata na osnovne molekulske kosture benzimidazolnih molekula je aktivno i atraktivno područje istraživanja, osobito za razvoj novih fluorofora optimiziranih fluorescentnih odgovora. Dizajn i optimizacija molekulskog fluorescentnog sustava se u velikom broju radova temelji na molekulskom modeliranju i rezultatima prikupljenim prema principima računalne kemije. Sve je češća karakterizacija spojeva u krutom stanju ili tankim filmovima, osobito planarnih benzimidazolnih sustava koji se lako mogu primjenjivati u optoelektronici (OLED i slično).

Benzimidazolna jezgra je ključna strukturna jedinica u molekulskim senzorima za određivanje vrijednosti pH. Svi pH senzori se temelje na promatranju kiselo-bazne ravnoteže imino dušika, odnosno protonaciji / deprotonaciji dušika unutar benzimidazolne jezgre. Slobodan elektronski par na dušiku također sudjeluje u koordiniranju metalnih iona. Većina metalnih kationa koji se mogu određivati benzimidazolnim senzorima su kationi teških metala. Prema HSAB teoriji (teorija tvrdih i mekih kiselina i baza) baziranoj na polarizibilnosti i sličnim fizikalno-kemijskim parametrima, donorski imini su meki ligandi pogodni za vezanje prijelaznih metala, stoga ne čudi razvoj većeg broja senzora za prijelazne metale. Međutim, uspješno je predstavljen i manji broj senzora za alkalijske i zemnoalkalijske metale zahvaljujući lakoj funkcionalizaciji benzimidazola te mogućnosti stvaranja konjugata benzimidazola i drugih kationskih receptora (npr. krunastih etera). Optički senzori temeljeni na benzimidazolu rade na principu različitih mehanizama stvaranja fluorescentnog signala. Međutim, senzori temeljeni na PET mehanizmu su najčešća vrsta zbog jednostavnosti izvedbe mjerenja („*ON-OFF*“ princip).

Iako su uspješno predstavljeni kemosenzorski sustavi za detekciju velikog broja analita, vrlo je mali broj derivata prikladan za rad u čistom vodenom mediju. Stoga, daljnji razvoj optičkih kemijskih senzora temeljenih na derivatima benzimidazola se mora usmjeriti prema primjeni spojeva u vodenom mediju na temelju adekvatne funkcionalizacije ili imobilizacije u (nano)materijale. Većina senzora pokazuje odziv u spektralnom području 200 – 600 nm, što je prikladno za većinu primjena u pogledu optoelektroničkih instrumentacijskih zahtjeva. Međutim, odziv na višim valnim duljinama (oko 700 – 800 nm) pruža mogućnost primjene spojeva u biologiji i biokemiji, gdje su derivati benzimidazola vrlo atraktivna klasa spojeva za ispitivanja zahvaljujući svojoj biološkoj aktivnosti. Stvaranje senzorskih (nano)materijala imobilizacijom spojeva na određeni supstrat u ovoj klasi optički osjetljivih molekula je demonstrirano kroz tek nekoliko znanstvenih radova. Većina funkcionalnih optičkih materijala opisanih u literaturi su karakterizirani elektrokemijskim ili drugim metodama, stoga su optički materijali za senzorsku primjenu temeljeni na benzimidazolu još uvijek nedovoljno istraženo područje.

4. CILJEVI ISTRAŽIVANJA

Cilj ovog doktorskog rada je razvoj novih kemosenzorskih molekula i funkcionalnih optičkih materijala temeljenih na benzimidazolu. Sustavna karakterizacija fotofizičkih, kiselo-baznih i kompleksirajućih svojstava novosintetiziranih skupina kromofora (fluorofora) temeljenih na benzimidazolu u otopinama i polimernim matricama omogućuje prikupljanje bitnih znanja o odnosu strukture i svojstava ispitivane klase fluorofora. Rad izravno doprinosi širokom znanstvenom području istraživanja i primjene heterocikličkih fluorofora, u kojem interes pronalaze istraživači iz područja analitičke, organske i fizikalne kemije, kemije materijala, medicine i biokemije.

Konačni cilj doktorskog rada je razvoj novih kemosenzorskih molekula za određivanje pH ili metala u otopini i senzorskih materijala za primjenu u kemijskim optičkim sustavima. Detaljna fotofizička karakterizacija nekoliko klasa benzimidazolnih spojeva te ispitivanje njihovih senzorskih svojstava u otopinama i tankim filmovima omogućuje racionalni dizajn novih fluorofora u budućim istraživanjima.

Naposljetku, svaka karakterizacija novih i neistraženih spojeva, poput predstavljenih klasa benzimidazolnih spojeva, može rezultirati neočekivanim otkrićima novih svojstava, potencijalno primjenjivih u širokom istraživačkom području.

5. REZULTATI I RASPRAVA

U ovom poglavlju su kritički raspravljeni rezultati dobiveni u sklopu izrade doktorskog rada, objavljeni u znanstvenim časopisima te priloženi u nastavku disertacije:

Rad 1

E. Horak, R. Vianello, M. Hranjec, S. Krištafor, G. Karminski Zamola, I. Murković Steinberg, Benzimidazole acrylonitriles as multifunctional push-pull chromophores: spectral characterization, protonation equilibria and nanoaggregation in aqueous solutions, *Spectrochimica Acta Part A* 178 (2017) 225-233. (IF: 2,653, Q2)

Rad 2

E. Horak, M. Hranjec, R. Vianello, I.M. Steinberg, Reversible pH switchable aggregation-induced emission of self-assembled benzimidazole-based acrylonitrile dye in aqueous solution, *Dyes and Pigments* 142 (2017) 108-115. (IF: 4,055, Q1)

Rad 3

M. Hranjec, **E. Horak**, D. Babic, S. Plavljanin, Z. Srdovic, I. M. Steinberg, et al., Fluorescent benzimidazo[1,2-*a*]quinolines: synthesis, spectroscopic and computational studies of protonation equilibria and metal ion sensitivity, *New Journal of Chemistry*, 41 (2017) 358-71. (IF: 3,277, Q2)

Rad 4

E. Horak, P. Kassal, M. Hranjec, I.M. Steinberg, Benzimidazole functionalised Schiff bases: novel pH sensitive fluorescence turn-on chromoionophores for ion-selective optodes, *Sens. Actuator B-Chem.* (rad poslan na recenziju, IF: 4,758, Q1)

Rad 1 predstavlja karakterizaciju novih molekula iz obitelji akrilonitrilnih bojila (cijano-supstituirani stirilni derivati benzimidazola) za primjenu u senzorima za određivanje pH. Stiril-cijaninska bojila pronalaze široku primjenu u tehnologiji lasera, kao fluorescentne probe u biologiji i medicini (označavanju proteina i sekvencioniranje DNA), bojila, optički uređaji, solarni sustavi i kozmetički sastojci. Benzimidazolni derivati ove klase spojeva pružaju novu platformu za ispitivanje kiselo-baznih i kompleksirajućih svojstava novih kromofora (fluorofora) i razvoj novih kemosenzorskih sustava.

Organski sustavi s takozvanom *push- pull* strukturom (elektron donor- π konjugirani most - elektron akceptor sustavi) su široko upotrebljavani u području medicine, biologije ili

funkcionalnih materijala. Njihov senzorski mehanizam se temelji na intramolekulskom prijenosu naboja. Utjecaj prirode supstituenata i položaja na π-konjugiranom kosturu znatno utječu na fotofizička i senzorska svojstva ove vrste flurofora. Benzimidazolna jezgra u D-π-A sustavima može znatno modulirati fluorescentni odgovor kemosenzorske molekule. Planarna konjugirana struktura koja se lako funkcionalizira različitim supstituentima, delokalizirani elektroni i slobodni elektronski par na dušiku unutar benzimidazolne jezgre pružaju različite mogućnosti uporabe benzimidazolnih derivata u optički osjetljivim sustavima. Osim sastavnog dijela kromofora, benzimidazol u optičkim senzorima može biti i ključna funkcionalna jedinica odgovorna za prepoznavanje analita.

Fotofizička i kiselo-bazna svojstva četiri akrilonitrilna derivata benzimidazola su sustavno okarakterizirana spektrofotometrijskim metodama u različitim otapalima i plastificiranim PVC matricama. Spojevi **1** i **2** su uvođenjem elektron donorske *N*,*N*-dimetilamino skupine pretvoreni u D-π-A molekulske sustave (spojevi **3** i **4**), što čini temelj rasprave o odnosu strukture i svojstava. Dizajn kemosenzorskih molekula je prikladan za uporabu u optičkim senzorima za pH zbog postojećih protonabilnih mjesta i D-π-A molekulske strukture koja omogućava apsorpciju u vidljivom spektralnom području. Tumačen je odnos strukture i svojstava ispitivanih spojeva u različitim otapalima, pri čemu je uočen očekivani trend u fotofizičkim svojstvima spojeva u odnosu na polarnost otapala. Batokromni pomak u apsorpcijskim spektrima je uočen kod spojeva **3** i **4** u odnosu na roditeljske spojeve **1** i **2** zbog prisutnosti *N*,*N*-dimetilamino skupine koja zbog slobodnog elektronskog para na dušiku znatno doprinosi konjugiranosti sustava. Apsorpcija u vidljivom području elektromagnetskog spektra i visoka vrijednost molarnog apsorpcijskog koeficijenta omogućuje primjenu spojeva spojeva **3** i **4** kao kromofora u optičkim sustavima. Spojevi **3** i **4** su potom detaljno karakterizirani kao senzori za pH zahvaljujući izraženoj promjeni spektralnih svojstava pri protonaciji.

Određene su vrijednosti pK_a u vodenim otopinama (99:1 volumni omjer H_2O:MeOH) te su uz pomoć molekulskog modeliranja i računalne kemije (suradnja s dr. sc. Robertom Vianellom, Institut Ruđer Bošković) određena mjesta protoniranja spojeva. U istraživanim uvjetima najveću promjenu spektralnih svojstava donosi ravnoteža između neutralne i monokationske ionske vrste. Promatrana ravnoteža se odnosi na protoniranje benzimidazolnog dušika, a vrijednosti pK_a se nalaze u kiselom području (pK_a = 2,1 – 3,0). Međutim, imobilizacijom spojeva u plastificirane polimerne matrice uvjetne vrijednosti pK_a se, zbog različitih ionskih izmjena prisutnih u takvom heterogenom sustavu, pomiču prema višim vrijednostima (pK_a =

6,3), što omogućava potencijalnu primjenu pripravljenih membrana u optičkim kemijskim senzorima.

Usporedbom spojeva dostupnih u literaturi i novih cijano-supstituiranih akrilonitrila (stiril-cijanina) dobiva se uvid u značaj i utjecaj cijano skupine supstitiranih stirilnih derivata. Utjecaj cijano skupine se najviše očituje za ispitivani spoj **3**. Naime, spojevi **1**-**4** su vrlo slabo fluorescentni u svim ispitivanim medijima, stoga je njihov potencijal za primjenu u senzorima za pH isključivo kolorimetrijski. Međutim, spoj **3** u vodenom mediju stvara nanokristalinične strukture koje zbog novonastalih interakcija emitiraju svjetlost nekoliko puta jačeg intenziteta. Narančasto-crvena emisija se uočava na visokim valnim duljinama (λ = 600 nm), a prisutnost nanokristala je dokazana Tyndallovim testom i raspodjelom veličina čestica dobivenom dinamičkim raspršenjem svjetlosti. Uočena pojava se naziva emisija izazvana agregacijom (engl. *Aggregation induced emission,* AIE) te se u literaturi opisuje tek u posljednjem desetljeću. AIE posjeduje velik potencijal za primjenu u različitim područjima, pa tako i u području optičkih senzorskih sustava. Izazov je primijeniti novu i nedovoljno istraženu pojavu u optičkom sustavu, kao što je AIE, no ujedno i velik potencijal za razvoj novih optičkih senzora.

Rad 2 opisuje primjenu fenomena emisije izazvane agregacijom u optičkom senzorskom sustavu. Emisija izazvana agregacijom (engl. *Aggregation induced emission*, AIE) je uočena kod ispitivanog 2-benzimidazolil supstituiranog akrilonitrilnog bojila, u ovom radu nazvanog **BIA**, te demonstrirana kao mehanizam reverzibilne pH osjetljivosti. Primjena klasičnih fluorofora u optičkim kemijskim senzorima je često ograničena, jer se zbog pojave agregacije i gašenja fluorescencije pri većim koncentracijama često moraju upotrebljavati vrlo razrijeđene otopine. Stoga, razvoj fluorofora s izraženom fluorescencijom u agregiranom obliku sasvim mijenja pogled na ovu vrstu nuspojave. Emisija izazvana agregacijom se naglo počinje primjenjivati u raznim područjima, no uglavnom se temelji na poznatim AIE molekulama (tetrafenileteneski ili heksafenilsilolni derivati). Vrlo malo benzimidazolnih derivata je opisano u AIE, pri čemu benzimidazolna jezgra najčešće nije ključna funkcionalna jedinica. AIE molekule su opisane i u području optičkih kemijskih senzora, no također treba naglasiti da je reverzibilnih AIE sustava za određivanje pH vrlo malo. Stoga, benzimidazolni derivat **BIA** predstavlja potpuno novu klasu spojeva u grupi agregacijom izazvanih emitera i njihove primjene u optičkim kemijskim senzorima.

BIA je donorsko-akceptorski molekulski sustav povezan π-konjugiranim mostom, pri čemu je benzimidazol glavna funkcionalna jedinica. Planarna benzimidazolna jezgra omogućuje

samoudruživanje molekula **BIA** u agregate (engl. *self assembly*). Osim benzimidazolne jezgre koja doprinosi rigidnosti sustava, položaj i vrsta supstituenta ima značajan utjecaj na pakiranje molekula i interakcije unutar novonastalih struktura koje omogućavaju AIE. Usporedbom sličnih spojeva u literaturi i prethodno opisanom radu (rad 1), koji ne posjeduju AIE svojstvo, dolazimo do zaključka da je ciano skupina jedan od ključnih faktora u opisanom AIE sustavu. Literaturno dostupni spoj iste strukture kao i **BIA**, no bez ciano supstituenta, ne pokazuje svojstvo emisije izazvane agregacijom, kao i mnogo drugih literaturno dostupnih primjera. Benzimidazolni protonabilni dušik omogućuje pH osjetljivost kemosenzorskog sustava, koja je u radu 1 demonstrirana u nevodenom mediju i polimernoj matrici. pH osjetljivost **BIA** se uočava i u vodenom mediju, pri čemu se ionske vrste razlikuju u fotofizičkim svojstvima zbog procesa agregacije molekula **BIA** u neutralnom stanju. Predstavljen je novi AIE molekulski sustav čija se osjetljivost na pH pripisuje mehanizmu agregacije-deagregacije.

Ispitana su fotofizička svojstva **BIA** u otopinama, agregiranom i krutom stanju. Apsorpcija i emisija **BIA** je karakterizirana u smjesama otapala etanol-H_2O, THF-H_2O i DMSO-H_2O. Dodatkom vode u otopinu **BIA** apsorpcijski i emisijski spektar ostaje nepromijenjen sve do 80% vode, nakon čega je vidljivo nastajanje novog apsorpcijskog maksimuma na 350 nm i emisijskog maksimuma na 600 nm. Narančasto-crvena emisija u vodenim otopinama (λ = 600 nm) se pripisuje stvaranju nanokristaliničnih struktura **BIA**. Prisutnost nanoagregata je dokazana Tyndallovim testom i raspodjelom veličina čestica dobivenom dinamičkim raspršenjem svjetlosti. Nanoagregati pripravljeni iz etanola, DMSO-a i THF-a se razlikuju po strukturi i veličini, što se može pripisati različitim utjecajima molekula otapala na brzinu i način stvaranja agregata. Pripravljeni agregati su karakterizirani SEM mikroskopijom.

Najatraktivnija karakteristika opisanog **AIE** sustava je njegova pH osjetljivost temeljena na mehanizmu agregacije-deagregacije. pH titracijama je dokazana reverzibilna protonacija i deprotonacija spoja, pri čemu je on u neutralnom mediju u agregiranom stanju. Intenzivna narančasto-crvena fluorescencija se uočava u rangu vrijednosti pH 5 do 8, dok u području 1,5 do 5 fluorescira slabom tirkiznom fluorescencijom, te u području 9 do 13 slabom zelenom fluorescencijom. Vrijednosti pri kojima dolazi do agregacije-deagregacije blisko odgovaraju pK_a vrijednostima izračunatim molekulskim modeliranjem. Dobiveni rezultati pokazuju potencijalnu primjenu za određivanje unutarstanične vrijednosti pH, a **BIA** svojom narančasto-crvenom emisijom u krutom stanju može pronaći potencijalnu primjenu u optoelektroničkim sustavima.

Rad 3 predstavlja novu klasu benzimidazolnih derivata kao novih senzora za pH i metalne ione. Benzimidazo[1,2-*a*]kinolini su ciklički derivati benzimidazola koji u svojoj strukturi imaju 4 aromatska kondenzirana prstena, tj. benzimidazolni prsten kondenziran s kinolinskom jezgrom. Ciklički derivati benzimidazola posjeduju vrlo izraženu antitumorsku aktivnost i stupaju u interakciju s biološki važnim molekulama poput molekule DNA. Također, ciklički derivati benzimidazola pokazuju svojstva intenzivne fluorescencije i širokog ranga primjenjivosti i uporabe u optičkim senzorskim sustavima.

Novosintetizirani derivati **3-6** spektrofotometrijski su okarakterizirani u različitim otapalima te je ispitan utjecaj pH i mogućnost kompleksiranja metalnih iona. Sinteza i spektralna karakterizacija osnovnih fotofizičkih svojstava ispitivanih spojeva je provedena na Zavodu za organsku kemiju u istraživačkoj grupi izv. prof. dr. sc. Marijane Hranjec. Visoki kvantni prinos fluorescencije se općenito uočava kod amino-supstituiranih derivata na položaju 2 zbog olakšanog intamolekulskog prijenosa naboja. Nekoliko protonabilnih mjesta na položajima koji mogu znatno utjecati na ICT proces omogućuje primjenu ove vrste molekula u senzorima za pH. Spojevi su detaljno karakterizirani spektrofotometrijskim metodama te su određene njihove uvjetne vrijednosti pK_a u vodenom mediju (99:1 volumni omjer H_2O:EtOH). Spoj **3** je izdvojen kao potencijalni kadnidat za razvoj novog senzora za pH obzirom na visoku vrijednost kvantnog prinosa fluorescencije (Φ = 0.65), no vrijednost pK_a u kiselom području (pK_a = 3,31) ne odgovara u većini područja primjene. Međutim, fotofizička svojstva spoja **6** su također prikladna za uporabu u optičkim kemijskim senzorima. Protoniranjem spoja **6** intenzitet fluorescencije raste i nekoliko desetaka puta. Vrijednosti pK_a ispitivanog spoja su pK_{a1} = 3,45 i pK_{a2} = 9,14 te se blisko slažu s izračunatim vrijednostima pK_a. Potaknuti prethodno dobivenim rezultatima selektivnog kompleksiranja cinka sličnog cikličkog benzimidazolnog derivata, provedene su titracije s metalnim ionima. Svi ispitivani spojevi su osjetljivi na prisutnost metala što se uočava po gašenju fluroescencije i smanjenju intenziteta apsorbancije. Međutim, selektivnost ispitivanih kemosenzorskih molekula nije dovoljno izražena. Detaljna karakterizacija kompleksiranja spoja **6** i Cu^{2+} i teorijski izračun vrijednosti pK_a su provedeni računalnim metodama u suradnji s dr.sc. Robertom Vianellom (Institut Ruđer Bošković).

Razvoj novih senzora za pH temeljenih na Schiffovim bazama je prikazan u **radu 4**. Schiffove baze su jedna od najistraživanijih skupina organskih spojeva. Osim širokog spektra biološke primjene, često su korištene kao kelatni ligandi u koordinacijskoj kemiji prijelaznih metala. Schiffove baze temeljene na benzimidazolu čine zanimljivu klasu kemosenzorskih

molekula zbog izraženih promjena spektralnih svojstava pri interakciji s analitom. Ispitivani derivati benzimidazola, strukturno opisani kao Schiffove baze, mogu se promatrati kao D-π-A molekulski sustavi. Spojevi posjeduju slabu fluorescenciju u većini otapala, a intenzitet i valna duljina emitirane svjetlosti ovisi o polarnosti otapala. Batokromni pomak se uočava s porastom polarnosti otapala za sve ispitivane spojeve, kako je i pretpostavljeno za D-π-A molekulske sustave. Detaljna karakterizacija kiselo-bazne ravnoteže i spektralnih svojstava ispitivanih spojeva u ovisnosti o pH je provedena u vodenom i nevodenom mediju. Izračunate su uvjetne vrijednosti pK_a (95:5 volumni omjer EtOH:H_2O) koje iznose p$K_a \approx 4$. Međutim, kao i većina senzora za određivanje pH temeljena na Schiffovim bazama, imino veza u kiselom ili bazičnom mediju hidrolizira te se ova vrsta spojeva ne može upotrebljavati u vodenom mediju. Iz navedenog razloga su Schiffove baze vrlo rijetko opisane kao pH senzori, no imobilizacijom ispitivanih spojeva su uspješno predstavljeni novi senzorski sustavi. Fotofizička svojstva ispitivanih spojeva se mijenjaju mobilizacijom u plastificirane polimerne matrice te se dobivaju tanki filmovi izražene fluorescencije. Plastificirani PVC tanki filmovi su takozvane „*bulk*“ membrane prikladne za optičku detekciju H^+ iona. Spojevi su unutar membrana stabilni, fluorescentni i osjetljivi na pH. Senzorski mehanizam se temelji na ionskoj izmjeni između polimerne mebrane i vodenog medija. Pripravljene ion-selektivne optode imaju vrijednosti uvjetne pK_a (5,5 – 6,9) te dobru stabilnost i reverzibilnost mjerenja. Supstituenti i u ovom slučaju omogućuju optimiranje fluorescentnog odgovora kemosenzorskog sustava, pa su tako pripravljeni funkcionalni optički materijali različitih emisijskih svojstava. Predstavljeni rezultati izravno doprinose području razvoja fluorescentnih membrana za detekciju pH, a osobito senzorskih sustava temeljenih na Schiffovim bazama. Primjena razvijenog sustava je predstavljena na primjeru selektivnog prepoznavanja kalija u ion-selektivnim optodama.

Radovi 1 – 4 predstavljaju dio sustavne karakterizacije benzimidazolnih derivata za primjenu u optičkim kemijskim senzorima. Razvojem novih pH osjetljivih sustava ostvaren je napredak u istraživanju navedene klase spojeva. Ispitivana skupina heterocikličkih kromofora posjeduje različita fotofizička svojstva, pri čemu je benzimidazolna jedinica ključna u gotovo svim mehanizmima stvaranja i prijenosa signala te receptorskoj moći novih kemosenzora. Benzimidazol u mnogočemu doprinosi u molekulskim sustavima za optičku detekciju iona:

- povećava stupanj konjugiranosti molekule,

- olakšava prijenos naboja unutar molekule i ostale mehanizme stvaranja i prijenosa signala poput prijenosa elektrona ili protona u pobuđenom stanju,
- planarna benzimidazolna jezgra doprinosi rigidnosti sustava,
- dušikovi atomi u molekuli benzimidazola i njihovi slobodni elektronski parovi izravno sudjeluju u konjugaciji sustava i određuju mogućnost kompleksiranja iona,
- različiti supstituenti na osnovnom molekulskom kostruru mogu izravno utjecati na fotofizička svojstva molekulskog sustava i selektivno prepoznavanje analita,
- poznavanjem odnosa strukture i svojstava u ispitivanoj klasi spojeva, moguće je fino podešavanje spektralnih i senzorskih svojstava budućih kemosenzorskih sustava temeljenih na benzimdiazolu.

Sažeti prikaz fotofizičkih i senzorskih svojstava benzimidazolnih derivata ispitivanih u ovom doktorskom radu je prikazan u sljedećoj tablici. Odnos strukture i svojstava ispitivanih derivata, detaljno opisan u radovima **1-4**, temelj je za ciljani dizajn novih benzimidazolnih senzorskih sustava u budućim istraživanjima. Pojava agregacije u vodi kod benzimidazolnih spojeva, tj. emitirajućih agregata na čiji se mehanizam agregacije-deagregacije može utjecati vanjskim čimbenicima, prvi je korak za daljnja istraživanja novih senzorskih mehanizama. Emitirajući agregati i fluorescencija u krutom stanju su široko primjenjive pojave. Fluorofori koji u krutom stanju emitiraju crvenu fluorescenciju su izrazito traženi, a često se upotrebljavaju u optoelektroničkim uređajima, solarnim ćelijama i slično [243, 244].

	Struktura i klasa spojeva	Ispitani spojevi (struktura – svojstvo)	Glavne karakteristike ispitivane klase	Spektoskopska svojstva	pH osjetljivost u otopinama	Osjetljivost na metalne ione i ostale analite	Imobilizacija / uvjetne pK_a vrijednosti u PVC membranama
Rad 1; Rad 2	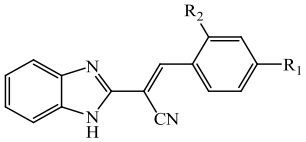 Akrilonitrilna bojila (stiril-cijaninska bojila)	**1a** R_1=H, R_2=H **1b** R_1=H, R_2= 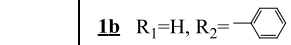 **1c** R_1=N$(CH_3)_2$, R_2=H **1d** R_1=N$(CH_3)_2$, R_2= 	• BI kao dio D-π-A sustava • **Visoke vrijednosti *ε*** • Promjena apsorpcijskih svojstava pri protoniranju • Određena mjesta protonacije i ionske vrste prisutne u otopinama i bulk membranama • Emisija pri visokim valnim duljinama izazvana agregacijom (AIE) spoj **1c**	250-500 nm (AIE 600 nm) Stokesovi pomaci 3162-8299 cm^{-1}	Da. Izražena kolorimetrijska promjena spektralnih svojstava pri protoniranju. pK_{a1}= 2,2 – 3,0 pK_{a2}= 10,3	**DNA** izravno utječe na stvaranje agregata kod spoja **1c**.	Da. Pripravljeni homogeni plastificirani PVC filmovi intezivno žute boje. **p$K_{a\ app}$ = 6,3**
Rad 3	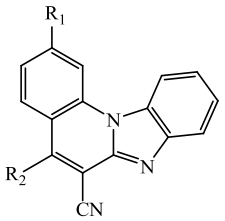 Derivati benzimidazo[1,2-*a*] kinolina	**2a** R_1= H , R_2= H **2b** R_1= −N⬡, R_2= H **2c** R_1= H , R_2= −N⬡ **2d** R_1= −N⬡, R_2= −N⬡ **2e** R_1= $NHCH_2CH_2CH_2N(CH_3)_2$, R_2= H **2f** R_1= $N(CH_2CH_3)_2$, R_2= H **2g** R_1= $NHCH_2CH(CH_3)_2$, R_2= H **2h** R_1= −N⬡NH, R_2= H **2i** R_1= H, R_2=  **2j** R_1= NH_2, R_2=  **2k** R_1= NH_2, R_2= **2l** R_1= $NHCH_2CH_2CH(CH_3)_2$, R_2=H **2lj** R_1= H, R_2=$NHCH_2CH_2CH(CH_3)_2$ **2m** R_1=  R_2=H **2n** R_1= R_2= 	• *push – pull* struktura omogućuje **intenzivnu plavu fluorescenciju** i značajnu promjenu fotofizičkih svojstava ovisno o pH i okolnom mediju • Istraživano podrijetlo fluorescencije pojedinih vrsta i odnos strukture i svojstva (neobjavljeni rezultati) • Određena mjesta protonacije i ionske vrste prisutne u otopinama i bulk membranama	400 – 500 nm Stokesovi pomaci 1261-7414 cm^{-1} Φ = 0,65	Da. Intenzitet i valna duljina fluorescencije ionskih vrsta se znatno razlikuju. pK_{a1}= 1,7 -3,45 pK_{a2}= 7,8-9,14	Da. Derivat **2j** pokazuje selektivan **fluorescentni odziv na cink** [56]. Derivati **2l-2n** su karakterizirani kao receptori za bakar u vodenim otopinama.	Da. Pripravljeni homogeni plastificirani PVC filmovi **intenzivne plave fluorescencije**. p$K_{a\ app}$ = 2,8 – 5,77

Rad 4	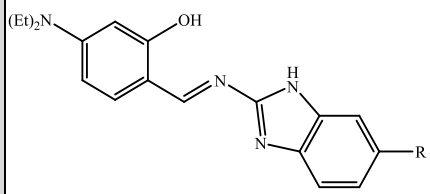 Schiffove baze temeljene na benzimidazolu	**3a** R=H **3b** R=CN **3c** R=NO_2	• BI kao dio D-π-A sustava • Visoke vrijednosti ε • Promjena boje pri protoniranju uočljiva golim okom • Slaba fluorescencija u otopinama, intenzivna fluorescencija u imobiliziranom obliku • **Agregacija** spojeva u vodi	400 – 550 nm Stokesovi pomaci 2366-3614 cm^{-1}	Da. Promjena spektralnih svojstava pri protoniranju. pK_a = 2,9 – 4,2	Da. Spektralne promjene prikladne za senzorsku primjenu se uočavaju pri vezivanju Cu^{2+} i Al^{3+} (neobjavljeni rezultati).	Da. Pripravljeni homogeni plastificirani PVC filmovi žute boje, **intenzivne plavo-zelene do zeleno-žute fluorescencije**. **p$K_{a\ app}$ = 5,5 – 6,9**

6. ZAKLJUČAK

Rezultati prikazani u ovom doktorskom radu predstavljaju doprinos u razvoju i pripravi novih optičkih kemijskih senzora temeljenih na derivatima benzimidazola.

- **Akrilonitrilna klasa benzimidazolnih derivata** pripravljena je kao skupina *push-pull* kromofora s izraženim spektralnim odgovorom na promjenu vrijednosti pH u vidljivom području elektromagnetskog spektra i **visokim molarnim apsorpcijskim koeficijentima**. Ispitivani spojevi su se pokazali kvalitetnim pH senzorima u kiselom području u otopinama (pK_a u području 2 do 4), no bliže fiziološkim pH vrijednostima u polimernim matricama, **pK_a oko 6**. Pripravljene polimerne membrane posjeduju potencijal za primjenu u kemijskim optičkim senzorima (analitičkim uređajima).

- **Akrilonitrilna bojila** su vrlo slabo fluorescentna, stoga je vrlo zanimljiva pojava uočena kod spoja *E*-2-(2-benzimidazolil)-3-(4-*N*,*N*-dimetilaminofenil)akrilonitrila – **emisija izazvana agregacijom (AIE)** koja se ostvaruje promjenom udjela otapala i vrijednosti pH u vodenom mediju. Protoniranjem i deprotoniranjem navedenog derivata benzimidazola uočava se vrlo slaba tirkizna i zelena emisija, no u neutralnom obliku spoj tvori nanokristalinične strukture, te se uočava narančasto-crvena emisija. Ovisnost procesa **stvaranja nanoagregata o vrijednosti pH je prvi put pokazana za derivate benzimidazola**, otvorivši pritom vrata širokoj primjeni u biologiji stanica i medicini zahvaljujući upravo benzimidazolnom biološkom djelovanju. Bitno je napomenuti da su preliminarna istraživanja dokazala ovisnost procesa agregacije-deagregacije u prisutnosti molekula DNA.

- Skupina **benzimidazo[1,2-*a*]kinolina** je prikladna za primjenu u fluorescencijskim senzorima zbog **intenzivne emisije u plavom području, najviša vrijednost Φ = 0,65.** Fluorescencijski pH senzori pronalaze široku primjenu u medicini i biologiji, stoga ova grupa spojeva ima veliki potencijal obzirom na **izraženu promjenu emisijskih svojstava prilikom protoniranja ili deprotoniranja**. Ispitivana skupina spojeva je prethodno pokazala mogućnost selektivnog vezanja metala [56] i potencijal za primjenu kao kemosenzora za metalne ione.

- Imobilizacijom benzimidazolnih derivata **Schiffovih baza** u plastificirane polimerne membrane razvijeni su novi optički senzorski materijali. Fluorescentni filmovi s

mogućnosti primjene u različitim sustavima su predstavljeni kao novi senzori **za pH u biološki kompatibilnom području pH vrijednosti (pH 6-8).**

- Uočen je opći doprinos benzimidazola u heterocikličkim π-konjugiranim optičkim sustavima koji se očituje kroz povećanje stupnja konjugiranosti molekule, omogućavanje lakšeg prijenosa naboja, elektrona ili protona unutar molekule te doprinosi planarnosti (rigidnosti) molekulskog sustava. Time dovodi do učinkovite fluorescencije što je posebno uočeno kod derivatima benzimidazo[1,2-*a*]kinolina. Posjeduje dušikove atome koji također višestruko utječu na fotofizička i senzorska svojstva molekulskog sustava, a supstituentima na osnovnom benzimidazolnom kosturu moguće je fino podešavanje spektralnih i senzorskih svojstava ispitivane molekule. Dušikovi atomi uvode nova mjesta za potencijalne unutarmolekulske i međumolekulske elektrostatske interakcije (npr. nova mjesta za nastajanje vodikovih veza odgovornih za stvaranje nanoagregata).

- Zaključno, benzimidazol je multifunkcionalna gradivna jedinica u optičkim kemijskim senzorima s dokazanim potencijalom za razvoj novih funkcionalnih (nano)materijala.

Iako je uporaba benzimidazola u optičkim kemijskim senzorima i općenito funkcionalnim materijalima često zasjenjena zbog njegove izvanredne biološke aktivnosti, sve je veće zanimanje znanstvenika za ovu vrlo jednostavnu i atraktivnu heteroaromatsku organsku molekulu. Rezultati prikazani u ovom radu su doprinos širokom području istraživanja fotofizičkih i senzorskih svojstava benzimidazolnih spojeva i njihovoj primjeni te će svakako rezultirati daljnjim istraživanjima s ciljem poboljšanja optičkih i senzorskih svojstava i razvojem novih molekulskih senzora.

7. LITERATURA

[1] W. Al Zoubi, N. Al Mohanna, Membrane sensors based on Schiff bases as chelating ionophores – A review, Spectroc. Acta Pt. A-Molec. Biomolec. Spectr. 132 (2014) 854-870.

[2] X. Tang, J. Han, Y. Wang, L. Ni, X. Bao, L. Wang, W. Zhang, A multifunctional Schiff base as a fluorescence sensor for Fe^{3+} and Zn^{2+} ions, and a colorimetric sensor for Cu^{2+} and applications, Spectroc. Acta Pt. A-Molec. Biomolec. Spectr. 173 (2017) 721-726.

[3] P. Guo, L. J. Liu, Q. Shi, C. Y. Yin, X. F. Shi, A rhodamine 6G derived Schiff base as a fluorescent and colorimetric probe for pH detection and its crystal structure, J. Mol. Struct. 1130 (2017) 150-155.

[4] J. Yang, Z.-l. Yuan, G.-q. Yu, S.-l. He, Q.-h. Hu, Q. Wu, B. Jiang, G. Wei, Single Chemosensor for Double Analytes: Spectrophotometric Sensing of Cu^{2+} and Fluorogenic Sensing of Al^{3+} Under Aqueous Conditions, J. Fluoresc.26 (2016) 43-51.

[5] L. Zhang, X. Cui, J. Sun, Y. Wang, W. Li, J. Fang, 8-Aminoquinoline-based ratiometric zinc probe: Unexpected binding mode and its application in living cells, Bioorg. Med. Chem. Lett. 23 (2013) 3511-3514.

[6] S. B. Roy, K. K. Rajak, A quinoline appended naphthalene derivative based AIE active "turn-on" fluorescent probe for the selective recognition of Al^{3+} and colourimetric sensor for Cu^{2+}: Experimental and computational studies, J. Photochem. Photobiol. A-Chem. 332 (2017) 505-514.

[7] P. A. More, G. S. Shankarling, Reversible 'turn off fluorescence response of Cu^{2+} ions towards 2-pyridyl quinoline based chemosensor with visible colour change, Sens. Actuator B-Chem.241 (2017) 552-559.

[8] Z. L. Luo, K. Yin, Z. Yu, M. X. Chen, Y. Li, J. Ren, A fluorescence turn-on chemosensor for hydrogen sulfate anion based on quinoline and naphthalimide, Spectroc. Acta Pt. A-Molec. Biomolec. Spectr. 169 (2016) 38-44.

[9] M. Tasior, D. Kim, S. Singha, M. Krzeszewski, K. H. Ahn, D. T. Gryko, π-Expanded coumarins: synthesis, optical properties and applications, J. Mater. Chem. C 3 (2015) 1421-1446.

[10] L. Yang, C. Wang, G. J. Chang, X. Y. Ren, Facile synthesis of new coumarin-based colorimetric and fluorescent chemosensors: Highly efficient and selective detection of Pd^{2+} in aqueous solutions, Sens. Actuator B-Chem.240 (2017) 212-219.

[11] B. Sen, S. K. Sheet, R. Thounaojam, R. Jamatia, A. K. Pal, K. Aguan, S. Khatua, A coumarin based Schiff base probe for selective fluorescence detection of Al^{3+} and its application in live cell imaging, Spectroc. Acta Pt. A-Molec. Biomolec. Spectr. 173 (2017) 537-543.

[12] S. Chen, P. Hou, J. Wang, L. Liu, Q. Zhang, A highly selective fluorescent probe based on coumarin for the imaging of N_2H_4 in living cells, Spectroc. Acta Pt. A-Molec. Biomolec. Spectr. 173 (2017) 170-174.

[13] T. Deligeorgiev, A. Vasilev, S. Kaloyanova, J. J. Vaquero, Styryl dyes - synthesis and applications during the last 15 years, Color. Technol.126 (2010) 55-80.

[14] X. D. Yang, P. L. Zhao, J. Q. Qu, R. Y. Liu, Fluorescent sensors based on quinoline-containing styrylcyanine: determination of ferric ions, hydrogen peroxide, and glucose, pH-sensitive properties and bioimaging, Luminescence 30 (2015) 592-599.

[15] Z. Seferoglu, H. Ihmels, E. Sahin, Synthesis and photophysical properties of fluorescent arylstyrylimidazo 1,2-*a* pyridine-based donor-acceptor chromophores, Dyes Pigment.113 (2015) 465-473.

[16] J. Freudenberg, F. Rominger, U. H. F. Bunz, New Aggregation-Induced Emitters: Tetraphenyldistyrylbenzenes, Chem.-Eur. J.21 (2015) 16749-16753.

[17] Y. Bansal, O. Silakari, The therapeutic journey of benzimidazoles: A review, Biorg. Med. Chem. 20 (2012) 6208-6236.

[18] Y. L. Gao, C. Zhang, S. W. Peng, H. Y. Chen, A fluorescent and colorimetric probe enables simultaneous differential detection of Hg^{2+} and Cu^{2+} by two different mechanisms, Sens. Actuator B-Chem.238 (2017) 455-461.

[19] N. Perin, L. Uzelac, I. Piantanida, G. Karminski-Zamola, M. Kralj, M. Hranjec, Novel biologically active nitro and amino substituted benzimidazo 1,2-*a* quinolines, Biorg. Med. Chem. 19 (2011) 6329-6339.

[20] M. Malathi, P. S. Mohan, R. J. Butcher, C. K. Venil, Benzimidazole quinoline derivatives - An effective green fluorescent dye for bacterial imaging, Can. J. Chem. 87 (2009) 1692-1703.

[21] A. Hulanicki, S. Glab, F. Ingman, Chemical sensors definitions and classification, Pure Appl. Chem. 63 (1991) 1247-1250.

[22] E. Bakker, P. Buhlmann, E. Pretsch, Carrier-based ion-selective electrodes and bulk optodes. 1. General characteristics, Chem. Rev. 97 (1997) 3083-3132.

[23] O. S. Wolfbeis, Fiber optic chemical sensors and biosensors, CRS Press, 1991.

[24] C. McDonagh, C. S. Burke, B. D. MacCraith, Optical chemical sensors, Chem. Rev. 108 (2008) 400-422.

[25] X. Xie, E. Bakker, Ion selective optodes: from the bulk to the nanoscale, Anal. Bioanal. Chem.407 (2015) 3899-3910.

[26] J. R. Lakowicz, Principles of Fluorescence Spectroscopy, Springer US (2006) XXVI, 954.

[27] B. Valeur, M. N. Berberan-Santos, Molecular fluorescence: principles and applications. John Wiley & Sons, 2012

[28] B. Valeur, I. Leray, Design principles of fluorescent molecular sensors for cation recognition, Coord. Chem. Rev. 205 (2000) 3-40.

[29] A. P. Demchenko, Introduction to fluorescence sensing, Anal. Bioanal. Chem.395 (2009) 1195-1196.

[30] A. P. de Silva, H. Q. N. Gunaratne, T. Gunnlaugsson, A. J. M. Huxley, C. P. McCoy, J. T. Rademacher, T. E. Rice, Signaling recognition events with fluorescent sensors and switches, Chem. Rev. 97 (1997) 1515-1566.

[31] O. S. Wolfbeis, Materials for fluorescence-based optical chemical sensors, J. Mater. Chem. 15 (2005) 2657-2669.

[32] O. S. Wolfbeis, An overview of nanoparticles commonly used in fluorescent bioimaging, Chem. Soc. Rev. 44 (2015) 4743-4768.

[33] O. Wolfbeis, E. Fürlinger, H. Kroneis, H. Marsoner, Fluorimetric analysis, Fresenius J. Anal. Chem. 314 (1983) 119-124.

[34] A. P. de Silva, T. S. Moody, G. D. Wright, Fluorescent PET (Photoinduced Electron Transfer) sensors as potent analytical tools, Analyst 134 (2009) 2385-2393.

[35] B. Wang, E. V. Anslyn, Chemosensors: principles, strategies, and applications. 15, John Wiley & Sons, 2011

[36] Z. R. Grabowski, K. Rotkiewicz, W. Rettig, Structural changes accompanying intramolecular electron transfer: Focus on twisted intramolecular charge-transfer states and structures, Chem. Rev. 103 (2003) 3899-4031.

[37] S. Sasaki, G. P. C. Drummen, G.-i. Konishi, Recent advances in twisted intramolecular charge transfer (TICT) fluorescence and related phenomena in materials chemistry, J. Mater. Chem. C 4 (2016) 2731-2743.

[38] J. Kulhánek, F. Bureš, Imidazole as a parent π-conjugated backbone in charge-transfer chromophores, Beilstein J. Org. Chem. 8 (2012) 25-49.

[39] J. Zhao, S. Ji, Y. Chen, H. Guo, P. Yang, Excited state intramolecular proton transfer (ESIPT): from principal photophysics to the development of new chromophores and applications in fluorescent molecular probes and luminescent materials, Phys. Chem. Chem. Phys. 14 (2012) 8803-8817.

[40] F. Bures, Fundamental aspects of property tuning in push-pull molecules, RSC Advances 4 (2014) 58826-58851.

[41] J. Kulhanek, F. Bures, Imidazole as a parent pi-conjugated backbone in charge-transfer chromophores, Beilstein J. Org. Chem. 8 (2012) 25-49.

[42] J. Kulhanek, F. Bures, T. Mikysek, J. Ludvik, O. Pytela, Imidazole as a central π-linkage in Y-shaped push-pull chromophores, Dyes Pigment.90 (2011) 48-55.

[43] H. C. Kolb, M. G. Finn, K. B. Sharpless, Click Chemistry: Diverse Chemical Function from a Few Good Reactions, Angew. Chem. Int. Ed. 40 (2001) 2004-2021.

[44] J. J. Bryant, U. H. F. Bunz, Click To Bind: Metal Sensors, Chem.-Asian J.8 (2013) 1354-1367.

[45] Y. H. Lau, P. J. Rutledge, M. Watkinson, M. H. Todd, Chemical sensors that incorporate click-derived triazoles, Chem. Soc. Rev. 40 (2011) 2848-2866.

[46] P. D. Jarowski, Y.-L. Wu, W. B. Schweizer, F. Diederich, 1,2,3-Triazoles as Conjugative π-Linkers in Push−Pull Chromophores: Importance of Substituent Positioning on Intramolecular Charge-Transfer, Org. Lett. 10 (2008) 3347-3350.

[47] W. Tscharnuter, Photon Correlation Spectroscopy in Particle Sizing. John Wiley & Sons, Ltd, 2006

[48] H. Wang, E. Zhao, J. W. Y. Lam, B. Z. Tang, AIE luminogens: emission brightened by aggregation, Mater. Today 18 (2015) 365-377.

[49] L. L. Yan, Y. Zhang, B. Xu, W. J. Tian, Fluorescent nanoparticles based on AIE fluorogens for bioimaging, Nanoscale 8 (2016) 2471-2487.

[50] U. Kubitscheck, Fluorescence Microscopy: From Principles to Biological Applications, Wiley-Blackwell (2013) 539.

[51] A. Verma, S. Joshi, D. Singh, Imidazole: Having Versatile Biological Activities, J. Chem. (2013)

[52] O. O. Ajani, D. V. Aderohunmu, C. O. Ikpo, A. E. Adedapo, I. O. Olanrewaju, Functionalized Benzimidazole Scaffolds: Privileged Heterocycle for Drug Design in Therapeutic Medicine, Arch. Pharm. 349 (2016) 475-506.

[53] P. Molina, A. Tarraga, F. Oton, Imidazole derivatives: A comprehensive survey of their recognition properties, Organic & Biomolecular Chemistry 10 (2012) 1711-1724.

[54] S. Manoharan, S. Anandan, Cyanovinyl substituted benzimidazole based (D-pi-A) organic dyes for fabrication of dye sensitized solar cells, Dyes Pigment.105 (2014) 223-231.

[55] B. R. B, T. S. Varadarajan, T. Mukherjee, Benzimidazo Quinolines - Potential Laser Dyes, Spectrosc. Lett. 23 (1990) 821-829.

[56] M. Hranjec, E. Horak, M. Tireli, G. Pavlovic, G. Karminski-Zamola, Synthesis, crystal structure and spectroscopic study of novel benzimidazoles and benzimidazo 1,2-*a* quinolines as potential chemosensors for different cations, Dyes Pigment.95 (2012) 644-656.

[57] S. K. Dogra, Spectral characteristics of 2-(2′-hydroxy-3′-pyridyl)benzimidazole: effects of solvents and acid or base concentrations, J. Mol. Struct. 734 (2005) 51-60.

[58] A. Mishra, S. Chaterjee, G. Krishnamoorthy, Intramolecular charge transfer emission of trans-2- 4 '-(dimethylamino)styryl benzimidazole: Effect of solvent and pH, J. Photochem. Photobiol. A-Chem. 260 (2013) 50-58.

[59] V. S. Patil, V. S. Padalkar, A. B. Tathe, V. D. Gupta, N. Sekar, Synthesis, Photo-physical and DFT Studies of ESIPT Inspired Novel 2-(2',4'-Dihydroxyphenyl) Benzimidazole, Benzoxazole and Benzothiazole, J. Fluoresc. 23 (2013) 1019-1029.

[60] J. Kulhanek, F. Bures, O. Pytela, T. Mikysek, J. Ludvik, A. Ruzicka, Push-pull molecules with a systematically extended pi-conjugated system featuring 4,5-dicyanoimidazole, Dyes Pigment. 85 (2010) 57-65.

[61] B. Jędrzejewska, P. Krawczyk, M. Pietrzak, M. Gordel, K. Matczyszyn, M. Samoć, P. Cysewski, Styryl dye possessing donor-π-acceptor structure – Synthesis, spectroscopic and computational studies, Dyes Pigment. 99 (2013) 673-685.

[62] S. Santra, S. K. Dogra, Prototropism of the methylated derivatives of 2-(2′-aminophenyl) benzimidazole, J. Lumin. 81 (1999) 249-262.

[63] S. Santra, S. K. Dogra, Spectral characteristics of the monocations of 2-(2′-aminophenyl)benzimidazole in different solvents, J. Mol. Struct. 478 (1999) 169-183.

[64] M. M. Henary, Y. Wu, J. Cody, S. Sumalekshmy, J. Li, S. Mandal, C. J. Fahrni, Excited-state intramolecular proton transfer in 2-(2 '-arylsulfonamidophenyl)benzimidazole derivatives: The effect of donor and acceptor substituents, J. Org. Chem. 72 (2007) 4784-4797.

[65] K. K. Donkor, B. Kratochvil, Determination of thermodynamic aqueous acid-base stability-constants for several benzimidazole derivatives, J. Chem. Eng. Data 38 (1993) 569-570.

[66] H. K. Sinha, S. K. Dogra, Absorption and fluorescence of 2-(aminomethyl)benzimidazole - study of solvent and pH-dependence, Spectroc. Acta Pt. A-Molec. Biomolec. Spectr. 41 (1985) 961-966.

[67] A. K. Mishra, S. K. Dogra, Photoluminescence of 2-(o-aminophenyl)benzimidazole, Journal of Photochemistry 31 (1985) 333-344.

[68] A. K. Mishra, S. K. Dogra, Effects of solvents and pH on the spectral behavior of 2-(para-aminophenyl)benzimidazole, Bull. Chem. Soc. Jpn. 58 (1985) 3587-3592.

[69] H. Walba, R. W. Isensee, Acidity constants of some arylimidazoles and their cations, J. Org. Chem. 26 (1961) 2789.

[70] A. K. Mishra, S. K. Dogra, Effect of solvents and ph on the absorption and fluorescence-spectra of 2-phenylbenzimidazole, Spectroc. Acta Pt. A-Molec. Biomolec. Spectr.39 (1983) 609-611.

[71] J. Dey, S. K. Dogra, Dual fluorescence of 2-(4'-(n,n-dimethylamino)phenyl)benzothiazole and its benzimidazole analog - effect of solvent and pH on electronic-spectra, J. Phys. Chem. 98 (1994) 3638-3644.

[72] G. Krishnamoorthy, S. K. Dogra, Dual fluorescence of 2-(4′-N,N-dimethylaminophenyl)benzimidazole: effect of β-cyclodextrin and pH, J. Photochem. Photobiol. A-Chem. 123 (1999) 109-119.

[73] T. A. Fayed, S. S. Ali, Protonation dependent photoinduced intramolecular charge transfer in 2-(p-dimethylaminostyryl)benzazoles, Spectrosc. Lett. 36 (2003) 375-386.

[74] M. Ladinig, W. Leupin, M. Meuwly, M. Respondek, J. Wirz, V. Zoete, Protonation equilibria of Hoechst 33258 in aqueous solution, Helv. Chim. Acta 88 (2005) 53-67.

[75] V. S. Padalkar, A. Tathe, V. D. Gupta, V. S. Patil, K. Phatangare, N. Sekar, Synthesis and Photo-Physical Characteristics of ESIPT Inspired 2-Substituted Benzimidazole, Benzoxazole and Benzothiazole Fluorescent Derivatives, J. Fluoresc.22 (2012) 311-322.

[76] T. Iijima, A. Momotake, Y. Shinohara, T. Sato, Y. Nishimura, T. Arai, Excited-State Intramolecular Proton Transfer of Naphthalene-Fused 2-(2 '-Hydroxyaryl)benzazole Family, J. Phys. Chem. A 114 (2010) 1603-1609.

[77] X.-H. Zhang, S. H. Kim, I. S. Lee, C. J. Gao, S. I. Yang, K.-H. Ahn, Synthesis, photophysical and electrochemical properties of novel conjugated donor-acceptor molecules based on phenothiazine and benzimidazole, Bull. Korean Chem. Soc. 28 (2007) 1389-1395.

[78] B. Jedrzejewska, B. Osmialowski, R. Zalesny, Application of spectroscopic and theoretical methods in the studies of photoisomerization and photophysical properties of the push-pull styryl-benzimidazole dyes, Photochem. Photobiol. Sci. 15 (2016) 117-128.

[79] F. Wu, L. Ma, Y. Geng, S. Zhang, Z. Wang, X. Cheng, Optical nonlinearity of HBI in different solvents, Opt. Laser Technol. 57 (2014) 206-208.

[80] A. Carella, R. Centore, A. Fort, A. Peluso, A. Sirigu, A. Tuzi, Tuning Second-Order Optical Nonlinearities in Push-Pull Benzimidazoles, Eur. J. Org. Chem. 2004 (2004) 2620-2626.

[81] S. Ahn, J. N. Kim, Y. C. Kim, Solid state solvation effect of a donor-acceptor type fluorescent molecule and its application to white organic light-emitting diodes, Curr. Appl. Phys. 15 (2015) S42-S47.

[82] J. J. Huang, M. K. Leung, T. L. Chiu, Y. T. Chuang, P. T. Chou, Y. H. Hung, Novel Benzimidazole Derivatives as Electron-Transporting Type Host To Achieve Highly Efficient Sky-Blue Phosphorescent Organic Light-Emitting Diode (PHOLED) Device, Org. Lett. 16 (2014) 5398-5401.

[83] G. M. Saltan, H. Dincalp, M. Kiran, C. Zafer, S. C. Erbas, Novel organic dyes based on phenyl-substituted benzimidazole for dye sensitized solar cells, Mater. Chem. Phys. 163 (2015) 387-393.

[84] Y. Yang, B. Li, L. M. Zhang, Y. L. Guan, Triphenylamine based benzimidazole and benzothiazole: Synthesis and applications in fluorescent chemosensors and laser dyes, J. Lumin. 145 (2014) 895-898.

[85] R. Saito, Y. Matsumura, S. Suzuki, N. Okazaki, Intensely blue-fluorescent 2,5-bis(benzoimidazol-2-yl)pyrazine dyes with improved solubility: their synthesis, fluorescent properties, and application as microenvironment polarity probes, Tetrahedron 66 (2010) 8273-8279.

[86] T. Inouchi, T. Nakashima, T. Kawai, The Origin of the Emission Properties of pi-Conjugated Molecules that have an Acid-responsive Benzimidazole Unit, Asian J. Org. Chem. 2 (2013) 230-238.

[87] T. Inouchi, T. Nakashima, T. Kawai, Charge Transfer Emission of T-Shaped π-Conjugated Molecules: Impact of Quinoid Character on the Excited State Properties, The J. Phys. Chem. A 118 (2014) 2591-2598.

[88] T. Inouchi, T. Nakashima, M. Toba, T. Kawai, Preparation and Acid-Responsive Photophysical Properties of T-Shaped π-Conjugated Molecules Containing a Benzimidazole Junction, Chem.-Asian J. 6 (2011) 3020-3027.

[89] R. C. Lirag, H. T. M. Le, O. S. Miljanic, L-shaped benzimidazole fluorophores: synthesis, characterization and optical response to bases, acids and anions, Chem. Commun. 49 (2013) 4304-4306.

[90] H. T. M. Le, N. S. El-Hamdi, O. S. Miljanic, Benzobisimidazole Cruciform Fluorophores, J. Org. Chem. 80 (2015) 5210-5217.

[91] Y. Hong, J. W. Y. Lam, B. Z. Tang, Aggregation-induced emission, Chem. Soc. Rev. 40 (2011) 5361-5388.

[92] J. Luo, Z. Xie, J. W. Y. Lam, L. Cheng, H. Chen, C. Qiu, H. S. Kwok, X. Zhan, Y. Liu, D. Zhu, B. Z. Tang, Aggregation-induced emission of 1-methyl-1,2,3,4,5-pentaphenylsilole, Chem. Commun. (2001) 1740-1741.

[93] B. K. An, S. K. Kwon, S. D. Jung, S. Y. Park, Enhanced emission and its switching in fluorescent organic nanoparticles, J. Am. Chem. Soc. 124 (2002) 14410-14415.

[94] M. Yang, D. Xu, W. Xi, L. Wang, J. Zheng, J. Huang, J. Zhang, H. Zhou, J. Wu, Y. Tian, Aggregation-induced fluorescence behavior of triphenylamine-based schiff bases: the combined effect of multiple forces, J. Org. Chem. 78 (2013) 10344-59.

[95] Q. Zeng, Z. Li, Y. Dong, C. a. Di, A. Qin, Y. Hong, L. Ji, Z. Zhu, C. K. W. Jim, G. Yu, Q. Li, Z. Li, Y. Liu, J. Qin, B. Z. Tang, Fluorescence enhancements of benzene-cored luminophors by restricted intramolecular rotations: AIE and AIEE effects, Chem. Commun. (2007) 70-72.

[96] Z. Y. Yang, W. Qin, N. L. C. Leung, M. Arseneault, J. W. Y. Lam, G. D. Liang, H. H. Y. Sung, I. D. Williams, B. Z. Tang, A mechanistic study of AIE processes of TPE luminogens: intramolecular rotation vs. configurational isomerization, J. Mater. Chem. C 4 (2016) 99-107.

[97] Y. N. Hong, J. W. Y. Lam, B. Z. Tang, Aggregation-induced emission: phenomenon, mechanism and applications, Chem. Commun. (2009) 4332-4353.

[98] H. Yuning, Aggregation-induced emission—fluorophores and applications, Methods Appl. Fluoresc. 4 (2016) 022003.

[99] A. Gogoi, S. Mukherjee, A. Ramesh, G. Das, Aggregation-Induced Emission Active Metal-Free Chemosensing Platform for Highly Selective Turn-On Sensing and Bioimaging of Pyrophosphate Anion, Anal. Chem. 87 (2015) 6974-6979.

[100] P. Alam, V. Kachwal, I. Rahaman Laskar, A multi-stimuli responsive "AIE" active salicylaldehyde-based Schiff base for sensitive detection of fluoride, Sens. Actuator B-Chem. 228 (2016) 539-550.

[101] A. Malakar, M. Kumar, A. Reddy, H. T. Biswal, B. B. Mandal, G. Krishnamoorthy, Aggregation induced enhanced emission of 2-(2 '- hydroxyphenyl) benzimidazole, Photochem. Photobiol. Sci. 15 (2016) 937-948.

[102] Z. Wu, J. B. Sun, Z. Q. Zhang, P. Gong, P. C. Xue, R. Lu, Organogelation of cyanovinylcarbazole with terminal benzimidazole: AIE and response for gaseous acid, Rsc Advances 6 (2016) 97293-97301.

[103] Y. L. Cao, M. D. Yang, Y. Wang, H. P. Zhou, J. Zheng, X. Z. Zhang, J. Y. Wu, Y. P. Tian, Z. Q. Wu, Aggregation-induced and crystallization-enhanced emissions with time-dependence of a new Schiff-base family based on benzimidazole, J. Mater. Chem. C 2 (2014) 3686-3694.

[104] N. Boens, V. Leen, W. Dehaen, Fluorescent indicators based on BODIPY, Chem. Soc. Rev. 41 (2012) 1130-1172.

[105] C. Maeda, T. Todaka, T. Ueda, T. Ema, Color-Tunable Solid-State Fluorescence Emission from Carbazole-Based BODIPYs, Chem.-Eur. J.22 (2016) 7508-7513.

[106] S. S. Thakare, G. Chakraborty, P. Krishnakumar, A. K. Ray, D. K. Maity, H. Pal, N. Sekar, Supramolecularly Assisted Modulation of Optical Properties of BODIPY-Benzimidazole Conjugates, J. Phys. Chem. B 120 (2016) 11266-11278.

[107] H. Sakai, T. Kubota, J. Yuasa, Y. Araki, T. Sakanoue, T. Takenobu, T. Wada, T. Kawai, T. Hasobe, Protonation-induced red-coloured circularly polarized luminescence of [5]carbohelicene fused by benzimidazole, Org. Biomol. Chem.14 (2016) 6738-6743.

[108] D. Wencel, T. Abel, C. McDonagh, Optical Chemical pH Sensors, Anal. Chem. 86 (2014) 15-29.

[109] J. Han, K. Burgess, Fluorescent Indicators for Intracellular pH, Chem. Rev. 110 (2009) 2709-2728.

[110] W. Shi, X. Li, H. Ma, Fluorescent probes and nanoparticles for intracellular sensing of pH values, Methods Appl. Fluoresc. 2 (2014)

[111] R. Wang, C. Yu, F. Yu, L. Chen, Molecular fluorescent probes for monitoring pH changes in living cells, Trac-Trends Anal. Chem. 29 (2010) 1004-1013.

[112] I. E. Tolpygin, Y. V. Revinskii, A. G. Starikov, A. D. Dubonosov, V. A. Bren, V. I. Minkin, Effective pH sensors based on 1-(anthracen-9-ylmethyl)-1H-benzimidazol-2-amine, Chem. Heterocycl. Compds. 47 (2012) 1230-1236.

[113] H. J. Kim, C. H. Heo, H. M. Kim, Benzimidazole-Based Ratiometric Two-Photon Fluorescent Probes for Acidic pH in Live Cells and Tissues, J. Am. Chem. Soc. 135 (2013) 17969-17977.

[114] Q.-H. You, L. Fan, W.-H. Chan, A. W. M. Lee, S. Shuang, Ratiometric spiropyran-based fluorescent pH probe, Rsc Advances 3 (2013) 15762-15768.

[115] Z. Xue, M. Chen, J. Chen, J. Han, S. Han, A rhodamine-benzimidazole based sensor for selective imaging of acidic pH, Rsc Advances 4 (2014) 374-378.

[116] G. Sevinc, B. Kucukoz, H. Yilmaz, G. Sirikci, H. G. Yaglioglu, M. Hayvali, A. Elmali, Explanation of pH probe mechanism in borondipyrromethene-benzimidazole compound using ultrafast spectroscopy technique, Sens. Actuator B-Chem.193 (2014) 737-744.

[117] Z. Liu, C. Peng, C. Guo, Y. Zhao, X. Yang, M. Pei, G. Zhang, Novel fluorescent and colorimetric pH sensors derived from benzimidazo 2,1-*a* benzisoquinoline-7-one-12-carboxylic acid, Tetrahedron 71 (2015) 2736-2742.

[118] X. Zhu, Q. Lin, Y.-M. Zhang, T.-B. Wei, Nitrophenylfuran-benzimidazole-based reversible alkaline fluorescence switch accurately controlled by pH, Sens. Actuator B-Chem. 219 (2015) 38-42.

[119] Z. Li, L.-J. Li, T. Sun, L. Liu, Z. Xie, Benzimidazole-BODIPY as optical and fluorometric pH sensor, Dyes Pigment. 128 (2016) 165-169.

[120] K. Aich, S. Das, S. Goswami, C. K. Quah, D. Sarkar, T. K. Mondal, H. K. Fun, Carbazole-benzimidazole based dyes for acid responsive ratiometric emissive switches, New J. Chem. 40 (2016) 6907-6915.

[121] J. Liu, Q. Liu, C. Yang, Y. Sun, Y. Zhang, P. Huang, J. Zhou, Q. Liu, L. Chu, F. Huang, L. Deng, A. Dong, J. Liu, cRGD-Modified Benzimidazole-based pH-Responsive Nanoparticles for Enhanced Tumor Targeted Doxorubicin Delivery, ACS Appl. Mater. Interfaces 8 (2016) 10726-10736.

[122] L. Tomljenovic, Aluminum and Alzheimer's Disease: After a Century of Controversy, Is there a Plausible Link?, J. Alzheimers Dis. 23 (2011) 567-598.

[123] J.-M. Lehn, Molecular Recognition. Wiley-VCH Verlag GmbH & Co. KGaA, 200611-30

[124] T. Q. Duong, J. S. Kim, Fluoro- and Chromogenic Chemodosimeters for Heavy Metal Ion Detection in Solution and Biospecimens, Chem. Rev. 110 (2010) 6280-6301.

[125] K. P. Carter, A. M. Young, A. E. Palmer, Fluorescent Sensors for Measuring Metal Ions in Living Systems, Chem. Rev. 114 (2014) 4564-4601.

[126] M. Formica, V. Fusi, L. Giorgi, M. Micheloni, New fluorescent chemosensors for metal ions in solution, Coord. Chem. Rev. 256 (2012) 170-192.

[127] Z. Xu, J. Yoon, D. R. Spring, Fluorescent chemosensors for Zn^{2+}, Chem. Soc. Rev. 39 (2010) 1996-2006.

[128] N. Dash, A. Malakar, M. Kumar, B. B. Mandal, G. Krishnamoorthy, Metal ion dependent “ON” intramolecular charge transfer (ICT) and “OFF” normal switching of the fluorescence: Sensing of Zn2+ by ICT emission in living cells, Sens. Actuator B-Chem. 202 (2014) 1154-1163.

[129] K. Rurack, Flipping the light switch 'ON' – the design of sensor molecules that show cation-induced fluorescence enhancement with heavy and transition metal ions, Spectroc. Acta Pt. A-Molec. Biomolec. Spectr. 57 (2001) 2161-2195.

[130] Y. Jeong, J. Yoon, Recent progress on fluorescent chemosensors for metal ions, Inorg. Chim. Acta 381 (2012) 2-14.

[131] A. Bianchi, E. Delgado-Pinar, E. García-España, C. Giorgi, F. Pina, Highlights of metal ion-based photochemical switches, Coord. Chem. Rev. 260 (2014) 156-215.

[132] M. Dutta, D. Das, Recent developments in fluorescent sensors for trace-level determination of toxic-metal ions, Trac-Trends Anal. Chem. 32 (2012) 113-132.

[133] A. R. Firooz, A. A. Ensafi, N. Kazemifard, H. Sharghi, A highly sensitive and selective bulk optode based on benzimidazol derivative as an ionophore and ETH5294 for the determination of ultra trace amount of silver ions, Talanta 101 (2012) 171-176.

[134] B. Zhao, Y. Fang, M. J. Ma, Q. G. Deng, Y. Xu, L. Y. Wang, A new on-fluorescent sensor for Ag+ based on benzimidazole bearing bis(ethoxycarbonylmethyl)amino groups, Heterocycl. Commun. 21 (2015) 211-214.

[135] C. Chen, H. Liu, B. Zhang, Y. Wang, K. Cai, Y. Tan, C. Gao, H. Liu, C. Tan, Y. Jiang, A simple benzimidazole quinoline-conjugate fluorescent chemosensor for highly selective detection of Ag^{+}, Tetrahedron 72 (2016) 3980-3985.

[136] D. Jeyanthi, M. Iniya, K. Krishnaveni, D. Chellappa, A ratiometric fluorescent sensor for selective recognition of Al^{3+} ions based on a simple benzimidazole platform, Rsc Advances 3 (2013) 20984-20989.

[137] K. Velmurugan, S. Mathankumar, S. Santoshkumar, S. Amudha, R. Nandhakumar, Specific fluorescent sensing of aluminium using naphthalene benzimidazole derivative in aqueous media, Spectroc. Acta Pt. A-Molec. Biomolec. Spectr. 139 (2015) 119-123.

[138] M. Iniya, D. Jeyanthi, K. Krishnaveni, D. Chellappa, A bifunctional chromogenic and fluorogenic probe for F^{-} and Al^{3+} based on azo-benzimidazole conjugate, J. Lumin. 157 (2015) 383-389.

[139] W. Cao, X.-J. Zheng, J.-P. Sun, W.-T. Wong, D.-C. Fang, J.-X. Zhang, L.-P. Jin, A Highly Selective Chemosensor for AI(III) and Zn(II) and Its Coordination with Metal Ions, Inorg. Chem. 53 (2014) 3012-3021.

[140] G. Dhaka, N. Kaur, J. Singh, Spectroscopic evaluation of a novel multi-element sensitive fluorescent probe derived from 2-(2'-phenylbenzamide)benzimidazole: Selective discrimination of Al^{3+} and Cd^{2+} from their congeners, Inorg. Chem. Commun. 72 (2016) 57-61.

[141] H. Y. Liu, B. B. Zhang, C. Y. Tan, F. Liu, J. K. Cao, Y. Tan, Y. Y. Jiang, Simultaneous bioimaging recognition of Al3+ and Cu2+ in living-cell, and further detection of F- and S2- by a simple fluorogenic benzimidazole-based chemosensor, Talanta 161 (2016) 309-319.

[142] G. Li, D. B. Zhang, G. Liu, S. Z. Pu, A highly selective fluorescent probe for Cd^{2+} and Zn^{2+} based on a new diarylethene with quinoline-benzimidazole conjugated system, Tetrahedron Lett. 57 (2016) 5205-5210.

[143] O. Cimen, H. Dincalp, C. Varlikli, Studies on UV-vis and fluorescence changements in Co2+ and Cu2+ recognition by a new benzimidazole-benzothiadiazole derivative, Sens. Actuator B-Chem. 209 (2015) 853-863.

[144] A. K. Lal, M. D. Milton, Designed benzimidazolium salts: Modulation of fluorescence response towards metal cations in pure aqueous media, Sens. Actuator B-Chem.202 (2014) 257-262.

[145] L. Tang, M. Cai, Z. Huang, K. Zhong, S. Hou, Y. Bian, R. Nandhakumar, Rapid and highly selective relay recognition of Cu(II) and sulfide ions by a simple benzimidazole-based fluorescent sensor in water, Sens. Actuator B-Chem.185 (2013) 188-194.

[146] P. Saluja, N. Kaur, N. Singh, D. O. Jang, A benzimidazole-based fluorescent sensor for Cu2+ and its complex with a phosphate anion formed through a Cu^{2+} displacement approach, Tetrahedron Lett. 53 (2012) 3292-3295.

[147] J. Jayabharathi, V. Thanikachalam, K. Jayamoorthy, R. Sathishkumar, Selective quenching of benzimidazole derivatives by Cu^{2+} metal ion, Spectroc. Acta Pt. A-Molec. Biomolec. Spectr. 97 (2012) 384-387.

[148] K. Mahiya, P. Mathur, Bis-Benzimidazolyl Diamide Based Fluorescent Probe for Copper(II): Synthesis, Structural and Fluorescence Studies, J. Fluoresc. 23 (2013) 767-776.

[149] S. Goswami, S. Maity, A. C. Maity, A. K. Maity, A. K. Das, P. Saha, A FRET-based rhodamine-benzimidazole conjugate as a Cu2+-selective colorimetric and ratiometric fluorescence probe that functions as a cytoplasm marker, RSC Adv. 4 (2014) 6300-6305.

[150] Z. Liu, Y. Qi, C. Guo, Y. Zhao, X. Yang, M. Pei, G. Zhang, Novel fluorescent sensors based on benzimidazo 2,1-*a* benz de isoquinoline-7-one-12-carboxylic acid for Cu^{2+}, RSC Adv. 4 (2014) 56863-56869.

[151] A. Kumar, A. Kumar, M. Dubey, A. Biswas, D. S. Pandey, Detection of copper(II) and aluminium(III) by a new bis-benzimidazole Schiff base in aqueous media via distinct routes, RSC Adv. 5 (2015) 88612-88624.

[152] L. Tang, N. Wang, Q. Zhang, J. Guo, R. Nandhakumar, A new benzimidazole-based quinazoline derivative for highly selective sequential recognition of Cu^{2+} and CN, Tetrahedron Lett. 54 (2013) 536-540.

[153] D. Y. Lee, N. Singh, D. O. Jang, A benzimidazole-based single molecular multianalyte fluorescent probe for the simultaneous analysis of Cu^{2+} and Fe^{3+}, Tetrahedron Lett. 51 (2010) 1103-1106.

[154] F. A. S. Chipem, S. K. Behera, G. Krishnamoorthy, Ratiometric fluorescence sensing ability of 2-(2′-hydroxyphenyl)benzimidazole and its nitrogen substituted analogues towards metal ions, Sens. Actuator B-Chem.191 (2014) 727-733.

[155] L. Tang, X. Dai, M. Cai, J. Zhao, P. Zhou, Z. Huang, Relay recognition of Cu^{2+} and S^{2-} in water by a simple 2-(2 '-aminophenyl)benzimidazole derivatized fluorescent sensor through modulating ESIPT, Spectroc. Acta Pt. A-Molec. Biomolec. Spectr. 122 (2014) 656-660.

[156] C. Kar, G. Das, A retrievable fluorescence "TURN ON" sensor for sulfide anions, J. Photochem. Photobiol. A-Chem. 251 (2013) 128-133.

[157] Y. Fu, Q.-C. Feng, X.-J. Jiang, H. Xu, M. Li, S.-Q. Zang, New fluorescent sensor for Cu^{2+} and S^{2-} in 100% aqueous solution based on displacement approach, Dalton Trans. 43 (2014) 5815-5822.

[158] A. Paul, S. Anbu, G. Sharma, M. L. Kuznetsov, M. da Silva, B. Koch, A. J. L. Pombeiro, Intracellular detection of Cu^{2+} and S^{2-} ions through a quinazoline functionalized benzimidazole-based new fluorogenic differential chemosensor, Dalton Trans. 44 (2015) 16953-16964.

[159] H. Goh, Y. G. Ko, T. K. Nam, A. Singh, N. Singh, D. O. Jang, A benzimidazole-based fluorescent chemosensor for Cu^{2+} recognition and its complex for sensing H2PO4- by a Cu^{2+} displacement approach in aqueous media, Tetrahedron Lett. 57 (2016) 4435-4439.

[160] R. Khattar, P. Mathur, 1-(Pyridin-2-ylmethyl)-2-(3-(1-(pyridin-2-ylmethyl)benzimidazol-2-yl) propyl) benzimidazole and its copper(II) complex as a new fluorescent sensor for dopamine (4-(2-aminoethyl)benzene-1,2-diol), Inorg. Chem. Commun. 31 (2013) 37-43.

[161] Y. Yu, J.-P. Ma, C.-W. Zhao, J. Yang, X.-M. Zhang, Q.-K. Liu, Y.-B. Dong, Copper(I) Metal-Organic Framework: Visual Sensor for Detecting Small Polar Aliphatic Volatile Organic Compounds, Inorg. Chem. 54 (2015) 11590-11592.

[162] H. J. Jung, N. Singh, D. O. Jang, Highly Fe(3+) selective ratiometric fluorescent probe based on imine-linked benzimidazole, Tetrahedron Lett. 49 (2008) 2960-2964.

[163] A. K. Lal, M. D. Milton, Synthesis of new benzimidazolium salts with tunable emission intensities and their application as fluorescent probes for Fe^{3+} in pure aqueous media, Tetrahedron Lett. 55 (2014) 1810-1814.

[164] G. Li, J. Tang, P. Ding, Y. Ye, A Rhodamine-Benzimidazole Based Chemosensor for Fe3+ and its Application in Living Cells, J. Fluoresc. 26 (2016) 155-161.

[165] S. M. Prakash, K. Jayamoorthy, N. Srinivasan, K. I. Dhanalekshmi, Fluorescence tuning of 2-(1H-Benzirnidazol-2-yl)phenol-ESIPT process, J. Lumin. 172 (2016) 304-308.

[166] J. B. Li, Q. H. Hu, X. L. Yu, Y. Zeng, C. C. Cao, X. W. Liu, J. Guo, Z. Q. Pan, A Novel Rhodamine-Benzimidazole Conjugate as a Highly Selective Turn-on Fluorescent Probe for Fe^{3+}, J. Fluoresc.21 (2011) 2005-2013.

[167] D. Y. Lee, N. Singh, D. O. Jang, Fine tuning of a solvatochromic fluorophore for selective determination of Fe^{3+}: a new type of benzimidazole-based anthracene-coupled receptor, Tetrahedron Lett. 52 (2011) 1368-1371.

[168] Y. Wang, Z. Liu, J. H. Sun, X. G. Liu, M. S. Pei, G. Y. Zhang, A turn-on fluorescence probe for Fe^{3+} based-on benzimidazo 2,1-alpha benz de isoquinoline-7-one derivatives, J. Photochem. Photobiol. A-Chem. 332 (2017) 515-520.

[169] J. Liu, Q. Lin, Y. Zhang, T. Wei, A reversible fluorescent chemosensor for Fe^{3+} and $H_2PO_4^{(-)}$ with "on-off-on" switching in aqueous media, Sci. China-Chem.57 (2014) 1257-1263.

[170] Y. Yang, B. Li, L. Zhang, Y. Guan, Triphenylamine based benzimidazole and benzothiazole: Synthesis and applications in fluorescent chemosensors and laser dyes, J. Lumin. 145 (2014) 895-898.

[171] D. Y. Lee, N. Singh, D. O. Jang, Ratiometric and simultaneous estimation of Fe^{3+} and Cu^{2+} ions: 1,3,5-substituted triethylbenzene derivatives coupled with benzimidazole, Tetrahedron Lett. 52 (2011) 3886-3890.

[172] G. Saikia, P. K. Iyer, A Remarkable Superquenching and Superdequenching Sensor for the Selective and Noninvasive Detection of Inorganic Phosphates in Saliva, Macromolecules 44 (2011) 3753-3758.

[173] S. Madhu, D. K. Sharma, S. K. Basu, S. Jadhav, A. Chowdhury, M. Ravikanth, Sensing Hg(II) in Vitro and in Vivo Using a Benzimidazole Substituted BODIPY, Inorg. Chem. 52 (2013) 11136-11145.

[174] J. Hu, J. Li, J. Qi, J. Chen, Highly selective and effective mercury(II) fluorescent sensors, New J. Chem. 39 (2015) 843-848.

[175] K. L. Zhong, X. Zhou, R. B. Hou, P. Zhou, S. H. Hou, Y. J. Bian, G. Zhang, L. J. Tang, X. H. Shang, A water-soluble highly sensitive and selective fluorescent sensor for Hg^{2+} based on 2-(2-(8-hydroxyquinolin)-yl)benzimidazole via ligand-to-metal charge transfer (LMCT), RSC Adv. 4 (2014) 16612-16617.

[176] J. Tan, X.-P. Yan, 2,1,3-Benzoxadiazole-based selective chromogenic chemosensor for rapid naked-eye detection of Hg^{2+} and Cu^{2+}, Talanta 76 (2008) 9-14.

[177] J. Liu, Q. Lin, Y. M. Zhang, T. B. Wei, A reversible and highly selective fluorescent probe for monitoring Hg^{2+} and iodide in aqueous solution, Sens. Actuator B-Chem. 196 (2014) 619-623.

[178] P. Saluja, H. Sharma, N. Kaur, N. Singh, D. O. Jang, Benzimidazole-based imine-linked chemosensor: chromogenic sensor for Mg^{2+} and fluorescent sensor for Cr^{3+}, Tetrahedron 68 (2012) 2289-2293.

[179] D. Sarkar, A. K. Pramanik, T. K. Mondal, Benzimidazole based ratiometric and colourimetric chemosensor for Ni(II), Spectroc. Acta Pt. A-Molec. Biomolec. Spectr. 153 (2016) 397-401.

[180] S. H. Mashraqui, S. Sundaram, T. Khan, Benzimidazole-chalcone: A selective intramolecular charge-transfer probe for biologically important zinc ions, Chem. Lett. 35 (2006) 786-787.

[181] S. Lohar, D. Karak, S. Guha, A. Banerjee, A. Sahana, D. Das, Spectroscopic Studies of a New Multi-Element Sensitive Fluorescent Probe Derived from 2-(2-pyridyl)benzimidazole: Selective Discrimination of Zn^{2+} from Its Congeners, Spectrosc. Lett. 46 (2013) 28-35.

[182] K. Velmurugan, A. Raman, D. Don, L. J. Tang, S. Easwaramoorthi, R. Nandhakumar, Quinoline benzimidazole-conjugate for the highly selective detection of Zn(II) by dual colorimetric and fluorescent turn-on responses, RSC Adv. 5 (2015) 44463-44469.

[183] S. H. Mashraqui, M. Chandiramani, S. Ghorpade, J. Upathayay, R. Mestri, A. Chilekar, A simple 2,6-bis(2-benzimidazole)pyridyl incorporated optical probe affording selective ratiometric targeting of biologically and environmentally significant Zn^{2+} under buffer condition, J. Incl. Phenom. Macrocycl. Chem. 84 (2016) 129-135.

[184] K. Akutsu, S. Mori, K. Shinmei, H. Iwase, Y. Nakano, Y. Fujii, Investigation of substitution effect on fluorescence properties of Zn^{2+}-selective ratiometric fluorescent compounds: 2-(2 '-Hydroxyphenyl)benzimidazole derivatives, Talanta 146 (2016) 575-584.

[185] S. Sharma, C. P. Pradeep, A. Dhir, Benzimidazole Based 'Turn on' Fluorescent Chemodosimeter for Zinc Ions in Mixed Aqueous Medium, J. Fluoresc. 26 (2016) 1439-1445.

[186] B. Vosough Razavi, A. Badiei, N. Lashgari, G. Mohammadi Ziarani, 2,6-Bis(2-Benzimidazolyl)Pyridine Fluorescent Red-Shifted Sensor for Recognition of Zinc(II) and a Calorimetric Sensor for Iron Ions, J. Fluoresc. 26 (2016) 1723-8.

[187] A. El Majzoub, C. CadiouA, I. Dechamps-Olivier, F. Chuburu, M. Aplincourt, B. Tinant, Mono- and bis-N-functionalised cyclen with benzimidazolylmethyl pendant arms:

Sensitive and selective fluorescent probes for zinc and copper ions, Inorg. Chim. Acta 362 (2009) 1169-1178.

[188] L. Tang, M. Cai, P. Zhou, J. Zhao, K. Zhong, S. Hou, Y. Bian, A highly selective and ratiometric fluorescent sensor for relay recognition of zinc(II) and sulfide ions based on modulation of excited-state intramolecular proton transfer, RSC Adv. 3 (2013) 16802-16809.

[189] L. J. Tang, M. J. Cai, P. Zhou, J. Zhao, Z. L. Huang, K. L. Zhong, S. H. Hou, Y. J. Bian, Relay recognition by modulating ESIPT: A phenylbenzimidazole derived sensor for highly selective ratiometric fluorescent recognition of Zn^{2+} and S^{2-} in water, J. Lumin. 147 (2014) 179-183.

[190] C. I. C. Esteves, R. M. F. Batista, M. M. M. Raposo, S. P. G. Costa, Novel functionalised imidazo-benzocrown ethers bearing a thiophene spacer as fluorimetric chemosensors for metal ion detection, Dyes Pigment.135 (2016) 134-142.

[191] C. Reichardt, T. Welton, Solvent Effects on the Absorption Spectra of Organic Compounds. Wiley-VCH Verlag GmbH & Co. KGaA, 2010

[192] S.-J. Yoon, J. W. Chung, J. Gierschner, K. S. Kim, M.-G. Choi, D. Kim, S. Y. Park, Multistimuli Two-Color Luminescence Switching via Different Slip-Stacking of Highly Fluorescent Molecular Sheets, J. Am. Chem. Soc. 132 (2010) 13675-13683.

[193] H. E. Ratcliffe, G. M. Swanson, L. J. Fischer, Human Exposure to Mercury: A Critical Assessment of the Evidence of Adverse Health Effects, J. Toxicol. Environ. Health 49 (1996) 221-270.

[194] I. O. P. de Souza, C. M. L. Schrekker, W. Lopes, R. V. A. Orru, M. Hranjec, N. Perin, M. Machado, L. F. Oliveira, R. K. Donato, V. Stefani, A. M. Fuentefria, H. S. Schrekker, Bifunctional fluorescent benzimidazo[1,2-α]quinolines for Candida spp. biofilm detection and biocidal activity, J. Photochem. Photobiol. B - Biology 163 (2016) 319-326.

[195] N. H. Evans, P. D. Beer, Advances in Anion Supramolecular Chemistry: From Recognition to Chemical Applications, Angew. Chem.-Int. Edit. 53 (2014) 11716-11754.

[196] P. A. Gale, C. Caltagirone, Anion sensing by small molecules and molecular ensembles, Chem. Soc. Rev. 44 (2015) 4212-4227.

[197] T. Y. Joo, N. Singh, G. W. Lee, D. O. Jang, Benzimidazole-based ratiometric fluorescent receptor for selective recognition of acetate, Tetrahedron Lett. 48 (2007) 8846-8850.

[198] B. Chetia, P. K. Iyer, Acetate recognition by 2,6-bis(2-benzimidazolyl)pyridine, Spectroc. Acta Pt. A-Molec. Biomolec. Spectr. 81 (2011) 313-316.

[199] S. Kumar, P. Singh, S. Kumar, 1-(2-Naphthalenyl)benzimidazolium based fluorescent probe for acetate ion in 90% aqueous buffer, Tetrahedron Lett. 53 (2012) 2248-2252.

[200] Y. Abraham, H. Salman, K. Suwinska, Y. Eichen, Cyclo 2-benzimidazole: luminescence turn-on sensing of anions, Chem. Commun. 47 (2011) 6087-6089.

[201] J. Shao, Y. Qiao, H. Lin, H. Lin, Rational Design of Novel Benzimidazole-Based Sensor Molecules that Display Positive and Negative Fluorescence Responses to Anions, J. Fluoresc. 19 (2009) 183-188.

[202] S. Kumar, S. Kumar, 1-(4-Nitrophenyl)-benzimidazolium-based ratiometric chromogenic probes for cyanide ion, Tetrahedron Lett. 50 (2009) 4463-4466.

[203] J.-B. Li, J.-H. Hu, J.-J. Chen, J. Qi, Cyanide detection using a benzimidazole derivative in aqueous media, Spectroc. Acta Pt. A-Molec. Biomolec. Spectr. 133 (2014) 773-777.

[204] D. Wang, J.-Q. Zheng, X. Yan, X.-J. Zheng, L.-P. Jin, Cu(II) complex-based fluorescence chemosensor for cyanide in aqueous media, RSC Adv. 5 (2015) 64756-64762.

[205] A. Sen Gupta, K. Paul, V. Luxami, Benzimidazole based ratiometric chemosensor for detection of CN^- and Cu^{2+} ions in protic/aqueous system: Elaboration as XOR logic operation, Inorg. Chim. Acta 443 (2016) 57-63.

[206] V. Luxami, R. Rani, A. Sharma, K. Paul, Quinazoline-benzimidazole hybrid as dual optical sensor for cyanide and Pb^{2+} ions and Aurora kinase inhibitor, J. Photochem. Photobiol. A-Chem. 311 (2015) 68-75.

[207] M. Yu, H. Lin, G. Zhao, H. Lin, A benzimidazole-based chromogenic anion receptor, J. Mol. Recognit. 20 (2007) 69-73.

[208] B. Chetia, P. K. Iyer, Selective fluoride anion sensing by simple benzimidazolyl based ligand, Sens. Actuator B-Chem.201 (2014) 191-195.

[209] S. Madhu, M. Ravikanth, Boron-Dipyrromethene Based Reversible and Reusable Selective Chemosensor for Fluoride Detection, Inorg. Chem. 53 (2014) 1646-1653.

[210] Y. C. Wu, J. P. Huo, L. Cao, S. Ding, L. Y. Wang, D. R. Cao, Z. Y. Wang, Design and application of tri-benzimidazolyl star-shape molecules as fluorescent chemosensors for the fast-response detection of fluoride ion, Sens. Actuator B-Chem.237 (2016) 865-875.

[211] K. S. Moon, N. Singh, G. W. Lee, D. O. Jang, Colorimetric anion chemosensor based on 2-aminobenzimidazole: naked-eye detection of biologically important anions, Tetrahedron 63 (2007) 9106-9111.

[212] A. Sen Gupta, A. Garg, K. Paul, V. Luxami, Differential sensing of fluoride and cyanide ions by using Dicyano substituted benzimidazole probe, J. Lumin. 173 (2016) 165-170.

[213] G. Wang, H. Qi, X.-F. Yang, A ratiometric fluorescent probe for bisulphite anion, employing intramolecular charge transfer, Luminescence 28 (2013) 97-101.

[214] X. Dai, T. Zhang, Z. F. Du, X. J. Cao, M. Y. Chen, S. W. Hu, J. Y. Miao, B. X. Zhao, An effective colorimetric and ratiometric fluorescent probe for bisulfite in aqueous solution, Anal. Chim. Acta 888 (2015) 138-145.

[215] L. J. Zhang, Z. Y. Wang, X. J. Cao, J. T. Liu, B. X. Zhao, An effective ICT-based and ratiometric fluorescent probe for sensing sulfite, Sens. Actuator B-Chem.236 (2016) 741-748.

[216] B. Roubinet, L. Bailly, E. Petit, P. Y. Renard, A. Romieu, A FRET-based probe for fluorescence sensing of sulfide/sulfite analytes, using a novel long-wavelength water-soluble 7-hydroxycoumarin as reporter fluorophore, Tetrahedron Lett. 56 (2015) 1015-1019.

[217] N. Singh, D. O. Jang, Benzimidazole-based tripodal receptor: Highly selective fluorescent chemosensor for iodide in aqueous solution, Org. Lett. 9 (2007) 1991-1994.

[218] K. Ghosh, I. Saha, A new benzimidazolium receptor for fluorescence sensing of iodide, Supramol. Chem. 22 (2010) 311-317.

[219] R. Kumar, S. Kumar, P. Singh, G. Hundal, M. S. Hundal, S. Kumar, A fluorescent chemosensor for detection of perchlorate ions in water, Analyst 137 (2012) 4913-4916.

[220] K. Ghosh, I. Saha, R. Frohlich, A. Patra, Selective Sensing of Fumarate Over Maleate by Benzimidazolium - Based Fluororeceptors, Mini-Reviews in Organic Chemistry 8 (2011) 31-37.

[221] V. Amendola, D. Esteban-Gomez, L. Fabbrizzi, M. Licchelli, What anions do to N-H-containing receptors, Acc. Chem. Res. 39 (2006) 343-353.

[222] L. Zhang, B. Li, A highly selective optical sensor for aniline recognition, Spectrochimica Acta Part a-Molecular and Biomolecular Spectroscopy 74 (2009) 1060-1063.

[223] M. Ishida, P. Kim, J. Choi, J. Yoon, D. Kim, J. L. Sessler, Benzimidazole-embedded N-fused aza-indacenes: synthesis and deprotonation-assisted optical detection of carbon dioxide, Chem. Commun. 49 (2013) 6950-6952.

[224] A. Singh, A. Singh, N. Singh, D. O. Jang, A benzimidazolium-based organic trication: a selective fluorescent sensor for detecting cysteine in water, RSC Adv. 5 (2015) 72084-72089.

[225] B. Fernandez, A. Gomez-Vilchez, C. Sanchez-Gonzalez, J. Bayon, E. San Sebastian, S. Gomez-Ruiz, C. Lopez-Chaves, P. Aranda, J. Llopis, A. Rodriguez-Dieguez, Novel anti-diabetic and luminescent coordination compounds based on vanadium, New J. Chem. 40 (2016) 5387-5393.

[226] S. Wang, Y.-T. Chang, Discovery of heparin chemosensors through diversity oriented fluorescence library approach, Chem. Commun. (2008) 1173-1175.

[227] S. Pal, M. Mukherjee, B. Sen, S. Lohar, P. Chattopadhyay, Development of a rhodamine-benzimidazol hybrid derivative as a novel FRET based chemosensor selective for trace level water, RSC Adv. 4 (2014) 21608-21611.

[228] S. Nandi, S. Mandal, J. S. Matalobos, A. Sahana, D. Das, Interaction of water with a benzimidazole derivative: fluorescence and colorimetric recognition of trace level water involving intramolecular charge transfer process, J. Mol. Recognit. 29 (2016) 5-9.

[229] K. Ghosh, D. Tarafdar, A. Samadder, A. R. Khuda-Bukhsh, A benzimidazolium-based new flexible cleft built on the piperazine unit: a case of selective fluorometric sensing of ATP, RSC Adv. 4 (2014) 58530-58535.

[230] J. Ouyang, H. Hong, C. Shen, Y. Zhao, C. G. Ouyang, L. Dong, J. H. Zhu, Z. J. Guo, K. Zeng, J. N. Chen, C. Y. Zhang, J. F. Zhang, A novel fluorescent probe for the detection of nitric oxide in vitro and in vivo, Free Radical Biol. Med. 45 (2008) 1426-1436.

[231] S. Das, S. Guha, A. Banerjee, S. Lohar, A. Sahana, D. Das, 2-(2-Pyridyl) benzimidazole based Co(II) complex as an efficient fluorescent probe for trace level determination of aspartic and glutamic acid in aqueous solution: A displacement approach, Org. Biomol. Chem. 9 (2011) 7097-7104.

[232] J. Ding, Y. Q. Ge, B. C. Zhu, A Highly Selective Fluorescent Probe for Quantitative Detection of Hydrogen Sulfide, Anal. Sci. 29 (2013) 1171-1175.

[233] B. Dumat, E. Faurel-Paul, P. Fornarelli, N. Saettel, G. Metge, C. Fiorini-Debuisschert, F. Charra, F. Mahuteau-Betzer, M. P. Teulade-Fichou, Influence of the oxazole ring connection on the fluorescence of oxazoyl-triphenylamine biphotonic DNA probes, Org. Biomol. Chem.14 (2016) 358-370.

[234] L. J. Tang, J. Z. Shi, Z. L. Huang, X. M. Yan, Q. Zhang, K. L. Zhong, S. H. Hou, Y. J. Bian, An ESIPT-based fluorescent probe for selective detection of homocysteine and its application in live-cell imaging, Tetrahedron Lett. 57 (2016) 5227-5231.

[235] L. Basabe-Desmonts, D. N. Reinhoudt, M. Crego-Calama, Design of fluorescent materials for chemical sensing, Chem. Soc. Rev. 36 (2007) 993-1017.

[236] F. Canfarotta, M. J. Whitcombe, S. A. Piletsky, Polymeric nanoparticles for optical sensing, Biotechnol. Adv. 31 (2013) 1585-1599.

[237] M. Montalti, E. Rampazzo, N. Zaccheroni, L. Prodi, Luminescent chemosensors based on silica nanoparticles for the detection of ionic species, New J. Chem. 37 (2013) 28-34.

[238] J. W. Aylott, Optical nanosensors - an enabling technology for intracellular measurements, Analyst 128 (2003) 309-312.

[239] P. K. Tomar, S. Chandra, I. Singh, A. Kumar, A. Malik, A. Singh, Development of a new copper(II) ion-selective PVC membrane electrode based on tris(2-benzimidazolylmethyl)amine, J. Indian Chem. Soc. 88 (2011) 1739-1744.

[240] Z. N. Yan, S. Y. Zhang, H. X. Wang, Y. X. Kang, Preparation and analytical application of new Cr3+-selective membrane electrodes based on acylhydrazone-containing benzimidazole derivatives, J. Iran Chem. Soc. 13 (2016) 411-420.

[241] P. C. A. Jeronimo, A. N. Araujo, M. C. B. S. M. Montenegro, Optical sensors and biosensors based on sol-gel films, Talanta 72 (2007) 13-27.

[242] H. S. Hoffmann, V. Stefani, E. V. Benvenutti, T. M. H. Costa, M. R. Gallas, Fluorescent silica hybrid materials containing benzimidazole dyes obtained by sol-gel method and high pressure processing, Mater. Chem. Phys. 126 (2011) 97-101.

[243] M. Shimizu, Y. Takeda, M. Higashi, T. Hiyama, 1,4-Bis(alkenyl)-2,5-dipiperidinobenzenes: Minimal Fluorophores Exhibiting Highly Efficient Emission in the Solid State, Angew. Chem. 121 (2009) 3707-3710.

[244] Z. Zhang, B. Xu, J. Su, L. Shen, Y. Xie, H. Tian, Color-Tunable Solid-State Emission of 2,2′-Biindenyl-Based Fluorophores, Angew. Chem. Int. Ed. 50 (2011) 11654-11657.

PRILOZI

RAD 1

E. Horak, R. Vianello, M. Hranjec, S. Krištafor, G. K. Zamola,I. M. Steinberg, *Benzimidazole acrylonitriles as multifunctional push-pull chromophores: Spectral characterisation, protonation equilibria and nanoaggregation in aqueous solutions*, Spectrochimica Acta Part A: Molecular and Biomolecular Spectroscopy **178** (2017) 225-33.

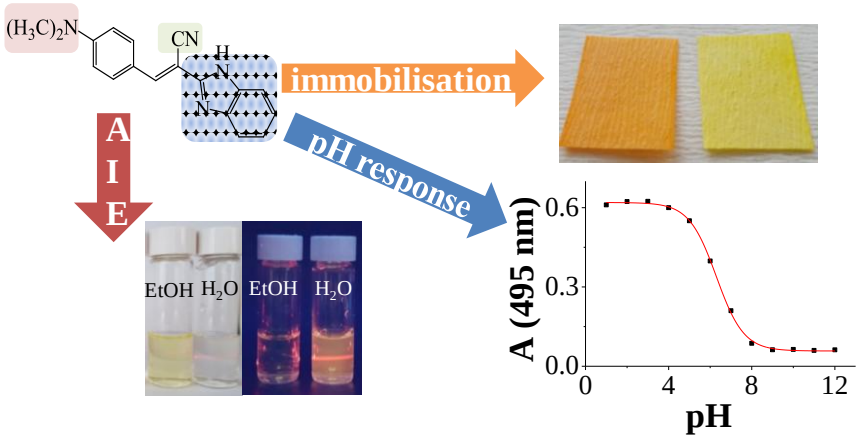

Benzimidazole acrylonitriles as multifunctional push-pull chromophores: spectral characterisation, protonation equilibria and nanoaggregation in aqueous solutions

Ema Horak[a], Robert Vianello[b], Marijana Hranjec[c], Svjetlana Krištafor[a], Grace Karminski Zamola[c] and Ivana Murković Steinberg[a]*

[a]*Department of General and Inorganic Chemistry, Faculty of Chemical Engineering and Technology, University of Zagreb, Marulićev trg 19, HR 10000 Zagreb, Croatia*
[b]*Computational Organic Chemistry and Biochemistry Group, Ruđer Bošković Institute, Bijenička cesta 54, HR 10000 Zagreb, Croatia*
[c] *Department of Organic Chemistry, Faculty of Chemical Engineering and Technology University of Zagreb, Marulićev trg 20, HR 10000 Zagreb, Croatia*

*Corresponding author:
Ivana Murković Steinberg, Department of General and Inorganic Chemistry, Faculty of Chemical Engineering and Technology, University of Zagreb, Marulićev trg 19, HR-10000 Zagreb, Croatia, Phone No. ++38514597287; e-mail: ivana.murkovic@fkit.hr

Abstract

Heterocyclic donor-π-acceptor molecular systems based on an *N*,*N*-dimethylamino phenylacrylonitrile benzimidazole skeleton have been characterised and are proposed for potential use in sensing applicatons. The benzimidazole moiety introduces a broad spectrum of useful multifunctional properties to the system including electron accepting ability, pH sensitivity and compatibility with biomolecules. The photophysical characterization of the prototropic forms of these chromophores has been carried out in both solution and on immobilisation in polymer films. The experimental results are further supported by computational determination of pK_a values. It is noticed that compound **3** forms

nanoaggregates in aqueous solutions with aggregation-induced emission (AIE) at 600 nm. All the systems demonstrate spectral pH sensitivity in acidic media which shifts towards near-neutral values upon immobilisation in polymer films or upon aggregation in an aqueous environment (compound **3**). The structure-property relationships of these functional chromophores, involving their spectral characteristics, acid-base equilibria, pK_a values and aggregation effects have been determined. Potential applications of the molecules as pH and biomolecular sensors are proposed based on their pH sensitivity and AIE properties.

Keywords: push-pull chromophores; benzimidazole; aggregation induced emission (AIE); pH sensitivity; prototropic equlibrium

1. Introduction

Intramolecular charge-transfer (ICT) organic systems based on electron donor-π-bridge-electron acceptor structures (D-π-A) are widely used as chromophores and fluorophores in advanced functional materials [1] and (bio)analytical or imaging applications [2].

The photophysical and chemical properties of such push-pull molecular systems are defined by the position, number and electron donating and accepting strengths of donor and acceptor groups and their chemical nature. Insight into the structure-property relationships allows fine tuning of their functional properties [3-5]. In this respect D-π-A systems based on heteroaromatic scaffolds such as styryl heterocycles [6-8] or imidazole derivatives [9] are especially interesting due to the additional functional molecular features they bring to chromophores: specific chemical and biological activity.

The benzimidazole moiety (BI) can serve as a multifunctional unit in such heteroaromatic molecular systems: its electron accepting and π bridging properties combined with chromogenic pH sensitivity/switching, metal-ion chelating properties and compatibility with biomolecules makes the BI moiety an especially attractive building block in D-π-A systems for different applications: optoelectronics and non-linear optics (NLO), photovoltaics, sensing and bioimaging. Representative examples of BI based ICT chromo- and fluorophores include materials for OLEDs [10], dye-sensitised solar cells (DSSCs) [11, 12] and molecular chemosensors [13], sensors for pH [14-17] metal-ions [18, 19], anions [20], biomolecules [21], and pH probes for bioimaging [22].

The structure-property impact of BI units within D-π-A heteroaromatic chromophores, especially pH sensitivity, have been studied in detail spectroscopically and theoretically [23-26] in potential sensing applications and for NLO pH switching. Studies involve computational prediction and determination of pK_a values and photophysical or non-linear properties and usually represent the first step in the design of novel multi-responsive molecular systems.

As a result of their dipolar structure, the ICT compounds can also form self-assembled functional molecular systems [27]. The cyano group, as a typical strong electron acceptor in D-π-A systems strongly affects the spectral characteristics of the molecules (λ_{abs} and ε), as well as the basicity of neighbouring nitrogen atoms and their corresponding pK_a values [28]. Additionally, the presence of a cyano group in these chromophores has been identified as a key factor in the creation of supramolecular interactions [29-32], leading to the formation of fluorescent organic nanoparticles (FONs) that exhibit aggregation induced emission (AIE) [33]. Aggregation induced emission is a photophysical phenomenon with great application promise, related to certain organic molecules which exhibit stronger fluorescence in their aggregated states than in the dissolved state.

Here we present multifunctional D-π-A molecular systems containing an *N*,*N*-dimethylamino group as a pH sensitive donor group connected via a π linker (styryl) to the electron accepting substituents: cyano group and the pH sensitive benzimidazole moiety (Fig. 1).

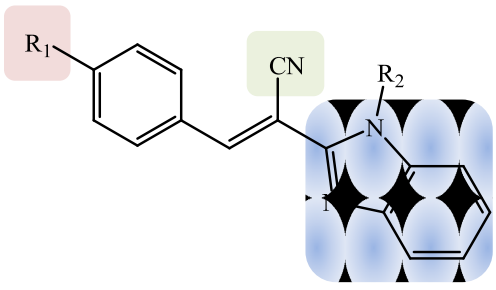

Fig. 1. D-π-A molecular system based on benzimidazole derivative.

The photophysical characterisation and computationally supported determination of species involved in prototropic equilibria, including their respective pK_a values, have been performed in order to better understand the effects of the D-π-A molecular structure on the UV-Vis spectral properties, nanoaggregation and pH sensing potential of these chromophores.

The results are critically evaluated in the light of structurally similar multifunctional compounds including cyanostilbenes [34], styrylbenzoxazoles [35] and cyanovinyl substituted

benzimidazoles [11, 19] as promising candidates for functional application as AIE-based pH probes, dye sensitisers in solar cells and as metal-ion sensors.

2. Materials and Methods

2.1. Reagents and instrumentation

Chemicals for synthesis and pure organic solvents were purchased from commercial suppliers Acros, Aldrich or Fluka. Hydrochloride acid and potassium hydroxide were obtained from Kemika d.d., Zagreb. Poly(vinylchloride) (PVC, high molecular weight) for thin film preparation was purchased from Fluka, whilst dioctyl sebacate (DOS) and potassium tetrakis(4-chlorophenyl)borate (PTCB) were obtained from Sigma-Aldrich. Polyester sheets (Laser + Copier Film 210 x 297 mm, d = 0.1 mm) were purchased from Zweckform. Milli-Q water was used for the preparation of aqueous solutions. pH was measured on commercially available pH electrode Blue Line 17 pH, Schott AG, Mainz, Germany. Absorption spectra were recorded by Cary 100 Scan Varian spectrophotometer. Fluorescence measurements were carried out by Varian Cary Eclipse fluorescence spectrophotometer. Quartz cells of 1 cm path length were used throughout measurements and absorbance and fluorescence values were recorded at 1 nm. Wavelength scan was performed between 250 nm and 800 nm. Baseline was recorded prior to each set of experiments in aqueous and non-aqueous solutions. Emission spectra corrected for the effects of time- and wavelength-dependent light-source fluctuations using a standard of Rhodamine 101, a diffuser provided with the fluorimeter and the software supplied with the instrument. Dynamic light scattering (DLS) experiments were conducted using Malvern Zetasizer Nano range light scattering instrument.

2.2. Synthesis of benzimidazole derivatives

All chemicals and solvents were purchased from commercial suppliers Aldrich and Acros. Melting points were recorded on SMP11 Bibby and Büchi 535 apparatus. NMR spectra were measured in DMSO-d_6 solutions using TMS as an internal standard. The ^{1}H and ^{13}C NMR spectra were recorded on a Varian Gemini 300 or Varian Gemini 600 at 300, 600 and 150 and 75 MHz, respectively. Chemical shifts are reported in ppm (δ) relative to TMS. All compounds were routinely checked by TLC with Merck silica gel 60F-254 glass plates.

The 2-benzimidazolyl substituted chromophores **1**-**4** (Fig. 2) were prepared in one-step condensation of 2-cyanomethylbenzimidazole or 2-cyanomethyl-*N*-phenylbenzimidazole with

corresponding heteroaromatic aldehydes in absolute ethanol by adding a few drops of piperidine [19, 36]. Detailed synthesis and structure properties of **1**-**4** can be found in supplementary material.

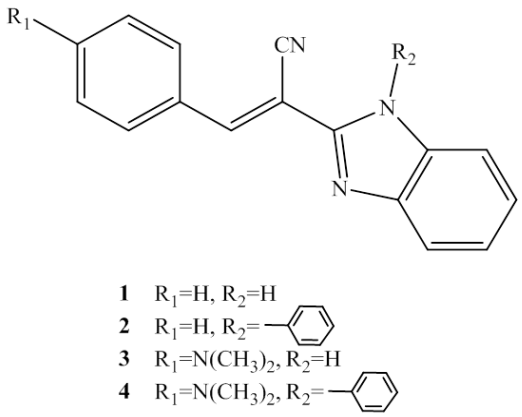

Fig. 2. Synthesised benzimidazole derivatives **1**-**4**.

2.3. Photophysical characterisation and acid-base properties

Basic photophysical properties of examined compounds were characterised by UV-visible absorption and fluorescence spectroscopy. Spectra were recorded in solvents with different $E_T(30)$ solvent polarity parameters [37]. The concentration of the chromophore solutions was $1x10^{-5}$ mol dm^{-3}. All the solvents were of high purity grade. Excitation wavelengths were determined from absorbance maxima. Quantum yields were determined by IUPAC method using quinine sulphate as standard (Φ = 0.546). The characterisation of benzimidazole derivatives **1**-**4** was conducted by diluting the stock solutions in methanol or ethanol (methanol or ethanol volume fraction in diluted solutions did not exceed 1.5 %). Concentrations of stock solutions were as it follows: c(**1**)=2.18×10^{-3} mol dm^{-3}; c(**2**)=1.35×10^{-3} mol dm^{-3} c(**3**)=6.4×10^{-4} mol dm^{-3}; c(**4**)=9.2×10^{-4} mol dm^{-3}.

The pH titration experiments were carried out using $1x10^{-5}$ mol dm^{-3} solutions of the compounds **1**-**4** in 0.1 M hydrochloric acid or 0.1 M potassium hydroxide solutions. The adjustment of pH was achieved through the acid or base addition until the change of pH within 0.5 units occurred. Following each addition of titrant, UV-visible absorption spectrum was recorded after the time required keeping the drift of pH electrode within 0.1 pH units per minute. Titrations were conducted at constant ionic strength I = 0.1 M, in potassium chloride solutions. The pK_a values were calculated as the x-coordinate of the inflection point of the Boltzmann function (1) obtained from spectrophotometric titrations data:

$$y = \frac{A_1 - A_2}{1 + e^{(x - x_0)/dx}} + A_2 \quad (1)$$

Dynamic light scattering (DLS) experiments were carried out in aqueous (f_w = 99% water/ethanol) and in ethanol solution, c = 10 μM.

2.4. Theoretical calculations of pK_a values

All of the molecular geometries were initially optimised in the gas-phase by the efficient and accurate M06–2X/6–31+G(d,p) model. The thermal corrections were extracted from the corresponding frequency calculations without the application of scaling factors. The final single-point energies were attained with a highly flexible 6–311++G(2df,2pd) basis set using the MP2 approach giving the MP2/6–311++G(2df,2pd)//M06–2X/6–31+G(d,p) model employed here for the gas-phase free energies. To account for the solvation effects, we reoptimized geometries employing the SMD polarisable continuum model [38] at the (SMD)/M06–2X/6–31+G(d,p) level with all parameters corresponding to pure water, and calculated solvation free energies as a difference between the corresponding SMD and gas-phase calculations at the same level of theory. The choice of such a computational setup was prompted by our success in estimating both pK_a and reaction thermodynamic values in solution [39, 40]. pK_a values were calculated in a relative fashion using $AH + B_{REF} \rightarrow A^- + B_{REF}H$ equation, and employing the following reference bases ($B_{REF}H$): benzimidazole (pK_a = 12.75 and 5.41) [41] for the deprotonation and protonation of this fragment, respectively, and *N*,*N*-dimethylaniline (pK_a = 5.15) [41] for the protonation of the dimethylamino group in investigated systems. All of the calculations were performed using the Gaussian 09 software [42].

2.5. Immobilisation of 3-4 in polymer films

Chromophores **3** and **4** were immobilised in plasticised PVC matrix starting from liquid mixture prepared by modified published method [43]. The “cocktail' contained 67 mg PVC, 134 mg DOS (the plasticiser), 2.4 mg (1 eq) of PTCB and 1 eq of compound **3** or **4** in 1.5 mL THF. Mixture was placed in ultrasonic bath for 15 min. Thin polymer films were prepared by spreading 100 μL mixture onto a 2.5 x 2.5 cm solid transparent polyester sheet by spin-coating technique. Obtained thin films were dried at room temperature for 18 h in dark. pH response of immobilised chromophores was examined in buffer solutions, pH 2 to 12.

2.6. DNA interaction experiments

A polynucleotide calf thymus DNA was purchased from Sigma and Aldrich, and used without further purification. Polynucleotide was dissolved in the BPE buffer (6mM Na_2HPO_4, 2mM NaH_2PO_4, 1mM EDTA), pH=7.0. Stock solution of compound **3** was prepared in ethanol. Respective aliquot of stock solution of **3** was added to the aqueous buffer (c = 1x10^{-5} mol dm^{-3}) and titration with DNA was conducted.

Spectral measurements were performed in aqueous buffer solution (BPE buffer, pH=7.0, and phosphate buffer, pH = 7.4). Absorbance and emission spectra were recorded after every addition of DNA aliquot. The partial volume of ethanol in water did not exceed 0.1%.

3. Results and Discussion

3.1. Design and D-π-A structure of chromophores

Compounds **1** and **2** as parent molecules were converted into D-π-A molecular systems (compounds **3** and **4**) by introduction of strong electron donating *N*,*N*-dimethylamino group, (D) into their phenylacrylonitrile benzimidazole conjugated skeleton.

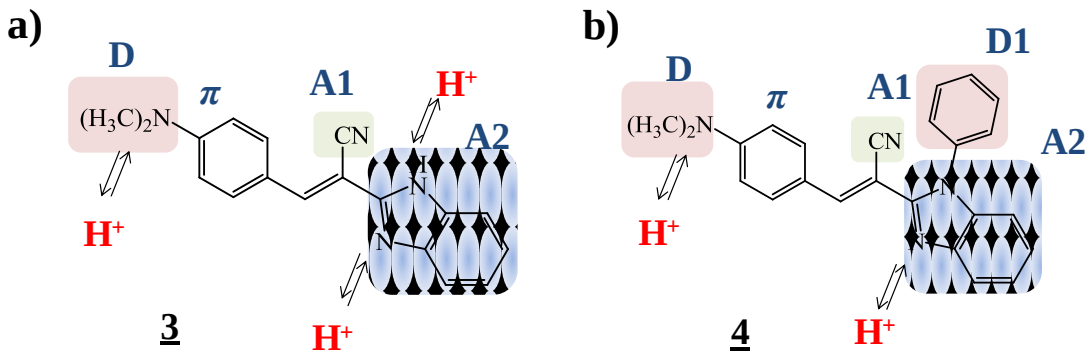

Fig. 3. D-π-A arrangement and protonable-deprotonable sites of (a) **3** and (b) **4.**

In terms of D-π-A arrangement the structures of chromophores **3** and **4** are shown in Fig. 3. In compound **3** the $-NMe_2$ as a strong donor group (D) is connected via π linker (styryl) to the very strong acceptor group A1 (cyano) and a weaker acceptor A2 (benzimidazole unit) forming a D-π-A1-A2 structure. In compound **4**, the benzimidazole moiety is modified with bulky electron donating phenyl substituent (D1) which increases the electron density of A2.

All structures contain acid-base active sites as a part of either donor or acceptor moiety and are marked in Fig. 3. These are amino nitrogen atom (in donor group D) and imino (azole)

nitrogen atom (in acceptor group A2) as protonable sites in **3** and **4**. The NH group on the benzimidazole ring in **3** is marked as deprotonable site.

Structural analogues of **3** previously reported in the literature included *N*,*N*-dimethylamino styryl benzimidazole [25] **(**D-π-A2), *N*,*N*-dimethylamino pyridyl acrylonitrile [32] (D-π-A1-pyrydyl), cyanostilbene derivatives [34] (D-π-A1-(phenyl or phenoyl)) and *N*,*N*-diethylamino analogue of **3** with carboxyl group attached to BI moiety [11].

The proposed donor- π- acceptor structures were used as a basis for discussion of structure-property relationships of **1-4** determined in this study (photophysical properties of prototropic species and the corresponding pK_a values).

3.2. Photophysical properties of chromophores 1-4

The chromophores were studied by UV-Vis absorption and fluorescence spectroscopy in different solvents. Absorption spectra of compounds **1-4** in ethanol are shown in Fig. 4a, and their basic photophysical properties in ethanol are summarised in Table 1.

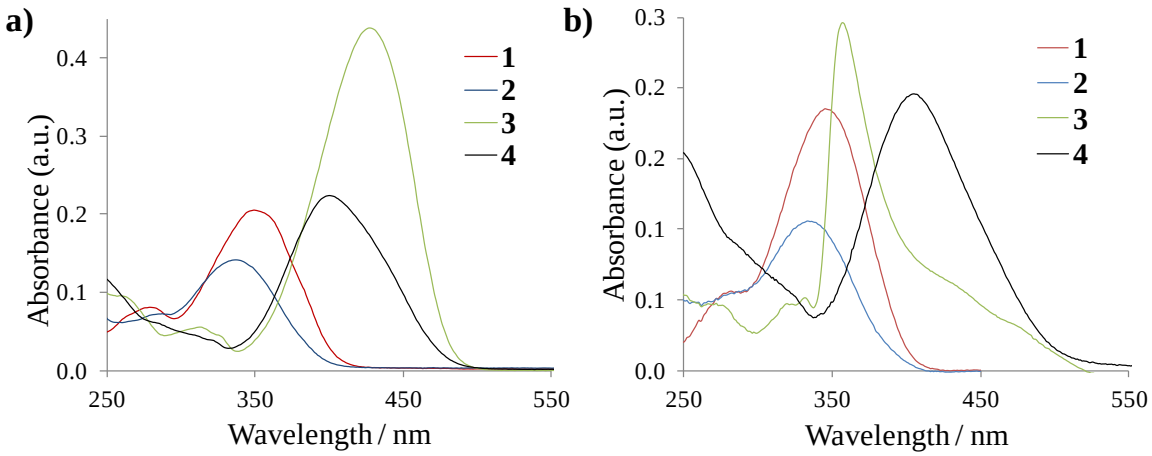

Fig. 4. Absorption spectra of compounds **1-4,** c = 1 x 10^{-5} M, in (a) ethanol and (b) water.

Table 1. Photophysical properties of compounds **1-4** in ethanol.

	Absorption		**Emission**		
Compound	λ_{abs} / nm	ε x 10^{-3} / $M^{-1}cm^{-1}$	λ_{em} / nm	Stokes shift / nm	Φ
1	204 350[a]	20.40	444	100	0.0027
2	202 335	14.13	464	136	0.0045
3	202 425	43.91	491	66	0.0021
4	202 400	22.38	486	86	0.0022

[a]underlined values were used to calculate molar absorption coefficients and Stokes shifts

Compounds **1** and **2** show the main absorption bands with maxima at 350 nm and 335 nm respectively. As expected, introduction of an *N*,*N*-dimethylamino group (−NMe_2) into **1** and **2** caused a bathochromic shift of 75 nm and 65 nm and considerable increase of molar absorption coefficients, as observed in compounds **3** and **4,** respectively (Table 1).

Both effects can be explained by the appearance of a strong intramolecular charge transfer (ICT) due to D-A interactions involving the electron donating −NMe_2 group.

As a result of its D-π-A1-A2 structure with enhanced push-pull effects, compound **3** shows the greatest red-shift with an absorption maximum at 425 nm, and a very high molar absorption coefficient of 43 910 dm^3 cm^{-1} mol^{-1}. In **4**, ICT effects are less pronounced due to D-π-A1-A2-D1 structure in which the electron donating phenyl substituent (D1) reduces the electron accepting power of the acceptor moiety. Previously reported *N*,*N*-dimethylamino styryl benzimidazole [25] has an absorption maximum at 374 nm. Introduction of a strong electron-withdrawing cyano group into its skeleton (compound **3**) results in a 50 nm bathochromic shift. All compounds show modest fluorescence in ethanol with quantum yields less than 0.01 and emission maxima that range from 444 nm to 491 nm. Due to relatively low fluorescence intensity in ethanol the compounds are not readily promising candidates for fluorimetric analytical applications.

The absorption spectra of **1-4** in aqueous solutions are shown in Fig. 4b, and the summary of absorption spectroscopy data in solvents of different polarity are presented in Table 2.

The absorption maxima of compounds **1** and **2** (λ_{abs}) recorded in solvents of varying polarity indicate a weak negative solvatochromic effect. A change of solvent from toluene to water induced a blue-shift in the absorption maxima of $\Delta\lambda$(**1**) = 18 nm and $\Delta\lambda$(**2**) = 10 nm. Compound **3** in water showed unusual spectral characteristics (Fig. 4b) indicating the presence of specific solvent effects, whilst **4** exhibited a very small positive solvatochromism with absorption maxima ranging from 390 nm in nonpolar aprotic toluene to 400 nm and 404 nm in hydrogen bond donating solvents, ethanol/methanol and water respectively. The reason for the different solvatochromic responses of **1-4** is most likely due to their different D-A structures, position and nature of ionisable sites (Fig. 3), and the corresponding polarity of the molecules in their respective ground and excited states. The small blue shift observed in **1** and **2** on increased solvent polarity suggests that these molecules possess a greater dipole moment in their ground state than in their respective excited states, whereas the red shift of **4** can be explained by a greater dipole moment in the excited state, leading to stronger stabilisation in solvents of higher polarity. A similar trend is observed for molar absorption coefficients (ε) which generally decrease on going from toluene to water for **3** and **4**. The spectral bandwidth expressed as FWHM value is fairly constant for **1** and **2** in all solvents (around 70 nm), but for **3** (except in water) and **4** increases with solvent polarity, as shown in Table 2. In comparison with other compounds, **3** has the highest values of ε and λ_{abs} in all solvents (except in water), which can be attributed to its stronger ICT character as discussed earlier based on its D-π-A1-A2 structure.

It is evident that compound **3** shows significantly different spectral characteristics in water in comparison to other solvents. Namely, **3** is yellow in all solvents except in water. Water solution is visually colourless and transparent, and spectrally it shows a sharp non-symmetrical (red-tailed) absorption band (FWHM value of 31 nm) with a maximum at around 350 nm (Fig. 4b). The water solution absorption peak wavelength λ_{abs} of **3** is blue-shifted by approximately 70 nm in comparison to other solvents. The ICT character of **3** becomes less pronounced in water solutions and is comparable to the spectral characteristics of compound **1**, its non-ICT analogue. These findings strongly indicate the presence of dye nanoaggregates, formed by the specific intermolecular interactions in aqueous environment. The shape of the absorption spectrum of **3** in water indicates presence light scattering effects on nanoparticles [44]. This was confirmed by Tyndall effect which occurred on visually transparent solution of **3** using a laser beam, as shown in Fig. S1A. In addition, the presence of nanometer and

micrometer sized aggregates of **3** in aqueous solutions (f_w = 99 %, c = 10 μM) was confirmed by dynamic light scattering experiments (Fig S1B).

It was also noticed that the water solution of **3** (colourless under ambient light) shows orange-red emission under UV light. Hence, the effects of nanoaggregation on spectroscopic properties of **3** were further studied in mixed solvent solutions (water-ethanol).

Table 2. Maximum absorbance wavelengths, molar absorption coefficients and FWHM values of benzimidazole chromophores in solvents of different polarities and $E_T(30)$ values.

		Solvent[a]				
		Toluene	**Ethyl acetate**	**EtOH**	**MeOH**	**H_2O**
		$E_T(30)$=33.9	$E_T(30)$=38.1	$E_T(30)$=51.9	$E_T(30)$=55.4	$E_T(30)$=63.1
1	λ_{abs} (nm)	362	350	350	346	344
	ε x 10^{-3} ($M^{-1}cm^{-1}$)	20.12	24.23	20.40	22.27	17.87
	FWHM (nm)	72	70	73	70	70
2	λ_{abs} (nm)	345	343	335	334	335
	ε x 10^{-3} ($M^{-1}cm^{-1}$)	28.23	32.97	14.13	27.11	10.56
	FWHM (nm)	70	71	65	69	63
3	λ_{abs} (nm)	430	420	425	425	356
	ε x 10^{-3} ($M^{-1}cm^{-1}$)	48.42	42.01	43.91	38.09	24.58[b]
	FWHM (nm)	77	75	86	81	31[b]
4	λ_{abs} (nm)	390	390	400	400	404
	ε x 10^{-3} ($M^{-1}cm^{-1}$)	30.42	25.87	22.38	32.42	19.61
	FWHM (nm)	59	64	68	64	89

[a] solvents contained 1 % of methanol (volume fraction of methanol, f_{MeOH}=1%) , [b]aggregation

3.3. Aggregation induced emission in aqueous solutions

The absorption and emission characteristics of **3** were investigated in water-ethanol mixtures of varying volume fraction of water, f_w. The resulting spectra are shown in Fig. 5a.

Compound **3** shows orange-red fluorescence emission at 600 nm in water, which gradually disappears upon addition of ethanol (Fig. 5). At a water fraction of f_w = 0.80 virtually no florescence emission at 600 nm is observable. The intensity of orange emission in aqueous solution (f_w = 99 %) is approximately 35-fold the emission in ethanol at 600 nm. This

photophysical phenomenon can be explained by aggregation induced emission, as first reported by Tang *et al*. [45] and Park *et al*. [30]. Unlike most organic fluorophores, some organic molecules exhibit strong fluorescence upon aggregation in poor solvents or in the solid-state. Different mechanisms have been proposed to explain AIE including restriction of intramolecular rotation (RIR), J-aggregate formation, twisted intramolecular charge transfer (TICT) and others [33].

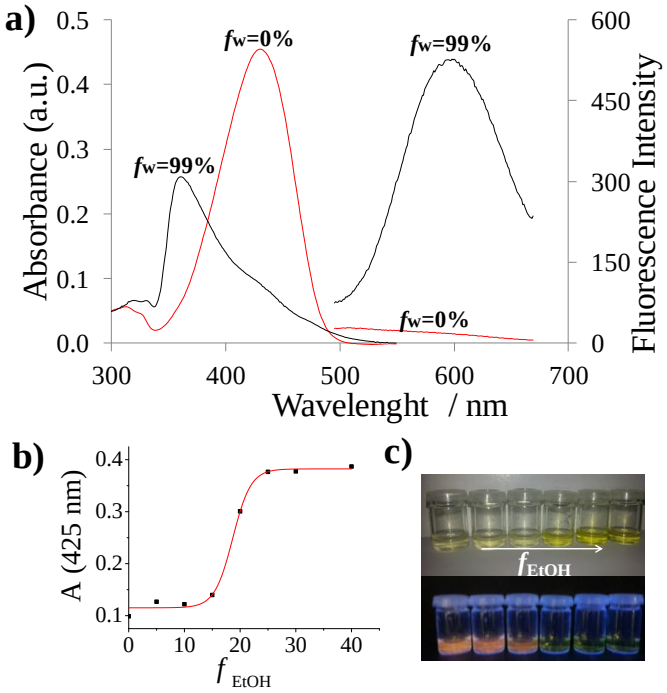

Fig. 5. (a) Absorbance and emission spectra of compound **3** in water and in ethanol, λ_{exc} = 350 nm; (b) Absorbance of **3** in ethanol/water mixtures recorded at 425 nm; (c) Photographs of **3** in water/ethanol mixtures under ambient light and under UV lamp (365 nm), volume fraction of ethanol in mixed solutions, f_{EtOH} = 0 – 40 %, *c* (**3**) = 1 x 10^{-5} M

Since a previously reported analogue of **3**, *N*,*N*-dimethylamino styryl benzimidazole [25], does not show aggregation in water, it is clear that the presence of the cyano group in **3** is responsible for intermolecular changes leading to the observed AIE. It is known that supramolecular interactions, especially hydrogen bonds and other dipole-dipole interactions involving cyano groups [46] may be responsible for the suppression of intramolecular motions in crystals resulting in tight molecular arrangements of increased rigidity leading to AIE phenomena [32, 47]. However, compound **4** also contains a cyano group but does not show aggregation in water. The BI moiety in **4**, with its bulky electron donating phenyl

substituent (D1), disturbs the molecular planarity and prevents certain dipole-dipole interactions that are possibly responsible for the aggregation observed in compound **3**. It is interesting to note that the observed blue-shift in the absorption band of **3** on going from ethanol (440 nm) to aqueous solution (350 nm) can easily be associated with the formation of non-emissive H-aggregates resulting from π–stacking interactions. However, in contrast to that, **3** shows red-shifted and significantly increased emission in nanoaggregated form. This can be related to a less common conformation of emissive H-aggregates [48] where the presence of the bulky and polar cyano group is known to affect the parallel face-to-face intermolecular interactions [30].

3.4. Protonation equilibria and pK_a *values*

3.4.1. Protonated species of 1-4 in ethanol

In order to define the species involved in neutral–monocation equilibria, spectral characterisation was first performed in acidified ethanol solutions to avoid possible complications due to observed nanoaggregation in aqueous solutions.

Absorption and emission spectra of neutral (M) and monoprotonated species (M^+) of **1**-**4** are shown in Fig. 6 and the summary of spectral properties of neutral and protonated chromophores in ethanol are presented in Table S1. Excitation and emission spectra of **3** and **4**, in neutral and protonated forms in ethanol, are shown in Fig. S2.

The absorption spectra of protonated species of compounds **1** and **2** in ethanol (Fig. 6) show no significant change of the longest wavelength peak, whilst compounds **3** and **4** exhibit bathochromic shifts with increased extinction coefficients. Since monoprotonated species of **3** and **4** contain two protonable sites (*N*,*N*-dimethylamino nitogen and imino nitrogen on BI moiety) the question is which nitrogen atom is more basic and would be protonated first.

It is generally known that protonation of a donor group (amino) in a push-pull system is reducing its electron-donating character and decreasing conjugation which results in a blue shift of the absorption spectrum and decreased extinction coefficient. On the other hand, protonation of acceptor moiety in a push-pull system is enhancing acceptor's electron-withdrawing character and results in a red-shift and increased extinction coefficients of molecules. The spectroscopic results indicate that protonation in **3** and **4** occurs first on imino nitrogen atom on BI moiety (the acceptor group), which is in agreement with previously reported styryl analogue of **3** [25] and the hydrochloride monohydrate of **3** whose crystal structure also confirmed that protonation occurs on imino nitrogen [36]. This is further corroborated by the computational results presented later.

Protonation of BI moiety on **1** and **2** (which are not typical ICT molecules) is not related to significant changes in absorption spectra. The lone electron pair on imino nitrogen occupies sp^2 hybrid orbital and is not involved in the π electron system. Its protonation does not considerably affect HOMO-LUMO energy levels, so the absorption spectra remain virtually unchanged. Fluorescence emission of neutral species in ethanol is relatively weak (Table 1). Protonation of **1** and **2** leads to increased fluorescence emission without shift of emission wavelength.

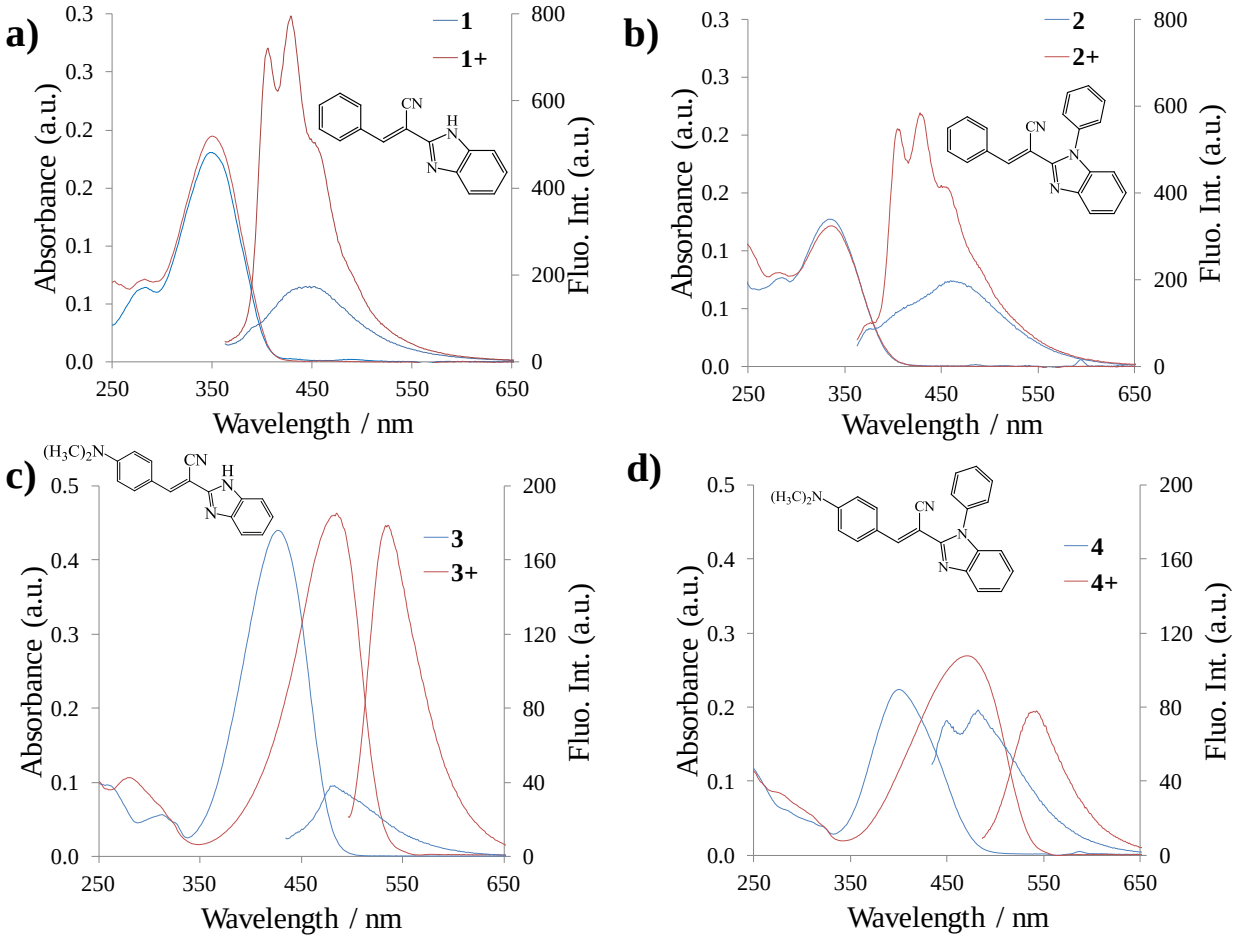

Fig. 6. Absorption and emission spectra of compounds **1** – **4,** c = 1 x 10^{-5} M, in neutral and protonated form in ethanol. (Excitation wavelength at absorption maximum of corresponding species.)

3.4.2. Spectroscopic pH titrations of 1-4 in aqueous solutions

General protonation-deprotonation equilibria and corresponding pK_a values of compounds **1-4** are shown in Scheme 1. (Note: under investigated conditions compounds **1** and **2** do not form M^{2+} species, while compounds **2** and **4** do not form M^- species)

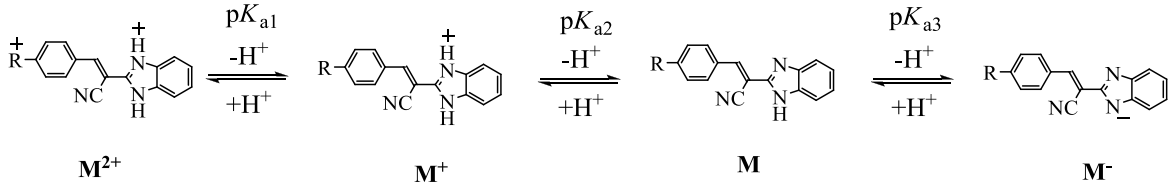

Scheme 1. General scheme of acid-base equilibria **1-4**.

The spectroscopic pH titrations were performed in aqueous solutions in the pH range 1.5 to 13.0 and the resulting absorption spectra for **3** and **4** are shown in Fig. 7a and 7b, respectively. The spectral identification of all species involved in respective protonation-deprotonation equilibria of **1-4** in aqueous solutions was performed, and the summary of spectroscopic properties is presented in Table S2. Spectral properties of dicationic and anionic (deprotonated) species are estimated from spectra obtained at pH = 1.0 and pH = 14.0, respectively.

As shown in Fig. 7a titration spectra of **3** show three distinct pH ranges corresponding to: i) protonation of neutral form (pH range 1.5 to 5); ii) neutral form (aggregate) at pH values ranging from approximately 5 to 8, and iii) deprotonation of neutral form (pH range 9 to 13). The protonation of monoprotonated form to dication form (amino-protonated species) occurs at pH values below 2 and is accompanied with blue shifted absorption maxima at 335 nm. The pH titration spectra of **4** show no evidence of aggregation and correspond to equivalent spectra obtained in ethanolic solutions.

Monoprotonated forms of both, **3** and **4** have considerably higher molar extinction coefficients than the corresponding neutral species, as expected from their ICT structure since protonation occurs at the acceptor moiety.

3.4.3. Experimental and theoretical pK_a *values in aqueous solutions*

The pK_a values are experimentally determined or estimated from spectroscopic titration data. Fig. 8 shows examples of plots used for experimental determination of pK_a values.

In order to rationalize the acid/base features of studied systems in aqueous solution we performed a computational analysis employing the implicit SMD solvation. The calculated

pK_a values (Table 3) show remarkable agreement with experimental data, which lends credence to the applied computational model. In comparison with the six precisely measured values, the average absolute deviation is only 0.6 pK_a units, which is remarkable for this kind of calculations. Nevertheless, we must emphasize that it would be even much lower if it would not include a 2 pK_a difference in the pK_{a2}(**3**) value that we attribute to the reported aggregation of this system in water, which complicates experimental pK_a determination.

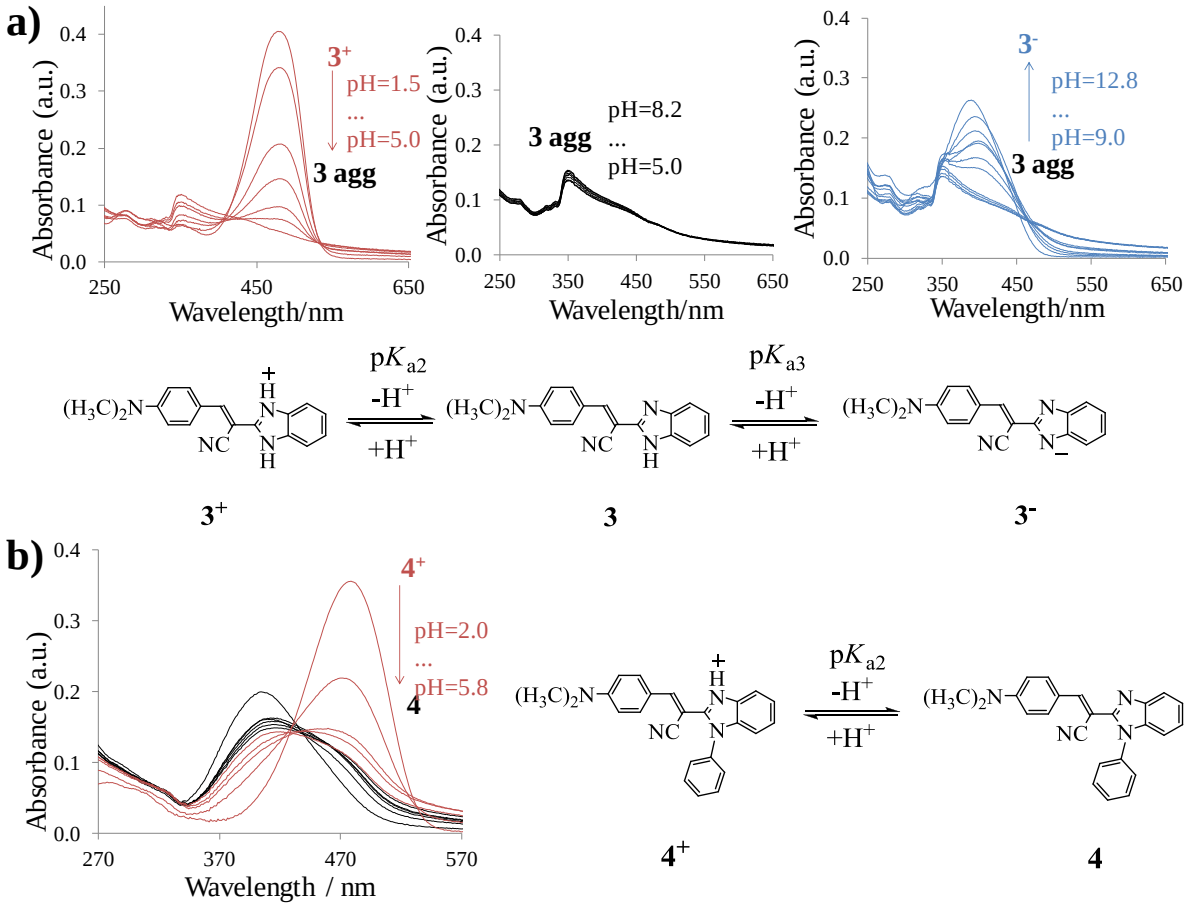

Fig. 7. Spectroscopic pH titration of (a) **3** and (b) **4,** c = 1 x 10^{-5} mol dm^{-3} in aqueous solutions and corresponding equilibria.

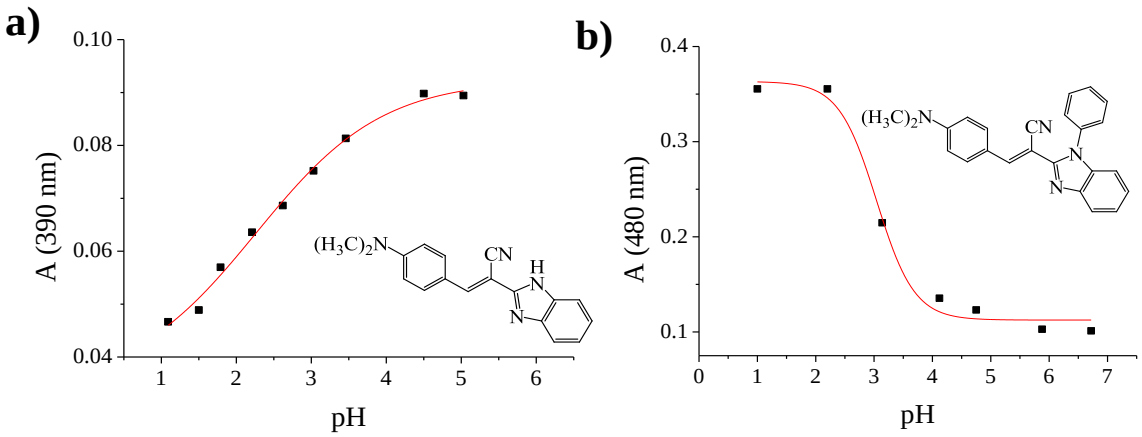

Fig. 8. Absorbance data plotted versus pH for (a) **3** and (b) **4** at selected wavelengths**.**

Table 3. Experimentally estimated and theoretically calculated pK_a values in water.

Compound	Acid-base equlibria	pK_a (I = 0,1M)	pK_a calculated
1	$\mathbf{1}^+ \rightleftharpoons \mathbf{1} + H^+$	pK_{a2}=2.7	pK_{a2}=3.0
	$\mathbf{1} \rightleftharpoons \mathbf{1}^- + H^+$	pK_{a3}>10.3	pK_{a3}=10.4
2	$\mathbf{2}^+ \rightleftharpoons \mathbf{2} + H^+$	pK_{a2}=2.5	pK_{a3}=2.4
3	$\mathbf{3}^{2+} \rightleftharpoons \mathbf{3}^+ + H^+$	pK_{a1}<1.5	pK_{a1}=1.1
	$\mathbf{3}^+ \rightleftharpoons \mathbf{3} + H^+$	pK_{a2}=2.2[a]	pK_{a2}=4.2
	$\mathbf{3} \rightleftharpoons \mathbf{3}^- + H^+$	pK_{a3}>10.4[a]	pK_{a3}=10.3
4	$\mathbf{4}^{2+} \rightleftharpoons \mathbf{4}^+ + H^+$	pK_{a1}<1.5	pK_{a1}=2.0
	$\mathbf{4}^+ \rightleftharpoons \mathbf{4} + H^+$	pK_{a2}=3.0	pK_{a2}=3.7
I	$\mathbf{I}^{2+} \rightleftharpoons \mathbf{I}^+ + H^+$	pK_{a1}=3.4[b]	pK_{a1}=3.3
	$\mathbf{I}^+ \rightleftharpoons \mathbf{I} + H^+$	pK_{a2}=6.0[b]	pK_{a2} =5.8
	$\mathbf{I} \rightleftharpoons \mathbf{I}^- + H^+$	-	pK_{a3}=12.5

[a]aggregation in aqueous solution

[b] from ref. [25]

Interestingly, the first protonation of all four systems **1**–**4** occurs on the benzimidazole imino nitrogen. This might be expected considering that benzimidazole (pK_a = 5.41) is slightly more basic than *N*,*N*-dimethylaniline (pK_a = 5.07) [41], together with the fact that the cyano group in **3** and **4** is in a direct resonance interaction with the latter fragment, thus reducing its basicity. In the parent system **1**, imino nitrogen protonation is associated with pK_{a2} = 3.0 making it significantly less basic than benzimidazole. This is a general trend in all **1**–**4**, which

strongly indicates that under normal conditions all four investigated systems are predominantly present as unionized neutral molecules, which is a significant observation. We attribute this trend to the presence of the electron withdrawing styryl moiety, which diminishes the basicity of the benzimidazole fragment. This effect is slightly compensated by adding the electron donating $–NMe_2$ group in **3** and **4**, where the corresponding pK_{a2} values increase to 4.2 and 3.7, but still not enough to make these systems more basic than benzimidazole. As expected, if we remove the strongly acidifying cyano group [49, 50] from **1** (model system **I**, Table 3) the corresponding pK_a value increases to 5.8.

The second protonation of **3** and **4** occurs at the dimethylamino group and, interestingly, it requires only slightly stronger acids than those able to allow the corresponding monocations. pK_{a1} values for **3** and **4** assume 1.1 and 2.0 (Table 3), which could be achieved with two equivalents of already moderately strong acids. As mentioned, dimethylamino positions are in a direct resonance with the attached cyano group, so these positions in **3** and **4** are significantly less basic than *N*,*N*-dimethylaniline (pK_a = 5.07). Differing effect of the –CN group is evident in the changes of bond distances induced upon protonation. For example, after the imino protonation of **3** to $\mathbf{3}^+$, the C–N distance of the cyano group is not changed and remains the same at 1.162 Å, but is subsequently reduced to 1.159 Å after amino protonation of $\mathbf{3}^+$ to $\mathbf{3}^{2+}$. In line with previous discussion, dication $\mathbf{I}^{2+}$ is even more easily attainable (pK_{a1} = 3.3). On the other hand, the unsubstituted benzimidazole amino groups in **1** and **3** are prone to deprotonation. Relative to benzimidazole deprotonation (pK_a = 12.75) [41], the presence of the cyano group increases the acidity of **1** and **3** by two orders of magnitude to the pK_{a3} values of 10.4 and 10.3 (Table 3), which is notable, yet not enough to make these systems monoanions under normal conditions. Since **I** is deprived of the cyano group, this effect is absent (pK_{a3} = 12.5).

In concluding this section, it is worth emphasizing that the calculations underline a significant electronic effect of the cyano group in affecting acid/base properties of **1**-**4**, and convincingly demonstrate that all investigated systems are neutral molecules under normal conditions, which become monoprotonated exclusively on the benzimidazole imino with moderately strong acids (pK_a values between 2-4).

The neutral species of **3** forms nanoaggregates in aqueous solution. The deaggregation process can be triggered either by protonation or deprotonation of molecules occurring at pH values lower than 5 or higher than 8, respectively. It is important to note that the aggregation-deaggregation process is reversibly switched by changing the pH of the aqueous solution, opening up interesting potential applications for compound **3** in AIE-based pH sensing and

imaging. Also, it has previously been shown that the hydrochloride monohydrate of **3** interacts with DNA molecules [36], a result which should now be explored further in light of the spectrally responsive and pH sensitive deaggregation processes we report here.

3.5. pH sensitivity of chromophores in polymer matrix

Thin polymer films based on plasticised PVC containing immobilised **3** and **4** were fabricated and initially tested as optically pH responsive materials for ion-selective optodes. The spectral and visual responses to pH, as well as the corresponding calibration plot of immobilised **3** are shown in Fig. 9.

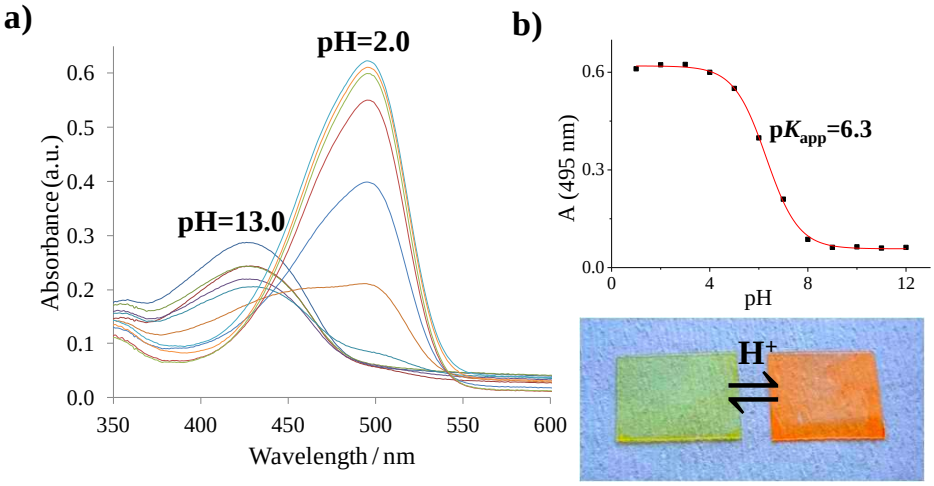

Fig. 9. a) Absorbance spectra of chromophore **3** immobilised in plasticised PVC film at different pH values; b) calibration plot of immobilised chromophore **3** (absorbance change in response to pH at 495 nm).

Table 4. Absorption maxima, emission maxima and apparent pK_a values of neutral and monocation form of **3** and **4** immobilised in thin polymer films.

Compound	λ_{abs}/nm **M**	λ_{em}/nm **M**	λ_{abs}/nm **M$^+$**	λ_{em}/nm **M$^+$**	pK_a **apparent**
3	428	494	495	544	6.30
4	400	481	490	548	6.32

Absorption and emission properties and the corresponding apparent pK_a values of neutral and monocation forms of immobilised **3** and **4** are summarised in Table S3. The spectral response of the immobilised chromophores corresponds to ethanolic solutions and no aggregation of **3**

was noticed. The apparent pK_a values increased by nearly 3 pK_a units in comparison to their aqueous values. Such changes are expected due to a number of known parameters affecting the complex heterogeneous ion-exchange equilibria in ion-selective optodes [51].

3.6. Effect of DNA on aggregation

The effect of DNA on the aggregation/deaggregation equilibrium of 3 has been studied. The absorption and emission spectral responses obtained in a *ct*-DNA titration experiment are shown in Fig. 10. In the presence of DNA the absorbance and emission intensities of the nanoaggregated form of **3** (at 350 nm and 600 nm, respectively) decrease. The corresponding titration plot is shown (Fig. 10, inset). The interaction between **3** and the *ct*-DNA molecules results in quenching of AIE. The interaction is most likely based on structural compatibility of the planar BI moiety and its ability to incorporate between adjacent base pairs of the DNA molecule during the intercalation process [36, 52].

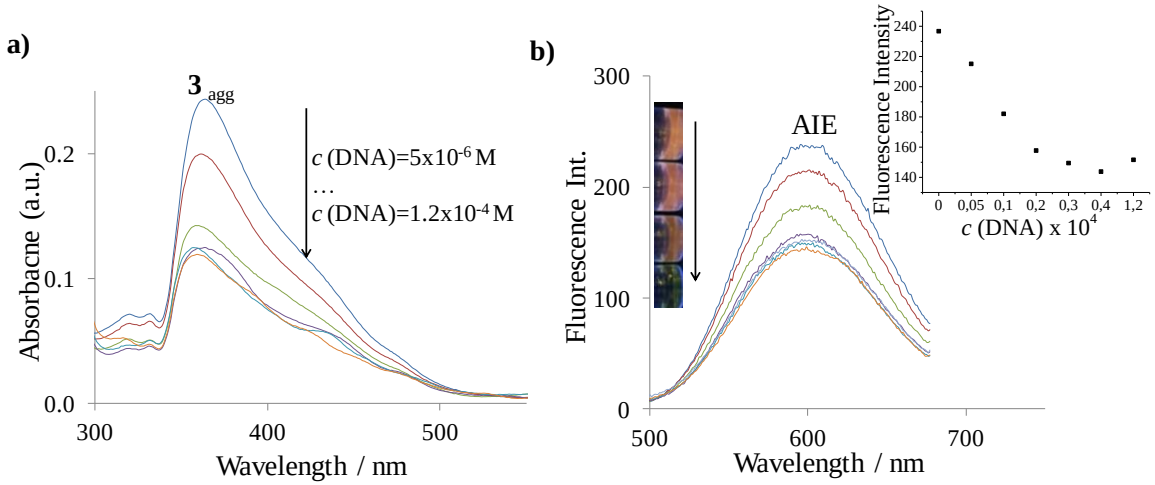

Fig. 10. a) Absorption and b) emission spectra (λ_{exc} = 350 nm) of **3** in aqueous solution (buffer pH = 7.0) upon titration with DNA.

4. Conclusion

The benzimidazole-based push-pull molecular systems presented in this work exhibit pH induced spectral responses in the visible region with relatively high molar absorption coefficients. In general, the fluorescence properties of the molecules are not promising for applications requiring high quantum yields, with the exception of **3** and the corresponding

aggregation-induced emission. All the chromophores demonstrate pH sensitivity with pK_a values in acidic (2.1-3.0) and basic (around 10) ranges, corresponding to neutral-monocation and neutral-anion equilibria. Computational analysis aided in rationalising acid/base features of the systems investigated, and demonstrated that all compounds are unionised under normal conditions, but become monoprotonated exclusively on the benzimidazole imino nitrogen with only moderately strong acids (pK_a values between 2-4). However, the apparent pK_a values of 3 and 4 when immobilised in polymer films shifted to 6.3, enabling possible future application of these chromophores as physiologically compatible pH sensitive materials. An important finding is the ability of **3** to form emissive nanoaggregates in solution triggered by either solvent composition or the pH value of the aqueous solution. Its near-neutral pH-switchable aggregation/deaggregation is accompanied by absorption and emission changes making it promising for pH sensing and imaging applications. An additional advantage for biological applications is the excitation at 350 nm resulting in a long wavelength emission at 600 nm.

Further studies exploring the effects of interactions of the BI moiety with biomolecules and metal-ions on AIE are underway in our laboratory.

Acknowledgments

This work was supported by the Croatian Science Foundation under grant number IP-2014-09-3386 entitled *Design and synthesis of novel nitrogen-containing heterocyclic fluorophores and fluorescent nanomaterials for pH and metal-ion sensing* which is gratefully acknowledged. We would like to thank Dr. Maja Dutour Sikirić and Dr. Darija Domazet Jurašin of Ruđer Bošković Institute, Zagreb, for use of the DLS instrumentation and for characterisation of the nanoaggregates. We would also like to thank Dr. Matthew D. Steinberg for reviewing the manuscript.

References

[1] T.D. Kim, K.S. Lee, D--A Conjugated Molecules for Optoelectronic Applications, Macromol. Rapid Commun., 36 (2015) 943-958.

[2] C. Barsu, R. Cheaib, S. Chambert, Y. Queneau, O. Maury, D. Cottet, H. Wege, J. Douady, Y. Bretonniere, C. Andraud, Neutral push-pull chromophores for nonlinear optical imaging of cell membranes, Organic & Biomolecular Chemistry, 8 (2010) 142-150.

[3] Y.Z. Wu, W.H. Zhu, Organic sensitizers from D-pi-A to D-A-pi-A: effect of the internal electron-withdrawing units on molecular absorption, energy levels and photovoltaic performances, Chemical Society Reviews, 42 (2013) 2039-2058.

[4] F. Bures, Fundamental aspects of property tuning in push-pull molecules, RSC Advances, 4 (2014) 58826-58851.

[5] L. Beverina, G.A. Pagani, pi-Conjugated Zwitterions as Paradigm of Donor-Acceptor Building Blocks in Organic-Based Materials, Accounts Chem. Res., 47 (2014) 319-329.

[6] S.L. Wang, T.I. Ho, Substituent effects on intramolecular charge-transfer behaviour of styrylheterocycles, Journal of Photochemistry and Photobiology a-Chemistry, 135 (2000) 119-126.

[7] M. Zajac, P. Hrobarik, P. Magdolen, P. Foltinova, P. Zahradnik, Donor-pi-acceptor benzothiazole-derived dyes with an extended heteroaryl-containing conjugated system: synthesis, DFT study and antimicrobial activity, Tetrahedron, 64 (2008) 10605-10618.

[8] Z. Seferoglu, H. Ihmels, E. Sahin, Synthesis and photophysical properties of fluorescent arylstyrylimidazo 1,2-a pyridine-based donor-acceptor chromophores, Dyes and Pigments, 113 (2015) 465-473.

[9] J. Kulhanek, F. Bures, Imidazole as a parent pi-conjugated backbone in charge-transfer chromophores, Beilstein J. Org. Chem., 8 (2012) 25-49.

[10] M.Y. Lai, C.H. Chen, W.S. Huang, J.T. Lin, T.H. Ke, L.Y. Chen, M.H. Tsai, C.C. Wu, Benzimidazole/amine-based compounds capable of ambipolar transport for application in single-layer blue-emitting OLEDs and as hosts for phosphorescent emitters, Angewandte Chemie-International Edition, 47 (2008) 581-585.

[11] S. Manoharan, S. Anandan, Cyanovinyl substituted benzimidazole based (D-pi-A) organic dyes for fabrication of dye sensitized solar cells, Dyes and Pigments, 105 (2014) 223-231.

[12] G.M. Saltan, H. Dincalp, M. Kiran, C. Zafer, S.C. Erbas, Novel organic dyes based on phenyl-substituted benzimidazole for dye sensitized solar cells, Materials Chemistry and Physics, 163 (2015) 387-393.

[13] Y.C. Wu, J.Y. You, L.T. Guan, J. Shi, L. Cao, Z.Y. Wang, Progress in the Synthesis and Application of Benzimidazole-Based Fluorescent Chemosensors, Chin. J. Org. Chem., 35 (2015) 2465-2486.

[14] M.A. Saeed, H.T.M. Le, O.S. Miljanic, Benzobisoxazole Cruciforrns as Fluorescent Sensors, Accounts Chem. Res., 47 (2014) 2074-2083.

[15] R.C. Lirag, H.T.M. Le, O.S. Miljanic, L-shaped benzimidazole fluorophores: synthesis, characterization and optical response to bases, acids and anions, Chemical Communications, 49 (2013) 4304-4306.

[16] Z.S. Li, L.J. Li, T.T. Sun, L.M. Liu, Z.G. Xie, Benzimidazole-BODIPY as optical and fluorometric pH sensor, Dyes and Pigments, 128 (2016) 165-169.

[17] R. Cinar, J. Nordmann, E. Dirksen, T.J.J. Muller, Domino synthesis of protochromic "ON-OFF-ON" luminescent 2-styryl quinolines, Org. Biomol. Chem., 11 (2013) 2597-2604.

[18] M.M. Henary, Y.G. Wu, C.J. Fahrni, Zinc(II)-selective ratiometric fluorescent sensors based on inhibition of excited-state intramolecular proton transfer, Chemistry-a European Journal, 10 (2004) 3015-3025.

[19] M. Hranjec, E. Horak, M. Tireli, G. Pavlovic, G. Karminski-Zamola, Synthesis, crystal structure and spectroscopic study of novel benzimidazoles and benzimidazo 1,2-a quinolines as potential chemosensors for different cations, Dyes and Pigments, 95 (2012) 644-656.

[20] N. Singh, D.O. Jang, Benzimidazole-based tripodal receptor: Highly selective fluorescent chemosensor for iodide in aqueous solution, Organic Letters, 9 (2007) 1991-1994.

[21] S.L. Wang, Y.T. Chang, Combinatorial synthesis of benzimidazolium dyes and its diversity directed application toward GTP-selective fluorescent chemosensors, Journal of the American Chemical Society, 128 (2006) 10380-10381.

[22] H.J. Kim, C.H. Heo, H.M. Kim, Benzimidazole-Based Ratiometric Two-Photon Fluorescent Probes for Acidic pH in Live Cells and Tissues, Journal of the American Chemical Society, 135 (2013) 17969-17977.

[23] S. Santra, S.K. Dogra, Excited-state intramolecular proton transfer in 2-(2 '-aminophenyl) benzimidazole, Chemical Physics, 226 (1998) 285-296.

[24] J. Dey, S.K. Dogra, DUAL FLUORESCENCE OF 2-(4'-(N,N-DIMETHYLAMINO)PHENYL)BENZOTHIAZOLE AND ITS BENZIMIDAZOLE ANALOG - EFFECT OF SOLVENT AND PH ON ELECTRONIC-SPECTRA, Journal of Physical Chemistry, 98 (1994) 3638-3644.

[25] A. Mishra, S. Chaterjee, G. Krishnamoorthy, Intramolecular charge transfer emission of trans-2- 4 '-(dimethylamino)styryl benzimidazole: Effect of solvent and pH, J. Photochem. Photobiol. A-Chem., 260 (2013) 50-58.

[26] S. Muhammad, H. Xu, M.R.S.A. Janjua, Z. Su, M. Nadeem, Quantum chemical study of benzimidazole derivatives to tune the second-order nonlinear optical molecular switching by proton abstraction, Physical Chemistry Chemical Physics, 12 (2010) 4791-4799.

[27] Y.J. Li, T.F. Liu, H.B. Liu, M.Z. Tian, Y.L. Li, Self-Assembly of Intramolecular Charge-Transfer Compounds into Functional Molecular Systems, Accounts Chem. Res., 47 (2014) 1186-1198.

[28] S.H. Kim, S.Y. Lee, S.Y. Gwon, Y.A. Son, J.S. Bae, D-pi-A solvatochromic charge transfer dyes containing a 2-cyanomethylene-3-cyano-4,5,5-trimethyl-2,5-dihydrofuran acceptor, Dyes and Pigments, 84 (2010) 169-175.

[29] B.K. An, J. Gierschner, S.Y. Park, pi-Conjugated Cyanostilbene Derivatives: A Unique Self-Assembly Motif for Molecular Nanostructures with Enhanced Emission and Transport, Accounts Chem. Res., 45 (2012) 544-554.

[30] B.K. An, S.K. Kwon, S.D. Jung, S.Y. Park, Enhanced emission and its switching in fluorescent organic nanoparticles, Journal of the American Chemical Society, 124 (2002) 14410-14415.

[31] Y. Li, F. Li, H. Zhang, Z. Xie, W. Xie, H. Xu, B. Li, F. Shen, L. Ye, M. Hanif, D. Ma, Y. Ma, Tight intermolecular packing through supramolecular interactions in crystals of cyano substituted oligo(para-phenylene vinylene): a key factor for aggregation-induced emission, Chemical Communications, (2007) 231-233.

[32] M.J. Percino, V.M. Chapela, M. Ceron, G. Soriano-Moro, M.E. Castro, F.J. Melendez, Fluorescence improvement of pyridylacrylonitrile by dimethylaminophenyl-substitutions: The effect of packing modes of conjugated compounds, Journal of Molecular Structure, 1034 (2013) 238-248.

[33] J. Mei, Y. Hong, J.W.Y. Lam, A. Qin, Y. Tang, B.Z. Tang, Aggregation-Induced Emission: The Whole Is More Brilliant than the Parts, Advanced Materials, 26 (2014) 5429-5479.

[34] V. Palakollu, S. Kanvah, alpha-Cyanostilbene based fluorophores: aggregation-induced enhanced emission, solvatochromism and the pH effect, New Journal of Chemistry, 38 (2014) 5736-5746.

[35] P. Xue, B. Yao, J. Sun, Z. Zhang, K. Li, B. Liu, R. Lu, Crystallization-induced emission of styrylbenzoxazole derivate with response to proton, Dyes and Pigments, 112 (2015) 255-261.

[36] M. Hranjec, G. Pavlovic, G. Karminski-Zamola, Spectroscopic characterization, crystal structure determination and interaction with DNA of novel cyano substituted benzimidazole derivative, Structural Chemistry, 18 (2007) 943-949.
[37] C. Reichardt, SOLVATOCHROMIC DYES AS SOLVENT POLARITY INDICATORS, Chemical Reviews, 94 (1994) 2319-2358.
[38] A.V. Marenich, C.J. Cramer, D.G. Truhlar, Universal solvation model based on solute electron density and on a continuum model of the solvent defined by the bulk dielectric constant and atomic surface tensions, The journal of physical chemistry. B, 113 (2009) 6378-6396.
[39] I. Picek, R. Vianello, P. Sket, J. Plavec, B. Foretic, Tandem beta-Elinnination/Hetero-Michael Addition Rearrangement of an N-Alkylated Pyridinium Oxime to an O-Alkylated Pyridine Oxime Ether: An Experimental and Computational Study, Journal of Organic Chemistry, 80 (2015) 2165-2173.
[40] D. Saftić, R. Vianello, B. Žinić, 5-Triazolyluracils and Their N1-Sulfonyl Derivatives: Intriguing Reactivity Differences in the Sulfonation of Triazole N1′-Substituted and N1′-Unsubstituted Uracil Molecules, European Journal of Organic Chemistry, 2015 (2015) 7695-7704.
[41] W.P. Jencks, J. Regenstein, Ionization Constants of Acids and Bases, in: Handbook of Biochemistry and Molecular Biology, Fourth Edition, CRC Press, 1976, pp. 305-351.
[42] M.J. Frisch, G.W. Trucks, H.B. Schlegel, G.E. Scuseria, M.A. Robb, J.R. Cheeseman, G. Scalmani, V. Barone, B. Mennucci, G.A. Petersson, H. Nakatsuji, M. Caricato, X. Li, H.P. Hratchian, A.F. Izmaylov, J. Bloino, G. Zheng, J.L. Sonnenberg, M. Hada, M. Ehara, K. Toyota, R. Fukuda, J. Hasegawa, M. Ishida, T. Nakajima, Y. Honda, O. Kitao, H. Nakai, T. Vreven, J.A. Montgomery Jr., J.E. Peralta, F. Ogliaro, M.J. Bearpark, J. Heyd, E.N. Brothers, K.N. Kudin, V.N. Staroverov, R. Kobayashi, J. Normand, K. Raghavachari, A.P. Rendell, J.C. Burant, S.S. Iyengar, J. Tomasi, M. Cossi, N. Rega, N.J. Millam, M. Klene, J.E. Knox, J.B. Cross, V. Bakken, C. Adamo, J. Jaramillo, R. Gomperts, R.E. Stratmann, O. Yazyev, A.J. Austin, R. Cammi, C. Pomelli, J.W. Ochterski, R.L. Martin, K. Morokuma, V.G. Zakrzewski, G.A. Voth, P. Salvador, J.J. Dannenberg, S. Dapprich, A.D. Daniels, Ö. Farkas, J.B. Foresman, J.V. Ortiz, J. Cioslowski, D.J. Fox, Gaussian 09, in, Gaussian, Inc., Wallingford, CT, USA, 2009.
[43] V.K. Gupta, A.K. Singh, L.K. Kumawat, Thiazole Schiff base turn-on fluorescent chemosensor for Al3+ ion, Sensors and Actuators B-Chemical, 195 (2014) 98-108.

[44] H. Auweter, H. Haberkorn, W. Heckmann, D. Horn, E. Luddecke, J. Rieger, H. Weiss, Supramolecular structure of precipitated nanosize beta-carotene particles, Angewandte Chemie-International Edition, 38 (1999) 2188-2191.

[45] J. Luo, Z. Xie, J.W.Y. Lam, L. Cheng, H. Chen, C. Qiu, H.S. Kwok, X. Zhan, Y. Liu, D. Zhu, B.Z. Tang, Aggregation-induced emission of 1-methyl-1,2,3,4,5-pentaphenylsilole, Chemical Communications, (2001) 1740-1741.

[46] F. Würthner, Dipole–Dipole Interaction Driven Self-Assembly of Merocyanine Dyes: From Dimers to Nanoscale Objects and Supramolecular Materials, Accounts Chem. Res., (2016).

[47] Y.P. Li, F. Li, H.Y. Zhang, Z.Q. Xie, W.J. Xie, H. Xu, B. Li, F.Z. Shen, L. Ye, M. Hanif, D.G. Ma, Y.G. Ma, Tight intermolecular packing through supramolecular interactions in crystals of cyano substituted oligo(para-phenylene vinylene): a key factor for aggregation-induced emission, Chemical Communications, (2007) 231-233.

[48] U. Rösch, S. Yao, R. Wortmann, F. Würthner, Fluorescent H-Aggregates of Merocyanine Dyes, Angewandte Chemie, 118 (2006) 7184-7188.

[49] R. Vianello, Z.B. Maksic, The engineering of powerful non-ionic superacids in silico-a DFT-B3LYP study of open chain polycyanopolyenes, New Journal of Chemistry, 33 (2009) 739-748.

[50] R. Vianello, Z.B. Maksic, Polycyano Derivatives of some Organic Tri- and Hexacyclic Molecules Are Powerful Super- and Hyperacids in the Gas Phase and DMSO: Computational Study by DFT Approach, Journal of Organic Chemistry, 75 (2010) 7670-7681.

[51] X. Xie, E. Bakker, Ion selective optodes: from the bulk to the nanoscale, Analytical and Bioanalytical Chemistry, 407 (2015) 3899-3910.

[52] M. Hranjec, G. Pavlović, M. Marjanović, M. Kralj, G. Karminski-Zamola, Benzimidazole derivatives related to 2,3-acrylonitriles, benzimidazo[1,2-a]quinolines and fluorenes: Synthesis, antitumor evaluation in vitro and crystal structure determination, European Journal of Medicinal Chemistry, 45 (2010) 2405-2417.

Electronic Supporting Information (ESI)

Synthesis of benzimidazole derivatives

General procedure for the synthesis of compounds 1-4

A solution of equimolar amounts of 2-cyanomethylbenzimidazole or 2-cyanomethyl-*N*-phenylbenzimidazole, benzaldehyde or 4-*N*,*N*-dimethylaminobenzaldehyde and a few drops of piperidine in absolute ethanol, was refluxed for 3 – 3.5 h. After cooling to the room temperature, the crude product was filtered off and recrystallized from ethanol.

*2-(1H-benzimidazol-2-yl)-3-acrylonitrile **1***

2-Cyanomethylbenzimidazole (2.00 g, 12.72 mmol) and benzaldehyde (1.35 g, 12.72 mmol) were refluxed in absolute ethanol (40 mL) and piperidine (0.25 mL) for 3 h. After recrystallization from ethanol compound **1** was isolated (2.52 g, 80%) as yellow powder; m.p. 217–218 °C; ^{1}H NMR (DMSO-d_6): δ = 13.20 (brs, 1H, $NH_{benzimidazole}$), 8.34 (s, 1H), 8.00 (d, 2H, *J* = 8.80 Hz, $H_{arom.}$), 7-63-7.61 (m, 2H, $H_{arom.}$), 7.60 (d, 1H, *J* = 7.72Hz, $H_{arom.}$), 7.57 (d, 2H, *J* = 8.77 Hz, $H_{arom.}$), 7.30-7.24 (m, 2H, $H_{arom.}$); ^{13}C NMR (DMSO-d_6): δ = 147.9, 145.9, 139.7, 133.2, 132.1, 130.0 (2C), 129.8 (3C), 123.5, 122.9, 121.0, 118.7, 116.7, 102.9; Anal. Calc. for $C_{16}H_{11}N_3$: C 78.35%, H 4.52%, N 17.13%; found: C 78.13%, H 4.75%, N 17.29%.

*E-3-phenyl-2-(1-phenylbenzimidazol-2-yl)acrylonitrile **2***

As described for **1**, the synthesis of **2** was performed. The reagents used were: 2-cyanomethyl-*N*-phenylbenzimidazole (1.00 g, 4.33 mmol), benzaldehyde (0.46 g, 4.33 mmol), absolute ethanol (20 mL) and piperidine (0.15 mL). After recrystallization from ethanol yellow crystals of compound **2** were isolated (0.90 g, 65%); m.p. 136-138 °C; ^{1}H NMR (300 MHz, DMSO-d_6): δ = 7.91 (s, 1H, $H_{arom.}$), 7.88-7.38 (m, 2H, H_{arom}), 7.81 (d, 1H, *J* = 7.68 Hz, H_{arom}), 7.69-7.65 (m, 3H, H_{arom}), 7.64 (d, 2H, *J* = 1.84 Hz, H_{arom}), 7.56-7.52 (m, 3H, H_{arom}), 7.40-7.34 (m, 2H, H_{arom}) , 7.23 (dd, 1H, J_1 = 7.60 Hz, J_2 = 1.83 Hz, H_{arom}); ^{13}C NMR (150 MHz, DMSO-d_6): δ = 150.9, 147.1, 142.4, 137.3, 135.6, 132.9, 132.5, 130.7 (2C), 130.0 (3C), 129.7 (2C), 127.9 (2C), 124.9, 123.9, 120.1, 116.0, 111.1, 101.1; Anal. Calcd for $C_{22}H_{15}N_3$ (321.1): C, 82.22; H, 4.70; N, 13.08. Found: C, 82.10; H, 4.62; N, 13.25.

*E-2-(2-Benzimidazolyl)-3-(4-N,N-dimethylaminophenyl)acrylonitrile **3***

According to procedure described for **1**, compound **3** was prepared by refluxing 2-cyanomethylbenzimidazole (0.80 g, 5.2 mmol), 4-*N*,*N*-dimethylaminobenzaldehyde (0.76 g, 5.2 mmol), absolute ethanol (15 ml) and piperidine (0.15 mL) for 2.5 h. Recrystallization of crude product from ethanol yielded 1.06 g (72%) compound **3** as orange powder; m.p. 253-255 °C; ^{1}H NMR (300 MHz, DMSO-d_6): δ = 12.44 (s, *NH*, 1H), 8.12 (s, 1H), 7.85 (d, *J*=8.88 Hz, H_{arom}, 2H), 7.60 (d, *J*=7.18 Hz, $H_{arom,}$ 1H), 7.45 (d, *J*=7.16 Hz, H_{arom}, 1H), 7.20-7.17 (m, H_{arom}, 2H), 6.82 (d, *J*=8.96 Hz, H_{arom}, 2H), 3.03 (s, 2CH3, 6H); ^{13}C NMR (75 MHz, DMSO-d_6): δ = 155., 150.7, 148.0, 136.3, 134.4 (2C), 127.5, 125.5, 124.3, 122.4, 121.1, 120.2, 118.6, 114.4 (2C), 113.6, 96.1, 25.1 (2C); Anal. Calcd for $C_{18}H_{16}N_4$: C 74.98, H 5.59, N 19.43. Found: C, 75.20; H, 5.68; N, 19.67.

*E-3-(4-N,N-dimethylaminophenyl)-2-(1-phenylbenzimidazol-2-yl)acrylonitrile **4***

As described for **1**, the synthesis of **4** was performed. The reagents used were: 2-cyanomethyl-*N*-phenylbenzimidazole (0.70 g, 3.03 mmol), 4-*N*,*N*-dimethylaminobenzaldehyde (0.44 g, 3.03 mmol), absolute ethanol (15 mL) and piperidine (0.15 mL). After recrystallization from ethanol orange crystals of compound 4 were obtained (0.26 g, 21%); m.p. 216-218 °C; ^{1}H NMR (600 MHz, DMSO-d_6): δ = 7.75 (d, 1H, *J* = 7.92 Hz, $H_{arom.}$), 7.70 (d, 2H, *J* = 9.06 Hz, H_{arom}), 7.69 (s, 1H, *J* = 5.64 Hz, $H_{arom.}$), 7.64 (t, 2H, *J* = 6.72 Hz, $H_{arom.}$), 7.61-7.57 (m, 3H, $H_{arom.}$), 7.32 (dt, 1H, J_1 = 7.53 Hz, J_2 = 1.15 Hz, $H_{arom.}$), 7.26 (dt, 1H, J_1 = 7.60 Hz, J_2 = 1.04 Hz, $H_{arom.}$), 7.15 (d, 1H, *J* = 7.87 Hz, $H_{arom.}$), 6.78 (d, 2H, *J* = 9.12 Hz, $H_{arom.}$), 3.03 (s, 6H, CH_3); ^{13}C NMR (150 MHz, DMSO-d_6): δ = 153.1, 150.5, 148.7, 147.6, 142.6, 137.4, 136.0, 132.5 (2C), 130.6 (2C), 129.7, 128.0 (2C), 124.4, 120.1, 119.7, 117.6, 112.1, 110.8, 91.9, 83.6, 47.7 (2C); Anal. Calcd for $C_{24}H_{20}N_4$ (364.2): C, 79.10; H, 5.53; N, 15.37. Found: C, 79.30; H, 5.67; N, 15.60.

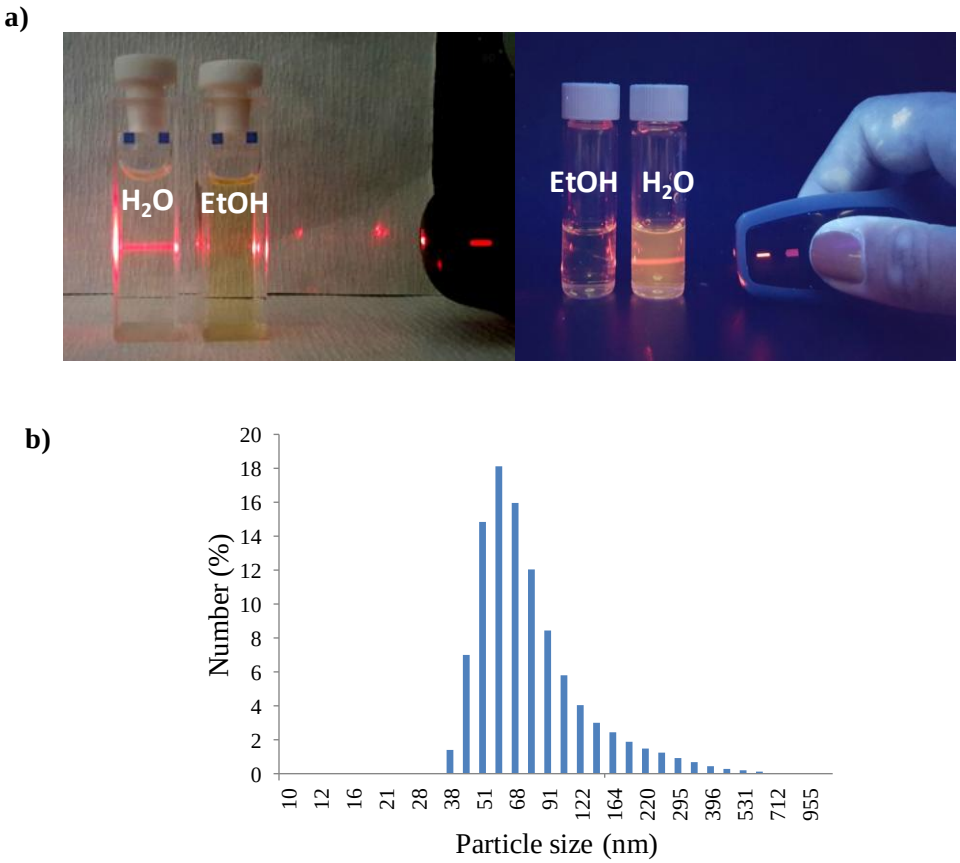

Fig. S1. (a) Tyndall probe observed on daylight and under UV lamp, c = 10 μM; (b) dynamic light scattering results in aqueous solution (f_w = 99%), , c = 10 μM.

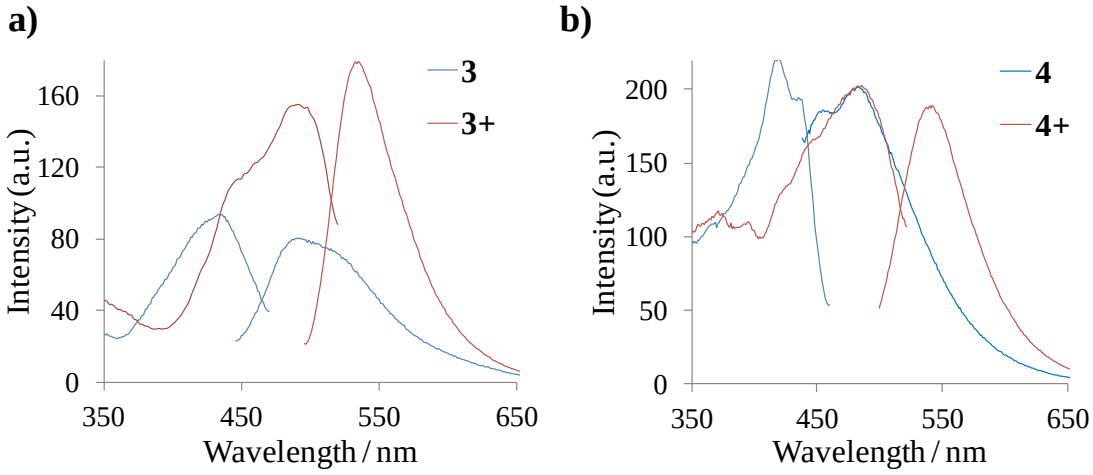

Fig. S2. Excitation and emission spectra of compounds **3** and **4**, c = 1 x 10^{-5} M, in neutral and protonated form in ethanol. (Excitation wavelength at absorption maximum of corresponding species.)

Table S1. Absorption, excitation and emission maxima and Stokes shifts for compounds **1 – 4** in pure and acidified ethanol (neutral, **M** and protonated, $\mathbf{M}^+$ forms in ethanol).

Compound	λ_{abs} / nm		λ_{exc} / nm		λ_{fluo} / nm (Stokes shift / nm)	
	M (ethanol)	$\mathbf{M}^+$ (acidified ethanol)	**M** (ethanol)	$\mathbf{M}^+$ (acidified ethanol)	**M** (ethanol)	$\mathbf{M}^+$ (acidified ethanol)
1	204 350	202 350	345	355 371	444 (94)	406 428 (78) 455 (sh)
2	202 335	202 335	268 352	266 354	464 (129)	405 430 (95) 455 (sh)
3	202 425	202 485	431	490	491 (64)	535 (50)
4	202 400	202 472	419 434	481	486 (86)	540 (68)

(sh) shoulder

Table S2. Absorption maxima wavelengths of all prototropic species of **1 – 4** in aqueous media, and molar extinction coefficients for neutral (M) and monocation (M^+) forms.

	M		$\mathbf{M}^+$		$\mathbf{M}^{2+}$	$\mathbf{M}^-$
Compound	λ_{abs} / nm	$\varepsilon \cdot 10^{-3}$ / M^{-1} cm^{-1}	λ_{abs} / nm	ε x 10^{-3} / M^{-1} cm^{-1}	λ_{abs} / nm pH=1.0	λ_{abs} / nm pH=14.0
1	270 344	17.87	345	21.67	-	355 270
2	335	10.56	340	13.12	-	-
3	356[a]	24.58[a]	480	46.63	480 335 280	390
4	404	19.61	479	35.04	479 325 278	-

RAD 2

E. Horak, M. Hranjec, R. Vianello,I. M. Steinberg, *Reversible pH switchable aggregation-induced emission of self-assembled benzimidazole-based acrylonitrile dye in aqueous solution*, Dyes and Pigments 142 (2017) 108-115.

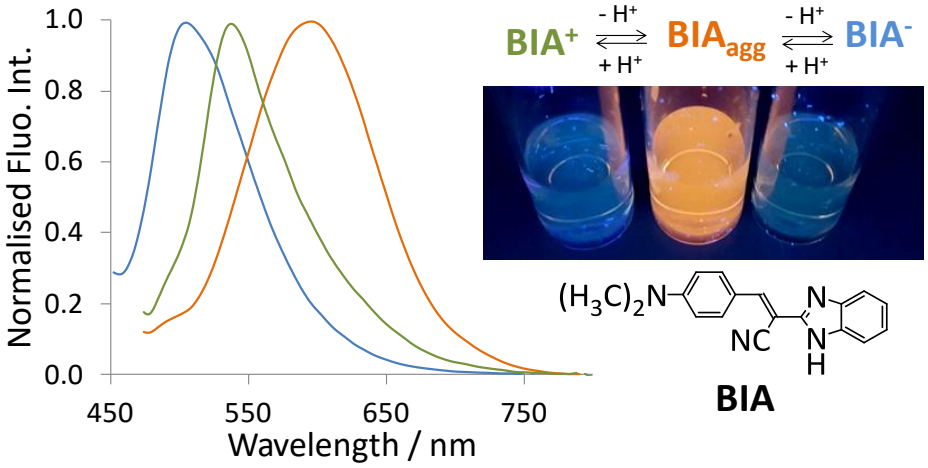

Reversible pH switchable aggregation-induced emission of self-assembled benzimidazole-based acrylonitrile dye in aqueous solution

Ema Horak,[a] Marijana Hranjec,[b] Robert Vianello[c] and Ivana Murković Steinberg*[a]

[a] *Department of General and Inorganic Chemistry, Faculty of Chemical Engineering and Technology, University of Zagreb, Marulićev trg 19, HR-10000 Zagreb, Croatia*

[b] *Department of Organic Chemistry, Faculty of Chemical Engineering and Technology, University of Zagreb, Marulićev trg 20, HR-10000 Zagreb, Croatia*

[c] *Computational Organic Chemistry and Biochemistry Group, Ruđer Bošković Institute, Bijenička cesta 54, 10000 Zagreb, Croatia*

[*] *Corresponding author:*
Ivana Murković Steinberg, Department of General and Inorganic Chemistry, Faculty of Chemical Engineering and Technology, University of Zagreb, Marulićev trg 19, HR-10000 Zagreb, Croatia, Phone No. ++38514597287; e-mail: ivana.murkovic@fkit.hr

Abstract

We report the pH switchable fluorescence and aggregation-deaggregation behaviour of a 2-benzimidazolyl substituted acrylonitrile dye (BIA). From the single molecular entity, three prototropic species (tri-state system) are derived that respectively emit in the red, green and cyan spectral regions. The neutral form is capable of self-assembly in an aqueous environment exhibiting stable red-orange aggregation-induced emission (AIE) at 600 nm in the physiologically relevant pH range. The aggregation and emission are pH switchable and fully-reversible. The molecule is shown to similarly function in the solid state where its emission can be modulated by exposure to acidic and basic vapours. Multicolour and reversibly pH switchable tri-state emission from a single fluorophore containing a biologically active benzimidazole moiety can find application in ratiometric optical chemosensing, bioimaging and functional materials.

Keywords: aggregation-induced emission; benzimidazole; pH probe; fluorescence; ICT chromophore; chemical sensor

1. Introduction

Application of conventional fluorophores is restricted and usually limited to diluted solutions because of the aggregation quenching effect at high concentrations. Aggregation is thus mostly investigated as an undesirable side effect in many biological or chemical applications. Tang and co-workers changed the prospects for analytical uses of aggregation phenomenon when they developed a novel class of organic luminophores with aggregation induced emission (AIE) [1]. Unlike conventional fluorophores, these molecules produce intense fluorescence upon aggregation [2]. Several classes of molecules showing AIE have been designed based on tetraphenylethene, hexaphenylsilole or similar molecular systems [3]. Since then, aggregation induced emitters (so called AIEgens) have been introduced as chemosensors [4-10], bioprobes [11-13] and as functional materials for OLEDs [14, 15].

There are several classes of pH sensor based on AIE presented in the literature [16-24]. A donor-acceptor molecular system based on carbazole and pyridine units, has been designed as a pH sensor based on aggregation–deaggregation mechanism [19]. A recently reported molecular chemodosimeter using AIE of salicylaldehyde Schiff-base derivatives showed great promise for irreversible multicolour pH sensing [25]. In general, AIEgens are not yet very common for reversible and multicolour pH sensing despite their attractive potential applications. Benzimidazole moiety (BI) is a multifunctional structural block used in the synthesis of novel heterocycles for drug development [26], chemosensors [27-29] and optoelectronics [30]. However, AIEgen molecules based on the benzimidazole unit are very rare [31]. The intramolecular charge transfer (ICT) compounds such as styryl cyanine dyes are strong candidates for the design and development of AIEGens due to their pronounced capacity for self-assembly [32-34]. The BI based styryl dyes can be designed as ICT systems (donor–π–acceptor) where the BI unit can act as an electron accepting or withdrawing group [35, 36]. As a part of our research effort on developing BI based ICT chromophores for pH and metal-ion sensing [29, 37, 38] we discovered that *E*-2-(2-Benzimidazolyl)-3-(4-*N*,*N*-dimethylaminophenyl)acrylonitrile (**BIA**) shows unique AIE properties. Furthermore, it is well known that suchlike benzimidazole derivatives are biologically active molecules which

display cytotoxic activity against human cancer cells and one of the mechanisms of their biological action is confirmed to be DNA binding [39].

In this work, we present the reversible pH switchable aggregation induced emission of **BIA** (Fig. 1.).

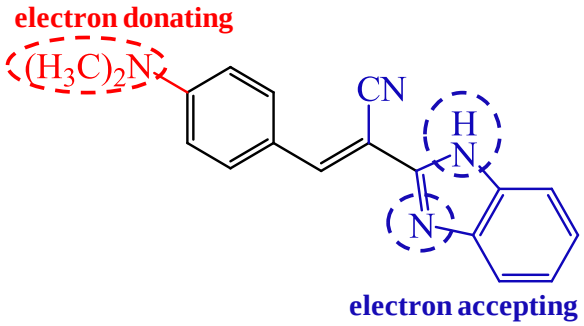

Figure 1. D-π-A arrangement and ionisable sites of **BIA.**

The ICT character of **BIA** originates from the interaction between the strong electron donating *N*,*N*-dimethylamino group and the electron accepting phenylacrylonitrile benzimidazole conjugated skeleton connected via a π linker. The molecule combines two additional functional features: proven self-assembly capacity of the styrylcyanine part, and the pH sensitivity of the planar BI moiety. The effects of pH on AIE and other photophysical properties of **BIA** in dissolved, aggregated and solid states are examined with a view to developing novel molecular systems relying on the pH induced aggregation–deaggregation mechanism.

2. Materials and methods

2.1. General methods

All chemicals and solvents for synthesis and characterisation were purchased from commercial suppliers Acros, Aldrich or Fluka. Methanol, hydrochloride acid, sodium hydroxide and organic solvents were obtained from Kemika d.d., Zagreb. Milli-Q water was used for the preparation of aqueous solutions. pH values in the range 1-13 were measured with a commercially available combination pH electrode BlueLine 17 pH (Schott AG, Mainz, Germany). Absorbance spectra were recorded on a Cary 100 Scan Varian spectrophotometer. Absorbance measurements were carried out using quartz cells of 1 cm path length and

absorbance values were recorded at 1 nm. Wavelength scan was performed between 200 nm and 700 nm. Baseline was recorded prior to each set of experiments. Fluorescence measurements were carried out on a Varian Cary Eclipse fluorescence spectrophotometer at 25ºC using 1 cm path quartz cells. Excitation wavelengths were determined from absorbance maxima. Emission spectra were recorded from 300 nm to 700 nm and corrected for the effects of time and wavelength dependent light source fluctuations using a standard of Rhodamine 101, a diffuser provided with the fluorimeter and the software supplied with the instrument.

2.2. Synthesis of E-2-(2-Benzimidazolyl)-3-(4-N,N-dimethylaminophenyl)acrylonitrile (BIA)

Compound **BIA** was prepared according to the reported method [40], using 2-cyanomethylbenzimidazole (0.80 g, 5.2 mmol) and 4-*N*,*N*-dimethylaminobenzaldehyde (0.76 g, 5.2 mmol) in absolute ethanol (15 mL) and piperidine (0.15 mL). After heating under reflux for 2,5 hours and recrystallisation from ethanol 1.06 g of orange powder was obtained (yield 72%). Characterisation details are described in ESI.

2.3. Photophysical characterisation of BIA

Absorption and fluorescence spectra of the compound were recorded in several organic solvents and aqueous solutions at different pH value. Due to low solubility in water, **BIA** was initially dissolved in ethanol or DMSO and stock solutions were prepared, c(stock)=1×10^{-3} mol dm^{-3}. Working solutions were prepared by dilution of concentrated stock solutions.

The pH titration experiments were carried out starting with 1x10^{-5} mol dm^{-3} solutions of **BIA** in 0.1 M hydrochloric acid or 0.1 M potassium hydroxide solutions. The adjustment of pH was achieved through the addition of acid or base until a change of pH within 0.5 units occurred. Following each addition of titrant, UV-visible absorption and fluorescence spectra were recorded after equilibration was achieved, defined as the drift of pH electrode < 0.1 pH unit per minute. Titrations were conducted at constant ionic strength I = 0.1 M, in potassium chloride solutions.

The pK_a values were calculated as the x-coordinate of the inflection point of the Boltzmann function (1) obtained from spectrophotometric titrations data:

$$y = \frac{A_1 - A_2}{1 + e^{(x - x_0)/dx}} + A_2 \quad (1)$$

Dynamic light scattering (DLS) experiments were carried out in aqueous (f_w = 99% water/ethanol) and in ethanol solution, c = 10 μM.

Crystalline structures were imaged by the scanning electron microscope TESCAN Vega3SEM Easyprobe at electron beam energy of 10 keV.

3. Results and Discussion

3.1. Photophysical properties of BIA

The photophysical properties of **BIA** were studied in pure organic solvents, in solvent-nonsolvent binary mixtures and in the solid state.

3.1.1. BIA in pure solvents

The compound is soluble in common organic solvents but insoluble in water. The *aqueous solution* in the text refers to solutions prepared by diluting stock ethanol solution of **BIA** in a large quantity of water (water volume fraction f_w = 99 %). Absorption and emission spectra and the summary of photophysical properties of **BIA** in solvents of varying polarities are shown in Fig. 2 (A and B) and Table 1, respectively.

Table 1. Optical properties of **BIA** in solvents of different polarity.

	$E_T(30)$[a] / (kcal mol^{-1})	**λ_{abs} / nm**	**$\varepsilon \cdot 10^{-3}$ / M^{-1} cm^{-1}**	**λ_{fluo} / nm**	**Rel. Fluo Int.**	**Stokes shift / nm**
diethylether	34.5	418	70.48	471	107	53
THF	37.4	423	58.12	491	137	68
ethylacetate	38.1	425	59.17	491	137	66
dichlormethane	40.7	434	70.00	501	165	67
acetone	42.2	425	59.60	498	130	73
DMSO	45.1	432	53.90	506	316	74
acetonitrile	45.6	425	59.84	503	130	78
ethanol	51.9	425	55.14	498	123	73
methanol	55.4	428	60.99	498	113	70
H_2O	63.1	358	21.80	600	272	238

[a] empirical parameter of solvent polarity [41]

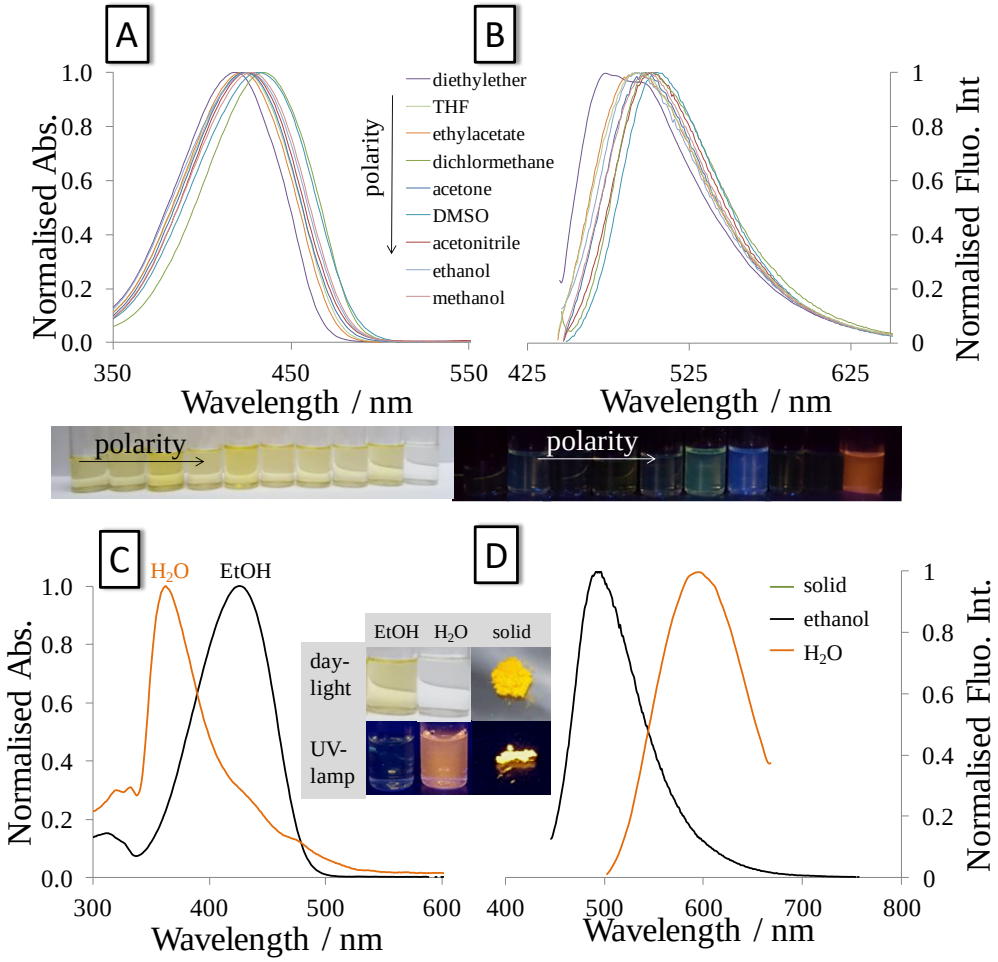

Figure 2. (A) Absorbance and (B) emission spectra of **BIA** in solvents of varying polarities, c = 10 μM, λ_{exc} = 425 nm; photographs show solvents in order of increasing polarity; the last sample presents **BIA** aggregates in aqueous solution; (C) Normalised absorbance and (D) emission spectra of **BIA** in aqueous solution and ethanol (c = 10 μM, λ_{exc} = 350 nm and 425nm respectively), and emission in solid state. Inset: photographs of samples taken in daylight and under UV lamp.

In all of the organic solvents tested, **BIA** shows absorption maxima in the range of 418 nm to 434 nm, giving yellow solutions with generally high molar absorption coefficients, the highest being in diethyl ether, ε = 70480 $dm^3\,cm^{-1}\,mol^{-1}$ (Fig. 2A). The fluorescence in all solvents is of moderate to low intensity (generally Φ < 0.01); in blue or green spectral region, ranging from 471 nm in diethyl ether to 506 nm in DMSO (Fig. 2B). The effect of solvent polarity on emission properties is demonstrated by a Lippert-Mataga plot of the Stokes shift against the orientation polarisibility of the solvent (Fig. S1). The best linear fit to the model is obtained in the polar aprotic solvents (R^2 = 0.90) with a slope of 3777 cm^{-1} indicating general, non-specific solvent-**BIA** interactions and a moderately strong ICT feature. Hydrogen bond

donating solvents do not fit into the Lippert-Mataga plot indicating the presence of specific solvent-**BIA** interactions in accordance with the availability of several ionisable sites in **BIA** (Fig. 1).

3.1.2. BIA in solvent-nonsolvent mixtures and solid state

Absorption and emission properties of **BIA** have also been studied in binary solvent-nonsolvent mixtures (ethanol-H_2O, THF-H_2O and DMSO-H_2O). **BIA** dissolved in each organic solvent was gradually diluted with water and followed spectroscopically, as shown for DMSO in Fig. 3 and for ethanol and THF in Fig. S2–S4, respectively.

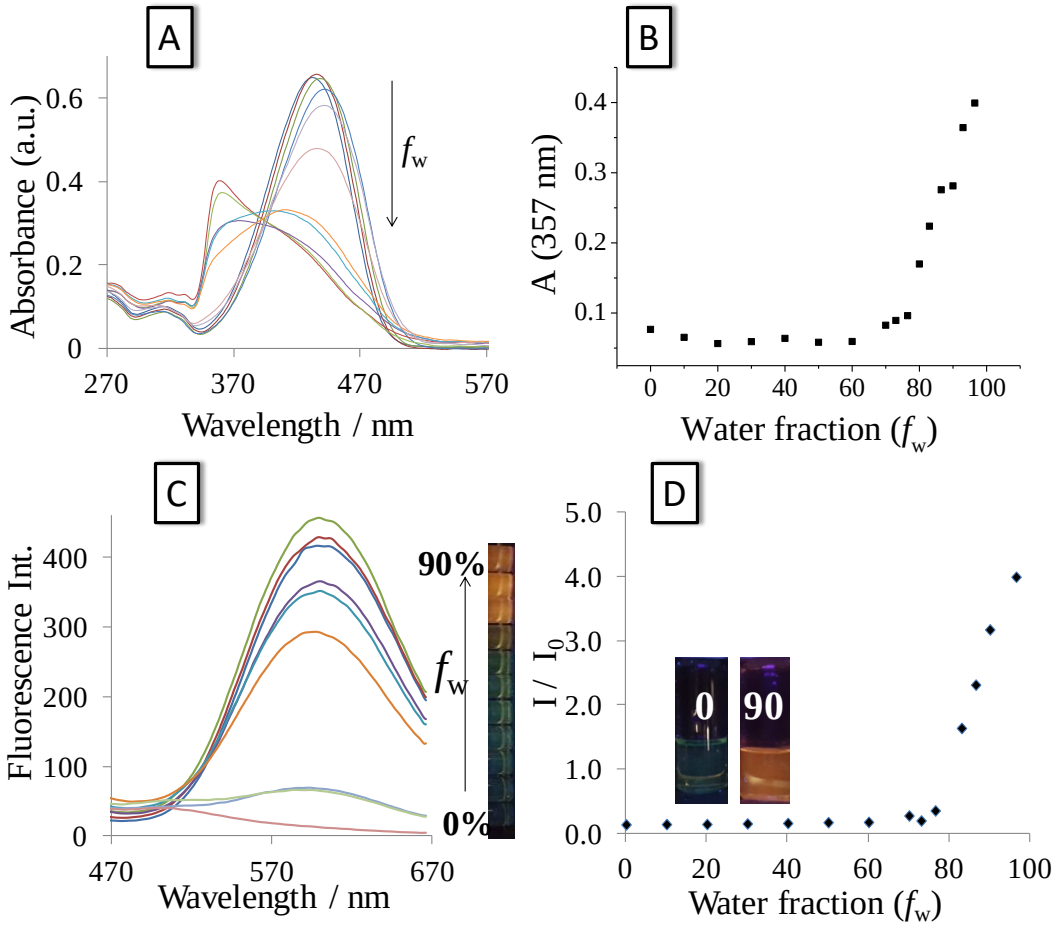

Figure 3. (A) Absorption and (C) emission spectra of **BIA** in DMSO at different volume fraction of water; effect of water fraction on the absorption (B) and emission (D) intensity, c = 10 μM, λ_{exc} = 350 nm.

On addition of water to a solution of **BIA** in DMSO and other solvents, the absorbance spectra remain virtually unchanged until the water fraction f_w reached the value 80% (Fig.

3A). Above this threshold value there is a significant change in absorption and emission spectra in all solvent-nonsolvent mixtures (ethanol-H_2O, THF-H_2O and DMSO-H_2O): the absorption spectra show a blue shift with a maximum at 350 nm and a *level-off* red tail indicating presence of light scattering effects on nanoparticles [42] (Fig. 2C). At the same time, yellow solution turns colourless under ambient light and a new intense fluorescence emission band appears at 600 nm observed as bright red-orange fluorescence under UV light (Fig. 2. inset photographs). The intensity of orange emission in aqueous solution (f_w = 99 %) is around 35-fold the emission in organic solvents at 600 nm (Fig. 3 and Figs. S2-S4). Aqueous mixtures appear completely homogenous, without precipitates, transparent and colourless under ambient light.

In the solid state **BIA** appears as a yellow powder and shows strong orange-red solid-state fluorescence with a maximum of emission at 595 nm (Fig. 2D). This emission is in full agreement with the emission spectra of **BIA** obtained in aqueous solutions.

3.2. Nanoaggregation and the mechanism of AIE

The presence of nanoaggregates in aqueous solution was confirmed by the occurrence of the Tyndall effect of **BIA** in solvent-nonsolvent mixtures (Fig S4). The dynamic light scattering (DLS) measurements showed no particles in pure ethanol but revealed the presence of aggregates in aqueous solutions with sizes in the range 30 nm to 1000 nm, depending on the solvent-nonsolvent composition and precipitation time (Fig S5). The SEM characterisation of aggregates precipitated under different conditions showed morphologies with more or less pronounced amphorous or crystalline character (Fig. S6). Interestingly, unlike some previously reported AIEgen molecules [43], all aggregates of **BIA** in solutions and in solid state show AIE at 600 nm regardless of their morphology or size. The self-assembly and packing modes of ICT molecules into nanoaggregate structures is dependent on supramolecular interactions, especially hydrogen bonds, other dipole-dipole interactions, and solvent-nonsolvent properties [44]. Suppression of intramolecular motion and the prevention of π–stacking result in tight molecular arrangements with increased rigidity leading to the suppression of non-radiative relaxation and AIE enhancement. The observed blue-shift in the absorption band of **BIA** on going from ethanol (440 nm) to aqueous solution (350 nm), can be associated with the formation of H-aggregates. It is known that H-type aggregates usually exhibit “aggregation-induced emission quenching“. In contrast to that, **BIA** shows red-shifted and significantly increased emission in nanoaggregated form. The same behaviour was reported for a cyano *para*-distyrylbenzene (DSB) derivative and has been associated with H-

type aggregation with the strongly red-shifted, unstructured emission spectrum similar to excimer emission [45]. In general, such behaviours can be ascribed to the formation of specific supramolecular stacking architectures related to the unique electronic and structural characteristics of the examined molecules. The presence of the bulky and polar cyano group plays a major role in preventing the parallel face-to-face intermolecular interactions [32]. The less common emissive H-aggregates [46] have recently been re-examined by Gierschner et al. [47] using DSB as a prototype example of a herringbone-arranged H-aggregate.

The effects of solvent viscosity and temperature changes on **BIA** spectral properties in solutions were studied. Absorption and fluorescence spectra were recorded in mixtures of varying viscosity (glycerol-methanol of different volume ratios) and varying temperatures (methanol solutions of **BIA**) (Figs. 4 and S7).

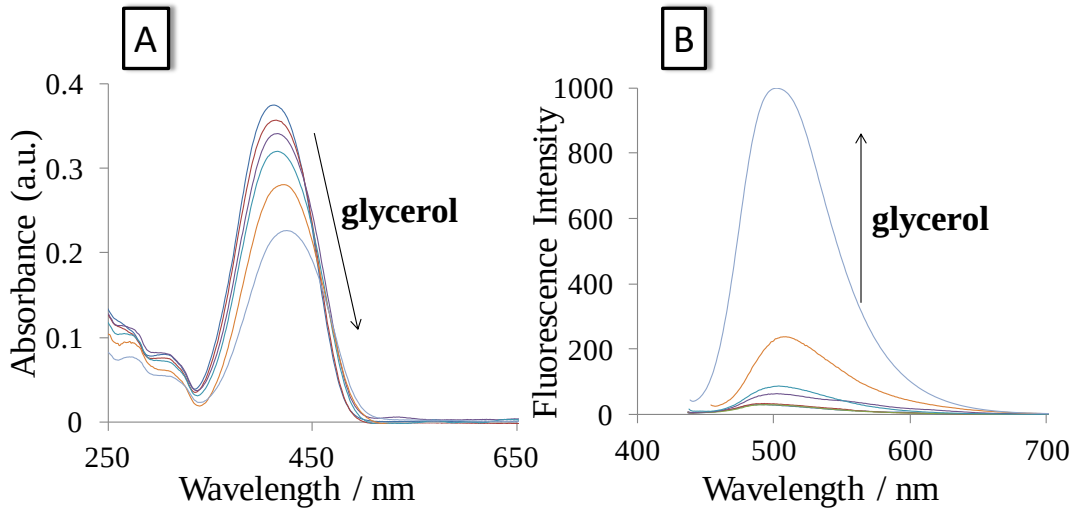

Figure 4. (A) Absorption and (B) fluorescence spectra of **BIA** in methanol – glycerol mixtures with different volume fractions of glycerol (glycerol fraction = 0 – 100%), *c* = 10μM.

As the volume fraction of glycerol increased, fluorescence intensity became stronger. Absorption spectra showed no evidence of aggregation (absence of *level-off* red tail). Fluorescence intensity of **BIA** in methanol increased with decreasing temperature. Both observed effects are closely related to the AIE mechanism [48] which in the case of **BIA** can be attributed to the restriction of the intramolecular rotation of the dimethylamino group conjugated to the aromatic ring, leading to a more rigid molecular arrangement. The restricted rotation in **BIA** enhances electron donating ability towards the acceptor moiety, thus stabilising the TICT state in viscous medium, as has been shown for a styryl analogue of **BIA**

[49]. These features are supported by our computations, which, at the M06–2X/6–31+G(d,p) level with the implicit SMD water solvation, reveal that the matching N(amino)–C(phenyl) bond in **BIA** is 1.368 Å, which is much shorter than, for example, in *N*,*N*-dimethylaniline where it is 1.401 Å, thus indicating increased electron donation of the $–N(Me)_2$ group in **BIA**. Concomitantly, the latter group is more planar in **BIA** with torsional angles of the methyl groups being 13.3° and 14.9° in **BIA**, and 20.8° and 24.5° in *N*,*N*-dimethylaniline. Analogously, the free energy barrier for the rotation of the dimethylamino group around the N(amino)–C(phenyl) bond in **BIA** is $\Delta G^{\ddagger}_{rot}$ = 7.5 kcal mol^{-1}, being significantly higher than in *N*,*N*-dimethylaniline ($\Delta G^{\ddagger}_{rot}$ = 4.7 kcal mol^{-1}), clearly suggesting increased rigidity in **BIA**.

3.3. Effect of pH on aggregation – deaggregation process of BIA

The effect of pH on AIE of **BIA** was studied by spectroscopic pH titrations in aqueous solution. The absorption spectra recorded during titration of **BIA** are shown in Fig. 5A.

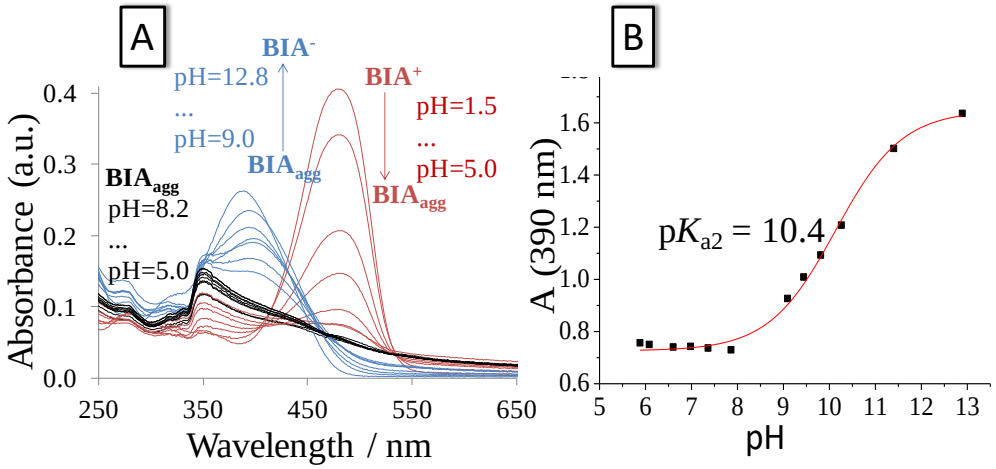

Figure 5. Effect of pH on the absorption properties caused by aggregation / deaggregation, *c* = 10 μM.

The absorption spectra show three distinct pH ranges corresponding to a) pH range 5 to 8 indicating presence of *neutral form* (aggregate); b) pH range from 1.5 to 5 (protonation of aggregated form) and c) pH range 9 to 13 (deprotonation of aggregated form). The corresponding apparent pK_a values estimated from the absorbance titration data are pK_{a1} = 2.2 and pK_{a2} = 10.4 (Fig. 5B), which are very well matched by the computed values of 4.2 and 10.3, respectively, showing good agreement with experimental data. These indicate that **BIA** is slightly less basic than benzimidazole (p$K_{a,EXP}$ = 5.41) [50] due to the presence of the electron-accepting cyano and vinyl groups, which reduce basicity. For the same reason, **BIA**

is two orders of magnitude more acidic than benzimidazole (p$K_{a,EXP}$ = 12.75) [50]. Prototropic equilibria and associated species of **BIA** in aqueous solutions are shown in Scheme 1.

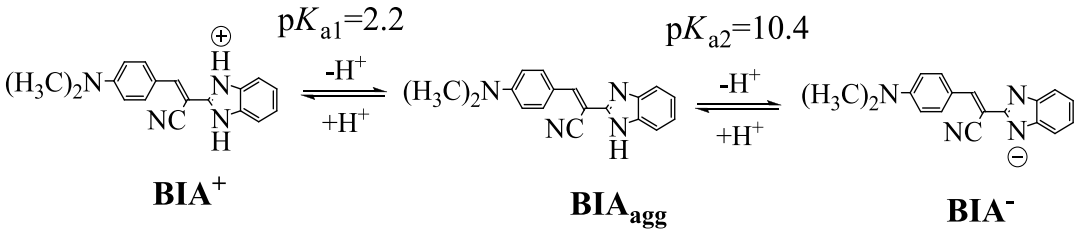

Scheme 1. Prototropic equilibria of **BIA** and associated species in aqueous solutions.

BIA is a pH responsive molecule due to the ionisable imino and amino groups of the BI moiety [34]. The absorption/emission maxima of prototropic species $\mathbf{BIA_{agg}}$, $\mathbf{BIA^+}$ and $\mathbf{BIA^-}$ were identified as 350/600 nm, 480/537 nm and 390/500 nm, respectively. The first protonation of **BIA** occurs on the imino nitrogen of the BI moiety and not on the dimethylamino group, and results in a red shift and increased extinction coefficient. This is explained by the enhanced electron accepting properties of the protonated BI moiety and additionally confirmed by theoretical calculations and crystallization data [40].

Normalised emission spectra of prototropic species $\mathbf{BIA_{agg}}$, $\mathbf{BIA^+}$ and $\mathbf{BIA^-}$**,** and the photographs of the corresponding solutions at different pH values taken under UV illumination are shown in Fig. 6A and Fig 6B.

The spectra show greenish-blue fluorescence emission of protonated (λ_{max} = 537 nm) and deprotonated forms (λ_{max} = 500 nm), in contrast to the orange-red emission of the aggregated form at near neutral pH values. The fluorimetric titration (Fig. S8) and the corresponding ratiometric plots with apparent pK^*_{a1} = 2.0 and pK^*_{a2} = 10.4 (Fig. 6D) are in good agreement with the pK_a values obtained from the absorption titrations.

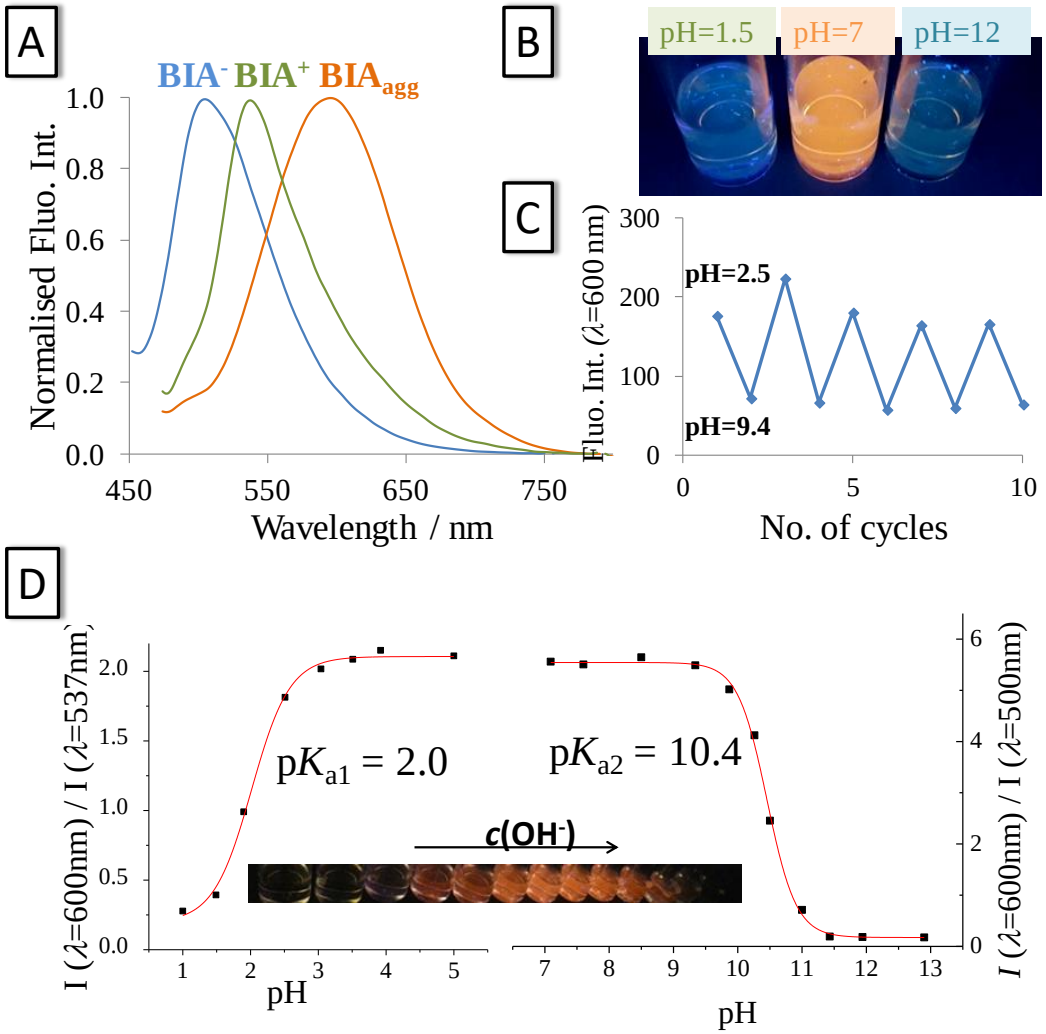

Figure 6. (A) Normalised emission spectra of prototropic species **BIA$_{agg}$**, **BIA$^+$** and **BIA$^-$** in aqueous solutions; (B) Photographs of the corresponding solutions at different pH values taken under UV illumination; (C) Reversible switching of the emission intensity of **BIA** with pH, λ_{exc} = 350 nm; (D) pH titration plots (ratiometric fluorescence intensity *vs* pH), *c* (BIA) = 10 μM, λ_{exc} = 425 nm; inset shows a photograph of **BIA** solutions at different pH values taken under UV illumination.

The aggregation – deaggregation process in solutions is bidirectionally pH switchable with the switching values around the apparent pK_a values. This allows the red-orange florescence of **BIA** aggregates to be turned-on and off by modulating environmental pH values.

The pH switching of aggregate absorption and emission is reversible (Fig. 6C, Fig. S9) and can also be observed in the solid state. On alternate exposure of **BIA** in solid state to the vapours of HCl and NH_3, the emission of **BIA** switches on and off (Fig. 7).

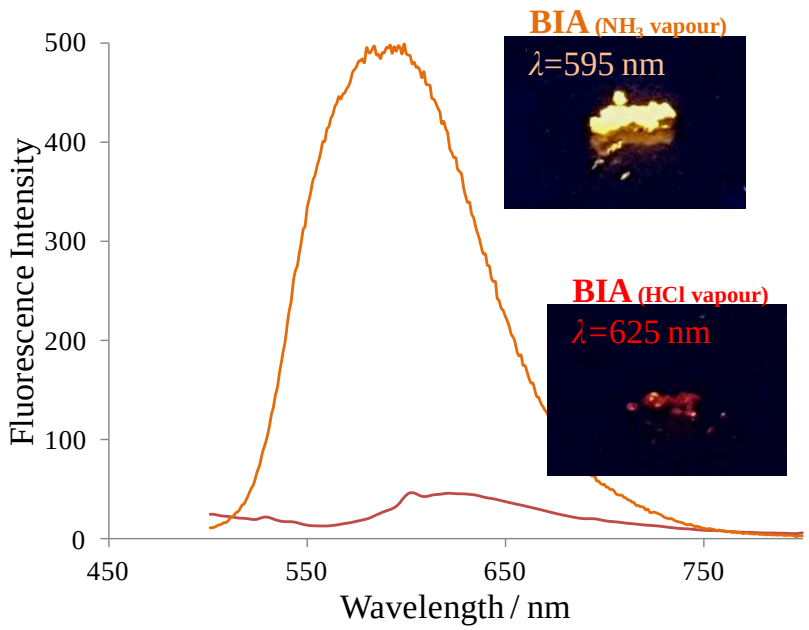

Figure 7. Emission spectra of **BIA** in solid state and upon exposure to the vapours of HCl (**BIA**$^+$), λ_{exc}=440 nm.

It is also known that **BIA** interacts with DNA molecules [40], and we plan to explore this phenomenon further in light of the AIE processes reported here.

4. Conclusion

To conclude, we present the bidirectional pH switchable fluorescence and aggregation behaviour of an ICT chromophore molecule (**BIA**) containing a benzimidazole moiety. From the single molecular entity, three prototropic species (tri-state system) are derived that respectively emit in the red, green and cyan spectral regions. The neutral form is capable of self-assembly in aqueous environment exhibiting stable red-orange aggregation-induced emission (AIE) in physiologically relevant pH range. The aggregation and emission are pH switchable and fully-reversible. The molecule is shown to similarly function in the solid state where emission can be modulated by exposure to acidic and basic vapours. Such novel optical behaviours are promising for future developments in intracellular pH sensing and imaging [51], and intelligent organic optoelectronic materials [52].

Acknowledgements

This work was supported by the Croatian Science Foundation under grant number IP-2014-09-3386 entitled *Design and synthesis of novel nitrogen-containing heterocyclic fluorophores and fluorescent nanomaterials for pH and metal-ion sensing*. We would like to thank Dr. Maja Dutour Sikirić and Dr. Darija Domazet Jurašin from the Ruđer Bošković Institute, Zagreb, for the use of the DLS instrumentation and Dr. Anamarija Rogina from Faculty of Chemical Engineering and Technology, University of Zagreb for the SEM images.

Appendix A. Supplementary data

Supplementary material related to this article can be found online.

References

[1] Luo J, Xie Z, Lam JWY, Cheng L, Chen H, Qiu C, et al. Aggregation-induced emission of 1-methyl-1,2,3,4,5-pentaphenylsilole. Chem Commun 2001 (18):1740-1.

[2] Hong Y, Lam JWY, Tang BZ. Aggregation-induced emission. Chem Soc Rev 2011;40(11):5361-88.

[3] Wang H, Zhao E, Lam JWY, Tang BZ. AIE luminogens: emission brightened by aggregation. Mater Today 2015;18(7):365-77.

[4] Yang XD, Chen XL, Lu XD, Yan CG, Xu YK, Hang XD, et al. A highly selective and sensitive fluorescent chemosensor for detection of CN^-, SO_3^{2-} and Fe^{3+} based on aggregation-induced emission. J Matter Chem C 2016;4(2):383-90.

[5] Peng L, Zhou Z, Wang X, Wei R, Li K, Xiang Y, et al. A ratiometric fluorescent chemosensor for Al3+ in aqueous solution based on aggregation-induced emission and its application in live-cell imaging. Anal Chim Acta 2014;829:54-9.

[6] Gogoi A, Mukherjee S, Ramesh A, Das G. Aggregation-Induced Emission Active Metal-Free Chemosensing Platform for Highly Selective Turn-On Sensing and Bioimaging of Pyrophosphate Anion. Anal Chem 2015;87(13):6974-9.

[7] Alam P, Kachwal V, Rahaman Laskar I. A multi-stimuli responsive "AIE" active salicylaldehyde-based Schiff base for sensitive detection of fluoride. Sensor Actuat B-Chem 2016;228:539-50.

[8] Fang W, Zhang G, Chen J, Kong L, Yang L, Bi H, et al. An AIE active probe for specific sensing of Hg^{2+} based on linear conjugated bis-Schiff base. Sensor Actuat B-Chem 2016;229:338-46.

[9] Kaur N, Kaur P, Singh K. Ferrocene-BODIPY Push–Pull dyad: A common platform for the sensing of Hg^{2+} and Cr^{3+}. Sensor Actuat B-Chem 2016;229:499-505.

[10] Lu W, Xiao P, Gu J, Zhang J, Huang Y, Huang Q, et al. Aggregation-induced emission of tetraphenylethylene-modified polyethyleneimine for highly selective CO2 detection. Sensor Actuat B-Chem 2016;228:551-6.

[11] Ding D, Li K, Liu B, Tang BZ. Bioprobes Based on AIE Fluorogens. Accounts Chem Res 2013;46(11):2441-53.

[12] Yan LL, Zhang Y, Xu B, Tian WJ. Fluorescent nanoparticles based on AIE fluorogens for bioimaging. Nanoscale 2016;8(5):2471-87.

[13] Zhu Z, Qian J, Zhao X, Qin W, Hu R, Zhang H, et al. Stable and Size-Tunable Aggregation-Induced Emission Nanoparticles Encapsulated with Nanographene Oxide and Applications in Three-Photon Fluorescence Bioimaging. ACS Nano 2016;10(1):588-97.

[14] Li Z, Dong YQ, Lam JWY, Sun J, Qin A, Haeussler M, et al. Functionalized Siloles: Versatile Synthesis, Aggregation-Induced Emission, and Sensory and Device Applications. Adv Funct Mater 2009;19(6):905-17.

[15] Huang J, Sun N, Chen PY, Tang RL, Li QQ, Ma DG, et al. Largely blue-shifted emission through minor structural modifications: molecular design, synthesis, aggregation-induced emission and deep-blue OLED application. Chem Commun 2014;50(17):2136-8.

[16] Lin N, Chen X, Yan S, Wang H, Lu Z, Xia X, et al. An aggregation-induced emission-based pH-sensitive fluorescent probe for intracellular acidity sensing. RSC Advances 2016;6(30):25416-9.

[17] Lu HG, Xu B, Dong YJ, Chen FP, Li YW, Li ZF, et al. Novel Fluorescent pH Sensors and a Biological Probe Based on Anthracene Derivatives with Aggregation-Induced Emission Characteristics. Langmuir 2010;26(9):6838-44.

[18] Chen SJ, Liu JZ, Liu Y, Su HM, Hong YN, Jim CKW, et al. An AIE-active hemicyanine fluorogen with stimuli-responsive red/blue emission: extending the pH sensing range by "switch+knob" effect. Chem Sci 2012;3(6):1804-9.

[19] Yang Z, Qin W, Lam JWY, Chen S, Sung HHY, Williams ID, et al. Fluorescent pH sensor constructed from a heteroatom-containing luminogen with tunable AIE and ICT characteristics. Chem Sci 2013;4(9):3725-30.

[20] Wang LY, Yang LL, Cao DR. Probes based on diketopyrrolopyrrole and anthracenone conjugates with aggregation-induced emission characteristics for pH and BSA sensing. Sensor Actuat B-Chem 2015;221:155-66.

[21] Zhou Z, Gu F, Peng L, Hu Y, Wang Q. Spectroscopic analysis and in vitro imaging applications of a pH responsive AIE sensor with a two-input inhibit function. Chem Commun 2015;51(60):12060-3.

[22] Wu D, Shao L, Li Y, Hu Q, Huang F, Yu G, et al. A boron difluoride dye showing the aggregation-induced emission feature and high sensitivity to intra- and extra-cellular pH changes. Chem Commun 2016;52(3):541-4.

[23] Yao X, Ma X, Tian H. Aggregation-induced emission encoding supramolecular polymers based on controllable sulfonatocalixarene recognition in aqueous solution. J Matter Chem C 2014;2(26):5155-60.

[24] Ma X, Sun R, Li W, Tian H. Novel electrochemical and pH stimulus-responsive supramolecular polymer with disparate pseudorotaxanes as relevant unimers. Polym Chem 2011;2(5):1068-70.

[25] Feng Q, Li Y, Wang L, Li C, Wang J, Liu Y, et al. Multiple-color aggregation-induced emission (AIE) molecules as chemodosimeters for pH sensing. Chem Commun 2016:(52):123-3126

[26] Ajani OO, Aderohunmu DV, Ikpo CO, Adedapo AE, Olanrewaju IO. Functionalized Benzimidazole Scaffolds: Privileged Heterocycle for Drug Design in Therapeutic Medicine. Arch Pharm 2016;349(7):475-506.

[27] Li Z, Li L-J, Sun T, Liu L, Xie Z. Benzimidazole-BODIPY as optical and fluorometric pH sensor. Dyes Pigment 2016;128:165-9.

[28] Gupta KC, Sutar AK. Catalytic activities of Schiff base transition metal complexes. Coordin Chem Rev 2008;252(12-14):1420-50.

[29] Hranjec M, Horak E, Tireli M, Pavlovic G, Karminski-Zamola G. Synthesis, crystal structure and spectroscopic study of novel benzimidazoles and benzimidazo 1,2-a quinolines as potential chemosensors for different cations. Dyes Pigments 2012;95(3):644-56.

[30] Saltan GM, Dincalp H, Kiran M, Zafer C, Erbas SC. Novel organic dyes based on phenyl-substituted benzimidazole for dye sensitized solar cells. Mater Chem Phys 2015;163:387-93.

[31] Cao YL, Yang MD, Wang Y, Zhou HP, Zheng J, Zhang XZ, et al. Aggregation-induced and crystallization-enhanced emissions with time-dependence of a new Schiff-base family based on benzimidazole. J Matter Chem C 2014;2(19):3686-94.

[32] An B-K, Gierschner J, Park SY. π-Conjugated Cyanostilbene Derivatives: A Unique Self-Assembly Motif for Molecular Nanostructures with Enhanced Emission and Transport. Accounts Chem Res 2012;45(4):544-54.

[33] Li YJ, Liu TF, Liu HB, Tian MZ, Li YL. Self-Assembly of Intramolecular Charge-Transfer Compounds into Functional Molecular Systems. Accounts Chem Res 2014;47(4):1186-98.

[34] Wang F, Li X, Wang S, Li CP, Dong H, Ma X, et al. New pi-conjugated cyanostilbene derivatives: Synthesis, characterization and aggregation-induced emission. Chinese Chem Lett 2016;27(10):1592-6.

[35] Jedrzejewska B, Osmialowski B, Zalesny R. Application of spectroscopic and theoretical methods in the studies of photoisomerization and photophysical properties of the push-pull styryl-benzimidazole dyes. Photoch Photobio Sci 2016;15(1):117-28.

[36] Jędrzejewska B, Krawczyk P, Pietrzak M, Gordel M, Matczyszyn K, Samoć M, et al. Styryl dye possessing donor-π-acceptor structure – Synthesis, spectroscopic and computational studies. Dyes Pigments 2013;99(3):673-85.

[37] Horak E, Vianello R, Hranjec M, Krištafor S, Zamola GK, Steinberg IM. Benzimidazole acrylonitriles as multifunctional push-pull chromophores: Spectral characterisation, protonation equilibria and nanoaggregation in aqueous solutions. Spectrochim Acta A 2017; 178:225-33.

[38] Hranjec M, Horak E, Babic D, Plavljanin S, Srdovic Z, Steinberg IM, et al. Fluorescent benzimidazo[1,2-a]quinolines: synthesis, spectroscopic and computational studies of protonation equilibria and metal ion sensitivity. New J Chem 2017;41(1):358-71.

[39] Hranjec M, Pavlović G, Marjanović M, Kralj M, Karminski-Zamola G. Benzimidazole derivatives related to 2,3-acrylonitriles, benzimidazo[1,2-a]quinolines and fluorenes: Synthesis, antitumor evaluation in vitro and crystal structure determination. Eur J Med Chem 2010;45(6):2405-17.

[40] Hranjec M, Pavlovic G, Karminski-Zamola G. Spectroscopic characterization, crystal structure determination and interaction with DNA of novel cyano substituted benzimidazole derivative. Struct Chem 2007;18(6):943-9.

[41] Reichardt C. Solvents and Solvent Effects in Organic Chemistry. Wiley-VCH Verlag GmbH & Co KGaA. 2004.

[42] Auweter H, Haberkorn H, Heckmann W, Horn D, Luddecke E, Rieger J, et al. Supramolecular structure of precipitated nanosize beta-carotene particles. Angew Chem Int Ed 1999;38(15):2188-91.

[43] Wang LK, Zheng Z, Yu ZP, Zheng J, Fang M, Wu JY, et al. Schiff base particles with aggregation-induced enhanced emission: random aggregation preventing pi-pi stacking. J Matter Chem C 2013;1(42):6952-9.

[44] Würthner F. Dipole–Dipole Interaction Driven Self-Assembly of Merocyanine Dyes: From Dimers to Nanoscale Objects and Supramolecular Materials. Accounts Chem Res 2016;49(5):868-76.

[45] Yoon S-J, Chung JW, Gierschner J, Kim KS, Choi M-G, Kim D, et al. Multistimuli Two-Color Luminescence Switching via Different Slip-Stacking of Highly Fluorescent Molecular Sheets. J Am Chem Soc 2010;132(39):13675-83.

[46] Rösch U, Yao S, Wortmann R, Würthner F. Fluorescent H-Aggregates of Merocyanine Dyes. Angew Chem 2006;118(42):7184-8.

[47] Gierschner J, Lüer L, Milián-Medina B, Oelkrug D, Egelhaaf H-J. Highly Emissive H-Aggregates or Aggregation-Induced Emission Quenching? The Photophysics of All-Trans para-Distyrylbenzene. J Phys Chem Lett 2013;4(16):2686-97.

[48] Hong YN, Lam JWY, Tang BZ. Aggregation-induced emission: phenomenon, mechanism and applications. Chem Commun 2009(29):4332-53.

[49] Mishra A, Chaterjee S, Krishnamoorthy G. Intramolecular charge transfer emission of trans-2-4'-(dimethylamino)styryl benzimidazole: Effect of solvent and pH. J Photoc Photobio A 2013;260:50-8.

[50] Jencks WP, Regenstein J. Ionization Constants of Acids and Bases. Handbook of Biochemistry and Molecular Biology, Fourth Edition: CRC Press; 1976. p. 305-51.

[51] Yue Y, Huo F, Lee S, Yin C, Yoon J. A review: the trend of progress about pH probes in cell application in recent years. Analyst 2017;142(1):30-41.

[52] Zhu L, Zhao Y. Cyanostilbene-based intelligent organic optoelectronic materials. J Matter Chem C 2013;1(6):1059-65.

Electronic Supplementary Material (ESI)

Synthesis of *E*-2-(2-Benzimidazolyl)-3-(4-*N*,*N*-dimethylaminophenyl)acrylonitrile (BIA)

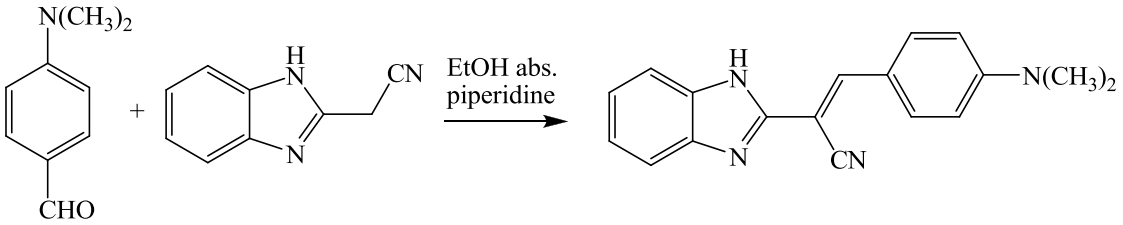

1 **2** **BIA**

Scheme S1. Reaction scheme for preparation of 2-(1*H*-benzimidazol-2-yl)-3-(4-N,N-dimethylamino-phenyl)-acrylonitrile (**BIA)**.

m.p. 253-255 °C; ^{1}H NMR (300 MHz, DMSO-d_6): δ = 12.44 (s, *NH*, 1H), 8.12 (s, 1H), 7.85 (d, *J*=8.88 Hz, H_{arom}, 2H), 7.60 (d, *J*=7.18 Hz, $H_{arom,}$ 1H), 7.45 (d, *J*=7.16 Hz, H_{arom}, 1H), 7.20-7.17 (m, H_{arom}, 2H), 6.82 (d, *J*=8.96 Hz, H_{arom}, 2H), 3.03 (s, 2CH3, 6H); ^{13}C NMR (75 MHz, DMSO-d_6): δ = 155., 150.7, 148.0, 136.3, 134.4 (2C), 127.5, 125.5, 124.3, 122.4, 121.1, 120.2, 118.6, 114.4 (2C), 113.6, 96.1, 25.1 (2C); Anal. Calcd for $C_{18}H_{16}N_4$: C 74.98, H 5.59, N 19.43. Found: C, 75.20; H, 5.68; N, 19.67.

All chemicals and solvents were purchased from commercial suppliers Aldrich and Acros. Melting points were recorded on SMP11 Bibby and Büchi 535 apparatus. All NMR spectra were measured in DMSO-d_6 solutions using TMS as an internal standard. The ^{1}H and ^{13}C NMR spectra were recorded on a Varian Gemini 300 or Varian Gemini 600 at 300, 600 and 150 and 75 MHz, respectively. Chemical shifts are reported in ppm (δ) relative to TMS. All compounds were routinely checked by TLC with Merck silica gel 60F-254 glass plates.

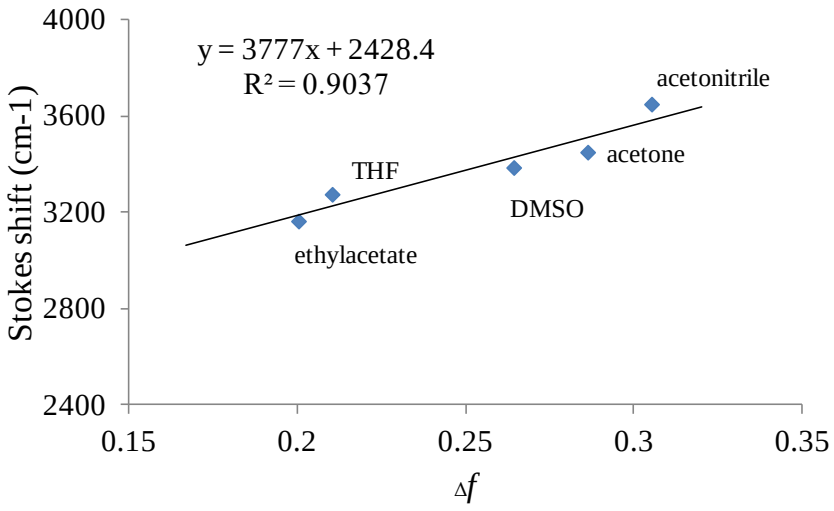

Fig. S1. Lippert-Mataga plot of **BIA** in solvents with different polarities, *c* = 10 μM, excitation wavelength 425 nm.

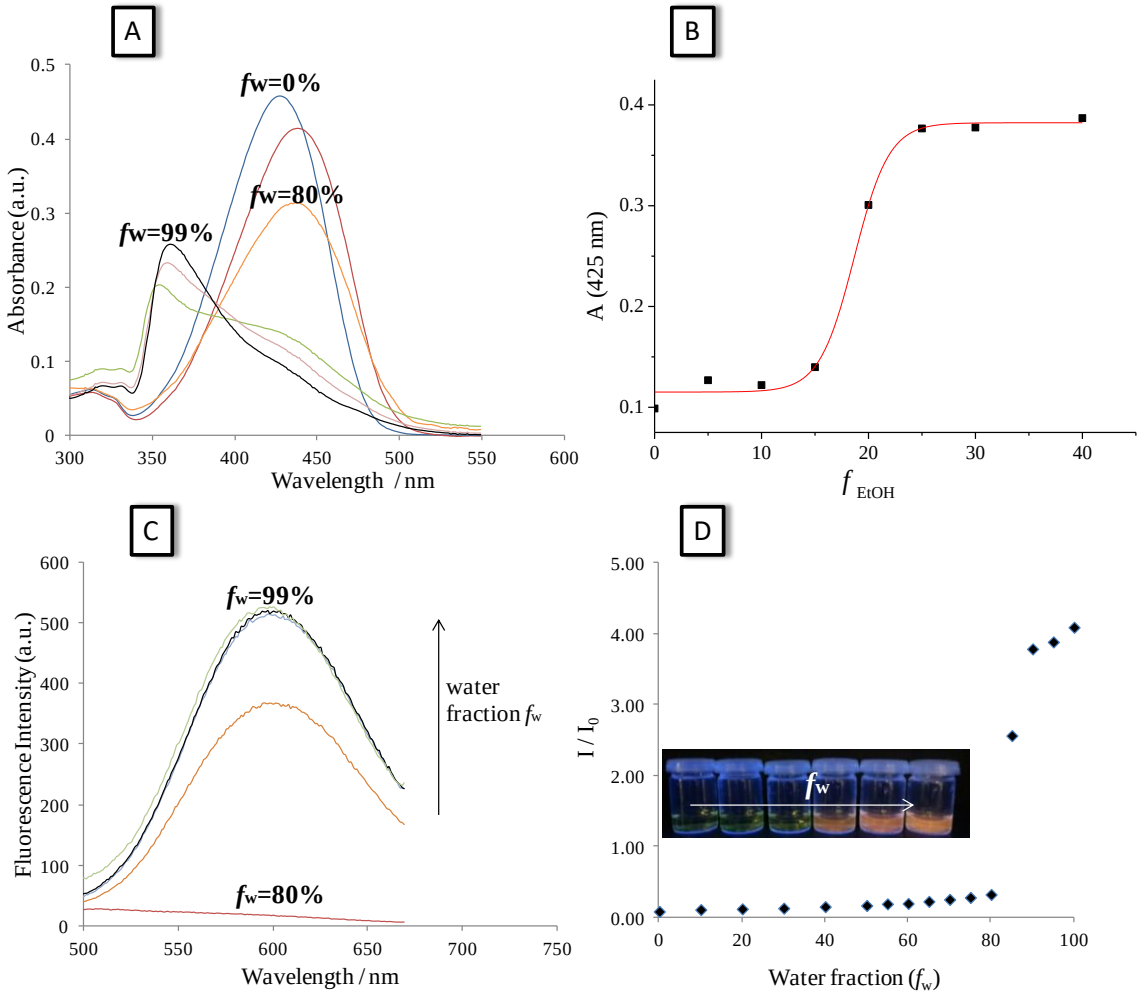

Fig. S2. (A) Absorption and (C) emission spectra of **BIA** in **ethanol** at different volume fraction of water; effect of water fraction on (B) absorbance and (D) emission intensity, *c* = 10μM, λ_{exc}=350 nm.

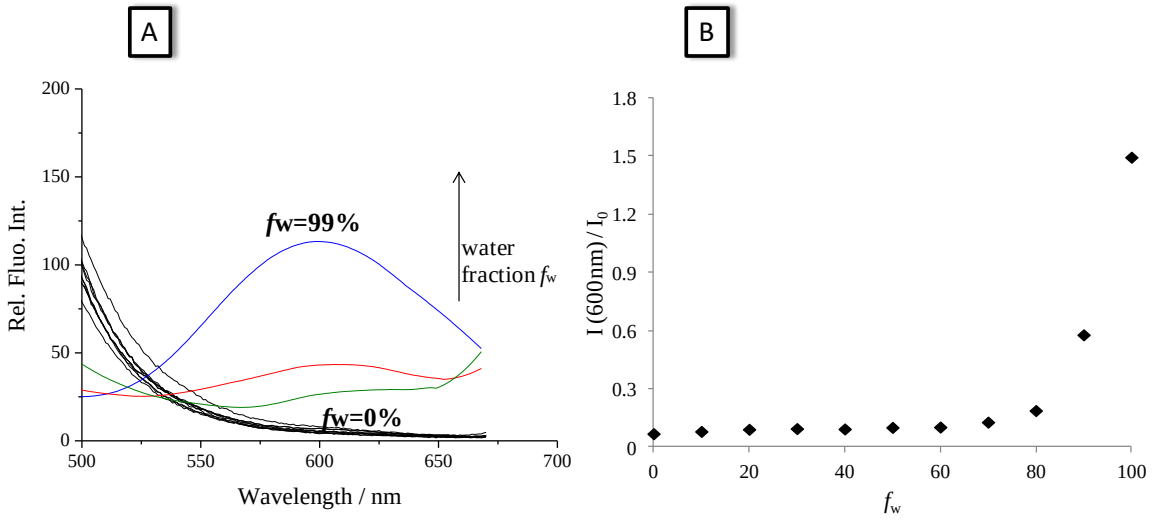

Fig. S3. (A) Emission spectra of **BIA** in **THF** at different volume fraction of water; (B) Effect of water fraction on emission intensity, c = 10μM, λ_{exc}=350 nm.

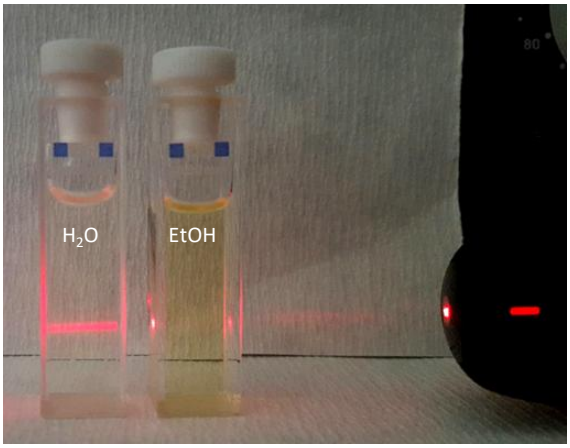

Fig. S4. Observation of the Tyndall effect on nanoaggregates; a red laser beam is directed through solutions of **BIA** in water (left) and ethanol (right). Nanoaggregates of **BIA** in the water cause light scattering, seen as a *red-line* through the solution. Light scattering in ethanol solution is not observed.

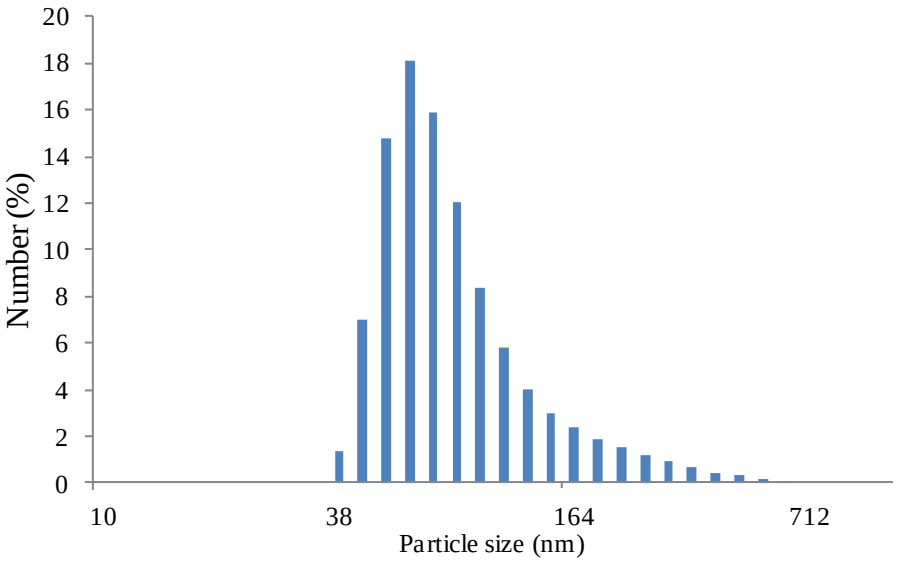

Fig. S5. Dynamic light scattering results of **BIA** in aqueous solution (f_w = 99%), c = 10μM.

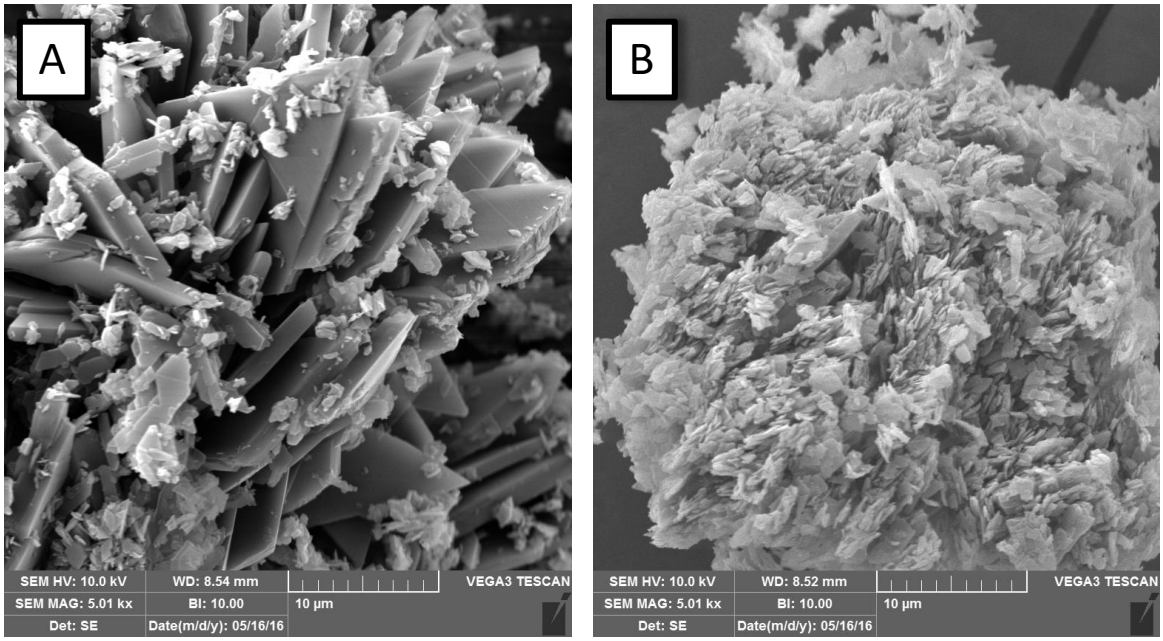

Fig. S6. SEM images of aggregates prepared by precipitation method in (A) **THF/water** and (B) **ethanol/water** mixtures. The former exhibits an irregular distribution of crystal sizes, where the larger crystals are of regular rhomboidal shape and tend to aggregate. The latter has a more uniform size distribution, with nanoparticles self-assembled in aggregates of dimension ~250 nm.

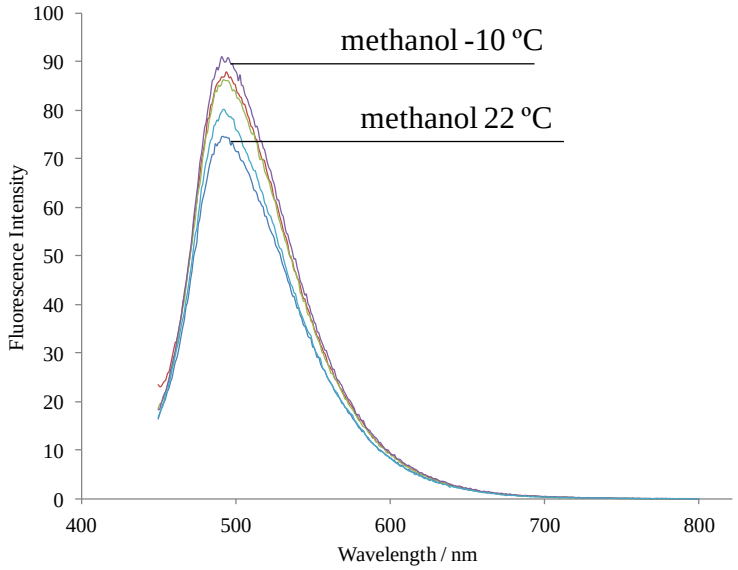

Fig. S7. Fluorescence spectra of **BIA** (c = 10 μM) in methanol at various temperatures.

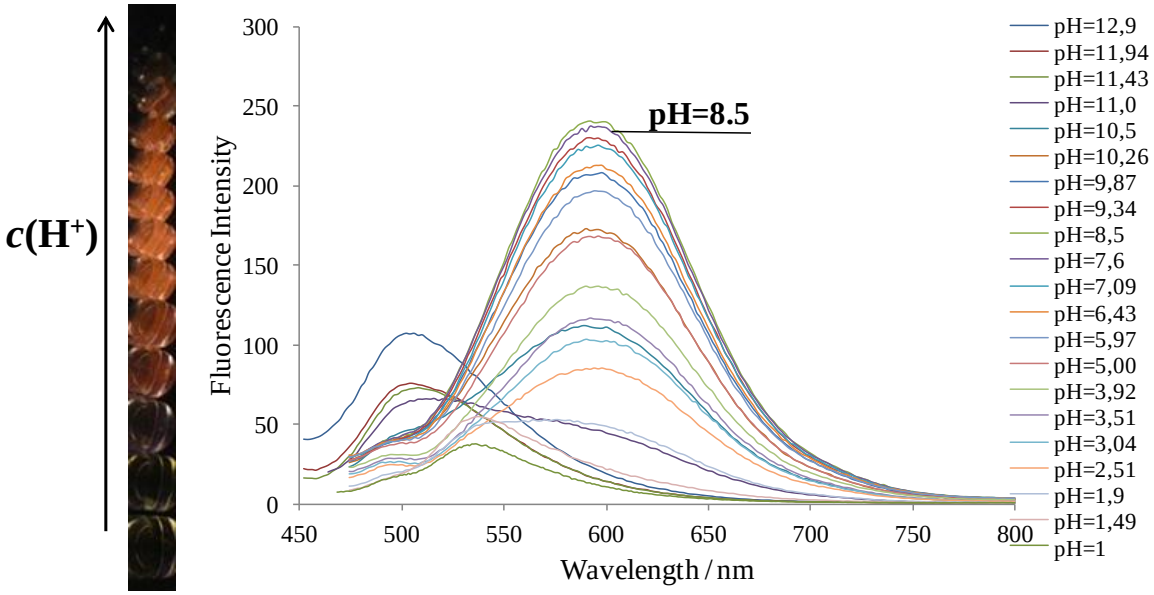

Fig. S8. Emission spectra of **BIA** upon titration, c = 10μM, λ_{exc}=425 nm.

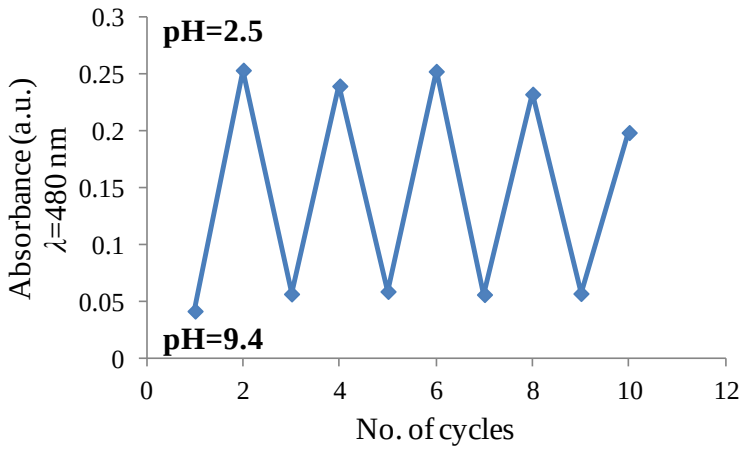

Fig. S9. Reversible switching of the absorption intensity of **BIA** by changing pH.

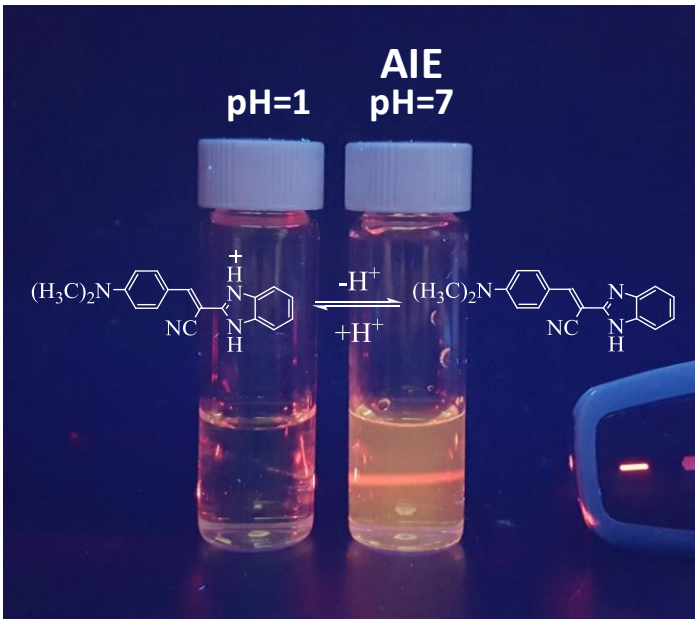

Fig. S10. Observation of the Tyndall effect on nanoaggregates; a red laser beam is directed through solutions of **BIA** in water at pH = 7 (right) and at pH = 1 (left). Nanoaggregates of **BIA** in the water cause light scattering, seen as a *red-line* through the solution. Light scattering at pH = 1 is not observed.

Computational details

All of the molecular geometries were initially optimized in the gas-phase by the efficient and accurate M06–2X/6–31+G(d,p) model. The thermal corrections were extracted from the corresponding frequency calculations without the application of scaling factors. The final single-point energies were attained with a highly flexible 6–311++G(2df,2pd) basis set using the MP2 approach giving the MP2/6–311++G(2df,2pd)//M06–2X/6–31+G(d,p) model employed here for the gas-phase free energies. To account for the solvation effects, we reoptimized geometries employing the SMD polarisable continuum model[1] at the (SMD)/M06–2X/6–31+G(d,p) level with all parameters corresponding to pure water, and calculated solvation free energies as a difference between the corresponding SMD and gas-phase calculations at the same level of theory. The choice of such a computational setup was prompted by our success in estimating both pK_a and reaction thermodynamic values in solution.[2] pK_a values were calculated in a relative fashion using $AH + B_{REF} \rightarrow A^- + B_{REF}H$ equation, and employing the following reference bases (B_{REF}): benzimidazole (pK_a = 12.75 and 5.41)[3] for the deprotonation and protonation of this fragment, respectively, and *N*,*N*-dimethylaniline (pK_a = 5.15)[3] for the protonation of the dimethylamino group. All of the calculations were performed using the Gaussian 09 software.[4]

References

1 A. V. Marenich, C. J. Cramer and D. G. Truhlar, *J. Phys. Chem. B*, 2009, **113**, 6378.

2 a) I. Picek, R. Vianello, P. Šket, J. Plavec and B. Foretić, *J. Org. Chem.*, 2015, **80**, 2165; b) D. Saftić, R. Vianello and B. Žinić, *Eur. J. Org. Chem.*, 2015, 2015, 7695.

3 W. P. Jencks and J. Regenstein, in *Handbook of Biochemistry and Molecular Biology, Fourth Edition*, CRC Press, 1976, pp. 305-351.

4 M. J. Frisch, G. W. Trucks, H. B. Schlegel, G. E. Scuseria, M. A. Robb, J. R. Cheeseman, G. Scalmani, V. Barone, B. Mennucci, G. A. Petersson, H. Nakatsuji, M. Caricato, X. Li, H. P. Hratchian, A. F. Izmaylov, J. Bloino, G. Zheng, J. L. Sonnenberg, M. Hada, M. Ehara, K. Toyota, R. Fukuda, J. Hasegawa, M. Ishida, T. Nakajima, Y. Honda, O. Kitao, H. Nakai, T. Vreven, J. A. Montgomery Jr., J. E. Peralta, F. Ogliaro, M. J. Bearpark, J. Heyd, E. N. Brothers, K. N. Kudin, V. N. Staroverov, R. Kobayashi, J. Normand, K. Raghavachari, A. P. Rendell, J. C. Burant, S. S. Iyengar, J. Tomasi, M. Cossi, N. Rega, N. J. Millam, M. Klene, J. E. Knox, J. B. Cross, V. Bakken, C. Adamo, J. Jaramillo, R. Gomperts, R. E. Stratmann, O. Yazyev, A. J. Austin, R. Cammi, C. Pomelli, J. W. Ochterski, R. L. Martin, K. Morokuma, V. G. Zakrzewski, G. A. Voth, P. Salvador, J. J. Dannenberg, S. Dapprich, A. D. Daniels, Ö. Farkas, J. B. Foresman, J. V. Ortiz, J. Cioslowski and D. J. Fox, Gaussian, Inc., Wallingford, CT, USA, 2009.

RAD 3

M. Hranjec, **E. Horak**, D. Babic, S. Plavljanin, Z. Srdovic, I. M. Steinberg, R. Vianello,N. Perin, *Fluorescent benzimidazo[1,2-*a*]quinolines: synthesis, spectroscopic and computational studies of protonation equilibria and metal ion sensitivity*, New Journal of Chemistry **41** (2017) 358-371.

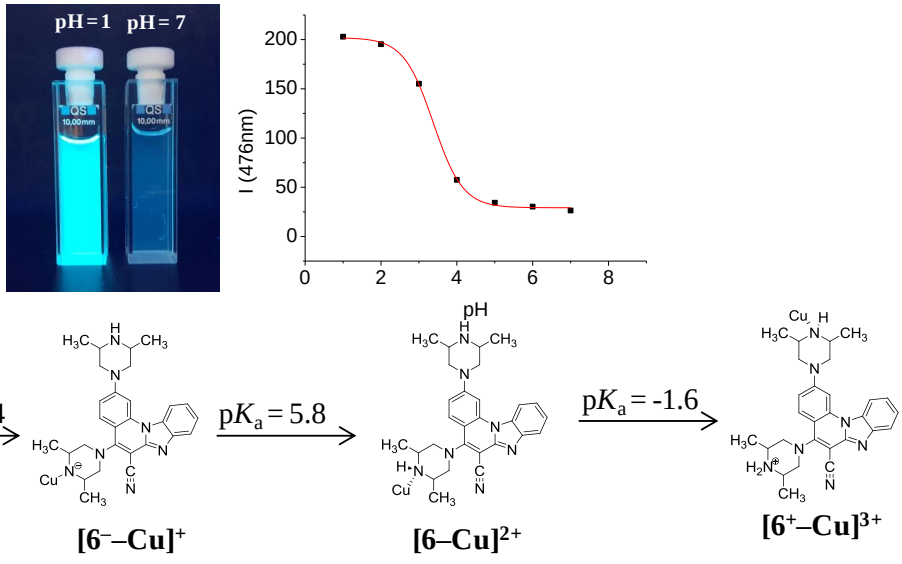

Fluorescent benzimidazo[1,2-*a*]quinolines: Synthesis, spectroscopic and computational studies of protonation equilibria and metal ion sensitivity

Marijana Hranjec,[a] Ema Horak,[b] Darko Babić,[c] Sanela Plavljanin,[a] Zrinka Srdović,[a] Ivana Murković Steinberg,[b] Robert Vianello*[d] and Nataša Perin*[a]

[a] *Department of Organic Chemistry, Faculty of Chemical Engineering and Technology, University of Zagreb, Marulićev trg 20, HR-10000 Zagreb, Croatia. E-mail: nperin@fkit.hr*
[b] *Department of General and Inorganic Chemistry, Faculty of Chemical Engineering and Technology, University of Zagreb, Marulićev trg 19, HR-10000 Zagreb, Croatia*
[c] *Group for Computational Life Sciences, Ruđer Bošković Institute, Bijenička 54, HR–10000 Zagreb, Croatia.*
[d] *Computational Organic Chemistry and Biochemistry Group, Ruđer Bošković Institute, Bijenička 54, HR–10000 Zagreb, Croatia. E-mail: robert.vianello@irb.hr*

Abstract

We describe the UV-Vis and fluorescence spectroscopic characterization of newly synthesised amino and diamino substituted benzimidazo[1,2-*a*]quinolines and their various 1:1 metal complexes together with the related computational analysis on their acid/base properties and metal binding affinities. The work was performed in order to evaluate the photophysical features of these compounds and assess their potential chemosensor activity towards pH and metal ions in several polar and non-polar organic solvents. In addition, pH titrations and titration with metal chloride salts were carried out to determine the selectivity towards Co^{2+}, Cu^{2+}, Ni^{2+} and Zn^{2+} cations and explore the potential as chemosensors and pH probes. While all systems exhibit notable but impractical differences in sensitivities and spectral responses with the used metals, computational analysis aided in identifying benzimidazo[1,2-*a*]quinolines mono- and disubstituted with the piperazine fragment as very promising and efficient pH sensors in the acidic environment, particularly in the range of

pH≈3, which is extended to pH≈6 upon the addition of metal cations. Their analytical features are significantly better than those involving the chain amino substituents, and their further development is strongly suggested.

Introduction

Optical sensors are widely used in biochemical and medicinal studies for the detection of biologically important molecules, and various cations and anions. Fluorescence spectroscopy in particular has long been viewed as a powerful tool for basic research in the biological sciences due to the notable progress made in instrumentation, and the synthesis and availability of novel fluorophores.[1–4] The selective recognition and detection of transition metal cations has become of a great interest for many scientific studies due to their significant importance in chemical, biological, biomedical or environmental processes.[5–7] Many of them are involved in the most important biological and biochemical processes, such as transmission of nerve impulses, muscle contraction and regulation of cell activity.[8] For example, Zn^{2+} is an essential trace metal element responsible for the control of many cellular and enzymatic processes in living organisms, and it is also a contributory factor in neurological disorders, such as epilepsy and Alzheimer's disease.[9–10] Also, Zn has a specific structural function that allows the formation of peptides into multiple domains, or "zinc fingers", within the coordination to amino acids like cysteine and histidine. Importantly, high levels of Zn can be cytotoxic and may cause serious problems such as skin disease, diabetes and some types of carcinoma. Co^{2+} is mainly retrieved in the corrin ring of vitamin B12, which is the original Co storage in biological systems, and is essential for the growth and metabolism of plants. In addition, Cu^{2+} is another necessary and important trace element, the third most abundant transition metal in the body and in the brain, responsible for the normal function of many tissues, like immune, nervous system and heart.[11] Ni^{2+} is a nutritionally essential trace metal in several animal species, microorganisms and plants. On the other hand, fluorescent pH probes are widely used in analytical and biomedicinal chemistry,[12] for measuring intercellular pH[13–14] or monitoring pH in blood.[15] Such probes are vital for the development of chemical sensors for biomedical diagnostics, cell biology and environmental monitoring.[16,17] In summary, optical fluorescent sensors provide high sensitivity, good selectivity, rapid

response, are widely available and support multiple modes of detection.[18] Their structure requires at least two functional sites: a recognition site where the host binds to the analyte, and a fluorophore which provides a spectroscopic signal dependent on the interaction with the analyte. Such response is mostly guided by well-known photo-physical mechanisms of electron or charge transfer.[19] The main challenge in the design and synthesis of novel fluorescent compounds for sensing applications is in providing both essential functions, recognition and signal transduction, in one molecule.

One of the most extensively studied classes of organic fluorescent sensors are those based on heterocyclic compounds,[20–21] which have excellent spectroscopic properties and are capable of selectively binding essential cations and anions. Thus, they can be employed as sensitive and selective optical sensors in a wide range of biological, environmental, and chemical processes. Besides the fact that they are widely incorporated in the structure of numerous important natural and synthetic biochemical agents, benzimidazole and especially their benzannulated derivatives, due to the possession of a highly conjugated planar chromophore, offer promising applications in optoelectronics, optical lasers, fluorescence probes, organic luminophores or fluorescent dyes in traditional textile and polymer fields.[22–23] A great variety of heterocyclic molecules have been employed for the development of optical sensors where the benzimidazole unit is one of the most important key building blocks.[24–28] Additionally, the fluorescence of cyclic benzimidazole derivatives can be significantly altered by additional substituents placed on different positions of the planar chromophore or by condensation with other heterocycles which leads to the enhancement of the conjugated aromatic surface.[29] Recently, we explored the characteristics of 2-amino-5-phenylbenzimidazo[1,2-*a*]quinoline-6-carbonitrile as a selective chemosensor for detecting versatile metal cations. Importantly, the fluorescence intensity of this compound significantly increases upon the addition of Zn^{2+}.[30]

Encouraged by the confirmed optical properties and application possibility of biologically active amino substituted benzimidazo[1,2-*a*]quinoline skeleton for a detection of various cations in solution, we set out the spectroscopic and computational characterization of several 2-amino and 2,5-diamino substituted benzimidazo[1,2-*a*]quinolines by the means of UV-Vis and fluorescence spectroscopies, density

functional theory calculations, pH titrations and UV-Vis and fluorescence titrations with several metal cations in various polar and non-polar organic solvents.

Results and discussion

Synthesis

All newly prepared compounds were synthesized according to the previously published synthetic procedures. The main procedure is shown in Scheme 1. Based on the series of undertaken experiments in order to optimize the reaction times and yields, targeted amino and diamino substituted benzimidazo[1,2-*a*]quinolines **3**–**6** were finally prepared from corresponding halogeno or dihalogeno substituted precursors **1**–**2** using uncatalyzed microwave assisted amination in low to moderate yields (28% to 33%). This reaction was performed in acetonitrile with the excess of five equivalents of the corresponding amine by using 800 W power, 170 °C and 40 bar while targeted compounds were purified by using column chromatography on silicagel.

The structures of all prepared systems were determined by the NMR analysis based on inspecting H–H coupling constants, chemical shifts and by mass spectroscopy. Generally, ^{1}H NMR spectra of all amino substituted benzimidazo[1,2-*a*]quinolines showed a downfield shift of the aromatic protons in comparison to halogeno substituted precursors **1**–**2**. Also, the appearance of protons related to amino substituents in the aliphatic part can be observed in both ^{1}H and ^{13}C NMR.

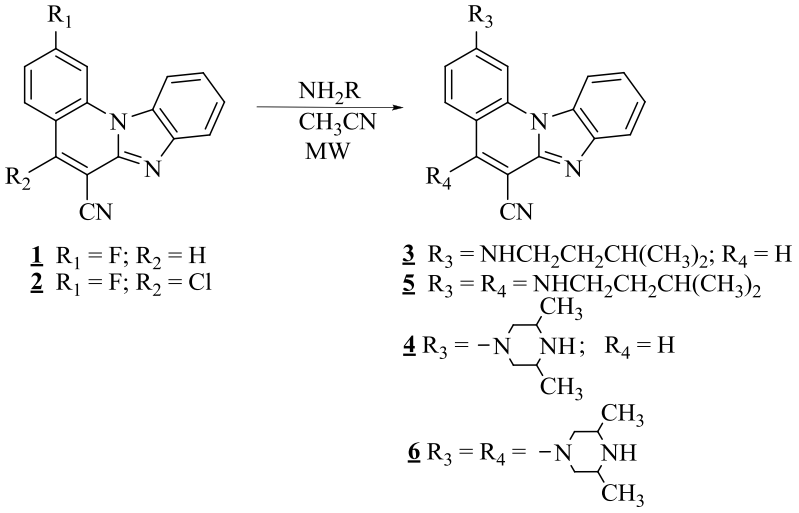

Scheme 1. Synthesis of compounds **3**–**6**.

Spectroscopic characterization

In order to study spectroscopic properties of prepared **3**–**6,** UV-Vis and fluorescence emission spectra were recorded in several organic solvents selected to ensure good solubility. To study the influence of chosen solvents on spectroscopic characteristics of tested compounds, stock solutions were prepared in two polar solvents, namely ethanol and acetonitrile and two non-polar solvents toluene and dioxane.

UV-Vis absorption spectra. UV-Vis spectra were measured in the range of 200–500 nm at the same concentration of 2×10^{-5} mol dm^{-3} at room temperature (Fig. 1). The UV-Vis absorption spectra of **3** and **4** showed two main bands at 380–440 nm while diamino substituted **5** and **6** displayed three main bands at 360–420 nm, which we assign to an n-π* electronic transition of amino substituents. Absorption bands in the region from 250–325 nm are assigned to the moderate energy transition of the tetracyclic conjugated aromatic π–system. Considering the UV-Vis spectra of **3**, measured in four mentioned solvents, the most intensive absorbance with strong hyperchromic shift and slightly batochromic shift were observed in ethanol, while in acetonitrile a significant hypochromic effect was noticed. Non-polar solvents, toluene and dioxane, also caused a significant hypochromic effect of the absorbance intensity as well as slightly hypsochromic shift of the absorbance maxima for 8 nm. The recorded spectra of **4** suggest that in non-polar solvents and ethanol this system shows the hyperchromic effect of the absorbance intensity relative to acetonitrile, and hypsochromic shift of the absorbance maxima for 5 ppm. The similar behaviour was observed for **5** since both non-polar solvents caused hyperchromic shift of absorbance intensity and bathochromic shift of absorbance maxima for around 8–10 nm. Furthermore, **6** showed the highest absorbance intensity in acetonitrile while in toluene the intensity drastically decreased.

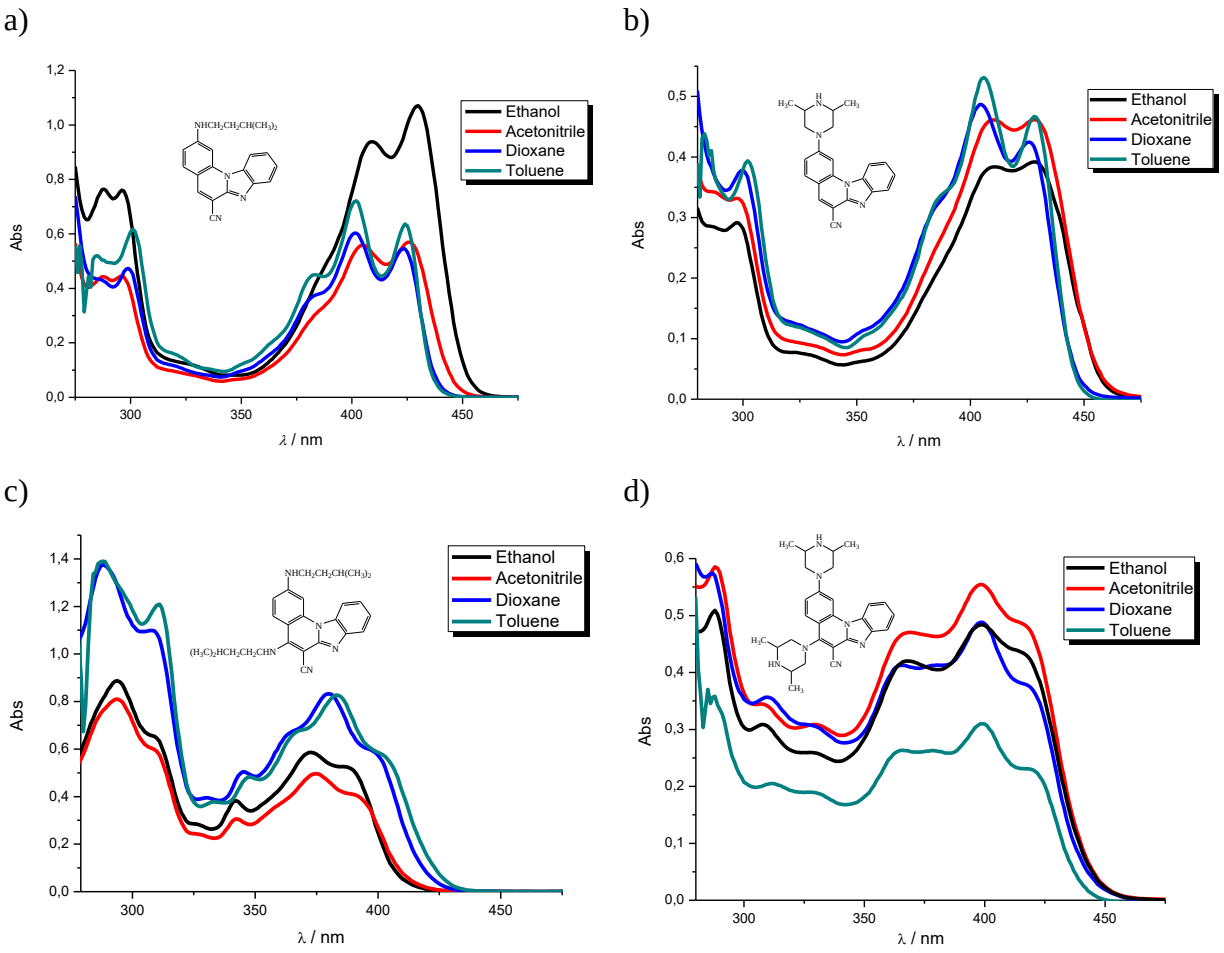

Figure 1. UV-Vis spectra recorded in ethanol, acetonitrile, dioxane and toluene at concentration of 2×10–5 mol dm–3 of 3 (a), 4 (b), 5 (c) and 6 (d).

Fluorescence emission spectra. Fluorescence emission spectra of **3**–**6** were recorded at the same concentration of 1×10^{-7} mol dm^{-3} at the room temperature (Fig. 2). Emission spectra of **3** in polar solvents showed one main emission band with slight bathochromic shift of maxima in ethanol while in toluene and dioxane it showed two main bands with maxima at 434 and 461 nm, respectively, with small bathochromic shift in dioxane at 437 and 464 nm. In addition, **3** showed a significant increase of the emission intensity in non-polar solvents. **4** also revealed very similar behaviour with a significant decrease of the emission intensity in acetonitrile. Furthermore, **5** showed one main band in all solvents with the highest emission intensity in ethanol and a bathochromic shift of maxima in dioxane and toluene for around 13 nm. **6** exhibited one main band in all solvents with the highest emission intensity in dioxane while in acetonitrile the latter drastically decreased. 2-*N*-isopentylamino substituted **3** revealed

the highest quantum yield while 2,5-diamino derivatives showed very low yields (0.04 for **5** and 0.01 for **6**). Electronic absorption and fluorescence data for **3**–**6** are summarized in Table 1, while analogous data for halogeno substituted precursors **1**–**2** are presented in Table S1 and Figures S2–S3 for comparison.

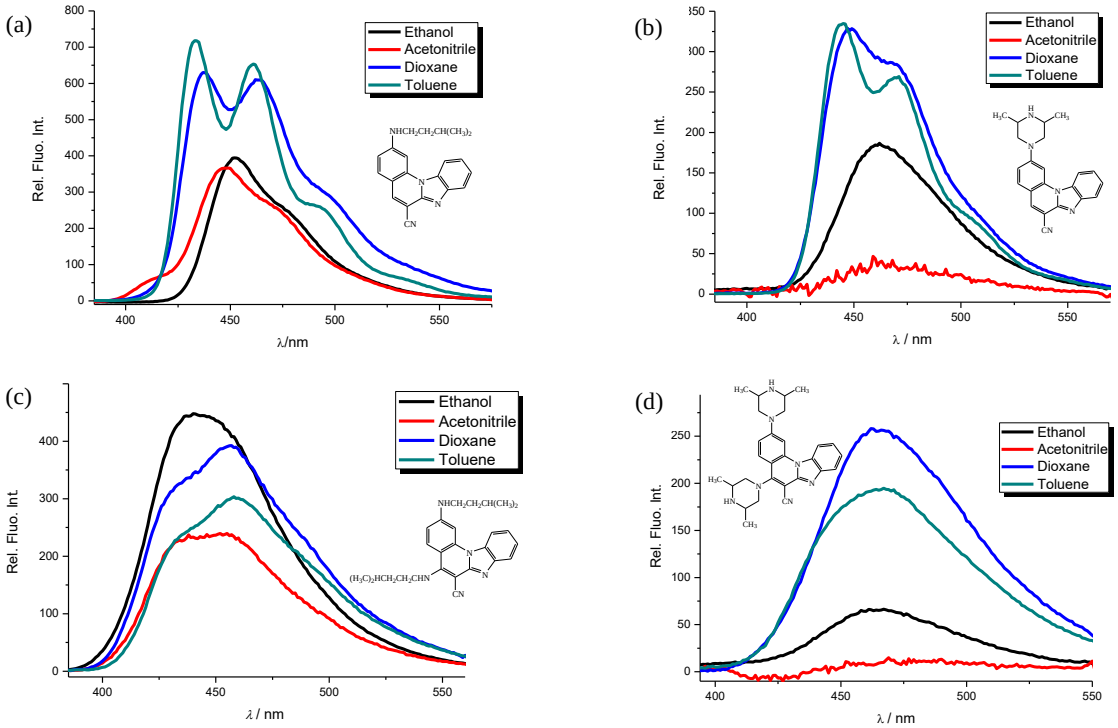

Figure 2. Fluorescence emission spectra in ethanol, acetonitrile, dioxane and toluene at concentration of 1×10^{-7} mol dm^{-3} of **3** (a), **4** (b), **5** (c) and **6** (d), $\lambda_{exc.}$=300nm.

Table 1. Electronic absorption and fluorescence emission data of studied compounds recorded at the same concentration in four organic solvents.[a,b]

Comp.	**3**				**5**				**4**				**6**			
solvent	Eth	Acn	Dxn	Tol	Eth	Acn	Dxn	Tol	Eth	Acn	Dxn	Tol	Eth	Acn	Dxn	Tol
λ_{max} (nm)	430	426	412	423	388	392	399	402	429	428	427	429	418	418	418	422
	409	403	399	401	372	374	380	382	409	410	404	405	399	397	399	400
	296	295	299	381	342	341	345	348	296	298	299	301	367	366	363	365
	287	270	274	300	294	294	308	311	272	272	267		330	331	328	
	271	250	252	283	262	263	297	287	250	250	252		307	309	310	
	248						264		232				288	289	280	
ε x 10^3 (dm^3 mol^{-1} cm^{-1})	53.2	28.3	27.3	31.7	25.9	20.2	28.9	19.6	19.6	23.1	21.0	23.2	21.3	23.9	18.8	11.4
	46.6	27.6	30.4	36.1	29.2	24.9	41.8	41.0	19.2	23.0	24.4	26.6	24.3	27.6	24.3	15.5
	37.8	22.2	23.3	22.4	19.4	14.9	24.7	24.0	14.5	16.5	18.8	19.5	21.2	23.6	20.7	13.1
	37.8	33.5	38.4	30.3	44.2	40.2	54.6	60.3	11.7	14.3	16.9		12.8	15.4	15.6	
	50.9	27.6	31.9	25.9	34.7	37.0	68.9	69.2	9.8	12.0	15.1		15.5	17.1	16.7	
	44.2						84.6		8.8				25.4	29.2	28.9	
λ_{emiss} (nm)	452	448	464	461	441	452	456	458	461	459	470	469	461	457	462	463
			437	433							449	444				
rel. fluor. int.	396	366	607	652	446	238	392	301	185	42	282	269	65	10	256	193
			624	719							328	333				
Φ	0.6760	–	–	–	0.114	–	–	–	0.0482	–	–	–	0.016	–	–	–

[a] Abbreviations Eth, Acn, Dxn and Tol correspond to ethanol, acetonitrile, dioxane and toluene, respectively. [b] The underlined wavelength values correspond to the most pronounced maximum in the visible region.

Effects of pH on spectral properties

Novel optical pH sensors and probes are usually characterized by their aqueous solution pK_a values using spectrophotometry or spectrofluorometry.[1–4] Optical evaluation of the concentrations of the acidic (HA) and basic forms (A^-) are based on the Henderson-Hasselbach equation (1):[31]

$$pH = pK_a + \log\frac{[A^-]}{[HA]}$$

Effects of pH on spectral properties of **3**–**6** were determined by spectroscopic pH titrations. Their fundamental acid-base features**,** such as absorption (λ_{abs}) and fluorescence maximum (λ_{emiss}), extinction coefficient (ε) and Stokes shifts ($\upsilon_A - \upsilon_F$) are presented in Table 2.

The potential use of **3**–**6** as pH sensing probes is based on the spectral changes caused by the protonation of the basic nitrogen atoms within the molecules. Protonation of **3** and **5** with 0.1 M HCl causes a hypsochromic (blue) shift (12 nm) of the absorption band in the visible spectrum. On the other hand, protonation of **4** and **6** results in a bathochromic (red) shift (5–9 nm) due to greater resonance effect and enhanced molecule stability. Different behaviour of these two sets of systems is significant for their application and will be rationalized using computational analysis (see later).

In general, the effect of pH is more pronounced in the fluorescence than in the absorption spectra. The binding of a proton alters and expands the π-conjugation and changes the electron-accepting nature of the aromatic moieties. Therefore, protonation can cause changes in both emission intensity and colour. It is known that the spectral properties of aminated benzimidazo[1,2-*a*]quinolines are related to charge transfer interactions.[32] As a result of protonation, the emission band of all compounds is bathochromicaly shifted (20–45 nm) whilst the fluorescence intensity considerably increases for **3**, **4** and **6**, while it decreases for **5**. The spectral responses to pH for compound **6** are shown in Fig. 3. The Stokes shifts for **3** and **4** (Table 2) do not indicate large differences in energy upon excitation (6–45 nm), whilst the diamino substituted **5** and **6** had Stokes shift of up to 75 nm, which is significant for their potential application.

Table 2. Effect of pH on the absorption and fluorescence emission properties of the studied compounds in universal buffer solutions.

Compound	λ_{abs} (nm)		ε x 10^3 ($dm^3mol^{-1}cm^{-1}$)		λ_{emiss} (nm)		Stokes shift (cm^{-1})		pK_a[c]
	acidic[a]	neutral[b]	acidic	neutral	acidic	neutral	acidic	neutral	
3	293 438	422 450	25.61 26.84	13.70 14.03	476	456	1822	292	2.91
5	238 305 343 379	294 344 375 392	21.38 18.20 10.32 9.42	21.32 11.22 14.77 14.57	461 503	460	4693	3513	3.31
4	290 425	267 284 397 416(sh)	31.00 31.03 16.20	24.10 16.90 19.45	470	453	2143	2863	2.70 7.89
6	238 283 317 359 399	298 358 394	30.70 28.10 17.70 24.60 25.80	17.50 16.60 18.70	475	461	3885	3496	3.45 9.14

*(sh) = shoulder, [a] 0,1M HCl, [b] MQ water, [c] '*apparent*' pK_a value

The typical UV-Vis spectral response of **6** at different pH values, and the corresponding titration curves are shown in Fig. 4. The relationship between the absorbance and pH is sigmoidal, so data points were fitted to a Boltzmann function:

$$A = A2 + \frac{A1 - A2}{1 + exp\left(\frac{pH - pK_{app}}{dx}\right)}$$

where *A* is the measured absorbance, *A2* is the maximum of absorbance, *A1* is the minimum of absorbance, and d*x* is the width in pH units of the most significant change in absorbance. The curve exhibits excellent adjustment (R^2 = 0.9978).

The acid-base properties are characterized by an '*apparent*' pK_a value (as opposed to a real thermodynamic pK_a, since pH titrations were not performed under strictly controlled conditions of temperature and ionic strength), and are shown in

Table 2. Unlike **3** and **5** which show p$K_{a,app}$ values of 2.91 and 2.7 respectively, **4** and **6** each show two values for p$K_{a,app}$ (2.7 and 7.9 for **4**, and 3.45 and 9.14 for **6**). This indicates that over the pH range examined, **4** and **6** exist in different pH sensitive forms, from neutral molecules to dications as shown by computations later, which are spectrally detectable.

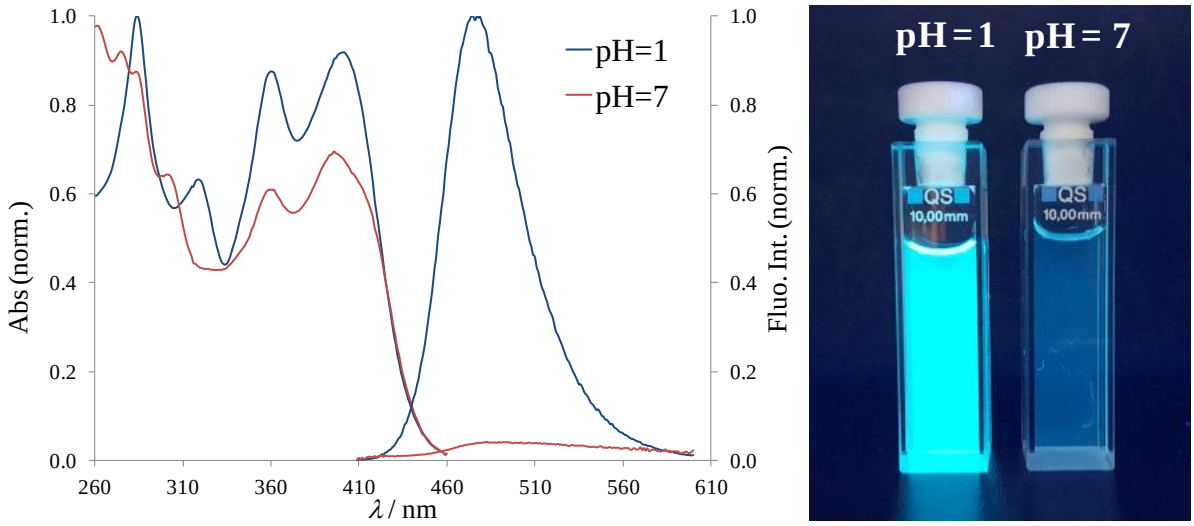

Figure 3. Typical absorption and fluorescence emission spectra of compound **6** ($\lambda_{exc.}$=397 nm) in buffer at pH = 7 and pH = 1 (bottom).

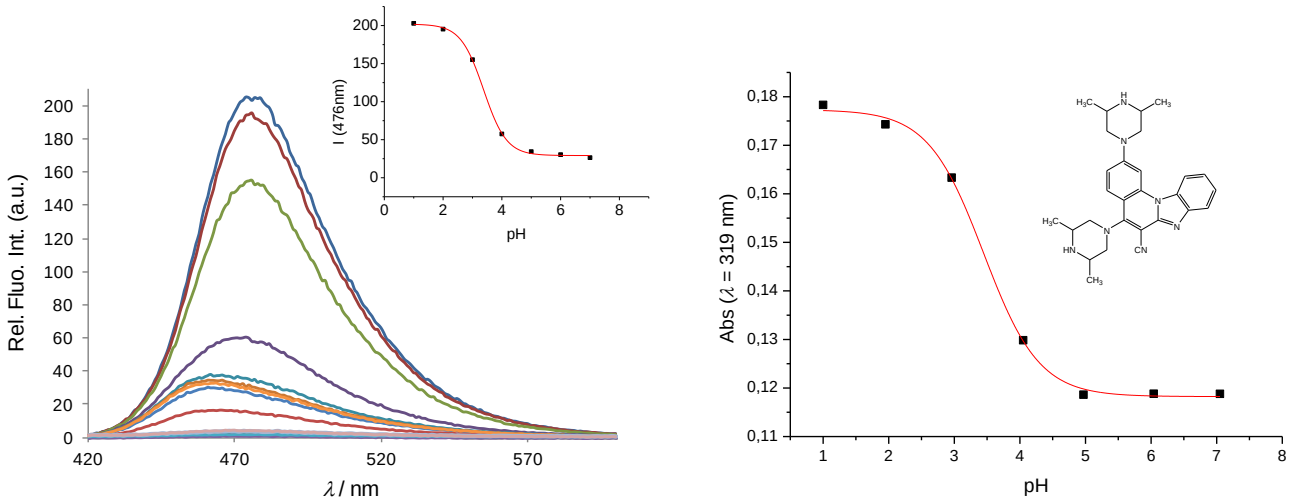

Figure 4. Fluorescence emission spectra of **6,** 2×10^{-6} mol dm^{-3} at different pH values (left) and its calibration curve (right); absorbance versus pH at 319 nm.

Titrations with metal chloride salts

In order to evaluate the chemosensing ability of studied amino and diamino substituted benzimidazo[1,2-*a*]quinolines **3**–**6** for the analytical detection of cations in aqueous solutions, their interaction with Co^{2+}, Cu^{2+}, Ni^{2+} and Zn^{2+} cations was evaluated through UV-Vis and fluorescence spectroscopies in spectrophotometric titrations. Stock solutions of compounds were prepared in ethanol, while, during the titrations, small aliquots of stock solutions were added in MQ aqua at room temperature. Preliminary UV-Vis titrations were performed at the system concentration of 2×10^{-5} mol dm^{-3} and 1.5×10^{-5} mol dm^{-3}, while metal chloride salts were added in the increasing concentrations, from 1×10^{-5} mol dm^{-3}, 2×10^{-5} mol dm^{-3}, and 5×10^{-5} mol dm^{-3} up to 1×10^{-4} mol dm^{-3}. Selected representative are presented in Fig. 5.

System **3** showed a decrease in absorbance intensity proportional to the concentration of Zn^{2+} (15% at both 422 and 449 nm) and Cu^{2+} cations (21% at 448 nm and 15% at 421 nm). We also noticed a slight (around 5 nm) bathochromic shift of both absorption maxima upon the Ni^{2+} addition. Moreover, **5** revealed a decrease in the absorbance intensity upon increasing the concentration of Zn^{2+} (21% at both 380 and 398 nm) and Ni^{2+} cations (20% at both 378 nm and 398 nm). All other tested systems showed very small or negligible changes in the absorbance intensity upon the cation addition. Our preliminary comparative fluorimetric titrations with the same metals were performed at the concentrations of 1×10^{-7} mol dm^{-3} for **3** and 5×10^{-7} mol dm^{-3} for **4**, **5** and **6**. Some selected results are presented in Fig. 6, which suggest that **3**–**6** display a consistent decrease in the fluorescence intensity with the added metal cations in concentrations from 1×10^{-7} to 1×10^{-5} mol dm^{-3}. Interestingly, Cu^{2+} and Zn^{2+} induced the largest intensity quenching in **5**, being 65% and 59%, respectively, while in **6** the effect of these two metals is significantly surpassed by the other two metals, namely Co^{2+} and Ni^{2+}, assuming 34% and 39%, in the same order (Fig.7), providing potential for different application of these two systems.

a) Compound **3** + Zn^{2+}

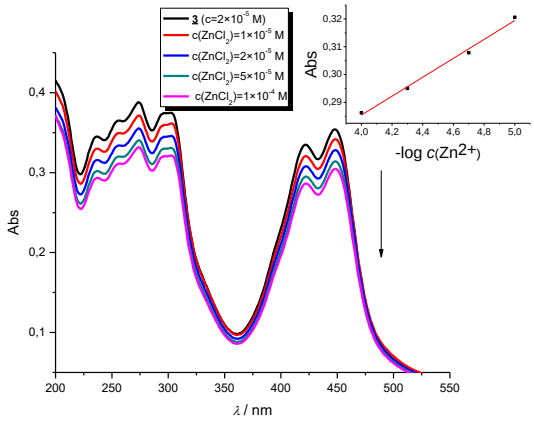

b) Compound **3** + Cu^{2+}

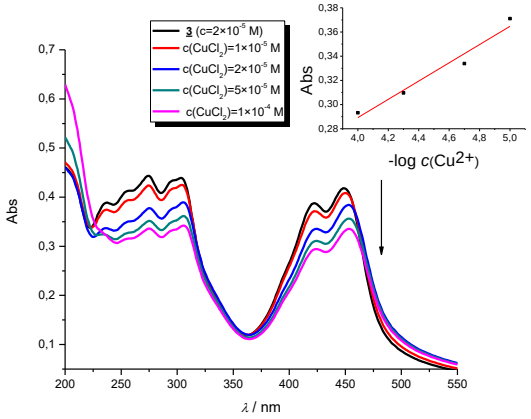

c) Compound **5** + Zn^{2+}

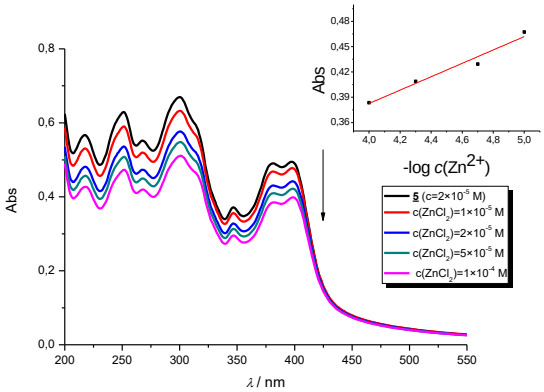

d) Compound **5** + Ni^{2+}

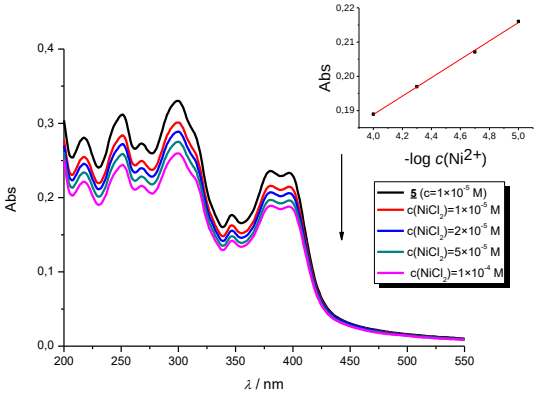

Figure 5. UV-Vis titrations of compound **3** with Zn^{2+} (a) and Cu^{2+} cations (b) and titrations of compound **5** with Zn^{2+} (c) and Ni^{2+} cations (d).

a) Compound **3** + Cu^{2+}

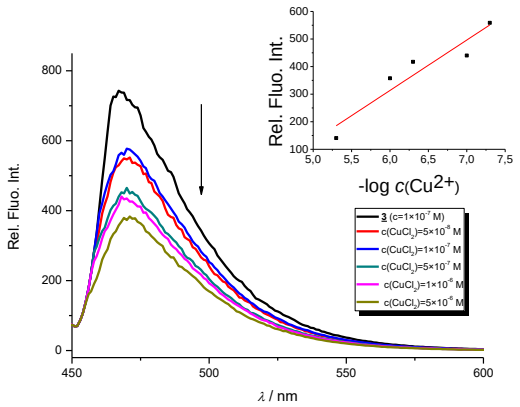

b) Compound **4** + Co^{2+}

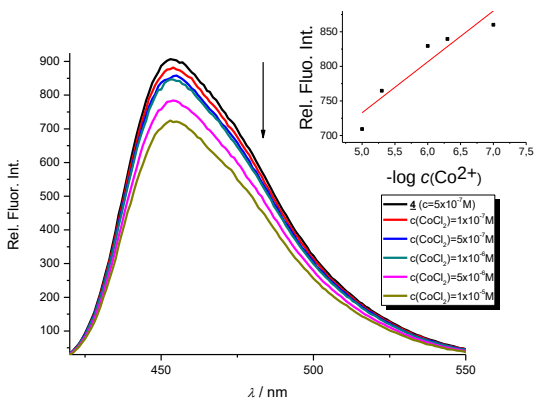

c) Compound **5** + Zn^{2+}

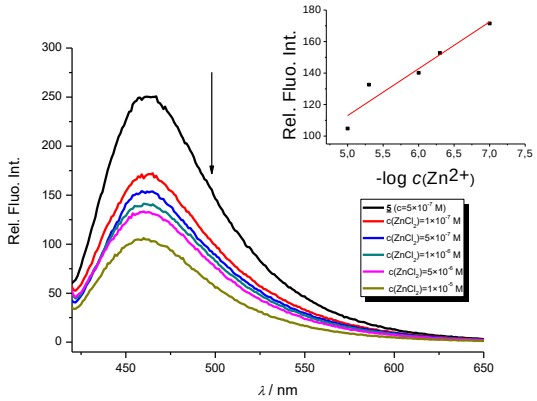

d) Compound **5** + Cu^{2+}

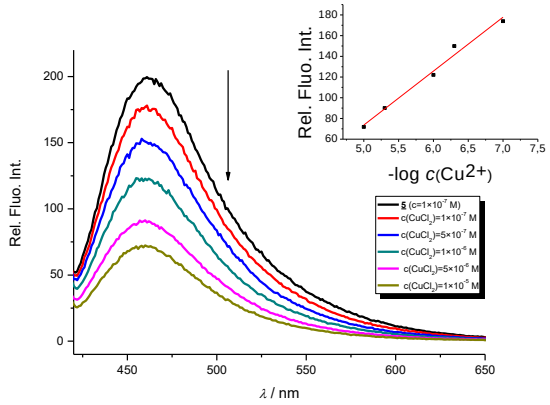

e) Compound **6** + Co^{2+}

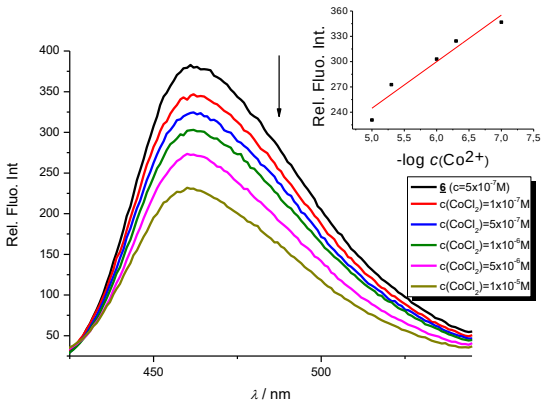

f) Compound **6** + Ni^{2+}

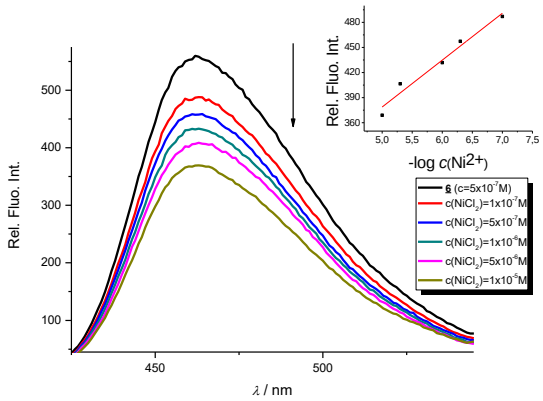

Figure 6. Fluorimetric titrations of compound **3** with Zn^{2+} (a), **4** with Co^{2+} (b), **5** with Zn^{2+} (c) and Cu^{2+} (d) and **6** with Co^{2+} (e) and Ni^{2+} cations (f).

In concluding this section, we employed the Job's continuous variation method[33] to reveal the metal binding stoichiometry of **3**–**6**. In doing so, we utilized the Cu^{2+} cation, which is selected as a representative example and to provide support for the

computational analysis presented latter. All four plots in Fig. S1 show a maximum intensity at mole fraction of Cu^{2+} of 0.5 strongly implying a 1:1 complexation.

Computational analysis

To rationalize the protonation states and the corresponding pK_a values of investigated systems, and aid in interpreting how the latter are affected by metal cations, we performed a computational analysis using the B3LYP DFT functional and implicit SMD solvation corresponding to pure water. The calculated pK_a values (Table 3) reveal that the selected computational methodology is very successful in predicting these parameters. In comparison with the six measured values, the average absolute deviation is only 0.4 pK_a units with the largest difference of 0.7 pK_a units for the first protonation of **6**, which is remarkable. This lends credence to the rest of computational data presented here.

Data in Table 3 suggest the calculated acid/base properties could classify the investigated systems into two separate groups. Namely, **3** and **5** having chain amino substituents show differences in several distinct features from those of **4** and **6** bearing cyclic piperazine amino fragments. **3** and **5** are weakly acidic. Deprotonation of **3** to $\mathbf{3}^-$ is associated with pK_a = 23.7, while **5** is slightly more acidic (pK_a = 21.1) because deprotonation occurs on the amino group next to the cyano moiety which is known to exhibit strong acidifying effect.[34]

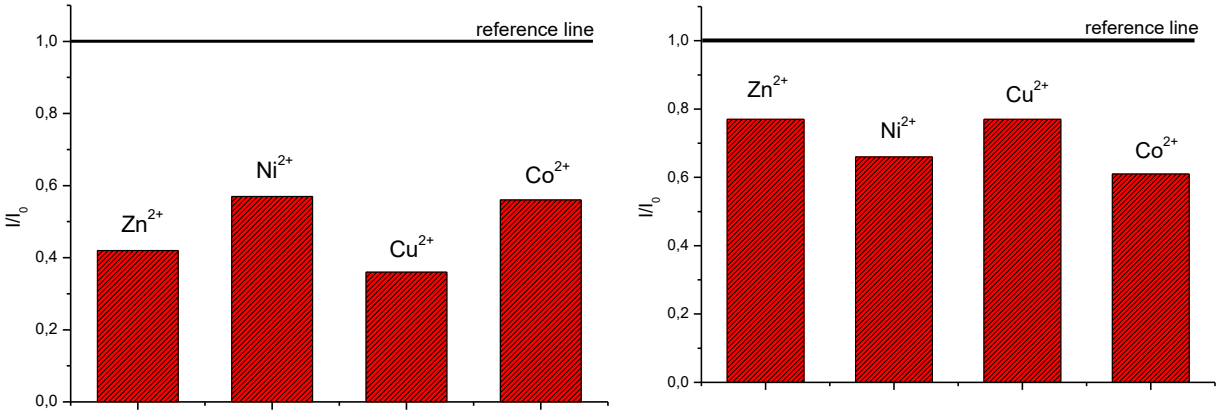

Figure 7. The selectivity of chemosensors **5** (left) and **6** (right) and towards different cations.

Still, deprotonation of **4** and **6** is much more difficult and it would require very strong bases with pK_a > 40 in water. More importantly, the first protonation of **3** and **5** occurs on the imidazole imino nitrogen with the pK_a values of 2.6 and 3.2, respectively, with **5**

being slightly more basic due to the electron donating effect of the additional neighbouring amino group that promotes basicity.[35] The former is expected knowing that benzimidazole (pK_a = 5.49) is more basic than, for example, *N*-methylaniline (pK_a = 4.85) and *N*-ethylaniline (pK_a = 5.12).[36] One also observes that the basicity of both **3** and **5** is lower than that of benzimidazole, which we attribute to the unfavourable effect of the attached cyano group. The second protonation of **3** and **5** takes place on the substituent amino group further away from the cyano moiety, pK_a values calculated as –6.0 and –1.1, respectively. This points to an important conclusion that, in water under normal conditions (pH = 7), both **3** and **5** are predominantly present as unionized neutral molecules, which will turn out to be the major and significant difference compared to **4** and **6** (see later).

The first protonation of **4** and **6** occurs on the unsubstituted piperazine nitrogen corresponding to the pK_a values of 8.1 and 9.8, respectively, the latter molecule already being appreciably basic and even surpassing the basicity of the isolated piperazine (pK_a = 9.73).[36] This leads to a conclusion that, unlike **3** and **5**, in aqueous solution systems **4** and **6** are predominantly monocations, being an important observation. Interestingly, the second protonation of **4** occurs on the imino nitrogen (pK_a = 2.1), while in **6** it takes place on the other piperazine unit (pK_a = 3.9), which is only then followed by the imino protonation (pK_a = 0.5) to yield $\mathbf{6}^{3+}$.

The calculated differences in the acid/base features of **3** and **5** on one hand, and **4** and **6** on the other, help rationalize their different spectral properties, thus being in excellent agreement with the observed spectral shifts induced by the protonation with HCl (Table 2). Namely, introducing HCl into the solution of either **3** or **5** gives monoprotonated systems, which causes hypsochromic (blue) shift of the absorption band. In contrast, for **4** and **6**, it produces diprotonated $\mathbf{4}^{2+}$ and $\mathbf{6}^{2+}$, which increases the stability of systems through the enhanced electron redistribution and cationic resonance resulting in the batochromic (red) shift. In this context, it is worth underlining the highest proton accepting abilities of **6**, for which the data in Table 3 indicate a relative ease in forming even tri- and tetra-protonated systems $\mathbf{6}^{3+}$ and $\mathbf{6}^{4+}$, with the corresponding equivalents of even moderately strong acids. This would be evident in the absorption spectra, thus suggesting **6** as the most promising framework for the efficient pH sensor in the broad range of pH values.

Table 3. Calculated aqueous solution pK_a values for each protonation state of investigated systems. Shaded protonation states indicate the dominant form at the neutral pH = 7.0.

system	protonation state	pK_a(calc)[a]	protonation reaction	structure at pH = 7
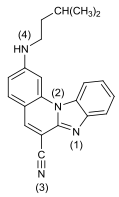	**3**$^{-}$	23.7	N4^{-} → N4–H	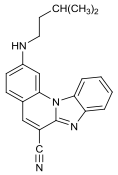
	3	2.6 [2.91]	N1 → N1–H^{+}	
	3^{+}	–6.0	N4–H → N4–H^{2+}	
	3^{2+}	–22.3	N3 → N3–H^{+}	
	3^{3+}	–38.1	N1–H^{+} → N1–H$_2$$^{2+}$	
	3^{4+}	–42.9	N2 → N2–H^{+}	
	3^{5+}			
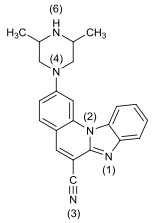	**4**$^{-}$	39.2	N6^{-} → N6–H	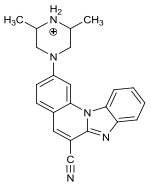
	4	8.1 [7.89]	N6–H → N6–H$_2$$^{+}$	
	4^{+}	2.1 [2.70]	N1 → N1–H^{+}	
	4^{2+}	–6.5	N4 → N4–H^{+}	
	4^{3+}	–23.1	N3 → N3–H^{+}	
	4^{4+}	–39.8	N1–H^{+} → N1–H$_2$$^{2+}$	
	4^{5+}	–69.8	N2 → N2–H^{+}	
	4^{6+}			
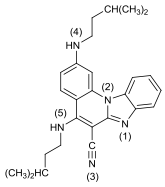	**5**$^{2-}$	28.7	N4^{-} → N4–H	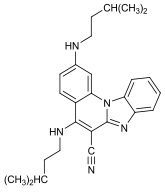
	5^{-}	21.1	N5^{-} → N5–H	
	5	3.2 [3.3]	N1 → N1–H^{+}	
	5^{+}	–1.1	N4–H → N4–H$_2$$^{+}$	
	5^{2+}	–13.4	N5–H → N5–H$_2$$^{+}$	
	5^{3+}	–26.9	N3 → N3–H^{+}	
	5^{4+}		unstable	
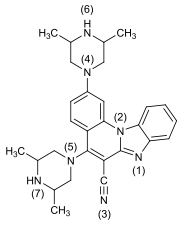	**6**$^{2-}$	40.4	N6^{-} → N6–H	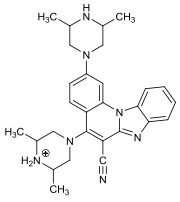
	6^{-}	38.8	N7^{-} → N7–H	
	6	9.8 [9.14]	N7–H → N7–H$_2$$^{+}$	
	6^{+}	3.9 [3.45]	N6–H → N6–H$_2$$^{+}$	
	6^{2+}	0.5	N1 → N1–H^{+}	
	6^{3+}	–3.5	N4 → N4–H^{+}	
	6^{4+}	–11.9	N5 → N5–H^{+}	
	6^{5+}	–26.7	N3 → N3–H^{+}	
	6^{6+}	–42.3	N1–H^{+} → N1–H$_2$$^{2+}$	
	6^{7+}	–71.3	N2 → N2–H^{+}	
	6^{8+}			

[a] Experimental data measured in this work are given in square brackets.

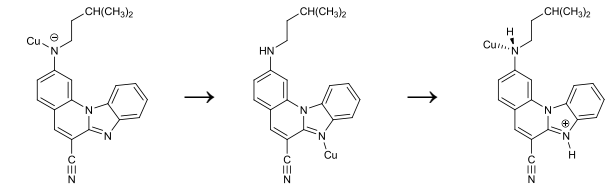

[3^{-}–Cu]$^{+}$ **[3–Cu]$^{2+}$** **[3^{+}–Cu]$^{3+}$**

pK_a 4.0 –4.7

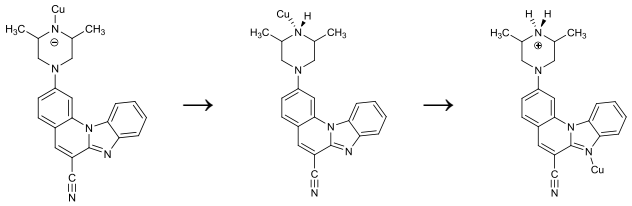

[4^{-}–Cu]$^{+}$ **[4–Cu]$^{2+}$** **[4^{+}–Cu]$^{3+}$**

pK_a 6.2 1.4

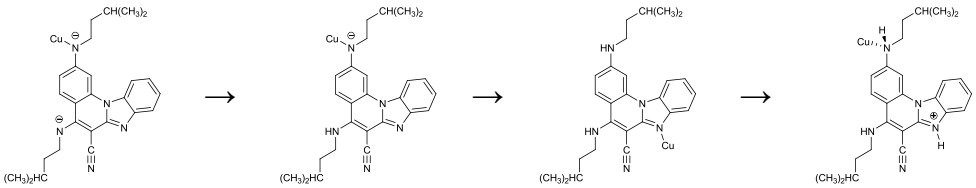

[5^{2-}–Cu] **[5^{-}–Cu]$^{+}$** **[5–Cu]$^{2+}$** **[5^{+}–Cu]$^{3+}$**

pK_a 17.7 5.3 –2.8

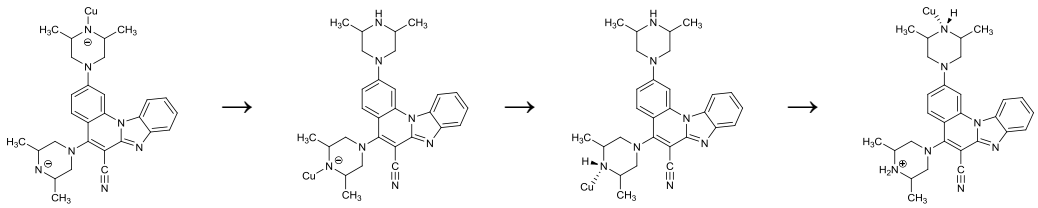

[6^{2-}–Cu] **[6^{-}–Cu]$^{+}$** **[6–Cu]$^{2+}$** **[6^{+}–Cu]$^{3+}$**

pK_a 31.4 5.8 –1.6

Figure 8. Calculated pK_a values for the investigated systems in the presence of the Cu^{2+} ions. Shaded protonation states indicate the dominant form at neutral pH = 7.0.

In order to discuss details of the excited state features of **3**–**6**, energies of the excited states responsible for the experimental UV/Vis spectra in Fig. 1 were calculated by the TD-DFT method (Figs. S4–S7). The results reveal that TD-DFT method quite well reproduced a trend within a very narrow range of the maxima of absorption, which are for **6**, taken as a representative example, calculated at 389, 388, 386 and 387 nm in toluene, dioxane, ethanol and acetonitrile, respectively (Figs. S4 and S6), being in a reasonable agreement with the measured values of 400, 399, 399 and 397 (Table 1), in the same order. This is despite the fact that calculations show only a single band in the visible region in all solvents (Fig. S4), while experiments display multiple bands in the same region (Fig. 1). Although the applied TD-DFT approach represents a state-of-the-art method for predicting electronic excitations of organic systems,[37] we assume that these inaccuracies are likely related to the recently reported problems with the low lying π–π* states of heteroaromatic molecules in TD-DFT calculations,[38] suggesting some further methodological developments are needed. As explained by Prlj and co-workers,[38] the problem is in an unbalanced description of the single and double excitations, which can, depending on the problem, result in both under- and overestimated energy differences in the first two π–π* transitions. Here, they are only overestimated with well reproduced energies of the lowest transitions. We note in passing that variations in the DFT functional and basis sets did not have significant impact on our results.

Nevertheless, on the overall, the calculated λ_{max} values show a reasonable correlativity with experimental values even when all four systems **3**–**6** in all four organic solvents are considered (Fig. S8). Differences between the lowest transition energies of **3**–**6** are in a good correlation with the shifts of their lowest bands. Experimental similarities between the spectra of monosubstituted **3** and **4**, and between disubstituted **5** and **6**, are also present in the calculated spectra (Fig. S4). On the other hand, the pronounced solvent effects of ethanol on **3** and of toluene on **6** were not found in the TD-DFT results. These effects must be due to some specific interactions with solvent molecules which are not involved at the present computational level. It can be noted that similar solvents, like acetonitrile with **3**, and dioxane with **6**, did not produce notable difference from other solvents. The spectral differences between mono- and diprotonated **6** (Figs. 3 and S5) were also well reproduced in terms of the lowest transition energies, while the agreement in relative intensities is modest.

We considered in more detail the excited states of **6**, which is a representative example among two piperazine derivatives with markedly better analytical features. The nature of the calculated excitations of **6** and its protonation forms was checked with the recently proposed φ_S descriptor.[39] For all states with the oscillator strength ≥ 0.1, φ_S values were safely above 0.4, the proposed threshold for states with significant charge transfer.[39] Only a few other states (with negligible intensities) were close to this value. At this point it is important to stress that we feel that, although we showed TD-DFT energies occasionally somewhat deviate from the exact values, the transition densities and oscillator strengths are very likely less affected and possibly well outlined here. The transition densities (obtained by subtracting the ground state from the excited state density) of all active states are dominated by π–electron contributions from the central benzimadozole-quinoline part extended by the peripheral nitrogen atoms and the cyano group (Fig. S6). The densities are approximately symmetric across the conjugation plane, which almost looks as a nodal plane, thus indicating that σ–electrons hardly participate in the lowest electronic transitions. Transition densities for the most intense transitions are not influenced much by the solvent; in almost all cases, their relative order is also the same (Fig. S6). Beside the conjugated part, photoinduced density redistribution in **6** involves, to a lesser extent, a transfer to piperazine rings. The second transition involves charge transfer from quinoline to the proximal part of the 5-piperazine, which is also active in few higher transitions, in contrast to mostly inactive 2-piperazine (apart from the linking nitrogen atom). Rydberg states were not present among the active sites. The nature of the four lowest active states is also well preserved in the neutral and two protonated species of **6** (Fig. S7), despite chemical perturbation by protonation.

Different acid/base properties of **3**–**6** are also reflected in their capabilities to bind metal cations, modelled here with the Cu^{2+} ions in a 1:1 ratio, in accordance with experiments presented earlier. The presence of Cu^{2+} significantly alters pK_a values of **3**–**6** (Fig. 8) as it favours their deprotonation so that, under normal conditions, all four systems are monoanions with Cu^{2+} bound to the most acidic site (Fig. 8). Since all **3**–**6** behave in the same way in this respect and assume the same monoanionic protonation state with $CuCl_2$, this explains why their UV-Vis spectra show considerable similarities and no clear spectroscopic distinction among molecules is obvious.

However, different behaviour is evident if one considers the strength of the interaction of the monoanionic $\mathbf{3}^-$–$\mathbf{6}^-$ with Cu^{2+}. It turns out that deprotonated

piperazine nitrogen in **4**$^{-}$ and **6**$^{-}$ forms significantly stronger interaction with Cu^{2+} than nitrogen of the chain amine fragment in **3**$^{-}$ and **5**$^{-}$ is. This is demonstrated in the calculated interaction free energies with the Cu^{2+} ion, which in **[M^{-}–Cu]$^{+}$**, where **M** = **3**–**6**, assume –46.4, –69.8, –44.5 and –70.5 kcal mol^{-1}, respectively. The second deprotonation of **[5^{-}–Cu]$^{+}$** and **[6^{-}–Cu]$^{+}$** is associated with pK_a values of 17.7 and 31.4. This implies it could occur under appreciably basic conditions, still much milder than without the Cu^{2+} ions, where it is associated with the pK_a values of 28.7 and 40.4, respectively (Table 3). This is a general trend, in which the Cu^{2+} ions increase the acidity of a particular amino centre by around 10 orders of magnitude, in accordance with our previous observations for the glutathione tripeptide and the Cd^{2+} ions.[40] Interestingly, only moderately strong acids are required (pK_a between 4–6) to revert the monoanionic **3**$^{-}$–**6**$^{-}$ to their unionized forms (Figure 8), which is worth further studies towards utilizing these systems as potential pH sensors in the presence of the metal cations and *vice versa*, since somewhat stronger acids (pK_a between 2–4) are required to change the protonation state of **3**–**6** without the metal ions (Table 3).

Conclusions

In this work novel 2-amino and 2,5-diamino substituted benzimidazo[1,2-*a*]quinolines **3**–**6** were synthesized in order to study their optical properties. UV-Vis and fluorescence spectroscopic characterizations were performed in polar and non-polar solvents as well as pH- and different metal chloride titrations in water.

The UV-Vis absorption spectra of **3**–**4** showed two main bands at 380–440 nm, while **5**–**6** displayed three main bands at 360–420 nm that can be assigned to *n*-π* electronic transitions, while bands at 250–325 nm correspond to the excitation of the aromatic π-system. **3** displayed the largest absorbance intensity in ethanol, while in other solvents significant hypsochromic effects were observed. **4** showed a hyperchromic effect in the absorbance intensity and slightly hypsochromic shift in non-polar solvents and ethanol, similarly to **5**. **6** demonstrated the highest absorbance intensity in acetonitrile and a decreased intensity in toluene.

Emission spectra suggest that, in polar solvents, all systems exhibit the fluorescence intensity quenching except **5**, which showed the highest intensity in ethanol. In addition, the fluorescence quantum yield is strongly influenced by both the position

and type of the amino substituent on the tetracyclic framework. Thus, 2-*N*-isopentylamino substituted **3** revealed the highest quantum yield while 2,5-diamino derivatives showed very low yields (0.04 for **5** and 0.01 for **6**).

Acid-base properties of **3**–**6** were examined and their pH sensing applicability evaluated. All compounds exhibited spectral changes in the pH range 1–12 and a very strong pH sensitivity of fluorescence (in the range 450–500 nm), the latter making them promising candidates for efficient pH sensors. Batochromic shift of the fluorescence emission band and a strong increase of the fluorescence intensity of **3, 4** and **6** occur on exposure to acidic solutions. It was found that **3**–**6** have a potential for the application in the acidic environment (pK_{app} in the range 2.70–3.45).

In order to determine the chemosensing ability of new systems, their interactions with Co^{2+}, Cu^{2+}, Ni^{2+} and Zn^{2+} cations were evaluated in 1:1 complexes. All compounds recognize metal cations in solution, as evidenced in the quenching of fluorescence intensity and a decrease in the UV-Vis absorbance, still without a significant practical selectivity among cations. The exception is offered by **5** and **6**, where a much higher relative intensity decrease was observed with Cu^{2+} and Zn^{2+}, and Co^{2+} and Ni^{2+} cations, respectively.

Computational analysis aided in rationalizing acid/base features of investigated molecules and their abilities to bind metal cations. The study of the pK_a values revealed that **3**–**6** could be divided in two distinct groups, which is experimentally evidenced in their different spectral properties, particularly in the shift of the absorption band in the visible spectrum. Namely, **3** and **5** having chain amino substituents are unionized under normal conditions, and upon the addition of HCl become monoprotonated at the corresponding imino centres to exhibit hypsochromic (blue) shift of the absorption band. In contrast, **4** and **6** are significantly more basic and are predominantly monocations, which become diprotonated in the same acidic media resulting in the batochromic (red) shift. The addition of Cu^{2+} favours monodeprotonation in all **3**–**6** under normal conditions, which diminishes their differences in spectral responses, however, produces systems which become more sensitive to very mild changes in the solution pH values (around pH ≈ 4–6, as opposed to pH ≈ 2–4 without the metal ions) opening the door for utilizing these systems as potential pH sensors in the presence of metal cations and *vice versa*.

Experimental section

Synthesis

General methods. All chemicals and solvents were purchased from commercial suppliers Acros, Aldrich or Fluka. Melting points were recorded on SMP11 Bibby and Büchi 535 apparatus. The ^{1}H and ^{13}C NMR spectra were recorded on a Varian Gemini 300 or Varian Gemini 600 at 300, 600, and 150 and 75 MHz, respectively. All NMR spectra were measured in DMSO-d6 solutions, while chemical shifts are reported in ppm (δ) relative to TMS as internal standard. Mass spectra were recorded on an Agilent 1200 series LC/6410 QQQ instrument. The electronic absorption spectra were recorded on Varian Cary 50 spectrometer using quartz cuvette (1 cm). All systems were routinely checked by TLC with Merck silica gel 60F-254 glass plates. Microwave-assisted synthesis was performed in a Milestone start S microwave oven using quartz cuvettes under pressure of 40 bar, power of 700 W at 180 °C. Elemental analysis for C, H and N were performed on a Perkin-Elmer 2400 analyzer. Where analyses are reported with element symbols, analytical results are within 0.4% of theoretical values.

General method for the preparation of systems. Systems **3**–**6** were prepared according to previous reports,[41] using microwave irradiation at optimized power and reaction time, from the corresponding halogeno substituted systems in acetonitrile (10 mL) with the excess of the matching amine.

2-*N*-*i*-pentylaminobenzimidazo[1,2-*a*]quinoline-6-carbonitrile 3. **3** was prepared from **1** (80 mg, 0.30 mmol) and isopentylamine (0.25 mL, 2.15 mmol) after 5 h of irradiation to yield 29 mg (29%) of yellow crystals; m.p. 200–205 °C. ^{1}H NMR (300 MHz, DMSO-d_6): □ 8.50 (d, J = 8.4 Hz, 1H, $H_{arom.}$), 8.46 (s, 1H, $H_{arom.}$), 7.94 (dd, J_1 = 1.4 Hz, J_2 = 7.8 Hz, 1H, $H_{arom.}$), 7.80 (d, J = 8.9 Hz, 1H, $H_{arom.}$), 7.74 (s, 1H, $H_{arom.}$), 7.57 (dt, J_1 = 1.0 Hz, J_2 = 7.4 Hz, 1H, $H_{arom.}$), 7.51 (dt, J_1 = 1.3 Hz, J_2 = 7.5 Hz, 1H, $H_{arom.}$), 7.31 (t, J = 5.2 Hz, 1H, NH), 6.90 (dd, J_1 = 1.7 Hz, J_2 = 8.9 Hz, 1H, $H_{arom.}$), 3.32 (q, J = 7.1 Hz, 2H, CH_2), 1.80–1.75 (m, 1H, CH), 1.57 (q, J = 6.9 Hz, 2H, CH_2), 0.98 (d, J = 6.5 Hz, 6H, CH_3) ppm; ^{13}C NMR (150 MHz, DMSO-d_6,): □ 153.8, 145.9, 144.2, 140.1, 138.1, 132.8, 130.4, 124.3, 122.3, 119.5, 116.7, 114.3, 111.2, 92.0, 40.6, 37.3, 25.2, 22.4 (2C) ppm ; elemental analysis: found C 76.93, H 5.99, N 17.08%; $C_{21}H_{20}N_4$ requires C 76.80, H 6.14, N 17.06%; MS (ESI): *m/z*= 329.3 ($[M+1]^+$).

2-[*N*-(3,5-dimethylpiperazinyl)]benzimidazo[1,2-*a*] quinoline-6-carbonitrile 4. Compound **4** was prepared from **1** (90 mg, 0.34 mmol) and 2,6-dimethylpiperazine (0.150 g, 1.30 mmol) after 6 h of irradiation to yield 39 mg (33%) of yellow powder; m.p. 263–268 °C. ^{1}H NMR (300 MHz, DMSO-d_6): □ 8.47 (s, 1H, $H_{arom.}$), 8.43 (dd, J_1 = 1.2Hz, J_2 = 7.1 Hz, 1H, $H_{arom.}$), 7.94 (dd, , J_1 = 1.4 Hz, J_2 = 7.6 Hz, 1H, $H_{arom.}$), 7.84 (d, J = 9.1 Hz, 1H, $H_{arom.}$), 7.68 (s, 1H, $H_{arom.}$), 7.58 (dt, J_1 = 1.2, J_2 = 6.6 Hz, 1H, $H_{arom.}$), 7.53 (dt, J_1 = 1.3 Hz, J_2 = 6.7 Hz, 1H, $H_{arom.}$), 7.27 (dd, J_1 = 1.7 Hz , J_2 = 9.1 Hz, 1H, $H_{arom.}$), 4.01 (d, J = 10.5 Hz, 2H, CH_2), 2.95–2,90 (m, 2H, CH), 2.55 (d, J = 11.7 Hz, 2H, CH_2), 1.13 (d, J = 6.2 Hz, 6H, CH_3) ppm ; ^{13}C NMR (75 MHz, DMSO-d_6): □ 154.2, 146.1, 144.5, 140.1, 138.5, 132.7, 130.7, 125.2, 123.3, 120.1, 116.9, 115.1, 112.9, 112.5, 97.8, 94.5, 53.6 (2C), 50.6 (2C), 19.5 (2C) ppm; elemental analysis: found C 74.40, H 6.08, N 19.52; $C_{22}H_{21}N_5$ requires C 74.34, H 5.96, N 19.70%; MS (ESI): *m/z*= 356.3 ($[M+1]^+$).

2,5-di-(*N*-*i*-pentylamino)benzimidazo[1,2-*a*]quinoline-6-carbonitrile 5. Compound **5** was prepared from **2** (200 mg, 0.72 mmol) and *i*-pentylamine (0.17 mL, 1.50 mmol) after 6 h of irradiation to yield 34 mg (28%) of white powder; m.p. 111–113 °C. ^{1}H NMR (300 MHz, DMSO-d_6): □ 8.27 (d, J = 8.2 Hz, 1H, $H_{arom.}$), 8.13 (d, J = 9.3 Hz, 1H, $H_{arom.}$), 7.68 (d, J = 7.5 Hz, 1H, $H_{arom.}$), 7.62 (s, 1H, $H_{arom.}$), 7.61 (t, J = 5.7 Hz, 1H, NH), 7.38 (t, J = 7.7Hz, 1H, $H_{arom.}$), 7.28 (t, J = 7.8 Hz, 1H, $H_{arom.}$), 6.93 (t, J = 4.6 Hz, 1H, NH), 6.78 (d, J = 9.3 Hz, 1H, $H_{arom.}$), 3.85 (q, J = 6.9 Hz, 2H, CH_2), 3.26 (q, J = 7.5 Hz, 2H, CH_2), 1.81–1.69 (m, 2H, CH), 1.66 (q, J = 7.1 Hz, 2H, CH_2), 1.55 (q, J = 6.8 Hz, 2H, CH_2), 0.97 (d, J = 5.3 Hz, 6H, CH_3), 0.94 (d, J = 5.3 Hz, 6H, CH_3) ppm; ^{13}C NMR (150 MHz, DMSO-d_6): □ 157.7, 150.9, 150.1, 145.0, 136.9, 130.8, 130.5, 125.9, 123.5, 120.9, 118.3, 117.9, 113.1, 108.1, 104.8, 96.8, 40.6, 40.1, 38.4, 37.5, 25.3, 25.2, 22.4 (4C) ppm; elemental analysis: found C 75.37, H 7.54, N 17.09; $C_{26}H_{31}N_5$ requires C 75.51, H 7.56, N 16.93%; MS (ESI): *m/z*= 414.3 ($[M+1]^+$).

2,5-di-[*N*-(3,5-dimethylpiperazinyl)]benzimidazo[1,2-*a*]quinoline-6-carbonitrile 6. Compound **6** was prepared from **2** (100 mg, 0.36 mmol) and 2,6-dimethylpiperazine (0.100 g, 0.90 mmol) after 3 h of irradiation to yield 51 mg (32%) of yellow powder; m.p. 233–236 °C. ^{1}H NMR (300 MHz, DMSO-d_6): □ 8.27 (d, J = 7.9 Hz, 1H, $H_{arom.}$), 7.86 (d, J = 9.4 Hz, 1H, $H_{arom.}$), 7.81 (d, J = 7.6 Hz, 1H, $H_{arom.}$), 7.61 (s, 1H, $H_{arom.}$), 7.47 (t, J = 7.7 Hz, 1H, $H_{arom.}$), 7.41 (t, J = 7.3 Hz, 1H, $H_{arom.}$), 7.23 (dd, J_1 = 1.4 Hz, J_2 = 9.7 Hz, 1H, $H_{arom.}$), 3.95 (d, J = 10.7 Hz, 2H, CH_2), 3.54 (d, J = 11.0 Hz, 2H, CH_2), 3.07 (m, 2H, CH), 3.00 (d, J = 11.3 Hz, 2H, CH_2), 2.89 (m, 2H,

CH), 2.46 (d, J = 9.5 Hz, 2H, CH_2), 1.11 (d, J = 6.2 Hz, 6H, CH_3), 1.05 (d, J = 6.18 Hz, 6H, CH_3) ppm; ^{13}C NMR (75 MHz, DMSO-d_6): □ □157.7, 153.6, 148.7, 145.0, 138.7, 130.6, 129.3, 124.7, 122.4, 119.3, 117.2, 114.4, 112.0, 109.6, 101.5, 98.1, 59.3 (2C), 53.6 (2C), 51.4 (2C), 50.5 (2C), 19.6 (2C), 19.2 (2C) ppm; elemental analysis: found C 71.72, H 7.15, N 21.13; $C_{28}H_{33}N_7$ requires C 71.92, H 7.11, N 20.97%; MS (ESI): *m/z*= 468.2 ($[M+1]^+$).

Spectroscopic characterization

UV-Vis absorption spectra were recorded, against the solvent, at (25±0.1) °C, using Varian Cary 50 spectrophotometer in double-beam mode. The wavelength range covered was 200–500 nm. Quartz cells of 1 cm path length were used throughout and absorbance values recorded at 0.1 nm. Fluorescence measurements were carried out on a Varian Cary Eclipse fluorescence spectrophotometer at 25 °C using 1 cm path quartz cells. Excitation maxima were determined from excitation spectra covering the range of 200–500 nm. Emission spectra were recorded from 400 to 600 nm and corrected for the effects of time- and wavelength-dependent light-source fluctuations using a standard of rhodamine 101, a diffuser provided with the fluorimeter and the instrument software. The measurements were done in ethanol, acetonitrile, toluene and dioxane (HPLC grade). Relative fluorescence quantum yields Φ were determined according to Miller using Eq. (3):

$$\Phi_x = \Phi_s \times A_s D_x n_x^2 / A_x D_s n_s^2$$

where A is the absorbance at the excitation wavelength, D is the area under the corrected emission curve, and n is the solvent refractive index. Subscripts s and x refer to standard and unknown, the former being quinine sulphate with a fluorescence quantum yield of 0.54.[28] All samples were purged with argon to displace oxygen. The quantum yield reproducibility after three independent measurements was better than 10%.

pH titrations

In order to study the effect of pH on the spectroscopic properties of **3**–**6**, UV-Vis and fluorescence emission spectra were recorded in universal buffer solutions covering pH range 2 to 12. Solutions of 0.1 M hydrochloric acid and 0.1 M sodium hydroxide were used as terminal acidic and basic points in the titration experiments with 1×10^{-5} mol dm^{-3} solutions of **3**–**6** for the absorbance and 2×10^{-6} mol dm^{-3} for the fluorescence

measurements. The excitation wavelengths were determined from the absorption spectra.

Computational details

As a good compromise between accuracy and feasibility, computational analysis was performed using the B3LYP DFT functional employing the 6–31+G(d) basis set for the carbon, nitrogen and hydrogen atoms and the Stuttgart-Dresden (SDD) effective core potentials[42] for the inner electrons of copper atoms and its associated double-ζ basis set for the outer ones. Thermal corrections were extracted from the corresponding un-scaled frequency calculations to obtain the free energies reported here. Gas-phase results were further refined with a single-point energy calculation employing a more flexible 6–311++G(2df,2pd) basis set. To account for the solvation effects, we included the SMD polarisable continuum model[43] with all parameters for pure water, giving rise to the B3LYP/6–311++G(2df,2pd)/SDD//(SMD)/B3LYP/6–31+G(d)/SDD model. The choice of this computational setup was prompted by its success in reproducing kinetic and thermodynamic parameters of various organic reactions,[44] and predicting accurate pK_a values for similar organic systems.[35,45] pK_a values were calculated in absolute fashion employing a gas-phase proton free energy of $G°(H^+)$ = 6.28 kcal mol^{-1} and experimentally determined value for the proton solvation free energy of $\Delta G_{SOLV}(H^+)$ = –265.9 kcal mol^{-1} in water,[46] to be consistent with the value used by Truhlar and co-workers[43] in parameterizing the SMD model. The latter value includes the free energy change associated with moving from a gas-phase pressure of 1 atm to a liquid-phase concentration of 1 M of –1.89 kcal mol^{-1}.

Excited state calculations were performed with the TD-DFT approach using the 6–31+G(d) basis set together with the M06 functional, which produced the best results among the four other DFT functionals tested here, namely B3LYP, CAM–B3LYP, PBE0 and ωB97XD. 32 lowest singlet electronic excitations were determined employing the IEF-PCM implicit solvation model on geometries optimized at the (SMD)/B3LYP/6–31+G(d) level. Descriptors for transition densities[39] were calculated with the program Nancy_EX 2.0,[47] while all other calculations were performed using the Gaussian 09 software.[48]

Acknowledgements

Financial support by the Croatian Science Foundation (project IP-2014-09-3386 entitled *Design and synthesis of novel nitrogen-containing heterocyclic fluorophores and fluorescent nanomaterials for pH and metal-ion sensing*) is gratefully acknowledged.

Notes and references

1 B. Wang and E. V. Anslyn, Chemosensors: *Principles, Strategies and Applications*, Wiley-VCH: Weinheim, **2011**.

2 B. Valeur, *Molecular fluorescence-principles and applications*, Wiley-VCH:Weinheim, **2002**.

3 U. S. Spichiger-Keller, *Chemical sensors and biosensors for medical and biological applications*, Wiley-VCH:Weinheim, **1998**.

4 P. A. Gale and C. Caltagirone, *Anion Sensors. In: B. Wang and E. V. Anslyn, editors. Chemosensors: Principles, Strategies and Applications*, Wiley-VCH:Weinheim, **2011**, p. 395−427.

5 Y. Jeong and J. Yoon, *Inorg. Chim. Acta*, 2012, **381**, 2−14.

6 (a) E. V. Anslyn, *J. Org. Chem.*, 2007, **72**, 687−699; (b) B. T. Nguyen and E. V. Anslyn, *Coord. Chem. Rev.*, 2006, **250**, 3118−3127.

7 (a) T. Gunnlaugsson, M. Glynn, G. M. Tocci, P. E. Kruger and F. M. Pfeffer, *Coord. Chem. Rev.*, 2006, **250**, 3094; (b) C. Caltagirone and P. A. Gale, *Chem. Soc. Rev.*, 2009, **38**, 520.

8 Y. Yang, Q. Zhao, W. Feng and F. Li, *Chem. Rev.*, 2013, **113**, 192−270.

9 (a) D. W. Choi and J. Y. Koh, *Annu. Rev. Neurosc.*, 1998, **21**, 347−375; (b) Z. Xu, J. Yoon and D. R. Spring, *Chem. Soc. Rev.*, 2010, **39**, 1996−2006.

10 (a) A. Ajayaghosh, P. Carol and S. Sreejith, *J. Am. Chem. Soc.*, 2005, **127**, 14962−14963; (b) A. E. Lee, M. R. Grace, A. G. Meyer and K. L. Tuck, *Tetrahedron Lett.*, 2010, **51**, 1161−1165.

11 R. A. Lovstad, *BioMetals*, 2004, **17**, 111−113.

12 D. Wencel, T. Abel and C. McDonagh, *Anal. Chem.*, 2014, **86**, 1529.

13 J. Han and K. Burgess K., *Chem. Rev.*, 2009, **110**, 2709−2728.

14 R. Wang, C. Yu, F. Yu and L. Chen, *Trends. Anal. Chem.*, 2010, **29**, 1004−1013.

15 M. I. Stich, L. H. Fischer and O. S. Wolfbeis, *Chem. Soc. Rev.*, 2010, **39**, 3102−3114.

16 W. Shi, X. Li and H. Ma, *Methods Appl. Fluoresc.*, 2014, **2**, 4.

17 M. Schaferling, *Angew. Chem. Int. Ed.*, 2012, **51**, 3532−3554.

18 B. Valeur and I. Leray, *Coord. Chem. Rev.*, 2000, **205**, 3−40.

19 A. P. de Silva, H. Q. N. Gunaratne, T. Gunnlaugsson, A. J. M. Huxley, C. P. McCoy, J. T. Rademacher and T. E. Rice, *Chem. Rev.*, 1997, **97**, 1515−1566.

20 N. Dash, A. Malakar, M. Kumar, B. B. Mandal and G. Krishnamoorthy, *Sen. Actuators B*, 2014, **202**, 1154–1163.

21 Y. Q. Ge, J. Jia, H. Yang, X. T. Tao and J. W. Wang, *Dyes Pigm.*, 2011, **88**, 344–349.

22 R. M. F. Batista, R. C. M. Ferreira, M. M. M. Raposo and S. P. G. Costa, *Tetrahedron*, 2012, **68**, 7322–7330.

23 M. Hranjec, G. Pavlović, M. Marjanović, M. Kralj and G. Karminski-Zamola, *Eur. J. Med. Chem.*, 2010, **45**, 2405–2417.

24 D. Y. Kim and H. J. Kim, *Sens. Actuators B*, 2015, **206**, 508.

25 A. Kumar, M. Chhatwal and T. Gupta, *Tetrahedron Lett.*, 2012, **53**, 5691–5694.

26 S. H. Mashraqui, S. Sundaram and T. Khan, *Chem. Lett.*, 2006, **35**, 786–787.

27 A. Mishra, S. Chaterjee and G. Krishnamoorthy, *J. Photochem. Photobiol. A*, 2013, **260**, 50–58.

28 (a) M. Yu, H. Lin, G. Zhao and H. Lin, *J. Mol. Recogn.*, 2007, **20**, 69–73; (b) F. A. S. Chipem, S. K. Behera and G. Krishnamoorthy, *Sensor. Actuat. B*, 2014, **191**, 727–733.

29 N. Perin, M. Hranjec, G. Pavlović and G. Karminski-Zamola, *Dyes. Pigm.*, 2011, **91**, 79–88.

30 M. Hranjec, E. Horak, M. Tireli, G. Pavlović and G. Karminski-Zamola, *Dyes. Pigm.*, 2012, **95**, 644–656.

31 A. P. Demchenko, *Anal. Bioanal. Chem.*, 2009, **395**, 1195.

32 A. P. de Silva, H. Q. Nimal Gunaratne, T. Gunnlaugsson, A. J. M. Huxley, C. P. McCoy, J. T. Rademacher and T. E. Rice, *Chem. Rev.*, 1997, **97**, 1515–1566.

33 (a) P. Job, *Ann. Chim.*, 1928, **9**, 113–203; (b) J. S. Renny, L. L. Tomasevich, E. H. Tallmadge and D. B. Collum, *Angew. Chem. Int. Ed.*, 2013, **52**, 11998–12013.

34 (a) R. Vianello and Z. B. Maksić, *J. Org. Chem.*, 2010, **75**, 7670–7681; (b) R. Vianello and Z. B. Maksić, *New J. Chem.*, 2009, **33**, 739–748; (c) R. Vianello and Z. B. Maksić, *New J. Chem.*, 2008, **32**, 413–427.

35 I. Despotović and R. Vianello, *Chem. Commun.*, 2014, **50**, 10941–10944.

36 D. D. Perrin, B. Dempsey and E. P. Serjeant, *pKa Prediction for Organic Acids and Bases*. Chapman and Hall:London, **1981**.

37 L. González, D. Escudero, and L. Serrano-Andrés, *ChemPhysChem*, 2012, **13**, 28–51.

38 A. Prlj, M. E. Sandoval-Salinas, D. Casanova, D. Jacquemin, and C. Corminboeuf, *J. Chem. Theory Comput.*, 2016, **12**, 2652–2660.

39 (a) T. Etienne, X. Assfeld, and A. Monari, *J. Chem. Theory Comput.*, 2014, **10**, 3896–3905; (b) T. Etienne, X. Assfeld, and A. Monari, *J. Chem. Theory Comput.*, 2014, **10**, 3906–3914; (c) T. Etienne, *J. Chem. Theory Comput.*, 2015, **11**, 1692–1699.

40 M. Glušič, J. Stare, J. Grdadolnik and R. Vianello, *J. Inorg. Biochem.*, 2013, **119**, 90–94.

41 N. Perin, R. Nhili, K. Ester, W. Laine, G. Karminski-Zamola, M. Kralj, M. H. David-Cordonnier and M. Hranjec, *Eur. J. Med. Chem.*, 2014, **80**, 218–227.

42 D. Andrae, U. Häussermann, M. Dolg, H. Stoll and H. Preuss, *Theor. Chim. Acta*, 1990, **77**, 123-141.

43 A. V. Marenich, C. J. Cramer and D. G. Truhlar, *J. Phys. Chem. B*, 2009, **113**, 6378–6396.

44 (a) D. Saftić, R. Vianello and B. Žinić, *Eur. J. Org. Chem.*, 2015, **35**, 7695–7704; (b) I. Picek, R. Vianello, P. Šket, J. Plavec and B. Foretić, *J. Org. Chem.*, 2015, **80**, 2165–2173.

45 (a) M. P. Coles, P. J. Aragón-Sáez, S. H. Oakley, P. B. Hitchcock, M. G. Davidson, Z. B. Maksić, R. Vianello, I. Leito, I. Kaljurand and D. C. Apperley, *J. Am. Chem. Soc.*, 2009, **131**, 16858–16868; (b) R. J. Schwamm, R. Vianello, A. Maršavelski, M. Á. García, R. M. Claramunt, I. Alkorta, J. Saame, I. Leito, C. M. Fitchett, A. J. Edwards and M. P. Coles, *J. Org. Chem.*, 2016, **81**, 7612–7625.

46 M. D. Tissandier, K. A. Cowen, W. Y. Feng, E. Gundlach, M. H. Cohen, A. D. Earhart, J. V. Coe and T. R. Tuttle, *J. Phys. Chem. A*, 1998, **102**, 7787−7794.

47 Nancy_EX-2.0 is a free post-processing tool for the analysis of the density and character of electronic excited states; https://sourceforge.net/projects/nancyex/ (accessed Oct 15, 2016).

48 Gaussian 09, Revision A.02, M. J. Frisch, G. W. Trucks, H. B. Schlegel, G. E. Scuseria, M. A. Robb, J. R. Cheeseman, G. Scalmani, V. Barone, B. Mennucci, G. A. Petersson, H. Nakatsuji, M. Caricato, X. Li, H. P. Hratchian, A. F. Izmaylov, J. Bloino, G. Zheng, J. L. Sonnenberg, M. Hada, M. Ehara, K. Toyota, R. Fukuda, J. Hasegawa, M. Ishida, T. Nakajima, Y. Honda, O. Kitao, H. Nakai, T. Vreven, J. A.

Montgomery, Jr., J. E. Peralta, F. Ogliaro, M. Bearpark, J. J. Heyd, E. Brothers, K. N. Kudin, V. N. Staroverov, R. Kobayashi, J. Normand, K. Raghavachari, A. Rendell, J. C. Burant, S. S. Iyengar, J. Tomasi, M. Cossi, N. Rega, J. M. Millam, M. Klene, J. E. Knox, J. B. Cross, V. Bakken, C. Adamo, J. Jaramillo, R. Gomperts, R. E. Stratmann, O. Yazyev, A. J. Austin, R. Cammi, C. Pomelli, J. W. Ochterski, R. L. Martin, K. Morokuma, V. G. Zakrzewski, G. A. Voth, P. Salvador, J. J. Dannenberg, S. Dapprich, A. D. Daniels, Ö. Farkas, J. B. Foresman, J. V. Ortiz, J. Cioslowski, and D. J. Fox, Gaussian, Inc., Wallingford CT, 2009.

Supplementary Information

CONTENTS

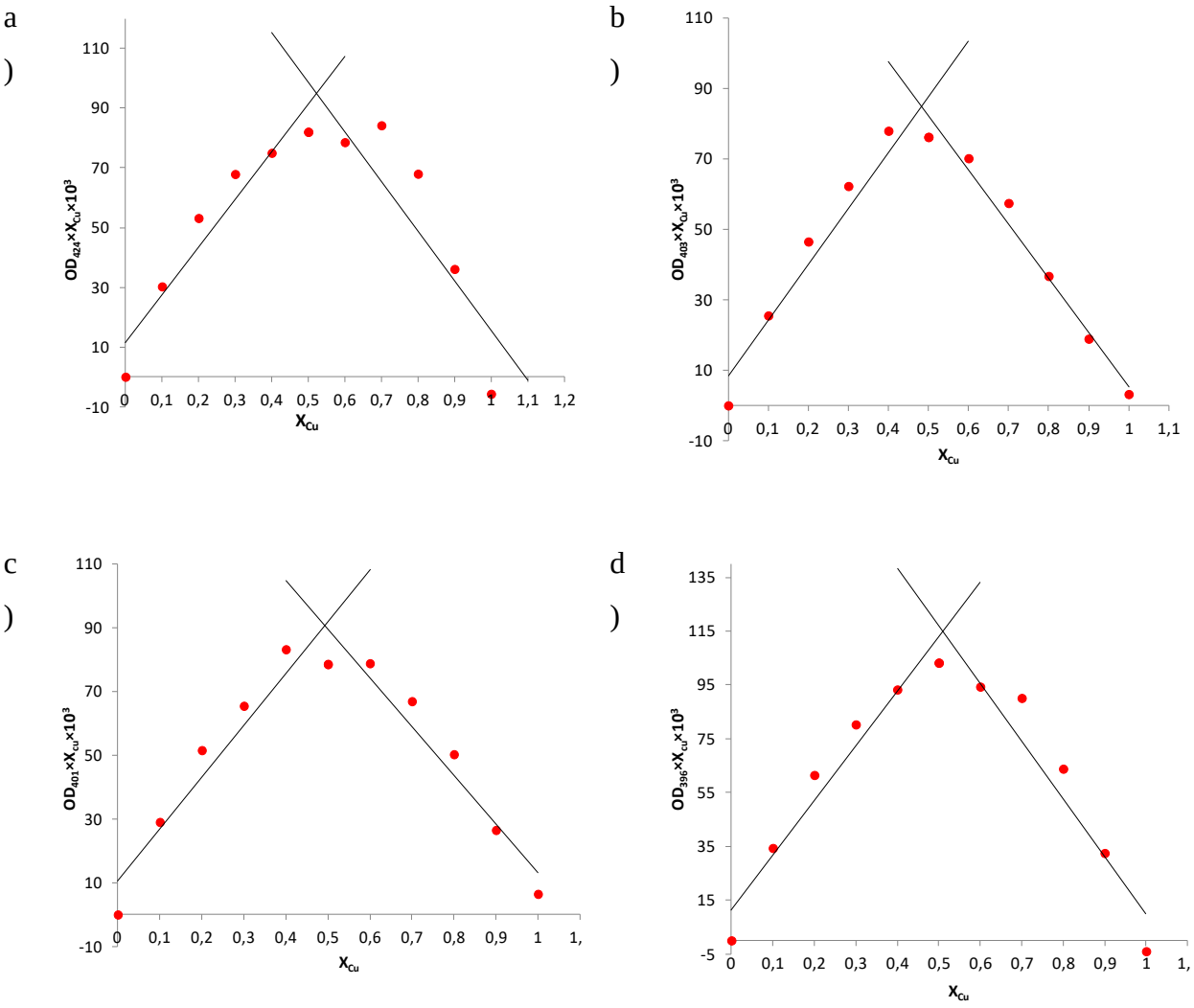

Figure S1. Job's plot for the determination of the stoichiometry of **3** (a), **4** (b), **5** (c) and **6** (d) with the Cu^{2+} ions in the complex. The total concentration of compounds **3**–**6** and Cu^{2+} is 2×10^{-5} mol dm^{-3}.

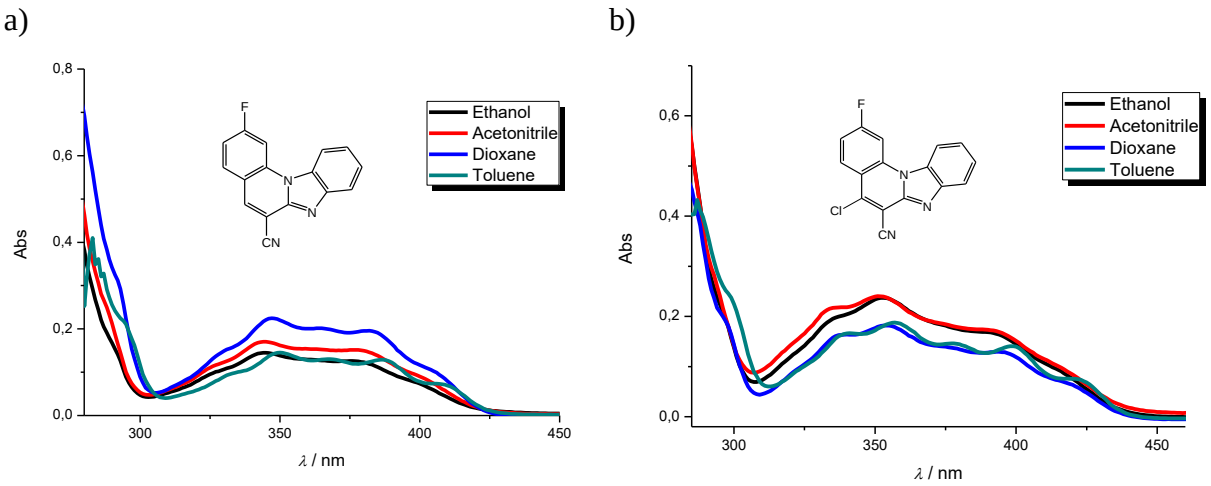

Figure S2. UV-Vis spectra recorded in ethanol, acetonitrile, dioxane and toluene at concentration of 2×10^{-5} mol dm^{-3} of **1** (a) and **2** (b).

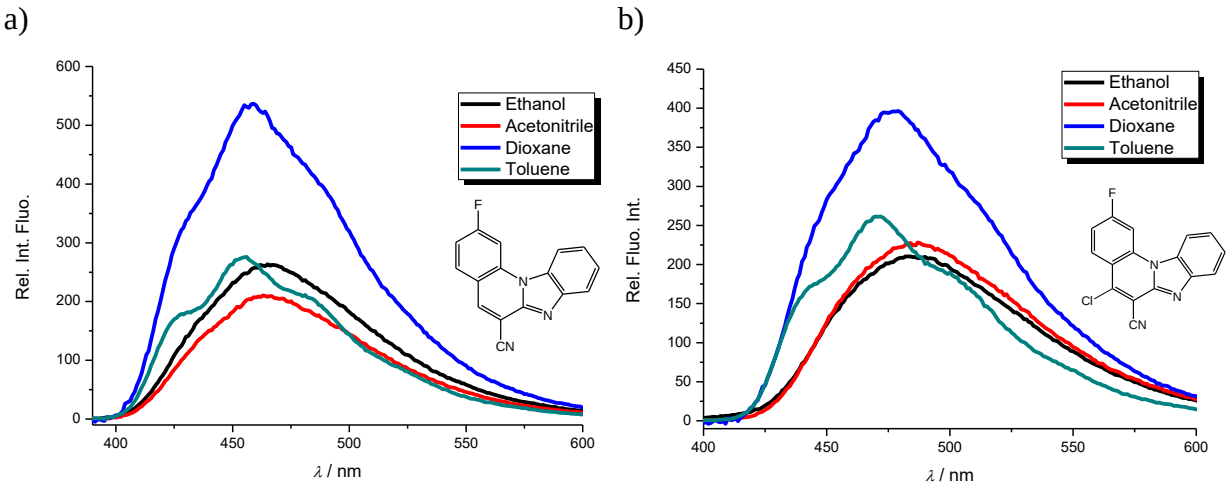

Figure S3. Fluorescence emission spectra in ethanol, acetonitrile, dioxane and toluene at concentration of 1×10^{-7} mol dm^{-3} of **1** (a) and **2** (b).

Table S1. Electronic absorption and fluorescence emission data of parent compounds **1** and **2** recorded at the same concentration in four organic solvents.

compound	**1**				**2**			
solvent[a]	Eth	Acn	Dxn	Tol	Eth	Acn	Dxn	Tol
λ_{max} (nm)	378	379	383	408	390	390	396	423
	343	344	346	387	352	352	353	399
	271	267	270	349	334	334	335	378
	260	259	261		269	272	273	357
	246	244	251		262	263	263	335
					248	248	252	
ε x 10^3 (dm^3 mol^{-1} cm^{-1})	6.2	7.5	9.7	3.5	8.6	8.6	6.3	3.6
	7.2	8.4	11.1	6.4	11.9	11.9	8.9	7.3
	26.3	33.3	44.2	7.3	9.7	10.9	8.2	7.4
	25.3	31.8	43.2		36.2	36.5	27.5	9.2
	24.4	31.1	43.3		36.8	35.7	27.2	8.2
					39.6	39.6	32.6	
λ_{emiss} (nm)[b]	465	464	458	429	486	486	476	443
				<u>454</u>				<u>470</u>
				483				501
relative fluorescence intensity	265	208	538	179	210	225	397	173
				275				262
				206				186
Φ	0.3361	-	-	-	0.2250	-	-	-

[a] Abbreviations Eth, Acn, Dxn and Tol correspond to ethanol, acetonitrile, dioxane and toluene, respectively.

[b] The underlined wavelength values correspond to the most pronounced maximum in the visible region.

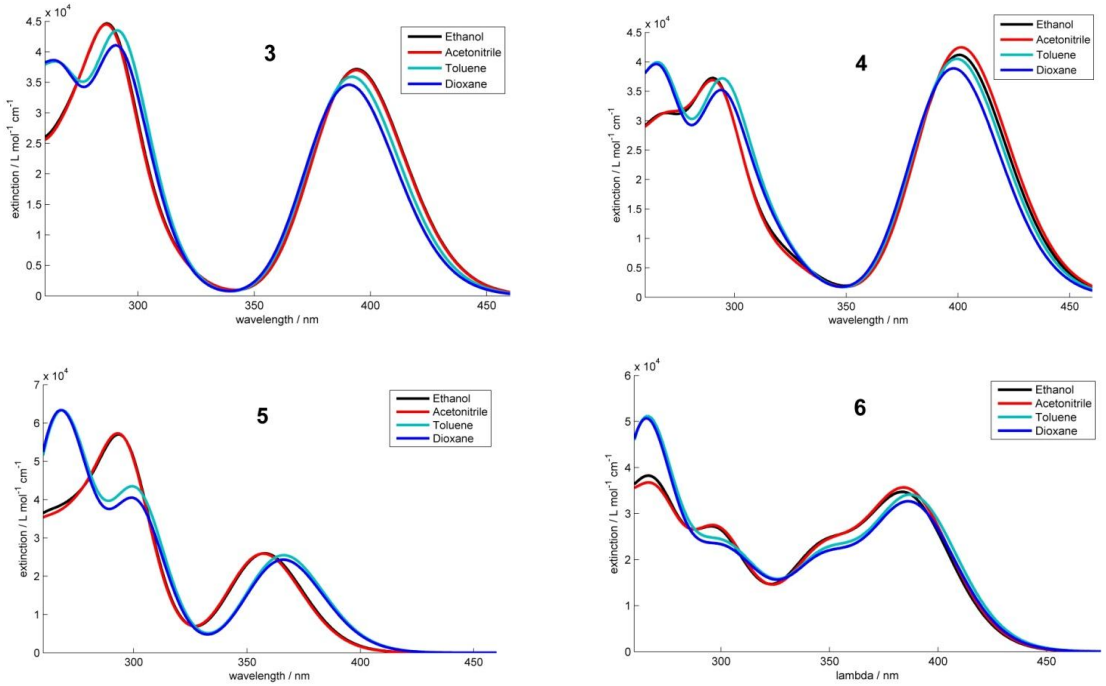

Figure S4. TD-DFT calculated UV/Vis spectra of molecules **3**–**6** in various solvents obtained at the (IEF–PCM)/M06/6–31+G(d) level of theory.

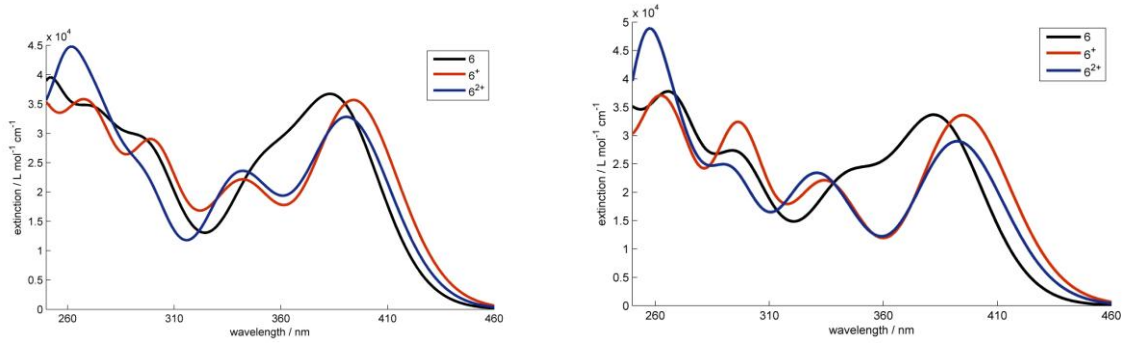

Figure S5. TD-DFT calculated UV/Vis spectra of **6** and its monoprotonated ($\mathbf{6}^{+}$) and diprotonated ($\mathbf{6}^{2+}$) derivatives in water obtained at the (IEF–PCM)/M06/6–311++G(2d,2p) (top) and (IEF–PCM)/M06/6–31+G(d) (bottom) levels of theory.

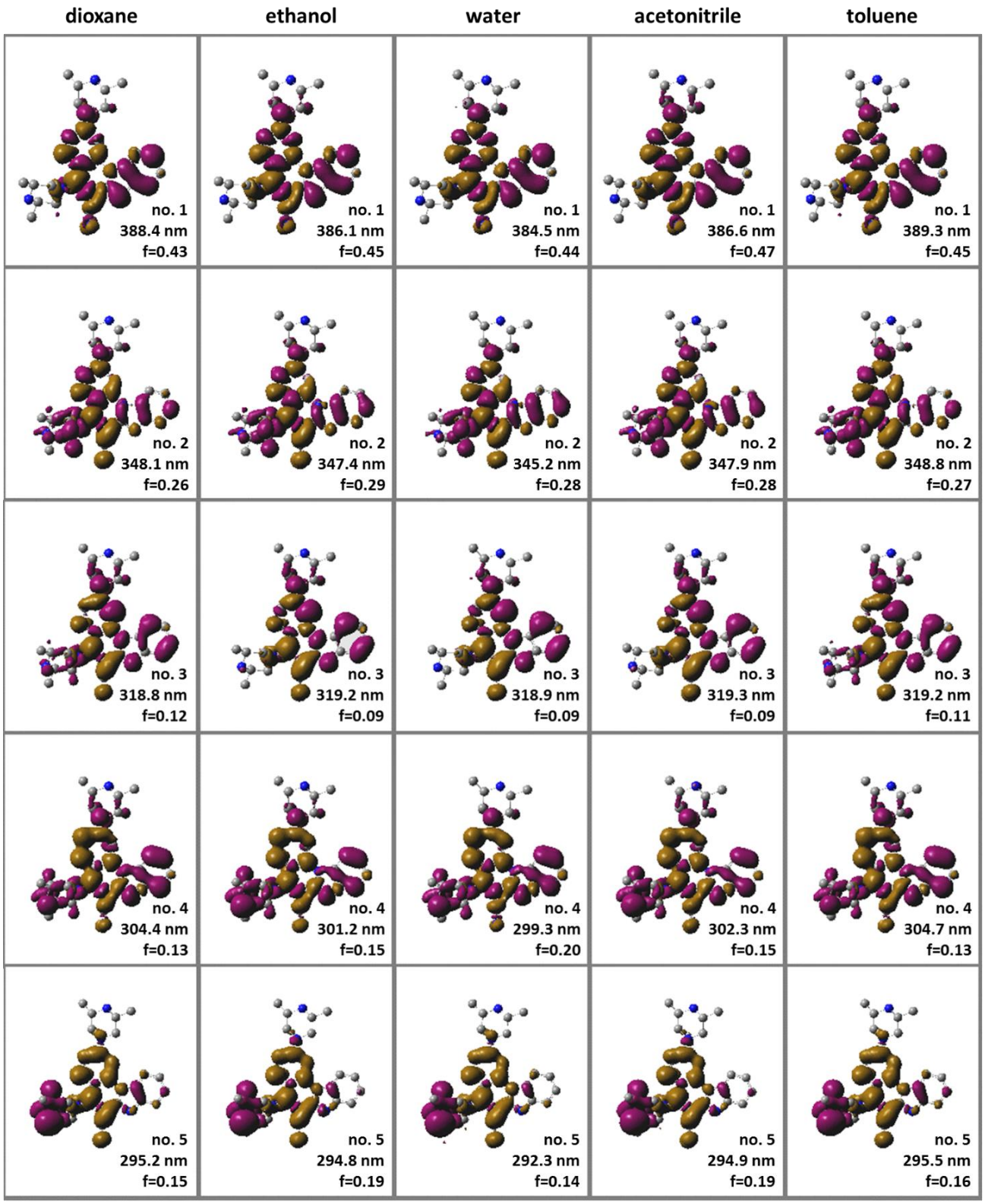

Figure continues on the next page

Continued from the previous page

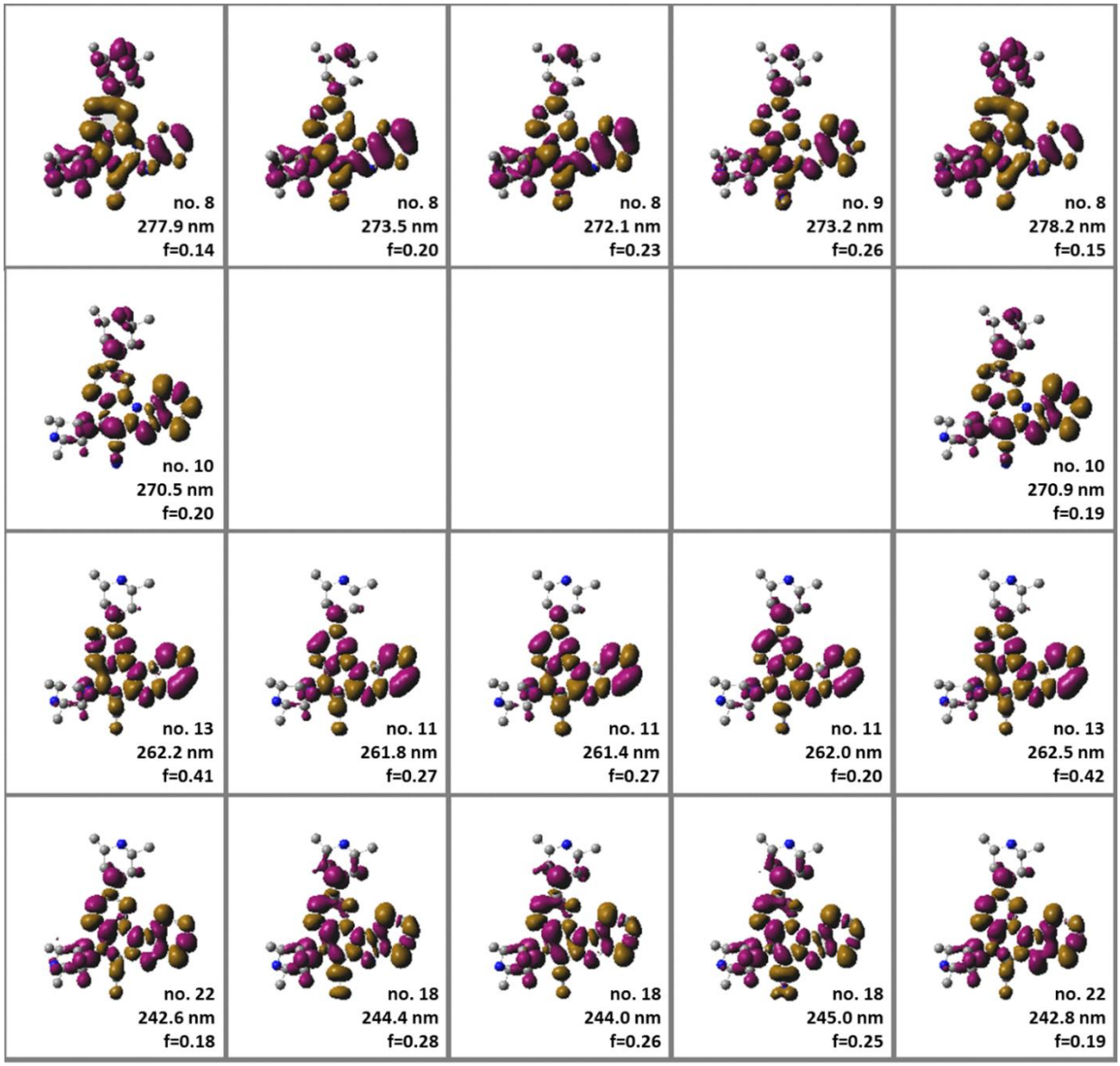

Figure S6. Transition densities of the lowest active excited states of **6**, calculated for various solvents. Electron enriched regions are coloured in purple, and those depleted in charge in drab. Excitation wavelength (in nm) is written below the ordinal number of the excited state, while *f* denotes the oscillator strength. The excited states are calculated by the TD-DFT method at the (IEF–PCM)/M06/6–31+G(d) level of theory.

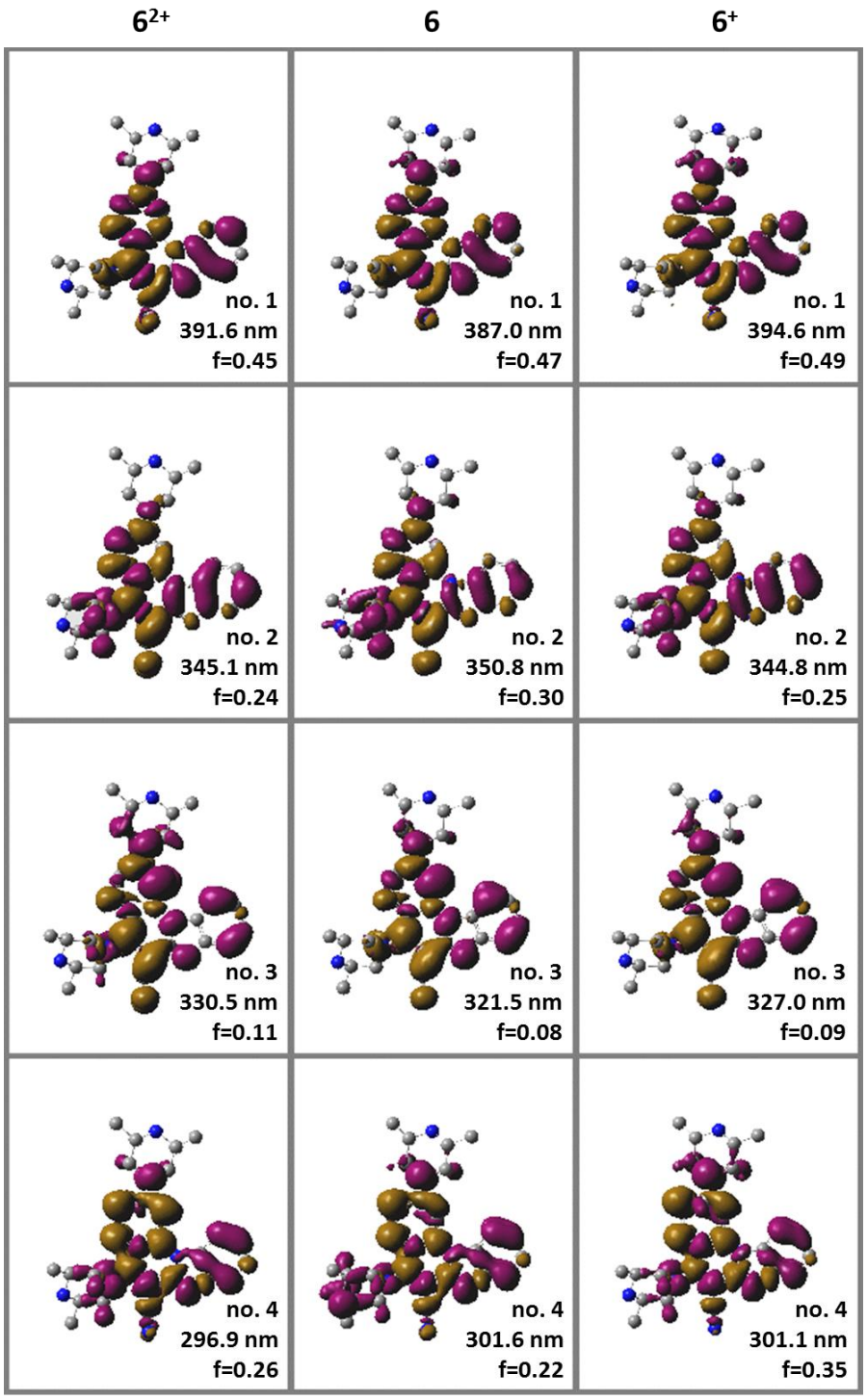

Figure S7. Transition densities of the lowest active excited states of **6** and its monoprotonated (**6**$^{+}$) and diprotonated (**6**$^{2+}$) derivatives in water. Electron enriched regions are coloured in purple, and those depleted in charge in drab. Excitation wavelength (in nm) is written below the ordinal number of the excited state, while *f* denotes the oscillator strength. The excited states are calculated by the TD-DFT method at the (IEF–PCM)/M06/6–31+G(d) level of theory.

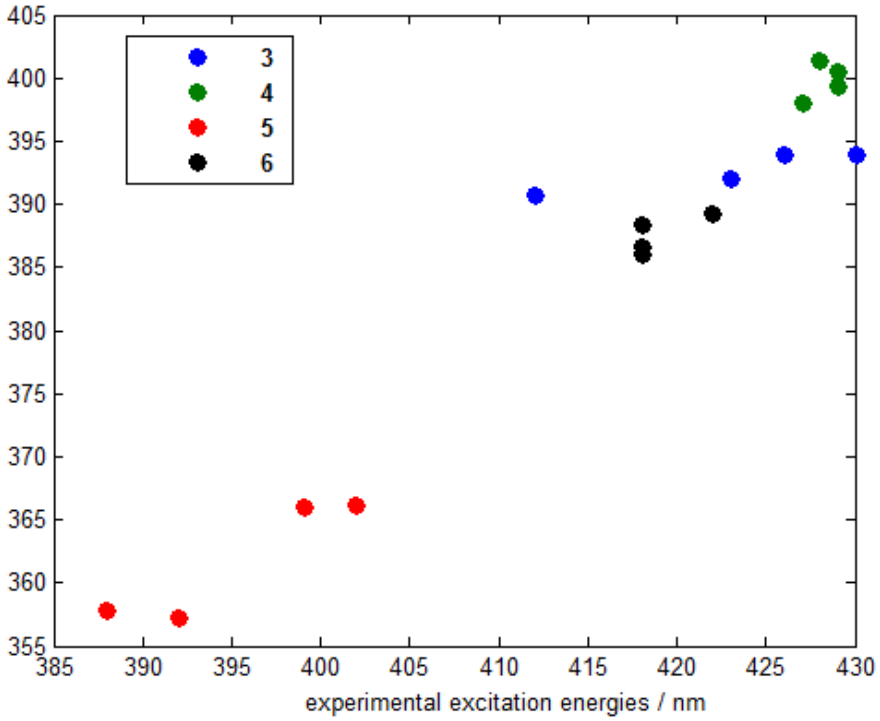

Figure S8. Correlation between the calculated and experimental lowest excitations for systems **3**–**6** in different solvents. Only the first excitation energies are shown (the solvents are not labeled). Linear regression reveals a reasonable correlation ($\lambda_{CALC} = 1.058 \cdot \lambda_{EXP} - 55.07$) with the regression coefficient of $R^2 = 0.94$.

RAD 4

E. Horak, P. Kassal, M. Hranjec, I.M. Steinberg, Benzimidazole functionalised Schiff bases: novel pH sensitive fluorescence turn-on chromoionophores for ion-selective optodes, *Sens. Actuator B-Chem.* (rad poslan na recenziju, IF: 4,758, Q1)

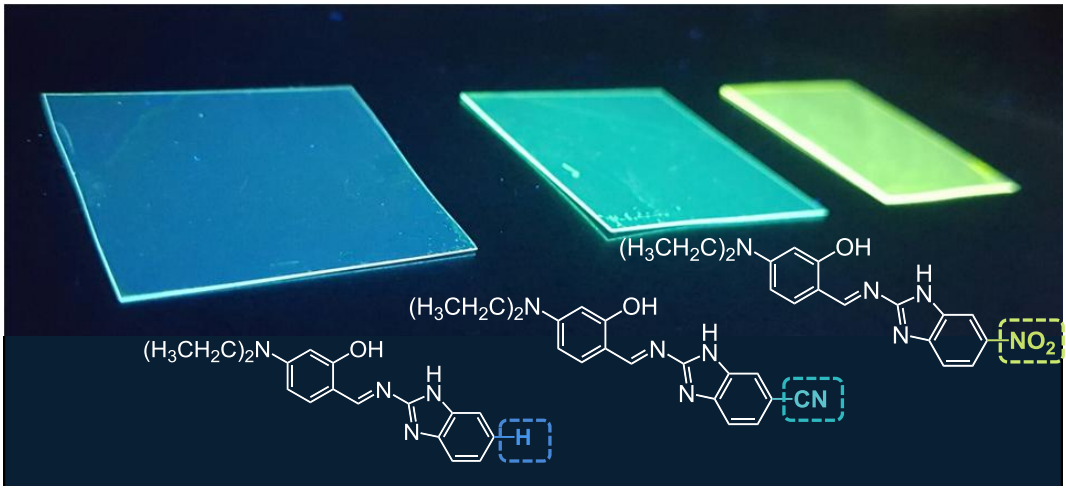

Benzimidazole functionalised Schiff bases: novel pH sensitive fluorescence turn-on chromoionophores for ion-selective optodes

Ema Horak,[a] Petar Kassal,[a] Marijana Hranjec[b] and Ivana Murković Steinberg[a]*

[a] *Department of General and Inorganic Chemistry, Faculty of Chemical Engineering and Technology, University of Zagreb, Marulićev trg 19, P. O. Box 177, HR-10000 Zagreb, Croatia*

[b] *Department of Organic Chemistry, Faculty of Chemical Engineering and Technology, University of Zagreb, Marulićev trg 20, P. O. Box 177, HR-10000 Zagreb, Croatia*

Abstract

Benzimidazole-based Schiff bases **1**-**3**, designed as D-π-A chromophores, are presented as novel pH responsive chromo- and fluoroionophores for ion-selective optodes. Tuning of their ICT character and photophysical properties has been achieved by introduction of an electron donating *N*,*N*-diethyl amino group and strong electron withdrawing groups -CN and $–NO_2$ on the benzimidazole acceptor moiety. The core molecular structure also contains a salicylidene moiety that potentially introduces photoinduced proton transfer reactivity. In general, pH chemosensors based on Schiff bases are relatively rare due to the common problem of protonation induced hydrolysis of the imino bond in water. The photophysical and sensing properties of **1**-**3** are characterised in solutions and thin polymer films, and the corresponding apparent pK_a and pK_a^* values are determined. In ethanol/water solutions, Schiff bases **1**-**3** show very weak fluorescence with reversible naked-eye visible colour change upon protonation (apparent pK_a ~ 4). Upon immobilisation in plasticised PVC films the photophysical properties and pH responses of **1**-**3** significantly change resulting in a reversible fluorimetric turn-on and turn-off pH sensitivity with apparent pK_a values in the physiologically relevant pH range (apparent pK_a ~ 6-7). A reversible spectroscopic response to pH is achieved because protonation of the immobilised benzimidazole Schiff bases occurs on the stable benzimidazole moiety (electron acceptor), whilst the imino bond remains preserved. An application for these novel fluoroionophores is demonstrated with a

fluorescence turn-on potassium selective optode, based on an ion-exchange sensing mechanism.

Keywords: fluorescence sensor; pH sensor; benzimidazole; Schiff base; ion-selective optode

1. Introduction

Electron donor-π-electron acceptor molecular systems (D-π-A systems) based on charge-transfer interactions are suitable for design of optical chemosensors due to their excellent properties as chromophores and fluorophores, as well as their varied ability to interact with potential analytes. Schiff bases play an important role in such systems, and represent one of the most investigated classes of organic compounds [1]. Besides their broad spectrum of biological activity [2, 3], they are often used as catalysts and intermediates in organic synthesis [4], as corrosion inhibitors [5, 6], as chelating agents [7, 8] and consequently in optical chemical sensors for detection of metal ions [9, 10] and as chemodosimeters [11].

pH responsive Schiff bases are often used as fluorescent probes for imaging [12-18], as colorimetric indicators [19], and as fluorescent chemosensors based on aggregation induced emission (AIE) [20, 21]. However, the use of Schiff bases for pH sensing in an aqueous environment is often problematic due to complex protonation and tautomeric equilibria involving a number of different species, and due to hydrolysis of the imino bond in polar solvents [22]. Hence, development of reversible pH sensors based on Schiff base derivatives is challenging and requires careful consideration of their structure-property relationships.

The benzimidazole moiety is another attractive building block of D-π-A molecular structures due to the multifunctionality of its heteroaromatic conjugated planar structure. The photophysical properties of benzimidazole based compounds can significantly change upon protonation/deprotonation [23-26], during metal-ion chelating and in interaction with biomolecules [27-29]. The combination of benzimidazole and Schiff base building blocks in a single molecular entity have been successfully used for optical detection of various metal ions [30-34], and the fluoride anion [35] in solutions.

One way of improving the stability of Schiff bases and preserving their pH sensitivity is by immobilisation in an appropriate material, as has been demonstrated with pH test strips based on organometal complexes [12, 36], fiber optic pH sensors [37, 38] and pH sensitive optodes [39]. In optodes, Schiff bases are typically incorporated into PVC thin films as metal ion

responsive chromophores or fluorophores [40-44], and less often as pH sensitive fluoroionophores.

In this work as part of our ongoing research effort on developing benzimidazole based ICT chromophores for pH and metal-ion sensing [23, 24, 29], we have designed and characterised benzimidazole based Schiff bases **1-3** (Scheme 1) for the reversible fluorimetric determination of pH and for potential use in ion-selective optodes. The multifunctional pH responsive benzimidazole moiety offers an alternative imino nitrogen as a protonation site and contributes to the photophysical and sensing properties of **1-3**. Immobilisation of **1-3** in lipophilic PVC matrices prevents hydrolysis of the Schiff bases, shifts the pK_a values and improves their fluorescence intensity as a result of the change of molecular microenvironment. The function of synthesised benzimidazole based Schiff bases as fluoroionophores is demonstrated in an ion-selective optode for potassium ion determination.

2. Experimental

2.1. Materials and instrumentation

All chemicals and solvents for synthesis and characterisation were purchased from commercial suppliers Acros, Aldrich or Fluka. Methanol, hydrochloride acid, sodium hydroxide and organic solvents were obtained from Kemika d.d., Zagreb. High molecular weight poly(vinylchloride) (PVC), bis(2-ethylhexyl) sebacate (DOS), cation-exchanger potassium tetrakis(4-chlorophenyl) borate, bis(2-ethylhexyl) sebacate (DOS), Potassium ionophore I (valinomycin), and tetrahydrofuran (THF) were purchased from Fluka (Switzerland). Milli-Q water was used for the preparation of aqueous solutions. pH in the range 1-13 was measured on commercially available combination pH electrode BlueLine 17 pH (Schott AG, Mainz, Germany). Absorbance spectra were recorded on a Carry 100 Scan Varian spectrophotometer. Fluorescence measurements were carried out on a Varian Cary Eclipse fluorescence spectrophotometer.

2.2. Synthesis and spectral characterisation of 1-3

All compounds presented in Fig. 1 were prepared by method previously reported by our research group [3] and characterised by ^{1}H NMR and ^{13}C NMR spectroscopy. Schiff bases were prepared from 2-aminobenzimidazoles and corresponding aromatic aldehydes in absolute ethanol for 12-24 h at reflux. Detailed description can be found in Electronic supporting information materials.

The stock solutions for **1**-**3** were prepared in ethanol (10 mM). Spectrophotometric titrations were carried out using $1x10^{-5}$ mol dm^{-3} solutions of the compounds **1**-**3** in ethanol or buffer solutions for the absorbance measurements and $2x10^{-6}$ mol dm^{-3} solutions for the fluorescence measurements. Absorbance measurements were carried out using quartz cells of 1 cm path length and absorbance values were recorded at 1 nm. Wavelength scan was performed between 200 nm and 800 nm. Baseline was recorded prior to each set of experiments. Fluorescence measurements were carried out on a Varian Cary Eclipse fluorescence spectrophotometer at 25 ºC using 1 cm path quartz cells. Excitation wavelengths were determined from absorbance maxima. Emission spectra were recorded from 300 nm to 800 nm and corrected for the effects of time and wavelength dependent light source fluctuations using a standard of Rhodamine 101, a diffuser provided with the fluorimeter and the software supplied with the instrument. Relative fluorescence quantum yields were determined according to *Miller* using Eq. (1):

$$\Phi_x = \Phi_s \times A_s D_x n_x^2 / A_x D_s n_s^2 \quad (1)$$

wherein Φ is the emission quantum yield, A is the absorbance at the excitation wavelength, D is the area under the corrected emission curve and n is the refractive index of the solvents used. The subscripts *s* and *x* refer to the standard and to the unknown, respectively. The standard employed was quinine sulphate with a published fluorescence quantum yield of 0.54 [45]. All samples were purged with nitrogen to displace oxygen. pH adjustment of ethanol solutions (EtOH:H_2O 95:5 v/v) was made with concentrated hydrochloride acid (HCl) and sodium hydroxide (NaOH). Apparent pK_a values were determined spectrophotometrically from fitted data points using the Boltzmann function.

Due to low solubility, measurements were conducted by diluting stock solutions of **1**-**3** in ethanol (volume fraction of ethanol in measured solutions is less than 1%).

2.3. Immobilisation and pH response of 1-3 in thin polymer films

Chromophores **1**-**3** were immobilised in plasticised PVC matrix starting from liquid mixture prepared by modified method found in literature [46]. The “cocktail' contained 67 mg PVC, 134 mg DOS (the plasticiser), 2.4 mg (1 eq) of PTCB and 1 eq of compound **1**-**3** in 1.5 mL THF. Mixture was placed in ultrasonic bath for 15 min. Thin polymer films were prepared by spreading 100 µL mixture onto a 2.5 x 2.5 cm solid transparent polyester sheet by spin-coating technique. Obtained thin films were dried at room temperature for 18 h in dark. pH response of immobilised chromophores was examined in buffer solutions pH 2 to 12.

Apparent pK_a values were determined spectrophotometrically from fitted data points using the Boltzmann function.

2.4. Preparation and characterisation of polymeric optodes

"Cocktails" for preparation of ion-selective optodes were prepared by diluting PVC in dry THF. The "cocktail' contained 67 mg PVC, 134 mg DOS (the plasticiser), 3.1 mg of PTCB, 7.1 mg of valinomycin and 0.9 mg of compound **3** in 1.5 mL THF. The mixture was placed in an ultrasonic bath for 15 min. Thin polymer films were prepared by spin-coating 100 µL of the mixture onto a 2.5 x 2.5 cm solid transparent polyester sheet. Different concentrations of potassium solutions were prepared by diluting 0.1 M KCl stock solution with a pH 4 buffer solution. The equilibrium time before each measurement was 5 min. For all measurements, the excitation wavelength was 433 nm.

3. Results and discussion

3.1. D-π-A structure of chromoionophores

Benzimidazole based Schiff bases **1-3** are designed as D-π-A molecular systems containing protonable and deprotonable sites (Scheme 1).

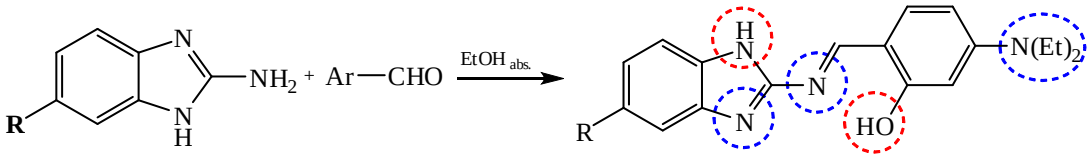

1 R = H
2 R = CN
3 R = NO_2

Scheme 1. Chemosensors **1-3** [3]. Protonable (blue) and deprotonable (red) sites are specified.

D-π-A molecules are widely used for chemosensing due to the variety of photophysical mechanisms and excited state reactions available for signalling the interaction with an analyte, such as photoinduced electron transfer (PET), intramolecular charge transfer (ICT) or excited state intramolecular proton transfer (ESIPT) [47]. The molecules designed here have an electron donating *N*,*N*-diethyl amino group on one side of the chromophore providing the extension of molecular conjugation, whilst the substituted benzimidazole moiety acts as an electron accepting unit. It is known that fine property tuning of push-pull molecules is achieved by introduction of electron withdrawing groups [48], achieved here by introduction

of -CN (**2)** and $–NO_2$ (**3)** on the benzimidazole core. In addition, the compounds contain a salicylidene moiety known for its ability to undergo photoinduced structural transformations, including ESIPT [49-51]. The presence of imino nitrogen on the benzimidazole moiety can offer an alternative protonation site [22], and improve the stability of the Schiff base by preventing hydrolysis of its imino bond.

3.2. Basic photophysical properties in different solvents

The spectral properties of Schiff bases **1-3** were characterised by UV-visible absorption and fluorescence spectrophotometry in different non-polar, aprotic and protic solvents. The basic photophysical properties of **1-3** in ethanol are presented in Figure 1 and summarised in Table 1.

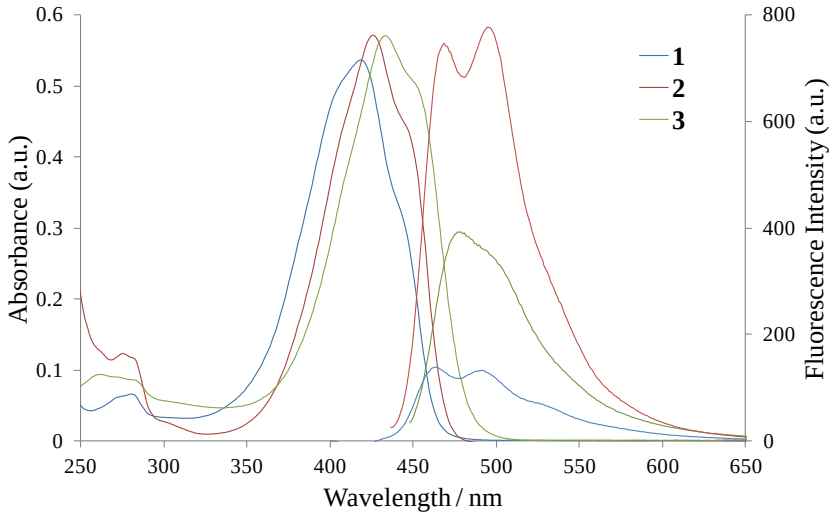

Figure 1. UV-vis absorption and emission spectra of chemosensors **1-3** in ethanol.

Table 1. Spectral properties of **1-3** in ethanol, and on immobilisation in a polymer film

		Ethanol							Polymer Film				
Comp.	**-R**	**λ_{abs} /nm**	**ε x 10^{-3} /M^{-1} cm^{-1}**	**λ_{em} /nm**	**Rel. Fluo. Int.[a]**	**Stokes shift /nm**	**FWHM (nm)**	**Φ**	**λ_{abs}/nm**	**Abs (a.u.)[a]**	**λ_{em}/nm**	**Fluo. Int. (a.u.)[b]**	**Stokes shift /nm**
1	-H	417	59.93	463 491	138.65 132.95	74	69.7	0.01495	420	0.1969	508 536	37.07 48.27	88
2	-CN	427 445	42.69 38.27	467 492	745.95 775.76	40	63.5	0.02974	426 446(sh)	0.4324 0.3346	469 495	195.97 214.00	43
3	-NO_2	433	60.85	480 495(sh)	392.04	62	65.0	0.00372	438 455(sh)	0.3642 0.3319	511	426.10	73

(sh) shoulder; [a] at given experimental conditions: c = 2 x 10^{-6} M. slit width = 10/10; [b] slit width = 2.5/5

Charge transfer in chromophores **1-3** induces strong absorption in the violet-blue region of the visible spectrum (λ_{abs} = 417 to 433 nm) with pronounced molar extinction coefficients (ε = 38000 to 60000 M^{-1} cm^{-1}). Electron withdrawing substituents –CN and –NO_2 on the benzimidazole core increased the ICT character of **2** and **3**, resulting in a bathochromic shift ($\Delta\lambda$ = 10 to 16 nm) in the absorption spectra. Compounds **1-3** exhibit weak blue-green fluorescence emission in ethanol (λ_{emiss} = 463 – 495 nm). This is a result of the structural arrangement of the molecular building blocks where free rotation of substituents around several single bonds promotes non-radiative relaxation pathways.

Further characterisation of photophysical properties of **1, 2** and **3** has been performed in different solvents as shown in Figures S1, 2 and S2 respectively, and summarised in Table S1.

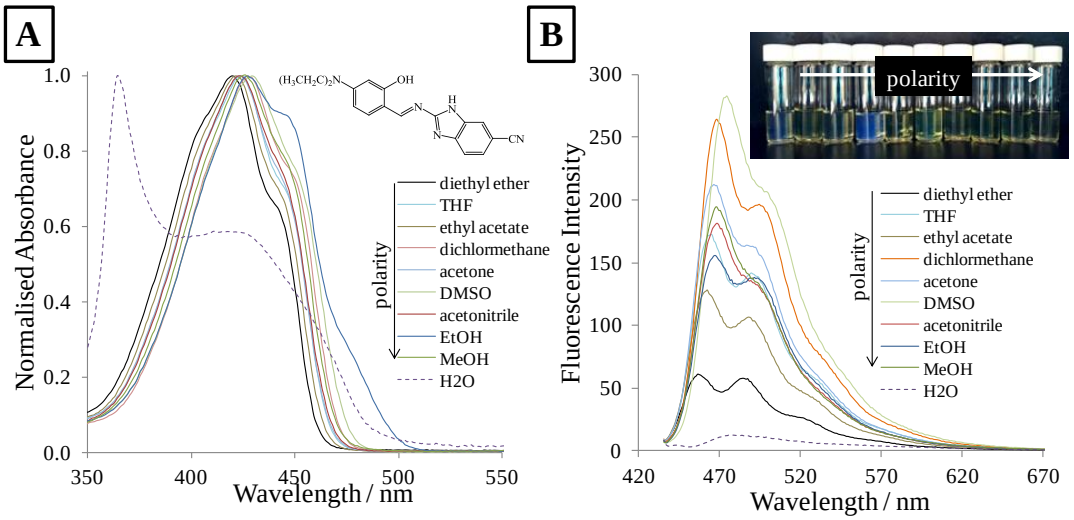

Figure. 2. UV-vis, c = 1x10^{-5} M (a) and emission (b) spectra, c = 2x10^{-6} M, of **2** in solvents of different polarity parameter, $\lambda_{exc} = \lambda_{abs}$.

In general, the UV-vis absorption peak wavelengths and molar extinction coefficients show a minor dependence on solvent polarity. Small bathochromic shifts with increasing solvent polarity are observed for absorbance and emission peaks in all compounds. However, the fluorescence intensity is substantially altered by solvent polarity. Fluorescence of all compounds was of highest intensity in DMSO (Figure 2 and Figures S1-S2), and the lowest in protic solvents: almost totally quenched in water. Schiff base **3** with a nitro substituent exhibited a strong and diverse spectral emission response in nonpolar and polar aprotic solvents (Figure 2 and Figures S1-S2). The sharp absorption peaks in water for **2** and **3** at λ_{abs} = 364 nm and 390 nm respectively indicate occurrence of aggregation [52]. All compounds exhibit moderate Stokes shifts and full width at half maximum values (FWHM) ranging from 63 nm to 69 nm.

3.3. Basic photophysical properties in thin films

Absorbance and emission spectra of **1-3** immobilised in DOS plasticised PVC thin films are shown in Figure 3. In general, they exhibit comparable spectral characteristics in thin films as in ethanol, however with significantly stronger fluorescence and slightly increased Stokes shifts (Table 1). Thin polymer films observed under UV lamp (λ_{exc} = 366 nm) exhibit strong blue, green and yellow-green emission (Figure 3). The most drastic increase in fluorescence intensity upon immobilisation occurred with compound **3,** where -NO_2, as an electron withdrawing substituent of an ICT structure, is also known to respond to microviscosity changes [53].

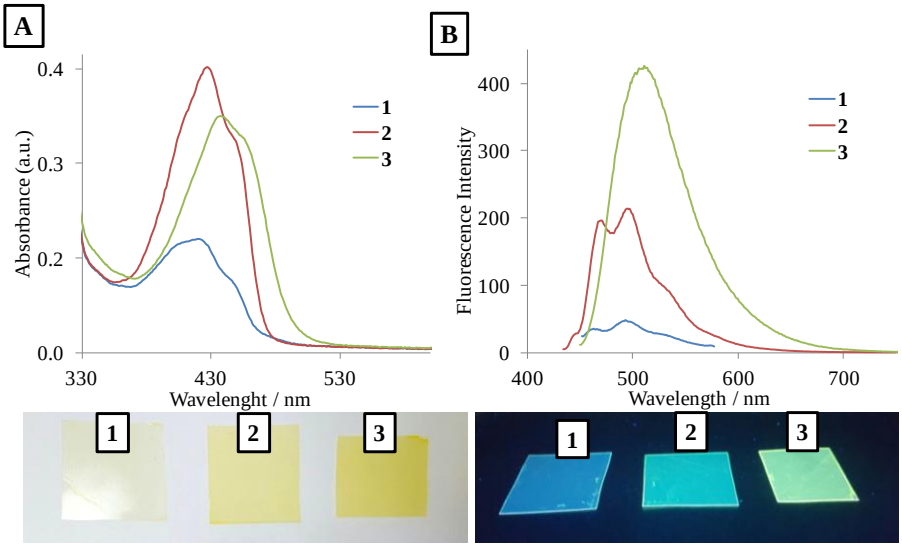

Figure 3. UV-vis absorption (a) and emission (b) spectra of chemosensors **1-3** in plasticised PVC thin films; photographs taken in daylight and under UV lamp (λ_{exc} = 366 nm).

3.4. Effect of protonation on spectral properties

Acid-base titrations of **1, 2** and **3** in ethanol/water mixtures were performed and the resulting spectral responses are shown in Figure 4 and Figures S3 and S4, respectively.

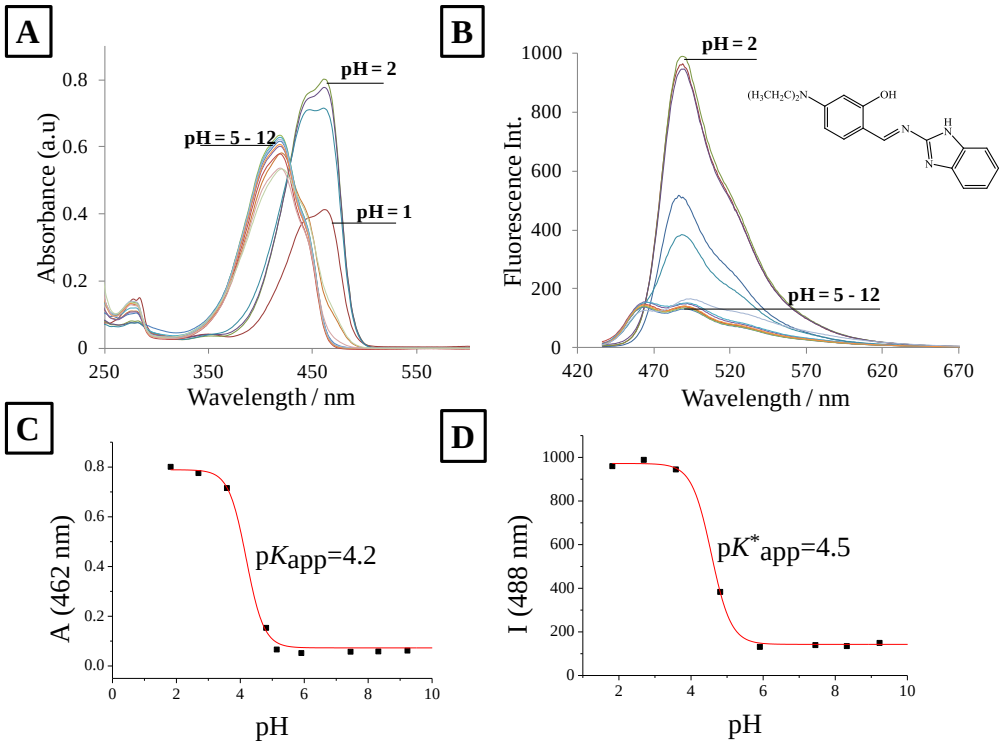

Figure 4. Effect of pH on absorbance (A) and emission (B) properties of **1**; pH response at selected absorbance (A) and emission wavelength (D); (c = 10 μM for absorbance and 2 μM for fluorescence data, λ_{exc} = 417 nm).

Protonation of **1**-**3** causes a bathochromic shift of absorption wavelength ($\Delta\lambda$ ranging from 28 nm for **1** to 37 nm for **3**) and an increase in their respective molar extinction coefficients. This is visually observable as a change of the solution colour from yellow to orange. Very strong acidic medium (pH = 1) causes a decrease in absorbance and formation of a novel absorption band at lower wavelengths ($\lambda_{abs} \approx 280$ nm). Based on our recent experimental and computational work on similar classes of compounds [24] it is presumed that the protonation occurs on the imino nitrogen atom on the benzimdiazole moiety. As shown in Scheme 1, charge transfer chromophores **1**-**3** contain acid-base active sites as a part of either donor or acceptor moiety. Protonation can occur at amino nitrogen atom or at imino (azole) nitrogens, and can lead to formation of monocationic or dicationic forms. It is generally known that protonation of the acceptor moiety in a push-pull system enhances the acceptor's electron-withdrawing character and results in a red-shift and increased extinction coefficients - which also supports our hypothesis that protonation occurs on the imino nitrogen of the benzimidazole moiety. The effect of protonation on the fluorescence spectra of **1** are different from the effects observed for **2** and **3**. Upon protonation, **1** shows a strong increase, whilst **2** and **3** show a decrease of fluorescence. The lack of an electron accepting substituent on **1** reduces its ICT character and can be responsible for the observed difference in excited state reaction mechanisms.

Summary of spectroscopic properties for neutral **M** and protonated $\mathbf{M}^+$ forms of **1**-**3** and the corresponding apparent pK_a and pK_a^* are shown in Table 2.

Table 2. Absorption maxima, emission maxima for neutral **M** and protonated $\mathbf{M}^+$ forms of **1**-**3** and the corresponding apparent pK_a and pK_a^* values (95/5 v/v EtOH:H_2O).

Compound	**-R**	λ_{abs} **/ nm**		λ_{fluo} **/ nm (Stokes shift / nm)**			
		M (ethanol)	$\mathbf{M}^+$ (acidified ethanol)	**M** (ethanol)	$\mathbf{M}^+$ (acidified ethanol)	pK_a **apparent**	pK_a* **apparent**
1	-H	417 441(sh)	445 461	463 (46) 488	488 (43)	4.2	4.5
2	-CN	427 445(sh)	466	467 (40) 492(sh)	495 (29)	3.6	2.7
3	$-NO_2$	433 452 (sh)	470	480 (47) 495(sh)	500 (30)	2.9	2.8

(sh) = shoulder; * = sharp; [a] possible aggregation

The pK_a values were experimentally determined from spectroscopic titration data (Figures 4c, 4d, S3, S4) in ethanol/water mixtures, thus calling them "apparent". The apparent pK_a values range from pK_a= 2.9 for compound **3,** to pK_a = 4.2 for compound **1** which is in agreement with the electron withdrawing character of the respective substituents and expected effect on basicity imino nitrogen. A small difference between excited state pK_a* and ground state pK_a can indicate that **2** and **3** in solutions are stronger acids when in their excited states.

3.5. Effect of protonation on immobilised 1-3

Spectral changes caused by protonation of **1, 2** and **3** in polymer films are shown in Figures S5 and S6, and Figure 5, respectively.

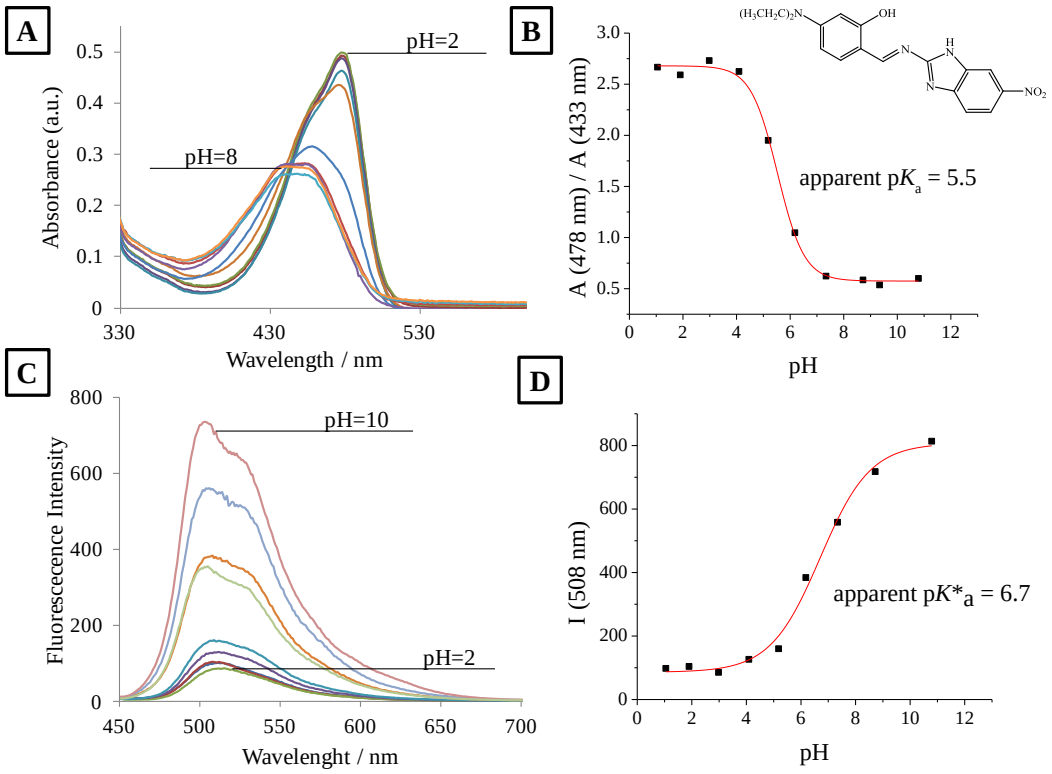

Figure 5. Effect of pH on absorption properties of immobilised **3** (A); pH response on selected absorbance wavelength (B); Effect of pH on emission properties of immobilised **3** (C); pH response on selected emission wavelength (D), λ_{exc} = 433 nm.

Qualitatively, the absorption spectral changes occurring upon protonation in the immobilised state are equivalent to those in solution: all chromophores exhibit a small bathochromic shift in absorbance spectra and an increase in molar extinction coefficient (Figure 5A), seen as a colour change from light yellow to dark yellow-orange (Figure 6).

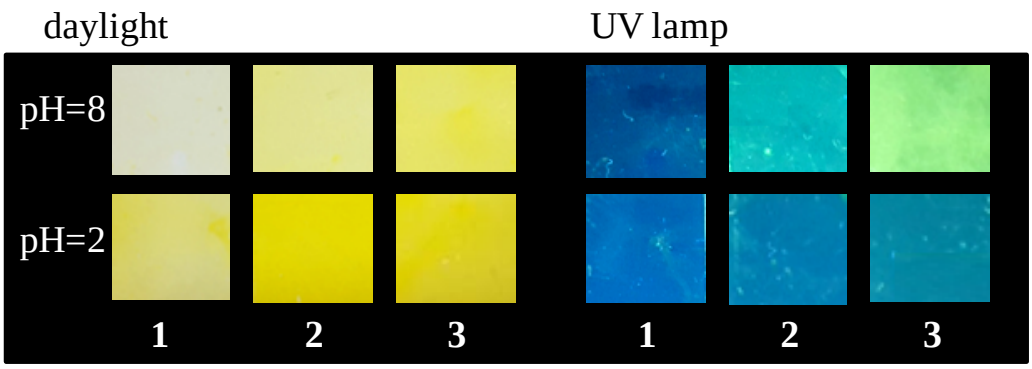

Figure 6. Photographs of thin polymer films of **1**-**3** taken in daylight and under UV lamp (λ_{exc} = 366 nm) showing the changes upon protonation

The strong fluorescence seen in all of the immobilised chromophores is quenched upon protonation, including compound **1** whose protonated form exhibited an increase of fluorescence in solution. Spectroscopic data for neutral **M** and protonated $\mathbf{M}^+$ forms of **1**-**3** in polymer films and the corresponding apparent pK_a and pK_a^* are summarised in Table 3.

Table 3. Absorption maxima, emission maxima and apparent pK_a values for compounds **1**-**3** in plasticised PVC films (neutral and protonated forms). The excitation wavelength was at the absorbance maxima of the neutral species.

		neutral (M)				protonated (M^+)					
Comp.	**-R**	**λ_{abs}/nm**	**Abs (a.u.)[a]**	**λ_{em}/nm**	**Fluo. Int. (a.u.)[a]**	**λ_{abs}/nm**	**Abs (a.u.)[a]**	**λ_{em}/nm**	**Fluo. Int. (a.u.)[a]**	**pK_a apparent**	**pK_a* apparent**
1	-H	417	0.1969	508 536	37.07 48.27	450(sh) 468	0.2057 0.2246	494	151.36	6.90	5.93
2	-CN	427 446(sh)	0.4324 0.3346	469 495	195.97 214.00	455(sh) 476	0.4565 0.5373	503	120.02	6.7	-
3	- NO_2	433 452(sh)	0.3642 0.3319	511	426.10	460(sh) 481	0.3576 0.4273	511	152.45	5.52	6.70

sh = shoulder; [a] at given experimental conditions: c = 1 x 10^{-3} M. slit width = 2.5/5

An important finding is that immobilisation of the compounds led to an increase in their apparent pK_a values by approx. 2 - 3 units. For example, immobilisation of **2** in the plasticised PVC matrix changed the apparent pK_a value from 3.6 to 6.7. Also, the differences between

corresponding apparent pK_a and pK_a^* values upon immobilisation have become more pronounced. Such effects have been observed for related compounds in solvents of different polarities [54], and may also be expected in polymer films where a number of parameters, including lipophilicity, polarity and microviscosity affect the complex heterogeneous ion-exchange equilibria [55]. The results indicate that the general sensing properties of chromophores have improved upon immobilisation in the plasticised films. Compond **3** demonstrated a reversible and stable response (Figure 7), has physiologically compatible pK_a values (pK_a = 5.5 and pK_a^*= 6.7), making it a promising candidate molecule for use as a fluorescent chromoionophore in ion-exchange optodes.

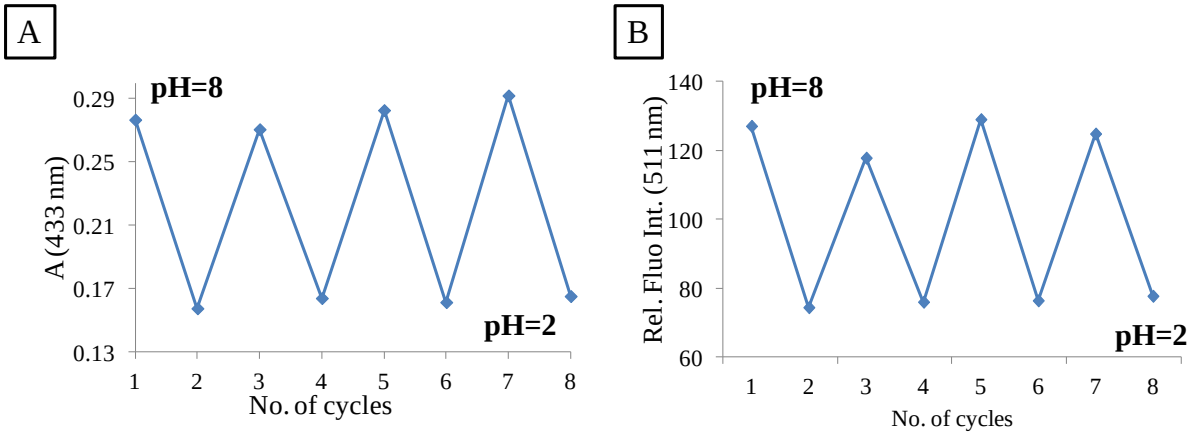

Figure 7. Reversible pH response of **3** (protonated – neutral) at selected absorbance (λ = 433 nm) and emission wavelength λ = 511 nm), λ_{exc} = 433 nm.

3.6. Optode for K^+ detection based on Schiff base 3

Based on the absorbance and emission properties of benzimidazole-based Schiff bases, an application for **3** as an ion-selective optode for the determination of potassium is demonstrated. Typically, the optical response of an ion-selective optode is a switch in the absorbance or fluorescence signal due to extraction of the target cation causing deprotonation of the pH indicator. pH indicators (chromoionophores) in thin films (bulk membranes) are responsible for the optical response. Most commercially available chromoionophores are colourimetric indicators and fluorescent ion selective optodes are less common. Recent examples of fluorescent pH sensitive chromoionophores are oxazinoindolines [56] and piperidine functionalised boron–dipyrromethenes [57]. Plasticised PVC is the most suitable substrate for the preparation of such optical systems, showing a variety of possible applications. Schiff bases have been used as chromoionophores in ion-selective optodes for

metal ion detection, however to the best of our knowledge benzimidazole-based Schiff bases have not been utilised as fluorescent chromoionophores in optodes.

The ion selective optode exhibits enhancement of fluorescence intensity due to an ion exchange mechanism. The ion exchange mechanism between bulk membrane (*org*) and aqueous solution (*aq*) is based on the following equation (1):

$$K^+(aq) + VAL\ (org) + \mathbf{3}^+\ (org) + R^-(org) \leftrightarrow KVAL^+(org) + \mathbf{3}(org) + R^-(org) + H^+(aq) \quad (1)$$

where VAL is the potassium selective ionophore (valinomycin), **3** is the benzimidazole-based pH sensitive Schiff base, and R is the cation exchanger [58]. The spectral response of **3** itself is not affected by potassium.

In the optode system, valinomycin is responsible for the reversible coordination of potassium ions. On exposure to potassium ion solutions, the optode film changes fluorescence intensity due to deprotonation of the chromoionophore **3** (Figure 8.). By fitting a Boltzmann curve to the fluorescence intensity at 511 nm *vs* log $c(K^+)$, the following calibration curve (2) was obtained:

$$I(511) = 526.7 + \frac{388.6-526.7}{1+\exp\frac{\log c+4.47}{0.475}} \quad (2)$$

The new fluorescent chromoionophore was fully functional in the ionophore-based polymeric optode.

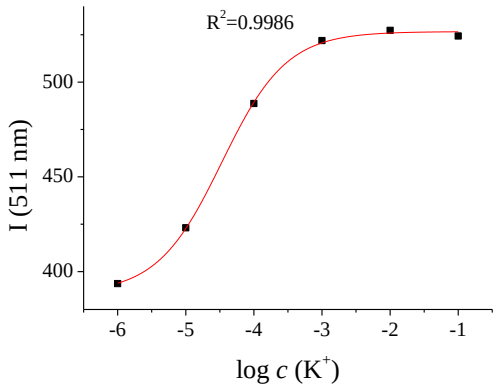

Figure 8. Response of the potassium-sensing thin films to different KCl concentrations. The Boltzmann function fit is used for calibration. KCl concentrations range from 10^{-6} M to10^{-1} M.

4. Conclusions

A new class of benzimidazole-based Schiff bases has been designed and are presented as novel pH responsive chromo- and fluoroionophores for ion-selective optodes. Tuning of their ICT character has been achieved by an electron donating *N*,*N*-diethyl amino group and strong electron withdrawing groups -CN and $–NO_2$ on the benzimidazole acceptor moiety. Schiff bases **1-3** show very weak fluorescence in ethanol solutions, with reversible naked-eye visible colour change upon protonation (apparent pK_a ~ 4).

Upon immobilisation in plasticised PVC films, the chromophores show a reversible fluorimetric turn-on and turn-off pH sensitivity with apparent pK_a values in the physiologically relevant pH range (apparent pK_a ~ 6-7). A reversible spectroscopic response to pH is achieved because protonation of the immobilised benzimidazole Schiff bases occurs on the stable benzimidazole moiety (electron acceptor), whilst the imino bond of the Schiff base remains preserved.

Compond **3** demonstrated a reversible and stable response to pH, with physiologically compatible pK_a values (pK_a = 5.5 and pK_a^*= 6.7) and has been successfully applied as a fluoroinophore in a fluorescence turn-on potassium selective optode based on an ion-exchange sensing mechanism.

Acknowledgements

This work was supported by the Croatian Science Foundation under grant number IP-2014-09-3386 entitled '*Design and synthesis of novel nitrogen-containing heterocyclic fluorophores and fluorescent nanomaterials for pH and metal-ion sensing*' which is gratefully acknowledged.

Appendix A. Supplementary data

Supplementary data associated with this article can be found in the online version.

Biographies

Ema Horak is a Teaching Assistant at Faculty of Chemical Engineering and Technology, University of Zagreb. She received her B.E. degree in Applied Chemistry from the same faculty in 2011 and continued her education as a graduate student under the supervision of Dr

Ivana Steinberg. Her research interest include development and characterisation of novel optical chemical sensors based on benzimidazole.

Petar Kassal is a postdoctoral researcher at the Faculty of Chemical Engineering and Technology, University of Zagreb, Croatia. He received an M.Sc. in chemical engineering (2010) and a Ph.D. in applied chemistry (2015) from this institution. His main research interest is the development of novel electrochemical and optical chemical sensors for wearable and wireless applications.

Marijana Hranjec obtained her Ph.D. at the Faculty of Chemical Engineering and Technology, University of Zagreb. Currently she is an associate professor at the Department of Organic Chemistry. Her interests are design, synthesis and spectroscopic characterization of versatile organic heterocyclic compounds, prepared as potential biologically active compounds or fluorescent probes for detection of biomacromolecules or cations in solutions.

Ivana Murković Steinberg is associate professor of chemistry at the Faculty of Chemical Engineering & Technology, University of Zagreb. Her current research involves development of novel functional material interfaces and sensing architectures for integration with wireless sensing systems. She graduated with a B.Eng. in Chemical Engineering from the University of Zagreb, and has a Ph.D. in chemistry from the Karl-Franzens University of Graz for research on optical sensors for the determination of metal ions.

References

[1] W.L. shi, S. Long, M. Panunzio, S. Biondi, Schiff Bases: A Short Survey on an Evergreen Chemistry Tool, Molecules, 18(2013) 12264-89.

[2] A. Kajal, S. Bala, S. Kamboj, N. Sharma, V. Saini, Schiff Bases: A Versatile Pharmacophore, Journal of Catalysts, 2013(2013) 14.

[3] M. Hranjec, K. Starčević, S.K. Pavelić, P. Lučin, K. Pavelić, G. Karminski Zamola, Synthesis, spectroscopic characterization and antiproliferative evaluation in vitro of novel Schiff bases related to benzimidazoles, Eur J Med Chem, 46(2011) 2274-9.

[4] P.G. Cozzi, Metal-Salen Schiff base complexes in catalysis: practical aspects, Chem Soc Rev, 33(2004) 410-21.

[5] J. Aljourani, K. Raeissi, M.A. Golozar, Benzimidazole and its derivatives as corrosion inhibitors for mild steel in 1M HCl solution, Corros Sci, 51(2009) 1836-43.

[6] M. Hosseini, S.F.L. Mertens, M. Ghorbani, M.R. Arshadi, Asymmetrical Schiff bases as inhibitors of mild steel corrosion in sulphuric acid media, Mater Chem Phys, 78(2003) 800-8.

[7] K.C. Gupta, A.K. Sutar, Catalytic activities of Schiff base transition metal complexes, Coord Chem Rev, 252(2008) 1420-50.

[8] H. Goh, Y.G. Ko, T.K. Nam, A. Singh, N. Singh, D.O. Jang, A benzimidazole-based fluorescent chemosensor for Cu2+ recognition and its complex for sensing H2PO4- by a Cu2+ displacement approach in aqueous media, Tetrahedron Lett, 57(2016) 4435-9.

[9] W. Al Zoubi, N. Al Mohanna, Membrane sensors based on Schiff bases as chelating ionophores – A review, Spectrochimica Acta Part A: Molecular and Biomolecular Spectroscopy, 132(2014) 854-70.

[10] V.K. Gupta, A.K. Singh, M.R. Ganjali, P. Norouzi, F. Faridbod, N. Mergu, Comparative study of colorimetric sensors based on newly synthesized Schiff bases, Sensors and Actuators B-Chemical, 182(2013) 642-51.

[11] Q. Feng, Y. Li, L. Wang, C. Li, J. Wang, Y. Liu, et al., Multiple-color aggregation-induced emission (AIE) molecules as chemodosimeters for pH sensing, Chem Commun, (2016).

[12] J.H. Cheng, F. Gou, X.H. Zhang, G.Y. Shen, X.G. Zhou, H.F. Xiang, A Class of Multiresponsive Colorimetric and Fluorescent pH Probes via Three Different Reaction Mechanisms of Salen Complexes: A Selective and Accurate pH Measurement, Inorg Chem, 55(2016) 9221-9.

[13] P. Guo, L.J. Liu, Q. Shi, C.Y. Yin, X.F. Shi, A rhodamine 6G derived Schiff base as a fluorescent and colorimetric probe for pH detection and its crystal structure, J Mol Struct, 1130(2017) 150-5.

[14] S. Halder, A. Bhattacharjee, A. Roy, S. Chatterjee, P. Roy, Chromogenic and fluorescence sensing of pH with a Schiff-base molecule, Rsc Advances, 6(2016) 39118-24.

[15] S. Halder, S. Dey, P. Roy, A quinoline based Schiff-base compound as pH sensor, Rsc Advances, 5(2015) 54873-81.

[16] U.C. Saha, K. Dhara, B. Chattopadhyay, S.K. Mandal, S. Mondal, S. Sen, et al., A New Half-Condensed Schiff Base Compound: Highly Selective and Sensitive pH-Responsive Fluorescent Sensor, Org Lett, 13(2011) 4510-3.

[17] Y. Sarkar, S. Das, A. Ray, S.K. Jewrajka, S. Hirota, P.P. Parui, A simple interfacial pH detection method for cationic amphiphilic self-assemblies utilizing a Schiff-base molecule, Analyst, 141(2016) 2030-9.

[18] P.S. Song, X.T. Chen, Y. Xiang, L. Huang, Z.J. Zhou, R.R. Wei, et al., A ratiometric fluorescent pH probe based on aggregation-induced emission enhancement and its application in live-cell imaging, J Mater Chem, 21(2011) 13470-5.

[19] J.Y. Noh, G.J. Park, Y.J. Na, H.Y. Jo, S.A. Lee, C. Kim, A colorimetric "naked-eye" Cu(II) chemosensor and pH indicator in 100% aqueous solution, Dalton Transactions, 43(2014) 5652-6.

[20] L.Q. Yan, T.T. Qing, R.J. Li, Z.W. Wang, Z.J. Qi, Synthesis and optical properties of aggregation-induced emission (AIE) molecules based on the ESIPT mechanism as pH- and Zn2+-responsive fluorescent sensors, Rsc Advances, 6(2016) 63874-9.

[21] Q. Feng, Y.Y. Li, L.L. Wang, C. Li, J.M. Wang, Y.Y. Liu, et al., Multiple-color aggregation-induced emission (AIE) molecules as chemodosimeters for pH sensing, Chem Commun, 52(2016) 3123-6.

[22] N. Galić, Z. Cimerman, V. Tomišić, Tautomeric and protonation equilibria of Schiff bases of salicylaldehyde with aminopyridines, Analytica Chimica Acta, 343(1997) 135-43.

[23] E. Horak, M. Hranjec, R. Vianello, I.M. Steinberg, Reversible pH switchable aggregation-induced emission of self-assembled benzimidazole-based acrylonitrile dye in aqueous solution, Dyes and Pigments, 142(2017) 108-15.

[24] E. Horak, R. Vianello, M. Hranjec, S. Krištafor, G.K. Zamola, I.M. Steinberg, Benzimidazole acrylonitriles as multifunctional push-pull chromophores: Spectral characterisation, protonation equilibria and nanoaggregation in aqueous solutions, Spectrochimica Acta Part A: Molecular and Biomolecular Spectroscopy, 178(2017) 225-33.

[25] M.A. Saeed, H.T.M. Le, O.S. Miljanic, Benzobisoxazole Cruciforrns as Fluorescent Sensors, Acc Chem Res, 47(2014) 2074-83.

[26] Z.S. Li, L.J. Li, T.T. Sun, L.M. Liu, Z.G. Xie, Benzimidazole-BODIPY as optical and fluorometric pH sensor, Dyes and Pigments, 128(2016) 165-9.

[27] M. Hranjec, E. Horak, M. Tireli, G. Pavlovic, G. Karminski-Zamola, Synthesis, crystal structure and spectroscopic study of novel benzimidazoles and benzimidazo 1,2-a quinolines as potential chemosensors for different cations, Dyes and Pigments, 95(2012) 644-56.

[28] S.L. Wang, Y.T. Chang, Combinatorial synthesis of benzimidazolium dyes and its diversity directed application toward GTP-selective fluorescent chemosensors, J Am Chem Soc, 128(2006) 10380-1.

[29] M. Hranjec, E. Horak, D. Babic, S. Plavljanin, Z. Srdovic, I.M. Steinberg, et al., Fluorescent benzimidazo[1,2-a]quinolines: synthesis, spectroscopic and computational studies of protonation equilibria and metal ion sensitivity, New Journal of Chemistry, 41(2017) 358-71.

[30] N. Ahmed, M. Riaz, A. Ahmed, M. Bhagat, Synthesis, Characterisation, and Biological Evaluation of Zn(II) Complex with Tridentate (NNO Donor) Schiff Base Ligand, Int J Inorg Chem, 2015(2015) 5.

[31] A. Kumar, A. Kumar, M. Dubey, A. Biswas, D.S. Pandey, Detection of copper(II) and aluminium(III) by a new bis-benzimidazole Schiff base in aqueous media via distinct routes, Rsc Advances, 5(2015) 88612-24.

[32] X.J. Wang, T. Xu, H.D. Duan, Schiff base fluorescence probes for Cu2+ based on imidazole and benzimidazole, Sensors and Actuators B-Chemical, 214(2015) 138-43.

[33] B. Zhao, Y. Fang, M.-j. Ma, Q.-G. Deng, Y. Xu, L.-y. Wang, A new on-fluorescent sensor for Ag+ based on benzimidazole bearing bis(ethoxycarbonylmethyl)amino groups, Heterocycl Commun2015, p. 211.

[34] Y.S. Kim, J.J. Lee, S.Y. Lee, T.G. Jo, C. Kim, A highly sensitive benzimidazole-based chemosensor for the colorimetric detection of Fe(II) and Fe(III) and the fluorometric detection of Zn(II) in aqueous media, Rsc Advances, 6(2016) 61505-15.

[35] K. Liu, X. Zhao, Q. Liu, J. Huo, B. Zhu, S. Diao, Fluoride-driven 'turn on' ESPT in the binding with a novel benzimidazole-based sensor, Beilstein journal of organic chemistry, 11(2015) 563-7.

[36] J.H. Cheng, Y.H. Zhang, X.F. Ma, X.G. Zhou, H.F. Xiang, Colorimetric and fluorescent pH and Cu2+ probes induced by photoisomerization of a maleonitrile-based Salen ligand, Chem Commun, 49(2013) 11791-3.

[37] S. Derinkuyu, K. Ertekin, O. Oter, S. Denizalti, E. Cetinkaya, Fiber optic pH sensing with long wavelength excitable Schiff bases in the pH range of 7.0-12.0, Anal Chim Acta, 588(2007) 42-9.

[38] S. Derinkuyu, K. Ertekin, O. Oter, S. Denizalti, E. Cetinkaya, Emission based fiber optic pH sensing with Schiff bases bearing dimethylamino groups, Dyes and Pigments, 76(2008) 133-41.

[39] C. Hazneci, K. Ertekin, B. Yenigul, E. Cetinkaya, Optical pH sensor based on spectral response of newly synthesized Schiff bases, Dyes and Pigments, 62(2004) 35-41.

[40] A.A.A. Aziz, S.H. Seda, S.F. Mohammed, Design of a highly sensitive and selective bulk optode based on fluorescence enhancement of N,N '-bis-(1-hydroxyphenylimine)2,2 '-pyridil Schiff base: Monitoring of zinc(II) ion in real samples and DFT calculation, Sensors and Actuators B-Chemical, 223(2016) 566-75.

[41] A.A.A. Aziz, R.G. Mohamed, F.M. Elantabli, S.M. El-Medani, A Novel Fluorimetric Bulk Optode Membrane Based on NOS Tridentate Schiff Base for Selective Optical Sensing of Al3+ Ions, Journal of Fluorescence, 26(2016) 1927-38.

[42] M. Shamsipur, M. Sadeghi, A. Garau, V. Lippolis, An efficient and selective flourescent chemical sensor based on 5-(8-hydroxy-2-quinolinylmethyl)-2,8-dithia-5-aza-2,6-pyridinophane as a new fluoroionophore for determination of iron(III) ions. A novel probe for iron speciation, Anal Chim Acta, 761(2013) 169-77.

[43] M. Arvand, Z. Lashkari, Sensitive and selective detection of trace copper in standard alloys, food and biological samples using a bulk optode based on N,N '-(4,4 '-ethylene biphenyl) bis(3-methoxy salicylidine imine) as neutral carrier, Spectrochimica Acta Part a-Molecular and Biomolecular Spectroscopy, 107(2013) 280-8.

[44] N. Aksuner, E. Henden, I. Yilmaz, A. Cukurovali, Development of a Highly Sensitive and Selective Optical Chemical Sensor for the Determination of Zinc Based on Fluorescence Quenching of a Novel Schiff Base Ligand, Sensor Lett, 8(2010) 684-9.

[45] W.H. Melhuish, QUANTUM EFFICIENCIES OF FLUORESCENCE OF ORGANIC SUBSTANCES - EFFECT OF SOLVENT AND CONCENTRATION OF FLUORESCENT SOLUTE, J Phys Chem, 65(1961) 229-&.

[46] E. Malavolti, A. Cagnini, G. Caputo, L. Della Ciana, M. Mascini, An optimized optrode for continuous potassium monitoring in whole blood, Anal Chim Acta, 401(1999) 129-36.

[47] B. Valeur, I. Leray, Design principles of fluorescent molecular sensors for cation recognition, Coord Chem Rev, 205(2000) 3-40.

[48] F. Bures, Fundamental aspects of property tuning in push-pull molecules, RSC Adv, 4(2014) 58826-51.

[49] M.E. Kletskii, A.A. Millov, A.V. Metelitsa, M.I. Knyazhansky, Role of structural flexibility in the fluorescence and photochromism of salicylideneaniline: the general scheme of the phototransformations, Journal of Photochemistry and Photobiology A: Chemistry, 110(1997) 267-70.

[50] W.H. Sun, S.Y. Li, R. Hu, Y. Qian, S.Q. Wang, G.Q. Yang, Understanding Solvent Effects on Luminescent Properties of a Triple Fluorescent ESIPT Compound and Application for White Light Emission, J Phys Chem A, 113(2009) 5888-95.

[51] S. Dalapati, S. Jana, N. Guchhait, Anion recognition by simple chromogenic and chromo-fluorogenic salicylidene Schiff base or reduced-Schiff base receptors, Spectroc Acta Pt A-Molec Biomolec Spectr, 129(2014) 499-508.

[52] A. Eisfeld, J.S. Briggs, The J- and H-bands of organic dye aggregates, Chem Phys, 324(2006) 376-84.

[53] R. Ghosh, A. Nandi, D.K. Palit, Solvent sensitive intramolecular charge transfer dynamics in the excited states of 4-N, N-dimethylamino-4 '-nitrobiphenyl, Phys Chem Chem Phys, 18(2016) 7661-71.

[54] T. Gunduz, E. Kilic, E. Canel, F. Koseoglu, PROTONATION CONSTANTS OF SOME SUBSTITUTED SALICYLIDENEANILINES IN DIOXAN-WATER MIXTURES, Analytica Chimica Acta, 282(1993) 489-95.

[55] X. Xie, E. Bakker, Ion selective optodes: from the bulk to the nanoscale, Anal Bioanal Chem, 407(2015) 3899-910.

[56] X. Xie, G.A. Crespo, E. Bakker, Oxazinoindolines as Fluorescent H+ Turn-On Chromoionophores For Optical and Electrochemical Ion Sensors, Analytical Chemistry, 85(2013) 7434-40.

[57] Y. Li, Y. Xu, J. Wu, Y. Qin, D. Jiang, Rational design of piperidine functionalized boron–dipyrromethene as fluorescent chromoionophore for ion-selective optodes, Sensors Actuators B: Chem, 232(2016) 37-42.

[58] E. Bakker, P. Buhlmann, E. Pretsch, Carrier-based ion-selective electrodes and bulk optodes. 1. General characteristics, Chem Rev, 97(1997) 3083-132.

Electronic supplementary information
Benzimidazole functionalised Schiff bases: novel pH sensitive fluorescence turn-on chromoionophores for ion-selective optodes

Ema Horak[a], Petar Kassal[a], Marijana Hranjec[b] and Ivana Murković Steinberg[a]*

[a] *Department of General and Inorganic Chemistry, Faculty of Chemical Engineering and Technology, University of Zagreb, Marulićev trg 19, P. O. Box 177, HR-10000 Zagreb, Croatia*

[b] *Department of Organic Chemistry, Faculty of Chemical Engineering and Technology, University of Zagreb, Marulićev trg 20, P. O. Box 177, HR-10000 Zagreb, Croatia*

Synthesis of benzimidazole based Schiff bases 1-3

Solutions of equimolar amounts of corresponding 5(6)-substituted-2-aminobenzimidazoles and aromatic aldehydes in absolute ethanol, were refluxed for 12-24 h. After cooling, the obtained product was filtered off and recrystallized from ethanol to obtain yellow powder products.

*Synthesis of 2-[(4-N,N-diethylamino-2-hydroxy)benz-2-ylideneamino] benzimidazole **1***

Compound **1** was prepared from 2-aminobenzimidazole (0.25 g, 1.90 mmol), 4-*N*,*N*-diethylamino-2-hydroxybenzaldehyde (0.36 g, 1.90 mmol) in absolute ethanol (10 mL) after 24 h and recrystallization from ethanol to obtain 0.13 g (32%) of orange powder. mp 228-230 °C; UV (EtOH) λ_{max}/ nm = 417; IR (diamond): ν/cm^{-1} = 3451, 2973, 1757, 1647, 1564, 1515; ^{1}H NMR (DMSO-d_6, 600 MHz): δ/ppm = 12.85 (s, 1H, $NH_{benzimidazole}$), 12.36 (bs, 1H, OH), 9.31 (s, 1H, $H_{arom.}$), 7.48 (d, 2H, J = 8.88 Hz, $H_{arom.}$), 7.38 (d, 1H, J = 8.70 Hz, H_{arom}), 7.12 (d, 2H, J = 8.80 Hz, H_{arom}), 6.39 (dd, 1H, J_1 = 8.92 Hz, J_2 ¼ 2.18 Hz, $H_{arom.}$), 6.14 (d, 1H, J = 2.20 Hz, H_{arom}), 3.45-3.41 (m, 4H, CH_2), 1.15 (t, 6H, J = 7.09 Hz, CH_3); ^{13}C NMR (DMSO-d_6, 75 MHz): δ/ppm = 164.62 (d), 163.96 (s), 155.23 (s), 153.16 (s), 143.18 (s), 135.72 (d), 131.55 (s), 124.56 (d), 121.89 (d), 116.54 (d), 108.77 (s), 105.29 (d), 102.44 (d), 97.17 (d),

44.58 (t), 44.56 (t), 13.02 (q), 13.00 (q); Anal. ($C_{18}H_{20}N_4O$) Calcd.: C, 70.11; H, 6.54; N, 18.17; Found: C, 70.33; H, 6.82; N, 18.37.

*Synthesis of 2-[(4-N,N-diethylamino-2-hydroxy)benz-2-ylideneamino]-5(6) cyanobenzimidazole **2**.*

Compound **2** was prepared from 2-amino-5(6)-cyanobenzimidazole (0.12g,0.76mmol), 4-*N*,*N*- diethylamino-2-hydroxybenzaldehyde (0.15 g, 0.76 mmol) in absolute ethanol (10 mL) after 24 h and recrystallization from ethanol to obtain 0.11 g (49%) of yellow powder. Mp 228-230 °C; UV (EtOH) λ_{max}/nm = 449, 426; IR (diamond): ν/cm^{-1} = 3486, 2971, 2219, 1729, 1619, 1577; ^{1}H NMR (DMSO-*d*6, 600 MHz): *d*/ppm = 12.67 (s, 1H, $NH_{benzimidazole}$), 9.34 (s, 1H, $H_{arom.}$), 7.94 (s, 1H, $H_{arom.}$), 7.58 (d, 1H, *J* = 8.22 Hz, H_{arom}), 7.53 (d, 1H, *J* = 8.66 Hz, H_{arom}), 7.51 (d, 1H, *J* = 8.42 Hz, H_{arom}), 6.42 (d, 1H, *J* = 8.20 Hz, H_{arom}), 6.15 (s, 1H, $H_{arom.}$), 3.80 (bs, 1H, OH), 3.47-3.43 (m, 4H, CH_2), 1.15 (t, 6H, *J* = 7.11 Hz, CH_3); ^{13}C NMR (DMSO-*d*6, 75MHz): *d*/ ppm = 165.72 (d), 164.32 (s), 153.72 (s), 142.87 (s), 135.99 (d), 131.48 (s), 125.59 (d), 120.66 (s), 118.35 (s), 108.87 (s), 105.68 (d), 104.95 (d), 97.07 (d), 96.42 (d), 44.64 (t), 44.58 (t), 13.02 (q), 12.89 (q); Anal. ($C_{19}H_{19}N_5O$) Calcd.: C, 68.45; H, 5.74; N, 21.01; Found: C, 68.11; H, 5.55; N, 20.78.

*Synthesis of 2-[(4-N,N-diethylamino-2-hydroxy)benz-2-ylideneamino]- 5(6)-nitrobenzimidazole **3**.*

Compound **3** was prepared from 2-amino-5(6)-nitrobenzimidazole (0.25 g, 1.40 mmol), 4-*N*,*N*- diethylamino-2-hydroxybenzaldehyde (0.27 g, 1.40 mmol) in absolute ethanol (10 mL) after 24 h and recrystallization from ethanol to obtain 0.23 g (52%) of orange powder. mp 232-234 °C; UV(EtOH) λ_{max}/nm = 436, 426; IR (diamond): ν/cm^{-1} = 3428, 2912, 2215, 1722, 1570, 1515; ^{1}H NMR (DMSO-d_6, 300 MHz): *d*/ ppm = 13.04 (s, 1H, $NH_{benzimidazole}$), 12.66 (bs, 1H, OH), 9.36 (s, 1H, $H_{arom.}$), 8.29 (s, 1H, $H_{arom.}$), 8.06 (dd, 1H, J_1 = 8.76 Hz, J_2 = 2.28 Hz, $H_{arom.}$), 7.60 (d, 1H, *J* = 8.78 Hz, H_{arom}), 7.55 (d, 1H, *J* = 8.80 Hz, H_{arom}), 6.43 (dd, 1H, J_1 = 8.90 Hz, J_2 = 2.34 Hz, $H_{arom.}$), 6.16 (d, 1H, *J* = 2.28 Hz, H_{arom}), 3.47-3.42 (m, 4H, CH_2), 1.14 (t, 6H, *J* = 7.06 Hz, CH_3); ^{13}C NMR (DMSO-d_6, 75 MHz): *d*/ppm = 165.87 (d), 164.43 (s), 153.87 (s), 141.54 (s), 136.07 (d), 133.61 (s), 126.44 (d), 124.47 (s), 121.53 (d), 117.92 (d), 113.92 (s), 108.93 (s), 105.80 (d), 97.03 (d), 44.67 (t), 44.51 (t),13.01 (q),12.99 (q); Anal. ($C_{18}H_{19}N_5O_3$) Calcd.: C, 61.18; H, 5.42; N, 19.82; Found: C, 60.97; H, 5.11; N, 19.66.

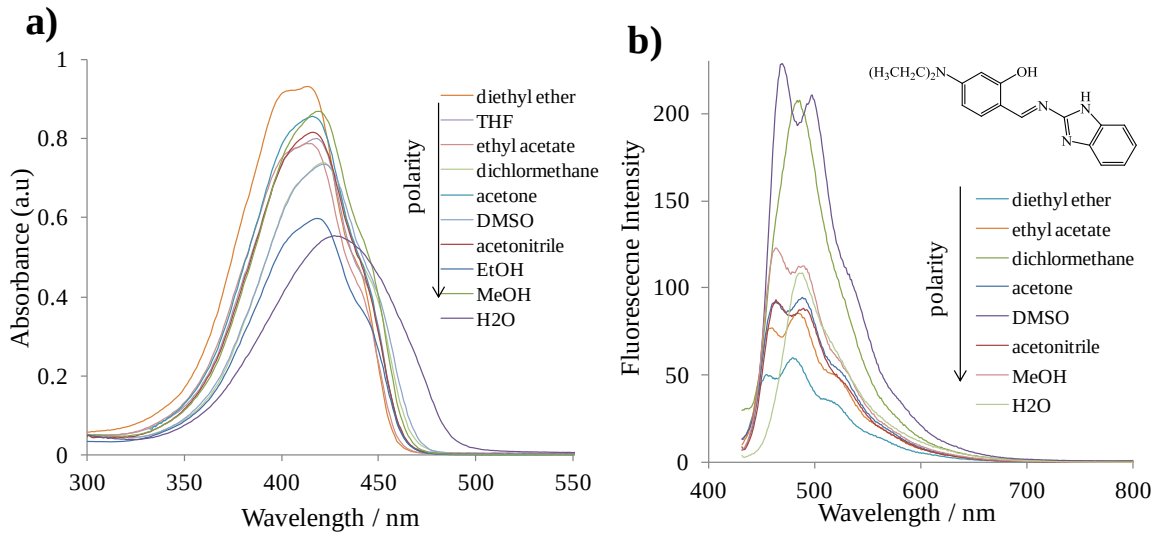

Figure S1. UV-vis, c = 1x10^{-5} M (a) and emission (b) spectra, c = 2x10^{-6} M of **1** in solvents of different polarity parameter, $\lambda_{exc} = \lambda_{abs}$.

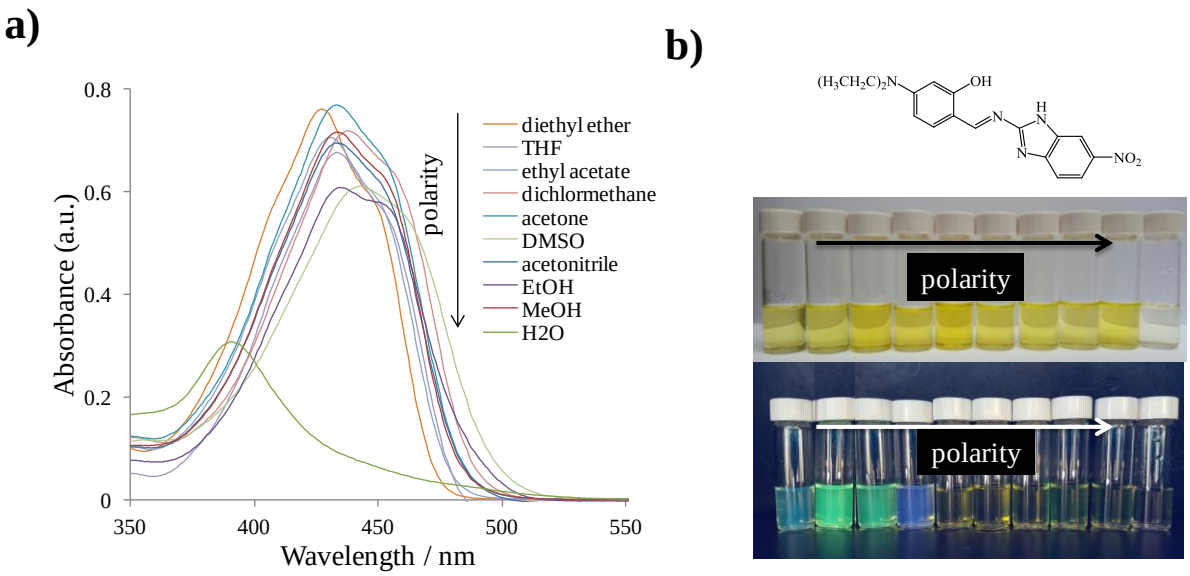

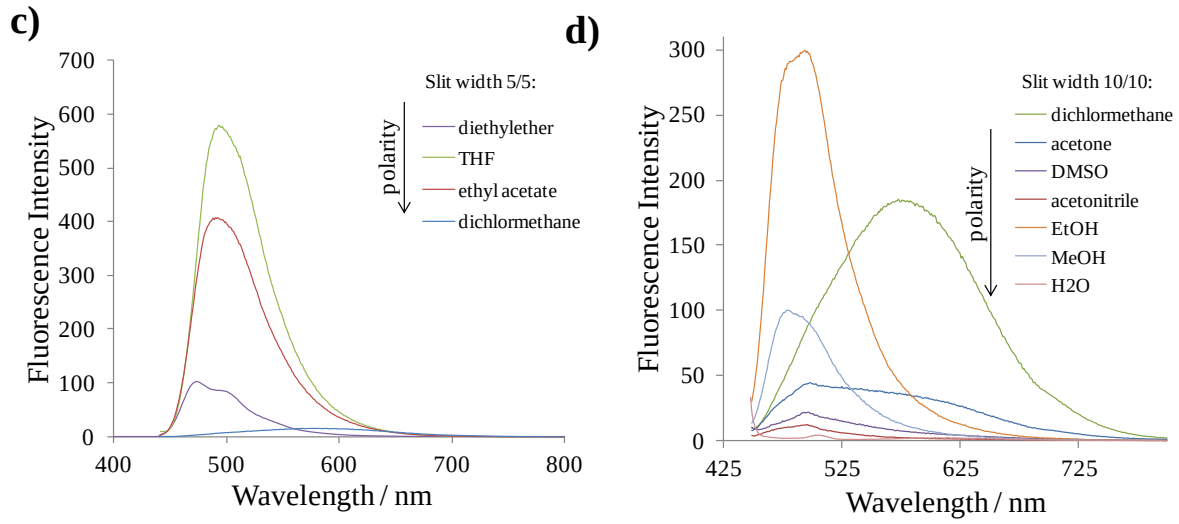

Figure S2. UV-vis, c = 1x10^{-5} M (a) and emission (c,d) spectra, c = 2x10^{-6} M of **3** in solvents of different polarity parameter, $\lambda_{exc} = \lambda_{abs}$; photographs of **3** in solvents of increasing polarity taken on day light and under UV lamp (b).

Table S1. Spectral properties of chemosensors **1-3** in in solvents of different polarity parameter.

		1					2					3				
Solvent	$E_T(30)$ / (kcal mol^{-1})	λ_{abs} / nm	$\varepsilon \cdot 10^{-3}$ / M^{-1} cm^{-1}	λ_{fluo} / nm	Rel. Fluo Int.[a]	Stokes shift (cm^{-1})	λ_{abs} / nm	$\varepsilon \cdot 10^{-3}$ / M^{-1} cm^{-1}	λ_{fluo} / nm	Rel. Fluo Int.[a]	Stokes shift (cm^{-1})	λ_{abs} / nm	$\varepsilon \cdot 10^{-3}$ / M^{-1} cm^{-1}	λ_{fluo} / nm	Rel. Fluo Int.[a]	Stokes shift (cm^{-1})
diethylether	34.5	413	93.36	480	16.58	3379	420	47.77	458	61.11	1975	427	75.97	475	-	2366
THF	37.4	418	79.47	489	31.22	3473	425	46.25	464	171.50	1977	433	67.62	493	-	2810
ethylacetate	38.1	415	78.69	485	24.11	3477	421	41.33	463	128.59	2154	431	70.38	490	-	2793
dichlormethane	40.7	423	73.5	484	59.30	2979	427	52.60	468	263.61	2051	438	71.86	576	-	5469
aceton	42.2	417	85.79	490	27.28	3572	423	52.19	465	205.22	2135	434	76.74	501	79.52	3081
DMSO	45.1	422	73.60	497	66.24	3575	430	41.34	475	282.76	2203	443	61.03	495	38.99	2371
acetonitrile	45.6	416	81.72	490	27.28	3630	423	50.00	468	187.80	2273	434	69.47	487	21.29	2507
ethanol	51.9	417	59.93	491	22.99	3614	427	42.69	467	155.55	2005	433	60.85	495	-	2892
methanol	55.4	418	87.04	486	33.17	3347	425	50.62	468	198.62	2161	434	71.45	480	196.50	2208
H_2O	63.1	429	56.29	486	30.78	2733	364	22.51	478	12.63	6552	390	31.16	500 608	6.80 4.56	5641

sh = shoulder; [a] at given experimental conditions: $c = 2 \times 10^{-6}$ M, slit width = 20/10

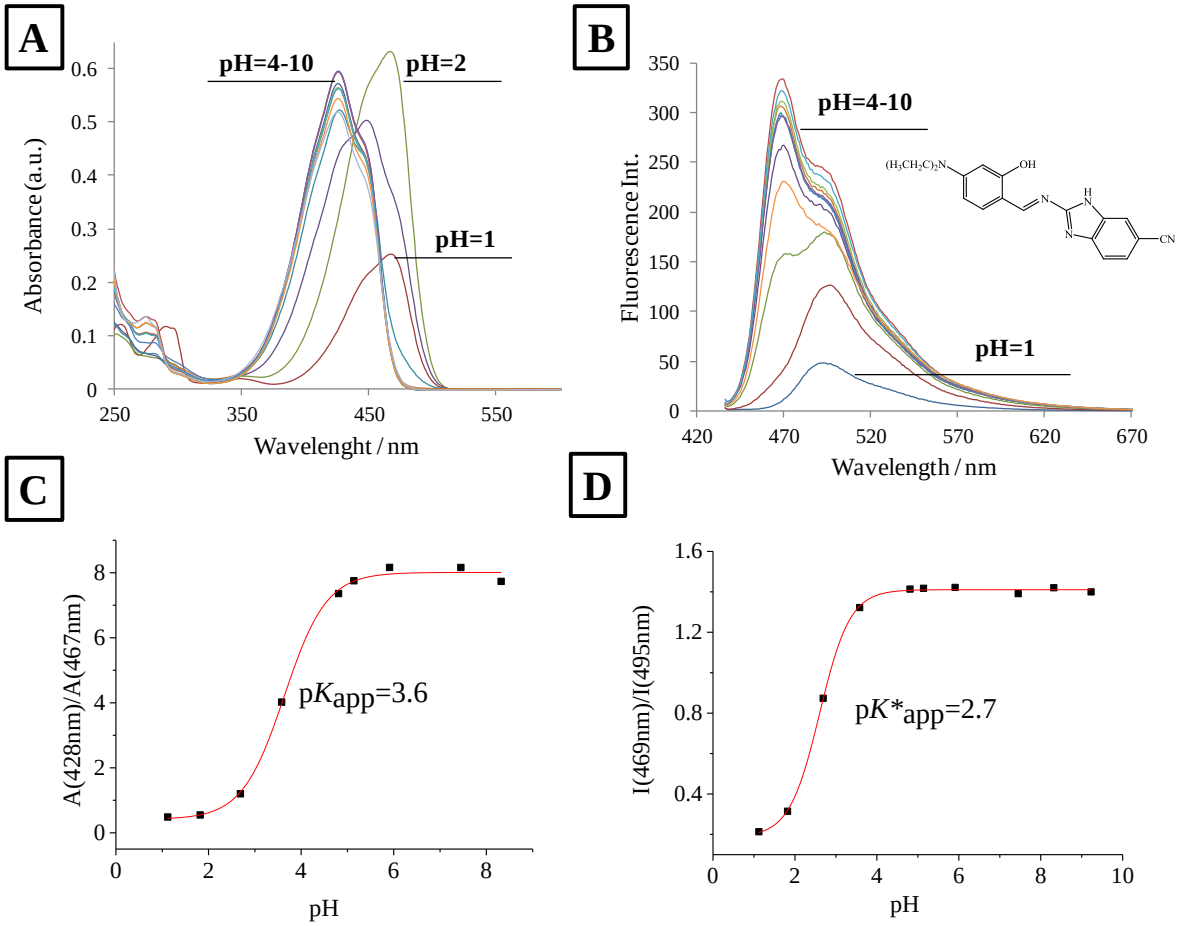

Figure S3. Effect of pH on absorbance (A) and emission (B) properties of **2**; pH response at chosen absorbance wavelength (A) and emission wavelength (D); (c = 10 μM and 2 μM, λ_{exc} = 425 nm).

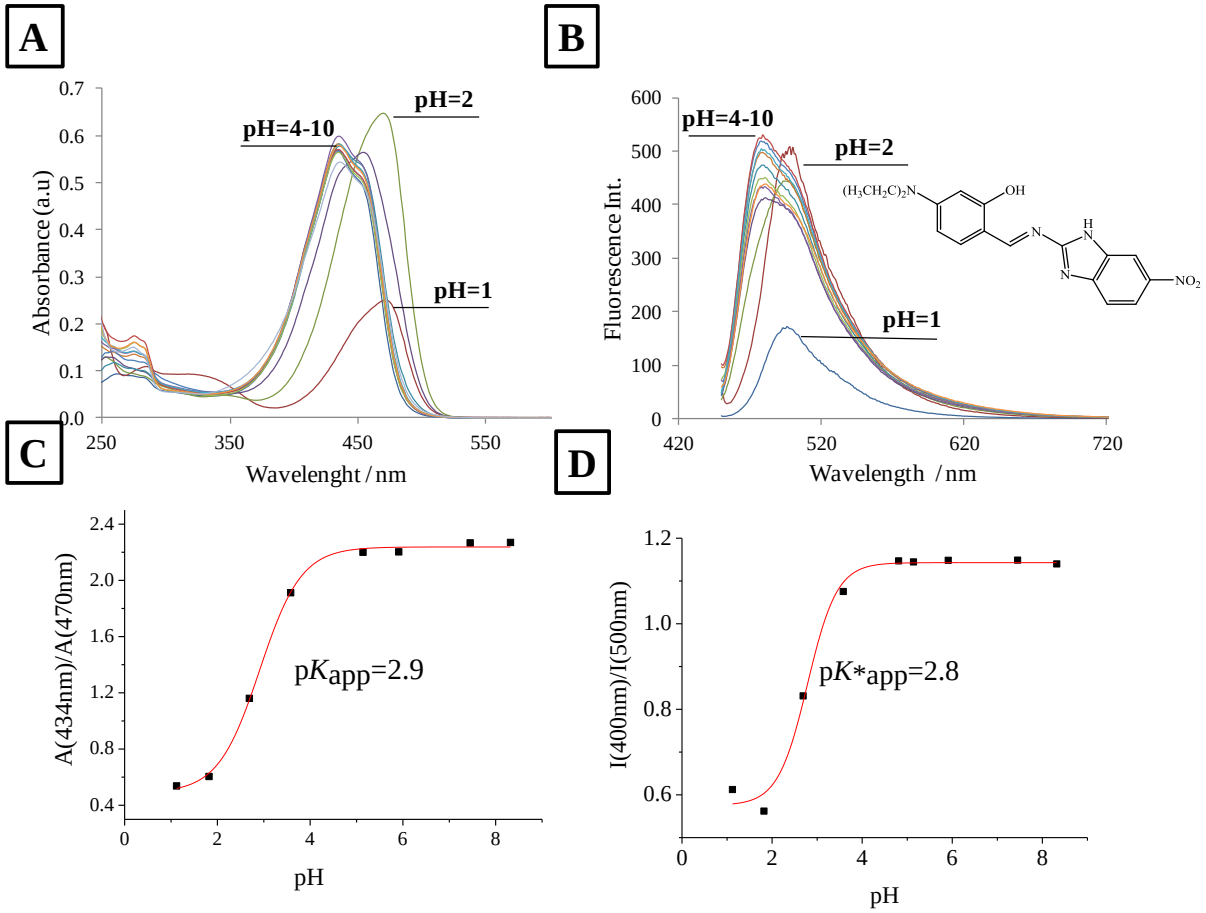

Figure S4. Effect of pH on absorbance (A) and emission (B) properties of **3**; pH response at chosen absorbance wavelength (A) and emission wavelength (D); (c = 10 μM and 2 μM, λ_{exc} = 433 nm).

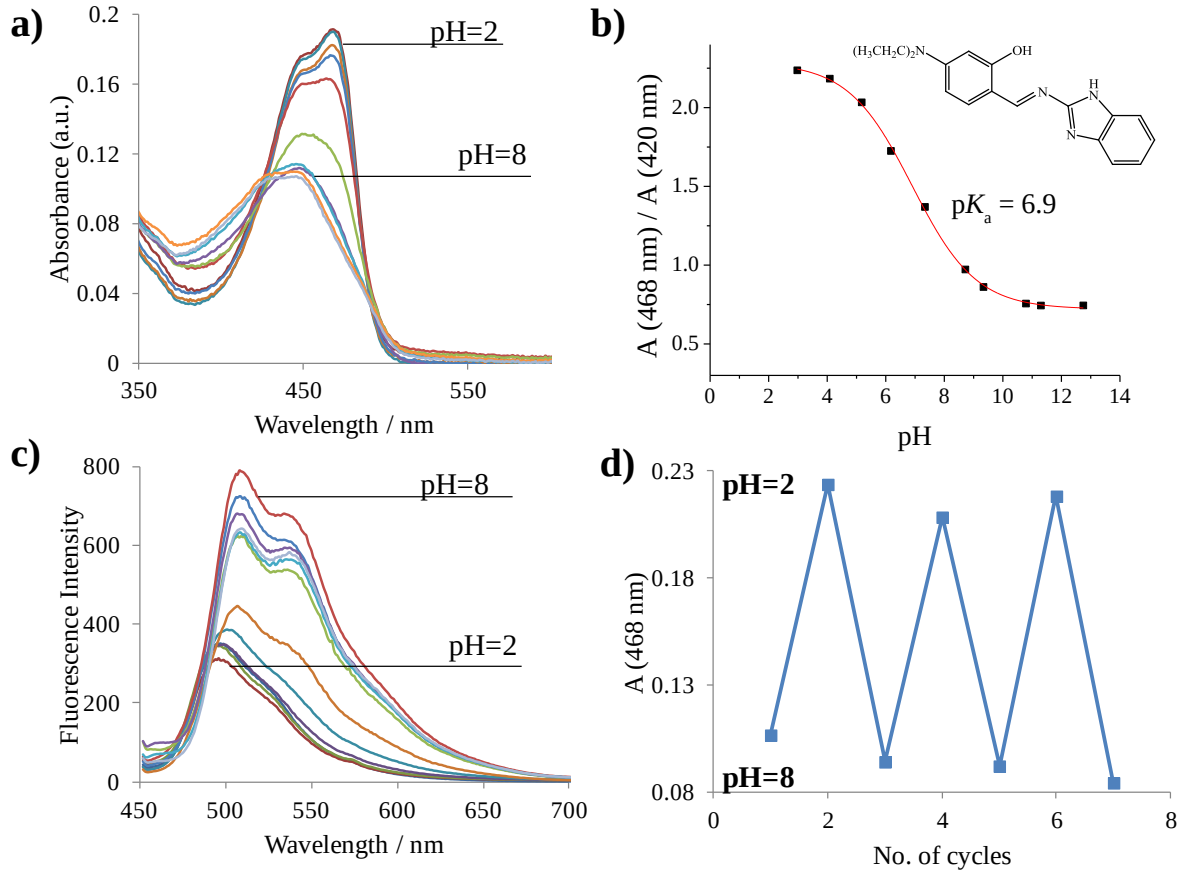

Figure S5. Effect of pH on absorbance (a) and emission (b) properties of immobilised **1**; pH response on selected wavelength (b) and results of reversibility of pH response (d), λ_{exc} = 417 nm.

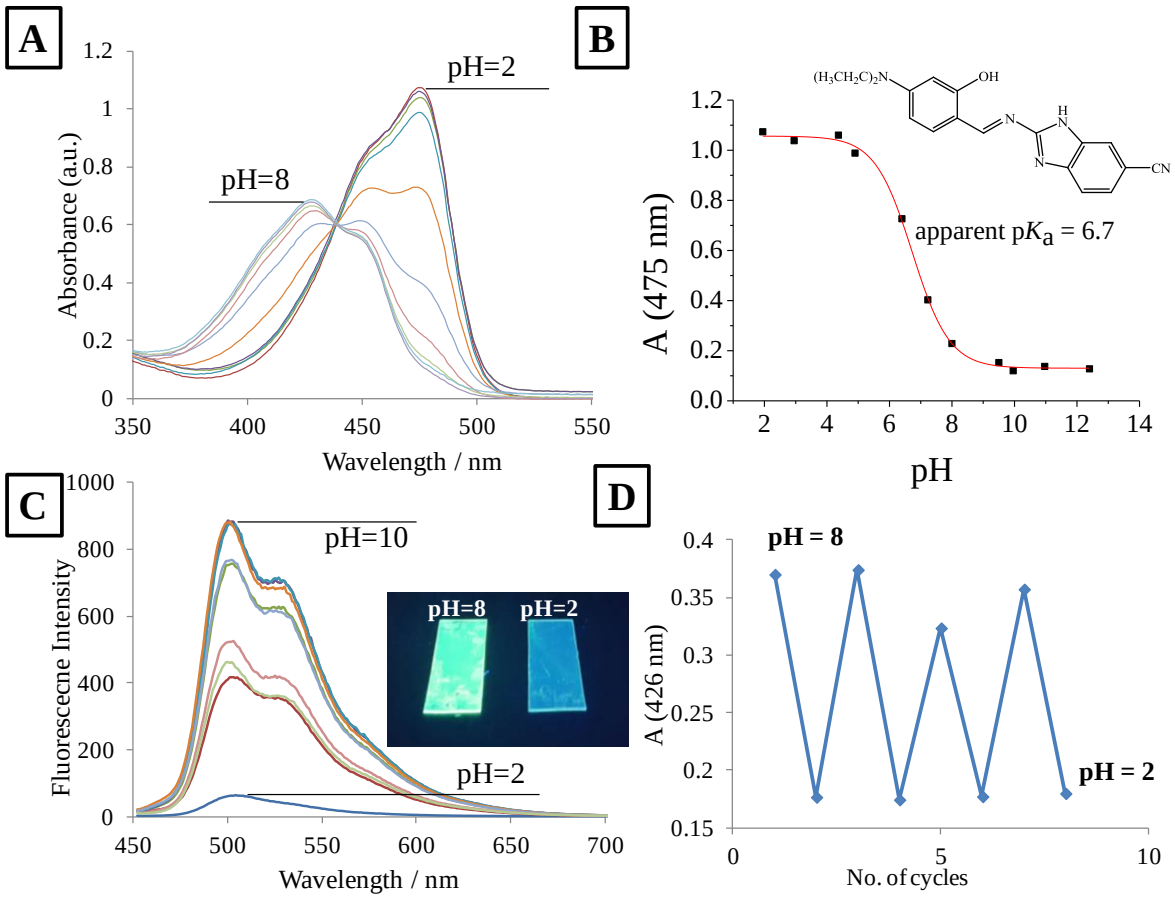

Figure S6. Effect of pH on absorbance (a) and emission (b) properties of immobilised **2**; pH response on selected wavelength (b) and results of reversibility of pH response (d), λ_{exc} = 427 nm. Inset: photographs of thin films taken under UV lamp.

ŽIVOTOPIS

Ema Horak [redacted] Svoje osnovnoškolsko i gimnazijsko obrazovanje završava u Bjelovaru, nakon čega 2006. godine upisuje studij Primijenjene kemije na Fakultetu kemijskog inženjerstva i tehnologije pri Sveučilištu u Zagrebu. Godine 2009. brani završni rad pod nazivom „*Priprava novih derivata 2-benzimidazo-amida i kinolona s potencijalnim antitumorskim djelovanjem*“ izrađen na Zavodu za organsku kemiju pod mentorskim vodstvom prof. dr. sc. Grace Karminski Zamola i time stječe titulu sveučilišne prvostupnice Primijenjene kemije. Iste godine upisuje diplomski studij Primijenjena kemija te 2011. godine brani diplomski rad „*Sinteza potencijalno biološki aktivnih amida i kinolona benzimidazolil-2(5)-karboksilne kiseline*„ izrađen na Zavodu za organsku kemiju pod mentorskim vodstvom prof. dr. sc. Marijane Hranjec te time stječe titulu magistre Primijenjene kemije. Tijekom studiranja je primila Rektorovu nagradu za studentski istraživački projekt „*Novi derivati benzimidazo[1,2-a]kinolina kao potencijalne fluorescentne probe za detekciju DNA/RNA*“ (mentorica dr. sc. Marijana Hranjec). Nakon kraćeg volontiranja na Zavodu za organsku kemiju, Ema Horak se zapošljava na radno mjesto asistenta na Zavodu za opću i anorgansku kemiju i priključuje istraživačkog grupi izv. prof. dr. sc. Ivane Steinberg. Pod njenim mentorskim vodstvom, započeto je istraživanje u području karakterizacije i razvoja novih kemosenzorskih molekula i optičkih senzorskih materijala u sklopu kojeg je izrađen doktorski rad. Tijekom izrade doktorskog rada Ema Horak je objavila 4 znanstvena rada citirana u bazi Current Contents i sudjelovala na međunarodnim i domaćim konferencijama s devet posterskih priopćenja. Sudjelovala je u zimskoj školi fizikalne organske kemije e-WiSPOC, (*European-Winter School on Physical Organic Chemistry*, e-WiSPOC), Bressanone, te u izvođenju laboratorijskih vježbi iz kolegija Opća kemija, Anorganska kemija, Integrirani kemijski sustavi i Tehnologijski management i inovacije.

Znanstvene publikacije:

[1] **E. Horak**, M. Hranjec, R. Vianello, I.M. Steinberg, Reversible pH switchable aggregation-induced emission of self-assembled benzimidazole-based acrylonitrile dye in aqueous solution, *Dyes Pigment.* 142 (2017) 108-115. (IF: 4,055, Q1)

[2] **E. Horak**, R. Vianello, M. Hranjec, S. Krištafor, G. Karminski Zamola, I. Murković Steinberg, Benzimidazole acrylonitriles as multifunctional push-pull chromophores: spectral characterization, protonation equilibria and nanoaggregation in aqueous solutions, *Spectroc. Acta Pt. A-Molec. Biomolec. Spectr.* 178 (2017) 225-233. (IF: 2,653, Q2)

[3] M. Hranjec, **E. Horak**, D. Babic, S. Plavljanin, Z. Srdovic, I. M. Steinberg, et al., Fluorescent benzimidazo[1,2-*a*]quinolines: synthesis, spectroscopic and computational studies of protonation equilibria and metal ion sensitivity, *New J. Chem.* 41 (2017) 358-71. (IF: 3,277, Q2)

[4] M. Hranjec, **E. Horak**, M. Tireli, G. Pavlovic, G. Karminski-Zamola, Synthesis, crystal structure and spectroscopic study of novel benzimidazoles and benzimidazo [1,2-*a*] quinolines as potential chemosensors for different cations, *Dyes Pigment.* 95 (2012) 644-56. (IF: 4,055, Q1)

Sudjelovanje na konferencijama:

1. **E. Horak**, M. Hranjec, N. Perin, R. Vianello, L. Furač, I. Steinberg, Aggregation-induced emission (AIE) of self- assembled benzimidazole based acrylonitrile dye, XXV. hrvatski skup kemičara i kemijskih inženjera, Poreč (Hrvatska), 2017.

2. **E. Horak**, M. Hranjec, N. Perin, R. Vianello, S. Krištafor, I. Steinberg, pH and metal sensing properties of benzimidazole based Schiff bases, XXV. hrvatski skup kemičara i kemijskih inženjera, Poreč (Hrvatska), 2017.

3. **E. Horak**, K. Bobanović, M. Sigurnjak, M. Marinović, N. Pantalon Juraj, I. Steinberg, S. Krištafor, Design, synthesis and immobilization of novel click-derived triazoles for the application in (bio)chemical sensor materials, *XIII Conference on Optical Chemical Sensors and Biosensors*, EUROPT(R)ODE 2016, Graz (Austrija), 2016.

4. **E. Horak,** Š. Kamenić, N. Perin, M. Hranjec, I. Steinberg, Optical properties of novel iminocoumarine derivatives in solutions and polymer matrices, *XIII Conference on Optical Chemical Sensors and Biosensors*, EUROPT(R)ODE 2016, Graz (Austrija), 2016.

5. **E. Horak**, S. Krištafor, N. Perin, M. Hranjec, I. Steinberg, Aminated benzimidazo[1, 2-*a*]quinolines as fluorescent pH sensors, *XXIV. Hrvatski skup kemičara i kemijskih inženjera*, Zagreb (Hrvatska), 2015.

6. M. Hranjec, N. Perin, **E. Horak**, Z. Srdović, S. Plavljanin, Novi benzimidazo[1, 2-*a*]kinolini kao pH senzori i kemosenzori, *XXIV. Hrvatski skup kemičara i kemijskih inženjera*, Zagreb (Hrvatska), 2015.

7. **E. Horak**, M. Hranjec, I. Steinberg, Optical sensing properties of novel benzimidazole-based dyes, E-*WISPOC 2015: Chemistry and chemical processes in confined spaces*, Bressanone (Italija), 2015.

8. **E. Horak**, R. Vianello, M. Hranjec, I. Murković Steinberg, Optička karakterizacija i imobilizacija novih derivata benzimidazola, akrilonitrilnih bojila, EUROPT(R)ODE XII, *Conference on Optical Chemical Sensors and Biosensors*, Atena (Grčka), 2014.

9. **E. Horak**, S. Krištafor, N. Perin, M. Hranjec, I. Murković Steinberg, Optička senzorska svojstva novih fluorescentnih amino benzimidazo[1,2-*a*] kinolina, EUROPT(R)ODE XII, *Conference on Optical Chemical Sensors and Biosensors*, Atena (Grčka), 2014.

10. M. Posavec, **E. Horak**, M. Hranjec, I. Murković Steinberg, Imobilizacija novih derivata benzimidazola u tanke polimerne filmove za optičku detekciju iona, *X. Susret mladih kemijskih inženjera*, Zagreb (Hrvatska), 2014.

11. **E. Horak**, S. Kostel, I. Sović, G. Karminski Zamola, Priprava novih derivata 2-benzimidazo-amida s potencijalnim antitumorskim djelovanjem, *VIII. Susret mladih kemijskih inženjera*, Zagreb (Hrvatska), 2010.